Physiology and Pathophysiology of the Dentine-Pulp Complex in Response to Dentine Exposure

Anas Falah Mahdee

MSc BDS

Thesis Submitted in Partial Fulfilment of the Requirements of the Regulations for the Degree of Doctor of Philosophy

Institute of Cellular Medicine and Centre for Oral Health Research

School of Dental Sciences

Newcastle University

October 2017

Abstract

Therapies to promote pulp repair and regeneration after injury should be underpinned by a deep understanding of normal tissue behaviour, and cellular signalling mechanisms. The objectives of this work were to understand normal structure of the tooth and to identify changes in its cellular elements and their complex interactions in response to dentine exposure. Revisiting pulp structure and function with a range of contemporary techniques may formalize observations into new concepts of tooth physiology and pathophysiology, and reveal new opportunities for therapeutic intervention.

Studies within this thesis employed rodent mandibular incisors and molars with structural and functional investigations on demineralised teeth, non-demineralised freshly extracted pulp tissues and tissue explants. Observations were made on ground sections, haematoxylin-eosin stained sections, immunohistochemically-stained sections, and on quantitative reverse transcription polymerase chain reaction (q-RT-PCR) examination of tissue explants.

Complex cellular structure and heterogeneity was observed within odontoblast and subodontoblast cellular populations. Previously undescribed odontoblast processes were identified within the predentine region during crown development and in the radicular pulp after tooth development. Programmed retraction of odontoblast processes was observed after dentine exposure by cavity preparation or tooth wear. Two phases of reactionary dentine deposition (atubular followed by tubular) was identified after tooth wear. This revealed a programmed cellular defensive mechanism which lead to tissue recovery and regeneration. This process could be controlled by autocrine or paracrine signalling mechanisms, as indicated by the presence of NGF and NGFR, in addition to a complex network of CGRP-IR axons.

Observations suggested revision of established hypotheses including the hydrodynamic theory of dentine sensitivity and the role of extracellular pH in biomineralisation. This hypothesis could provide coherent explanation for several well-known dental mysteries including pulp stone development, dentine sclerosis and the mode of action of high pH materials (calcium hydroxide, and hydraulic calcium silicate cements) in the repair of pulp wounds.

Certificate of approval

I confirm that, to the best of my knowledge, this thesis represents an original research carried out by **Anas Falah Mahdee** in fulfilment of the requirements for the degree of Doctor of Philosophy according to the regulations of Newcastle University.

Professor

John M. Whitworth

Supervisor

Acknowledgements

I would like to express my sincere gratitude to my PhD supervisors Prof. John Whitworth and Prof. James Gillespie for their expert advice and encouragement throughout every aspect of this work. Prof. Whitworth, your support, commitment, advice, reviewing efforts, and scientific questions helped me to produce this work. Prof. Gillespie, the expertise you taught me, lots of discussions we've had, the opportunities you have supported, and the thoughts you have given me, helped me become what I am today.

I would like to acknowledge and thank the research assistant Jane Eastham for her impressive laboratory efforts during immunohistochemistry. I would not be able to achieve what I have now without your help Jane. I also would like to thank my friend Ahmed Alhelal for his help in all part of this work, endless discussion, and sharing ideas and thoughts. Also great thanks to Mohammad Alhilal for his help and expert advice with the molecular work of this project.

I am extremely grateful to Prof. Leo Tjaderhane and Dr. Stephane Simon to their visits to Newcastle University and for their critical appraisal of this work during stages of its development.

I would like to acknowledge Dr. Ruth Valentine and Dr. Luisa Wakeling for their helpful advices in the genetic chapter of this project.

Special thanks go to Mrs Pamela Walton in Hard Tissue laboratory for her help in obtaining the ground sections. Also, I would like to thank Mrs Anna Long in the Cellular Pathology Department in RVI and her help in H&E staining.

I wish to thank all my colleagues and friends in Oral Biology Research Lab, especially Mrs Lesley Old, Nadia, Hala, Ahmed, Suhair, Ali, Nieka, Syatirah and Rebecca, and all other staff for their help and support whenever needed. Great thanks also to Catherine and Simone for their support and friendship.

I would like to thank all staff members of Newcastle University, especially Walton library and Kings Gate staff, for their friendly help and assistance on any occasion and under all circumstances.

Great thanks and gratitude to my sponsors, Iraqi Ministry of Higher Education and Baghdad University for granting me this sponsorship and valuable help and support throughout my study.

I am very lucky to have a lovely wife, Rasha and beautiful kids Melak, Yousif and baby Mayar. You are my entire life and hope this achievement makes you proud.

Finally, I would like to thank my Mum and brothers for all their love, patience and support in every situation of life, I wouldn’t be here without your help.

Table of contents

List of figures

List of tables

List of abbreviations

actin	α-smooth muscle actin
ASPA	animals Scientific Procedures Act 1986
ATP	adenosine triphosphate
BMP	bone morphogenic protein
bp	base pair
BV	blood vessel
Cav	cavity
Cb	cementoblast
cDNA	complementary DNA
Ce	cementum
CGRP	calcitonin gene-related peptide
CMZ	cavity measurement zone
CO_2	carbon dioxide
Col	collagen
Cp	capillary
CPC	central pulp cells
Ct	cycle threshold
D	distal
dapi	nuclear acid molecular probe stain
d	day
D-Den	distal nerve density
De	dentine

DEJ	dentino-enamel junction
DL	dentine thickness in control surfaces
DMEM	Dulbecco’s modified Eagle’s medium
DMP	dentine matrix protein
DNA	deoxyribonucleic acid
DP	dental papilla
DPP	dentine phophoprotein
DSP	dentine sialoprotein
DT	dentinal tubule
EDTA	ethylenediaminetetraacetic acid
En	enamel
EP	prostaglandin receptor
F-actin	filamentous actin
GAPDH	glyceraldehyde 3-phosphate dehydrogenase
gDNA	genomic DNA
Gi	gingiva
h	hour
HAP	hydroxyapatite
H&E	haematoxylin-eosin staining
HERS	Hertwig’s epithelial root sheath
IEE	inner enamel epithelium
IgG	immunoglobulin G
IHC	immunohistochemistry

IL	interleukin
IR	immunoreactivity
JC	junction complex
K^{+}_{Ca}	calcium activated potassium channel
L	estimated thickness of dentine after cavity
LPS	lipopolysaccharide
M	mesial
M-Den	mesial nerve density
MHC	major histocompatibility complex
MOA	mode of action
mRNA	messenger RNA
MTA	mineral trioxide aggregate
n	number
NaK-ATPase	sodium potassium adenosine tri-phosphatase
Na_v	sodium voltage gated channel
NBCe1	electrogenic sodium/bicarbonate cotransporter
NCPs	non-collagenous proteins
NCX	sodium/calcium exchanger
Nf	neurofilaments
NF-kB	nuclear transcription factor-kB
NGF	nerve growth factor
NGFR	nerve growth factor receptor
NHE	sodium/hydrogen antiporter

NOS	nitric oxide synthase
NS	non-significant
NTC	no template control
OCT	optimal cutting temperature medium
Od	odontoblast
OEE	outer enamel epithelium
OP	odontoblast process
P	pulp
PAm	pre-ameloblast
PBS	phosphate buffer saline
PBS-T	phosphate buffer saline-triton
PCR	polymerase chain reaction
PD	predentine
PDL	periodontal ligament
PFA	paraformaldehyde
PGs	proteoglycans
pH	potential of hydrogen
P_i	inorganic phosphate
PMCA	plasma membrane calcium ATP
POd	pre-odontoblast
qRT-PCR	quantitative reverse transcriptase polymerase chain reaction
Re-De	reactionary dentine
RNA	ribonucleic acid

RP	rhodamine-phalloidin stain
RT	reverse transcription
S	stage
SE	standard error
sec	second
SEM	scanning electron microscopy
SERCA	sacro/endoplasmic reticulum calcium ATP
SI	stratum intermedium
SIBLING	small integrin-binding ligand N-linked glycoproteins
SOd	subodontoblast
SR	stellate reticulum
TAE	tris-acetate-EDTA
TBS	tris buffer saline
TBS-T	tris buffer saline-tween
TD	tertiary dentine
T-Den	total nerve density
TEM	transmission electron microscopy
TGFbr	transforming growth factor beta receptor
TGFβ	transforming growth factor beta
TLR	Toll-like receptor
TP	Tome’s process
TREK	mechanosensitive potassium channel
trkA	tyrosine kinase receptors

TRPV	transient receptor potential
tub	tubulin
UOd	undifferentiated odontoblast
vim	vimentin
vs	versus
w	week

Chapter 1 **Literature review**

1.1 Introduction

Dental pulp is a unique soft tissue that resides in a hard tissue compartment of its own making. Its cells maintain an intimate spatial and functional relationship with surrounding tissues throughout life. This rigid compartment of dentine-enamel in the crown, and dentine-cementum in the root offers the required mechanical and microbial protection for the soft tissue of the pulp, and gives the pulp its distinctive anatomical features (Yu and Abbott, 2007; Luukko *et al.*, 2011). However, if this rigid chamber loses its structural integrity, the pulp is at a risk of adverse stimulation from the oral cavity. Caries, tooth wear, cracks, fractures, and open restoration margins provide an open route for the oral microflora and their toxins to access the pulp (Simon *et al.*, 2012).

The unique nature the dental pulp, relates most importantly to the presence of highly specialised odontoblasts (Ods) at its periphery and extension of cytoplasmic processes within dentinal tubules. The intimate embryological, physical and functional relationship between these cells and their surrounding hard shell is often referred to as the dentine-odontoblast complex (Goldberg and Lasfargues, 1995; Tjäderhane and Haapasalo, 2012; Simon and Goldberg, 2014). In addition to the primary role of Ods in dentine formation and mineralisation, their position within this complex enables them to play a crucial role in sensing danger and defensive responses. This could include sensing elements of the oral environment through their odontoblast processes (OPs), mechanosensitive functions related to fluid movement and tooth flexion (Magloire *et al.*, 2009), and maintaining hard tissue integrity to preserve pulp vitality (Tjäderhane and Haapasalo, 2012). Nevertheless, the overall pulp function is always limited by its low compliance surroundings, the absence of a collateral blood supply, at least in single rooted teeth, relative incompressibility and restricted ability to expand in the face of inflammation (Ikawa *et al.*, 2003; Smith, 2003).

Different models were used within published data to study dentine pulp complex including both human and animal teeth (Sloan *et al.*, 1998). Some of these models contain high crown and enamel extending under the gingival margin. These are called hypsodont such as the herbivores dentition (bovine and horse) (Raia *et al.*,

2011). This evolutionary pattern of teeth is to provide extra material for occlusal surface wear which occurs as a result of a fibrous diet (Jernvall and Fortelius, 2002). The opposite from that is the brachydont with normal crown size such as human teeth. Several studies also used rodent teeth which could provide two different growth patterns: continuous for incisors and limited for molars (Tjäderhane and Haapasalo, 2012). The former teeth contain an apical bud region with all generative cells for the pulp and enamel, to maintain tooth growth in order to compensate the incisal edge loss due to continuous wear (Smith and Warshawsky, 1975; Warshawsky *et al.*, 1981). The rodent molars, especially rat, show great similarity in their structure and growth pattern to human tissue (Sloan *et al.*, 1998).

1.2 Odontoblast differentiation and initial dentine formation

Odontoblasts originate from embryogenic ectomesenchymal cells which are parts of the cranial neural crest. The primitive oral epithelium proliferates and enlarges toward underlying ectomesenchyme, forming the basic structures of the tooth bud: dental lamina, enamel organ and dental papilla (Harada and Ohshima, 2004). Several epithelial-ectomesenchymal interactions administrate tooth formation (Tjäderhane and Haapasalo, 2012). During early stages of odontogenesis, proliferation of the oral epithelium changes the tooth germ from bud to cap and then bell stages. The differentiation of the Ods starts between the early and late bell stage after establishing the crown's morphology. Reciprocal signalling molecules between enamel organ and dental papilla cells regulate the differentiation of the outer, post-mitotic cells of the dental papilla into Ods (Ruch *et al.*, 1995). A number of growth factors have been recognised to participate in this inductive phenomenon. Nerve growth factor (NGF) belongs to the neurotrophin family, which is important for the development, survival, maintenance and repair of the neural system (Chao, 2003). Both NGF and its neurotrophic p^{75} receptors (NGFR) were reported to be localised within differentiating pulp cells (Byers *et al.*, 1990; Mitsiadis *et al.*, 1992). NGF protein was clearly identified within Ods, while NGFR labelled within inner enamel epithelium, then polarised Ods but was lost after the cells became functional. NGFR expression then begins in subodontoblast (SOd) cells. This indicates the possibility of reciprocal cellular paracrine and autocrine inductive mechanisms between these cells (Mitsiadis *et al.*, 1992). Transforming growth factor-β family (TGF-β1, TGF-β2, TGF-β3, BMP-2, BMP-4, BMP-7) also appear to be important molecules mediating Od differentiation (Ruch *et al.*, 1995; Sloan and Smith, 1999; Oka *et al.*, 2007). A

substantial delay in Od differentiation with decrease thickness of dentine formation and absence of dentinal tubules were reported in TGFbr2 mutant mice (Oka *et al.*, 2007). This indicated the role of TGF-β signalling in Od differentiation and dentine formation.

After the withdrawal of preodontoblast cells from the cell division cycle following the last division phase, these cells start to lie perpendicular to the basement membrane at the epithelia-mesenchymal junction. The differentiating Ods then elongate and their nuclei take an eccentric basal position with development of cisterna of rough endoplasmic reticulum apical to the nucleus and parallel to the cell axis (Couve, 1986). The redistribution of the cellular structural filaments within differentiating Ods was also reported to have a role in obtaining cellular polarity (Lesot *et al.*, 1982). This is associated with the dissociation of the basement membrane and the appearance of fibronectin and decorin near the apical side of the differentiating Ods (Ruch *et al.*, 1995). These basement membrane proteins were identified to be essential in terminal differentiation of the Ods. These cells then start to secrete predentine matrix protein prior to enamel matrix secretion by the ameloblasts. This initial predentine matrix is important in ameloblast terminal differentiation (Tjäderhane and Haapasalo, 2012).

The first protein matrix secreted by the differentiated Ods contains large fibrils of type III collagen (0.1-0.2 μm fibrillar diameter). These collagen fibrils and the extracellular material between the differentiating cells constitute the organic matrix of the initial dentine (mantle dentine) (Tjäderhane *et al.*, 2012). At the same time, the Ods enlarge and arrange in a uniform contacted cell layer, which starts to move in a pulpal direction leaving their OPs behind (Couve, 1986). Mineralisation of the mantle dentine begins throughout the matrix vesicles produced by the Ods. These vesicles are membrane-limited bodies and believed to originate from plasma membrane. They are reported to be enriched with tissue-nonspecific alkaline phosphatase (Golub, 2009). Although the role of matrix vesicles in the initiation of dentine and other hard tissue mineralisation is generally accepted, the extent of that role remains uncertain (Tjäderhane and Haapasalo, 2012). The matrix vesicles are also reported to be involved in reparative dentine mineralisation processes, but not in the formation of physiological primary and secondary dentine (Takano *et al.*, 2000). Additionally, the mantle dentine is devoid of dentinal tubules but contains occasional fine tubular branches. This may indicate that the mantle dentine is secreted by differentiated Ods

containing multiple branching of OPs (Couve, 1986), at a time before the development of the functional OPs that create patent dentinal tubules (Tjäderhane *et al.*, 2012).

1.3 Odontoblasts

Odontoblasts are terminally differentiated, post-mitotic, long living cells that do not turn over during the lifetime of the individual. They are located along the dental-pulp interface (Ruch *et al.*, 1995). The active Od is a highly polarized cell with a basally located nucleus. The polarization of the Od effects the cytoskeleton and results in apparent expression of the microtubules, intermediate filaments and microfilaments at the apical side of the cell (Lesot *et al.*, 1982; Nishikawa and Kitamura, 1986; Nishikawa and Kitamura, 1987). A well-developed Golgi complex is centrally located in the supra-nuclear cytoplasm. In addition, highly ordered rough endoplasmic reticulum and numerous mitochondria, ribosomes and secretory granules are also found in the Od, similar to other protein secretory cells (Sasaki and Garant, 1996). Od cell bodies are connected with gap junctions, occluding zone (tight junctions), adhesion belts and desmosomes. The tight junctions connect the cell bodies in their distal junctional complex with actin filaments. These insert into the junctions forming a terminal web, but still there are some openings in the inter-odontoblast spaces to permit the passage of some unmyelinated nerve fibres (Couve, 1986). In addition, tracer studies suggest the passage of small elements from the capillaries in the SOd cells, in between the Od cell bodies, to predentine and dentine (Linde and Lundgren, 1995). The gap junctions, places of cytoplasm-cytoplasm communication, also present in high numbers along the lateral surfaces of the Od cell bodies (Couve, 1986; Sasaki and Garant, 1996).

In the young pulp, where the Ods actively secrete collagen, they appear in a long columnar form and arrange in a single cell layer. After increasing dentine thickness the Ods actively slides over each other to form a pseudo-stratified cell layer of 3 to 5 cell thickness (Ohshima and Yoshida, 1992). In more mature pulp, the Od seems to be shorter with less cytoplasm, fewer cytoplasmic organelles, and lower numbers of cells within the layer. These cells appear to be in a less activity period after shifting from primary to secondary dentinogenesis (Couve, 1986; Lovschall *et al.*, 2002; Murray *et al.*, 2002). The reduced circumference of the pulp space due to ongoing primary and secondary dentine deposition creates crowding of the Ods, and

apoptosis may play a part in regulating cell numbers during ongoing tooth development (Mitsiadis *et al.*, 2008).

In addition to the Od cell bodies, capillaries, unmyelinated nerve fibres and dendritic cells are also found in the Od cell layer. It has been reported that, the peripheral capillaries invade in between the Ods and reach the mineralizing front during the active secretory stage (Ohshima and Yoshida, 1992; Sasaki and Garant, 1996). Unmyelinated nerve fibres have also been reported approaching the Od layer and terminating in the dentinal tubules in 25 day old mouse molars(Taylor and Byers, 1990). In addition to sensory conduction, these nerves are reported to release biologically active peptides (including calcitonin gene related peptide) during stimulation or injury (Mori *et al.*, 1989). Dendritic cells, and macrophages show marked increase in numbers during inflammatory stimulation (Ohshima *et al.*, 1995; Rungvechvuttivittaya *et al.*, 1998; Veerayutthwilai *et al.*, 2007).

The main function of the Od is secretion of dentine matrix to form tubular, primary dentine, and both physiological secondary and reactionary tertiary dentine. These functions may be preserved throughout life. The Ods secrete extracellular type I collagen-rich matrix to form predentine, in addition to a number of non-collagenous proteins including glycoprotein, proteoglycans, and dentine phosphoproteins to biomineralise the dentine organic matrix (Tjäderhane and Haapasalo, 2012). Unlike other formative cells such as cementoblast and osteoblast, the Od cell bodies are never entrapped by their collagen matrix during normal secretory conditions. When Ods secrete predentine matrix, they retreat towards the pulp, leaving their cytoplasmic processes within the tubular structure of the dentine, where they play a part in mineralisation of the dentine matrix (Ricucci *et al.*, 2014).

Odontoblasts also serve inflammatory, sensory and reparative roles in response to aging and injury, including dental caries, tooth wear and operative dental intervention (Ricucci *et al.*, 2014). The position of the Ods at the interface between the pulp and dentine with their cellular processes extending far within the dentinal tubules (Vongsavan *et al.*, 2000; Byers and Lin, 2003), and the presence of the partially impermeable barrier as a pseudo-epithelial layer (Sasaki and Garant, 1996), makes them the first cell line to encounter microorganisms and their products from the oral cavity. It has been reported that the Ods provide an innate immune barrier by expressing TLR2 and TLR4 receptors on their dentine interface. This suggests that

the pro-inflammatory cytokines and innate immune responses to tooth injury could be initiated from TLR4 signalling of the odontoblasts (Veerayutthwilai *et al.*, 2007).

The spatial arrangement of the Ods and their processes suggests their potential role in sensing both external stimuli and/or internal variation in pulp microcirculation (Magloire *et al.*, 2009). Further details are discussed in section 1.10.

1.4 Odontoblast processes

Odontoblast processes are the cellular extensions of the Od inside the dentine which act as the main element of the Od cells activity. They are the only cellular part of the pulp that resides within the dentinal tubules which they have formed, and highlight the vitality of this hard tissue. During Od differentiation and polarization, a few small and short OPs emerge facing the enamel organ (Arana-Chavez and Massa, 2004). After Ods start secreting the organic matrix and establishing the first dentine layer (mantle dentine) only one main process for each Od is believed to be left within the dentine to accomplish the mineralization process (Tjäderhane *et al.*, 2012).

1.4.1 Odontoblast process structure

At the ultrastructural level, the OP is a direct extension of the Od plasma membrane (Holland, 1985). The membrane of the processes is typically trilaminar in appearance. Although the surface of OPs look smooth, short projections extend from them which are more common in predentine and inner dentine (Holland, 1985). As the OPs extends through predentine to the mineralised dentine, it shows changes in its cytoplasmic contents. The most prominent organelles which have been reported by TEM studies are protein filaments which extend from the cell body into the process. The smallest are microfilaments or actin fibres (5-8 nm in diameter), somewhat larger intermediate filaments (10 nm in diameter) and hollow microtubules (27 nm in diameter) (Garant, 1972; Holland, 1985; Yoshiba *et al.*, 2002). These cytoplasmic proteins are polymers of different types of protein. They are required for numerous activities, including structural support primarily from the cytoskeleton, cellular movement and secretion (Pollard and Cooper, 2009). Other cytoplasmic organelles such as mitochondria, endoplasmic reticulum and ribosomes have also been identified within OPs, especially in the predentine area (Sasaki and Garant, 1996). Vesicles of various sizes and appearance, rod-shape dense bodies, and lysosome-like bodies may also be present (Thomas, 1979; Holland, 1985).

Within the dentinal tubules, the OPs occupy almost the entire space with scarce periodontoblastic space in between (Carda and Peydro, 2006). In demineralized sections, most of the peritubular dentine matrix has disappeared, causing space between the OPs and intertubular dentine (Yoshiba *et al.*, 2002). At the same time, incorrect fixation or inadequate demineralisation may change these proportions (Thomas, 1983). It has been reported that the average area of the OPs in a non-decalcified human molar is about 2.23 μm^2 and for the intratubular space is 2.85 μm^2 which reveals a difference of about 0.72 μm^2 for the intratubular space remaining (Carda and Peydro, 2006).

Nerve fibres are also reported within the tubular space accompanying the OPs. These nerves are limited to the inner dentine and extend no more than 150-200 µm. These nerves join only 30-70% of the odontoblast processes and occupy about 2.9% of the total tubular space area (Inoue *et al.*, 1992; Carda and Peydro, 2006). Although the nerve endings show very close proximity to the OPs, no real synaptic or gap junctions have been reported within or before entering the dentinal tubules. (Holland, 1985; Carda and Peydro, 2006).

1.4.2 Odontoblast process extension

Although the structure of the OPs appears to be well established and largely beyond debate, the distance to which the OPs extend within the dentinal tubules remains uncertain. Numerous studies, involving a range of methods including; scanning electron microscopy (SEM) (Thomas and Carella, 1983; Goracci *et al.*, 1999), transmission electron microscopy (Garant, 1972; Thomas, 1979; Yoshiba *et al.*, 2002), confocal laser microscopy (Grötz *et al.*, 1998; Goracci *et al.*, 1999), and immunofluorescence microscopy (Byers and Sugaya, 1995; Yoshiba *et al.*, 2002) have suggested that the odontoblast processes are limited to the inner third of the dentinal tubules. Other studies using SEM (Kelley *et al.*, 1981; Gunji and Kobayashi, 1983), TEM (Frank and Steuer, 1988), confocal laser microscopy (Grötz *et al.*, 1998; Tsuchlya *et al.*, 2002), and fluorescence microscopy (Sigal *et al.*, 1984a; Sigal *et al.*, 1985) have reported the existence of the OPs in peripheral dentine. It is an interesting area for further investigation to understand the role of these processes after tooth development such as sensing, maintaining dentine integrity, responding to different stimuli, and the consequential physiological and pathological reactions. Their response to operative dental procedures, including the cutting and restoration of enamel and dentine, which may disrupt an otherwise intact system, is also worthy

of further exploration (Byers and Narhi, 1999; Kawagishi *et al.*, 2006). Enhanced understanding of OP extension may provide important information for clinical practice and the optimisation of clinical procedures for pulp survival. Most of the previous studies agree with the full extension of the OPs through dentine during tooth development and the early life of teeth after eruption (Holland, 1985). In contrast, others insist that these processes retreat after that to the inner third of the dentine during normal tooth aging, attributing this to the inability of these processes to survive for a long period at that distance from the body of the pulp (Carda and Peydro, 2006). An important question could be raised about the ability of these processes to survive during the developmental period when their function is at its maximum due to dentinogenesis. There are various critical issues that should be considered when studying dentine. First is the complexity of this tissue, which is composed of a network of huge numbers of hard tubules with various sizes of lateral branches that could contain vital tissue (Tjäderhane *et al.*, 2012). Second is the technical difficulties during fixation and the type of fixative that can penetrate deeply into these very fine areas easily without adversely affecting the vital structures within dentine (Thomas, 1983). Third is the effect of other technical procedures such as demineralisation which could also harm some of the original existing cellular protein (Thomas, 1983; Carda and Peydro, 2006). Another technical issue which is especially relevant in TEM work is the impact of processing on delicate cellular structures, including tissue shrinkage (Brown *et al.*, 2002), which could happen to the processes within the dentinal tubules during tissue fixation and dehydration. Finally, there are recognised difficulties in distinguishing between the cellular living substances and the extracellular materials at an ultrastructural level. Most of the researchers who have claimed the limitation of the OPs to the inner third of dentine, have suggested the persistence of a membrane lining the peritubular dentine which could be mis-diagnosed as OPs. They called this limiting membrane the lamina limitans which was defined by Thomas (1984) as a sheet-like structure lining the dentinal tubules, which can be greatly enhanced during the demineralising procedure and appears as an electron dense structure in SEM and TEM images (Thomas and Carella, 1983).

On the other hand, the detection of intracellular proteins such as tubulin in the peripheral dentine could reveal the presence of cellular processes in that region. Actin immunoreactivity (IR) was also detected in the OPs, but its labelling was less intense, discontinuous, and only located in the inner third of the dentine (Sigal *et al.*,

1984a; Sigal *et al.*, 1985). The expression of the DiI and phalloidin have also been detected in the outer dentine by the use of confocal laser microscopy (Tsuchlya *et al.*, 2002). A histotomographical study using confocal laser microscopy with non-decalcified tooth samples revealed the presence of OPs with complex terminal branching at the DEJ (Grötz *et al.*, 1998). Using SEM, the presence of the OPs has been reported extending the full dentine thickness in coronal dentine. Sigal *et al.* (1985) observed bench dried and freshly extracted tooth samples both in SEM and immunofluorescence for cytoskeletal proteins. They reported the presence of process-like structures near the DEJ of the dried teeth by SEM which could be mummified remnants of the processes. Equally, these dry structures did not have immunofluorescence labelling compared with the fresh teeth. This may prove that the detection of the cytoskeletal protein fibres vimentin, tubulin, and actin within the OPs is a real intracellular structure of the processes and is not a remnant of these elements that would persist after the retraction of the OPs toward the pulp. Furthermore, in TEM studies, the detection of intracellular organelles was reported in the OPs residing within the outer dentine (Frank and Steuer, 1988).

The anatomical complexity of the OPs may reflect its likely functions. In the coronal dentine, the diameter of the OPs is about 1-3 µm with rare branches in the inner dentine. As the processes extend toward the DEJ, their diameters decrease, and their branches become more extensive. These branches are directed mainly toward the DEJ (Tsuchlya *et al.*, 2002), and some of them appear cross-bridging between two adjacent processes (Gunji and Kobayashi, 1983). In the outer dentine, the main processes reach about 0.1-0.2 µm in diameter with a similar branching pattern, but appear more extensive than in middle dentine. At the DEJ, the OPs terminate freely without special structure (Kelley *et al.*, 1981). Small branches also show anastomoses with each other (Grötz *et al.*, 1998). From a clinical perspective, the existence of the OPs within the dentine represents the appendages of the Od cells in the pulp, and this should be taken into consideration in treating dentine as a vital tissue. Destruction of dentine and its OPs may adversely impact on pulp integrity (Luukko *et al.*, 2011).

1.5 Dentinogenesis

In different mineralised tissues, biomineralisation is always a cellular responsible process in which cells direct the formation of mineralised tissue (Tjäderhane and

Haapasalo, 2012). Several simultaneous events are necessary to perform biomineralization of a collagenous matrix: i) cellular deposition of extracellular matrix including collagen type I and non-collagenous matrix molecules, ii) cellular translocation and accumulation of mineralising ions, iii) cellular organisation of the matrix contents to permit controlled mineralisation, iv) initiation of mineral crystallisation, v) regulation of the growth and accumulation of hydroxyapatite crystals, which could include further remodelling of the deposited matrix (Boskey, 2003). The rate of dentine deposition is dependent on several factors including the age and function of the tooth and the position of the depositing cells within the tooth. During primary dentinogenesis, the young Ods are actively secreting cells with a higher rate of dentine formation. In secondary dentinogenesis and after tooth eruption the Od cells decrease their dentine formation ability, but never lose their ability as long as they remain alive (Lovschall *et al.*, 2002; Murray *et al.*, 2002).

1.5.1 Extracellular matrix secretion

The extracellular dentine matrix is synthesised within Ods and excreted either directly from the main cell bodies or from OPs into the predentine region. This matrix is composed of 90% collagen and the remainder is non-collagenous proteins, including proteoglycans (Linde and Lundgren, 1995). This forms a region of about 10-40 µm of non-calcified predentine matrix, separating the apical border of the Ods from mineralisation front.

Collagen secretion

After collagen exocytosis from the Od cell bodies (Figure 1.1), an intra and inter-molecular cross-linking occurs before the start of matrix mineralisation. The collagenous matrix within predentine gradually matures from a poorly organised condition near the Od border, to a well organised, dense, covalent cross linked, insoluble network, with precisely located non-collagenous compounds at the distal part close to the mineralisation front (Linde and Goldberg, 1993; Linde and Lundgren, 1995). It has been suggested that the high intermolecular cross-linking of the collagenous network is important for mineralisation (Kuboki and Mechanic, 1982). However, the more accepted idea is that the collagen mesh acts only as a support for non-collagenous dentine molecules, which initiate and control crystal formation and growth (Linde and Goldberg, 1993; Boskey, 2003).

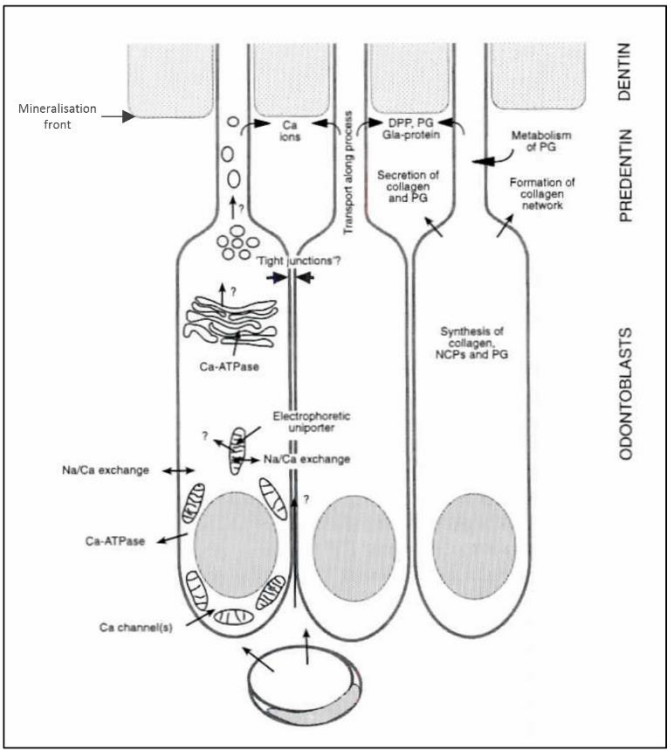

Figure 1.1: Schematic drawing of active secretory Ods showing Ca^{2+} ion transporter mechanisms (left part of the Fig) and dentine matrix macromolecule secretion (right part of the Fig).
Ca^{2+} ions are transferred via Od cell layer from pulp capillaries to the mineralisation front. A major way for the flow is transcellular, but the intercellular route can also be suggested. However, this can be restricted by the tight junctions between Ods. Ca^{2+} is transferred from pulp circulation into Od via Ca-channels and Na/Ca exchanger. To maintain cytosolic Ca^{2+} concentration, membrane ATP-dependant (Ca-ATPase) is used for extruding the excess of Ca^{2+}. Cellular organelles take part in buffering the activity of cytosolic Ca^{2+}. Mitochondria use electrophoretic uniporter for intrusion of and Na/Ca exchanger for extrusion of Ca^{2+}. Golgi and endoplasmic reticulum are also involved in regulation of Ca^{2+} concentration. Intavesicular Ca-ATPase is also used to accumulate Ca^{2+} within intracellular vesicles to obtain controlled transportation toward mineralisation front. The organic matrix of predentine is synthesised within Ods (right). Collagen and PGs are secreted from the apical border of the Ods to form predentine matrix. The collagen fibrinogenesis occurs within predentine region to obtained matured collagen fibrillar network near mineralisation front. A major portion of non-collagenous proteins including DPP, Gala-protein and other PGs are putatively secreted via OPs near mineralisation front. Fig reproduced from Linde and Lundgren (1995).

Non-collagenous matrix

Generally composed of non-collagenous proteins (NCPs) and proteoglycans (PGs), the NCP fraction comprises the highly phosphorylated phosphoproteins including mainly of dentine phosphoprotein (DPP), dentine sialoprotein (DSP), and dentine matrix protein-1 (DMP-1) (Goldberg and Smith, 2004). These have a high phosphate content, polyanionic type proteins composed of more than 80% of amino acids with negatively charged phosphate or carboxyl group (Linde and Lundgren, 1995). The PGs belong to a class of one or more glycosaminoglycane side chains attached to a

specific core protein. They also present with different compositions between predentine and dentine (Figure 1.1), and with different concentrations within different parts of the predentine implicating their significance in matrix maturation and the control of mineralisation (Goldberg and Takagi, 1993).

Both NCPs and PGs are widely accepted modulators of dentine biomineralisation due to their role in regulating matrix formation, modulating cellular activity, and controlling hydroxyapatite crystal growth and morphology (Goldberg and Takagi, 1993; Bègue-Kirn *et al.*, 1998).

Growth factors

As discussed in section 1.2, several growth factors are detected as inductive molecules for the differentiation of Ods during early developmental stages of the tooth germ. It is perhaps not unexpected to find traces of these molecules sequestered within dentine as fossilised by interaction with other dentine matrix components. These molecules are quantitatively minor in comparison to the other matrix components; however, they have the capacity to influence different processes that enhance tissue growth and repair (Smith *et al.*, 2012). When dentine is injured, these fossilised growth factors will be activated again and start their inductive function (Smith, 2003).

There are different growth factors which are described to be present within dentine and release during different dentinal injury processes. Among these are some which notably promote tissue regenerative process including transforming growth factor β1 (TGFβ1) and bone morphogenic protein-7 (BMP-7) (Sloan and Smith, 1999; Dobie *et al.*, 2002; Six *et al.*, 2002).

1.5.2 Mineralisation of extracellular matrix

When hydroxyapatite crystals form, there are several fundamental conditions controlling the type and rate of crystal development. Among these conditions are pH, concentrations of calcium and phosphate ions, the presence of mature collagen networks and cross linking non-collagenous proteins (Linde and Lundgren, 1995). Although there are many published studies about the concentration of mineral ions (Boyde and Reith, 1977; Wiesmann *et al.*, 1995), the effect of non-collagenous proteins on biomineralisation of dentine (Goldberg and Takagi, 1993; Goldberg and Smith, 2004), and the properties of collagen within mineralised tissue (Landis, 1996), there is little information on the role of pH in controlling the mineralisation process. A

study by Lundgren *et al.* (1992), used micro-electrodes to measure the pH in predentine, which was found to be 7. Another recent article also shows that Ods express special acid sensing ion channels which may play important roles in detecting a wide range of pH fluctuation during normal and pathological conditions (Solé-Magdalena *et al.*, 2011). However, none of the previous studies identify the role of the pH as a critical parameter in Od cellular homeostasis and its possible effect on mineral deposition and growth during different types of dentinogenesis.

In the predentine region, both calcium and phosphate ions are concentrated. This indicates the presence of translocating mechanisms to transfer these mineral ions through pulp cells to enrich predentine which nourish the biomineralisation process (Lundgren *et al.*, 1992; Wiesmann *et al.*, 1995). In addition, considerable amounts of carbonate and variable traces of other ions are found within mineralised dentine such as chloride, fluoride, sulphide, magnesium, strontium, zinc and lead (Linde and Goldberg, 1993).

In biomineralized tissue, the minerals are deposited within two distinct places in relation to type I collagen fibrils: the first is intrafibrillar (between collagen molecules within each fibril) and the second is extrafibrillar (attached externally on the collagen fibrils). In both cases, the mineral ions are either directly bound to the collagen molecules with the fibril or through a link provided by NCPs (Landis, 1996). The high mineral content significantly increases the mechanical properties of the collagen fibrils (Linde and Goldberg, 1993).

The nucleation of hydroxyapatite crystal requires a specific site which can be induced by electric or other properties that initiate the formation of solid calcium phosphate from a solution. Additionally, the growth of such crystals is reported to be dependent on crystal-protein interactions (Gajjeraman *et al.*, 2007). Most of the matrix NCPs should be modulated by specific enzymes to obtain their anionic characters. Therefore, the activities of these enzymes plus the nature of such modulation, may determine mineralised tissue specificity by modulating the position and size of the growing crystals (Boskey, 2003).

It has been reported that the circumpulpal dentine is the only mesodermal hard tissue in which the matrix vesicles are not involved in its mineralisation (Takano *et al.*, 2000). This mineralisation may be performed by heterogenous nucleation instead of matrix vesicle formation (Tjäderhane and Haapasalo, 2012). This depends

exclusively on the localisation of DPP within the apical part of the predentine region in order to induce appositional calcification at the mineralisation front (Lundgren and Linde, 1992).

Mineralisation front

This is a transitional zone, of 0.5-2µm thickness, occurring between the predentine and dentine where the collagen fibres are mineralised. This includes the total mineralisation of the inter-collagenous spaces within the predentine matrix (Goldberg and Septier, 1996). The shape of such a mineralisation interface is different according to the rate of the dentine deposition and mineralisation. It appears as a globular shape with mineralised protrusions, called calcospherites, which are thought to represent heterogenous deposition of crystals in the case of rapid dentinogenesis. This could occur during mantle and circumpulpal dentine deposition periods. Nevertheless, with slower dentine formation (secondary dentinogenesis), the mineralisation front looks more linear in shape (Nanci, 2012).

Transport of ions

During this process the mineral ions must be translocated from the pulp vascular circulation through the Od cell layer to pass the tight junctional complexes separating the pulp tissue from the predentine region. These ions should then be excreted through OPs into predentine matrix at the mineralisation front. Since Ods play a central role within this process, the main goal of the calcium transportation system is to maintain the cytosolic Ca^{2+} concentration at a low and steady level. Therefore, most of the intracellular Ca^{2+} must be complexed or stored within the intracellular organelles (Linde and Lundgren, 1995). The left part of Figure 1.1, represents what is known in the literature about the Ca^{2+} transportation process within Ods to perform dentine mineralisation (Linde and Lundgren, 1995; Tjäderhane and Haapasalo, 2012).

During calcification of the extracellular matrix of predentine, a large influx of Ca^{2+} and inorganic phosphate (P_i) ions is required to form hydroxyapatite induction and growth. Hence, predentine has 3 times more Ca^{2+} than the pulp, revealing the highly active Ca^{2+} transportation mechanism of the Ods (Lundgren *et al.*, 1992). Calcium was also reported to be accumulated in the apical cell body of the Od as well as OPs, and deposits of calcium have been shown within organelles at these sites (Boyde and Reith, 1977; Granström, 1984). The influx of Ca^{2+} into the Ods was also reported to

be controlled through L-type voltage gated Ca^{2+} channels, as their blocking *in vivo* caused severe impairment of radio-labelled Ca^{2+} uptake within dentine minerals. Additionally, these channels seem to be highly selective, with no mimicking by similar ions such as lanthanum (Lundgren and Linde, 1997).

There are several cellular homeostatic mechanisms to maintain intracellular calcium concentration (about few µM) in comparison to the extracellular level (about 3 mM and less than half of which is in ionised form) (Carafoli, 1987). Cellular extrusion of the excess Ca^{2+} can occur through an ATP-dependant process and Na^{+}/Ca^{2+} exchanger (NCX). Cell membrane Ca-ATPase (PMCA) is identified within the dentinogenically active Ods (Granström *et al.*, 1979), and also located in the vesicle membrane at the distal region of Od cell body (Granström *et al.*, 1978). The intra-vesicular accumulation of Ca^{2+} is demonstrated to be ATP-dependant using Ca-ATPase (Granström, 1984). Ca^{2+} extrusion mechanism in osteoblast and salivary gland is most likely to occur via NCX at the mineralisation face (Stains and Gay, 1998; Homann *et al.*, 2006). Both NCX-1 and NCX-3 are expressed by the distal membrane of the Od and believed to play a pivotal role in directing Ca^{+} transportation and extrusion. Ca^{2+} efflux is proven to be dependent on the extracellular Na^{+} concentration within culture media (Lundquist *et al.*, 2000). However, in living tissue the concentration of the intracellular Na^{+} is controlled by membrane ATP pumping mechanism through NaK-ATPase. This ATP-dependent transporter maintains the membrane gradient to Na^{+} which is necessary for the function of Na^{+}/Ca^{2+} antiporter (Therien and Blostein, 2000). However, this complementary role of the cellular homeostatic ion transported within Ods is not yet understood.

Although several researchers have demonstrated the Ca^{2+} transportation mechanism within Od cells, little interest has focused on the inorganic phosphate transport system. The presence of sodium phosphate cotransporter (Na/P_i) within differentiated cultured odontoblast-like cells indicates that this could be the mechanism for the Ods to provide P_i for dentine mineralisation (Lundquist *et al.*, 2002). This also emphasises the role of the NaK-ATPase as a complementary ion transporter.

The flux of Ca^{2+} within Od and between cellular compartments requires a buffering protein to regulate Ca^{2+} interactions with cytoskeletal proteins and membrane components. Several Ca^{2+}-binding proteins are expressed by dentinogenically active Ods such as calmodulin, parvalbumin, and calbindin (Celio *et al.*, 1984; Goldberg *et*

al., 1987; Berdal *et al.*, 1996). The latter is a high affinity, intracellular soluble protein, present in various Ca^{2+} transporting systems within different tissues such as salivary gland (Onishi *et al.*, 1999), enamel organ, and bone (Berdal *et al.*, 1996) in addition to odontoblasts (Onishi *et al.*, 1999). The role of the cellular organelles is also important in cytosolic buffering of Ca^{2+} activity, in addition to transmembraneous transport systems (Tjäderhane and Haapasalo, 2012). Inside Ods, Ca^{2+} can be taken up by mitochondria through electrophoretic uniporter and extruded through NCX (Lundgren and Linde, 1988). The ATP-dependant calcium intrusion seems to be located within Golgi and endoplasmic reticulum [sarco/endoplasmic reticulum Ca-ATP (SERCA)] and the cytoplasmic vesicles derived from them (Granström, 1984; Lundgren and Linde, 1987). These organelles act as intracellular store sites for calcium either to be secreted intracellularly as a secondary messenger to activate different cellular function (Shibukawa and Suzuki, 2003),or to be excreted extracellularly from the apical region of Ods at the mineralisation front (Granström, 1984).

1.6 Secondary dentinogenesis

This is the process of dentine deposition after eruption of the tooth crown to reach its functional contact. At this time, the crown has fully formed by enamel and dentine deposition, while the root is still developing. As described in section 1.3, Ods show morphological and structural changes after accomplishment of primary dentinogenesis. These cells are called transitional Ods (Couve, 1986), which become shorter and less polarised with nuclei displaced from the basal part of the cell. These Ods have less cellular organelles compared to the secretory cells with smaller rough endoplasmic reticulum and Golgi apparatus, but these cytoplasmic organelles are still supra-nuclear in location (Ohshima and Yoshida, 1992). After this period the Ods change to aged cells which appear shorter and more crowded. The nucleus moves more apically, creating a prominent infra-nuclear region where most of the cellular organelles are moved. The supra-nuclear region of the cells appears devoid of organelles except large vacuoles, some mitochondria, and cytoplasm filled with intermediate filament and microtubules (Couve, 1986).

After complete primary dentine formation, with a secretion rate of approximately 4 µm per day, the bulk of the tooth formation is already accomplished (Kawasaki *et al.*, 1979). However, the formation of secondary dentine is continuous, but at a much

slower rate of approximately 0.5 µm per day and decreasing throughout life (image A Figure 1.2) (Murray *et al.*, 2002). Secondary dentine is structurally similar to primary dentine and composed of intertubular and peritubular dentine. Slight differences in the curvature and regularity of dentinal tubules has been detected (Addy, 2002). The continuity in dentinal matrix secretion in predentine results in increased thickness of primary and/or physiologically deposited secondary dentine, i.e. decrease in pulp chamber volume (Smith *et al.*, 1995). This process is radiographically detectable especially on the floor and roof of the pulp chamber and results in limiting the space of the pulp chamber and canals in elderly patients (Luukko *et al.*, 2011). Other sign of the ageing process in teeth is the formation of excess cementosis at the apical region of the tooth. This process is mainly associated with cusp attrition to compensate for the length reduction of the physiological crown (Morse, 1991).

Age-related reduction in the available space of pulp chamber is eventually associated with elimination of a certain number of different pulp cellular populations by apoptosis. The continuous deposition of dentine progressively decreases both the volume occupied by pulp fibroblasts and the dentine/Od interface (Mitsiadis *et al.*, 2008). This possibly promotes reduction in the cellular densities of Ods, SOds, and pulp fibroblasts (Murray *et al.*, 2002). This age-dependant reduction in the cellular population possibly causes a decrease in the regenerative capacity (plasticity) of the pulp. This could be due to reduction in the number of Od as dentine forming cells in addition to restriction in the number of other pulp cells which could differentiate into Od-like cells following dentine/pulp injury. Furthermore, it has been reported that the nerve growth factor and its p75 receptors possibly has a role in inducing cellular apoptosis of the pulp cells during age progression (Mitsiadis *et al.*, 2008).

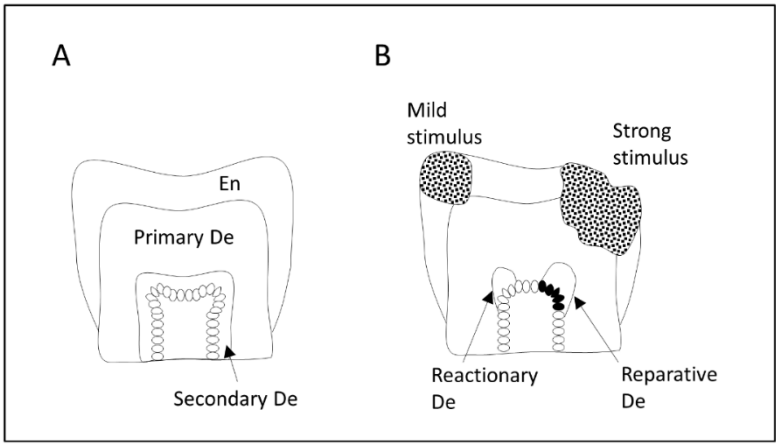

Figure 1.2: Schematic illustration of dentine types.
A shows primary dentine and secondary dentine. B shows tertiary dentine with two types reactionary and reparative. With mild stimulus, the original Od remains alive and formed reactionary De. When strong stimulation affects the dentine, this may lead to necrosis of the Od and recruitment of Od-like cells (black) and these cells forming reparative De.

1.7 Dentinal tubules

The tubular nature of dentine is the central characteristic which distinguishes it from other hard tissues of the body. This tubular pattern dramatically affects its mechanical properties, ability to withstand occlusal loads and the pulp responses to dentine injury (Tjäderhane *et al.*, 2012).

In three-dimensional study, the dentinal tubules show a wide range of tubular tilting angles beneath the DEJ and these tubules seem to twist or curl up to 90º. This disagrees with the popular idea that the dentinal tubules extend at right angles from DEJ and flow in s-shape coarse through the dentine and revealed a more complex pattern of the dentinal tubules (Zaslansky *et al.*, 2010). In terms of density, tubules are almost twice as densely packed near the pulp than at the DEJ due to packing of odontoblast as the pulp space and its circumference diminishes. Additionally, dentinal tubules appear denser under the cusp area in comparison to the other regions of the tooth (Mjör and Nordahl, 1996) and this could influence the pulp-dentine defensive system against wear (Tjäderhane *et al.*, 2012).

Dentinal tubules are not simple tube-like structures, but a complex tubular network with many branches and ramifications. These branches are most plentiful in regions of lower main tubule density, forming an abundant anastomosing system of canaliculi (Kagayama *et al.*, 1999). This allows the dentine to have a high degree of permeability and facilitates fluid movement (Pashley, 1985). There are three recognised types for dental tubule branches depending on their size, location and

anastomosing angle with the primary tubule. The major branches with a diameter similar to the main tubules (about 0.5-1µm), forked at an acute angle, and located more peripherally within dentine. Fine branches usually emerge at 45˚ angle from the primary tubule, ranging from 0.3-0.7 µm in diameter and usually limited to root dentine or crown dentine with low tubular density. Finally, microtubules are scattered throughout dentine with a very small diameter of 0.1 µm, emerging at right angles from the primary tubule (Mjör and Nordahl, 1996).

Dentinal tubules are surrounded by a collar of highly mineralised dentine called peritubular dentine. This type of dentine measures about 1µm in thickness, is more highly mineralised than intertubular dentine (about 40% more), with little or no collagen but rich in phosphoproteins (Gotliv and Veis, 2008). The thickness of this type of dentine varies greatly depending on the distance from the pulp, being very thin or completely absent near the pulp and with greatest thickness near the DEJ. The formation and mineralisation of this type of dentine may result from the mineral adsorption of the non-collagenous proteins on the peripheries of the dentinal tubules. The deposition of this type of dentine leads to a continuous decrease in the tubule lumen (Bertassoni *et al.*, 2012). Peritubular dentine has a porous nature, and the boundaries of dentinal tubules are fenestrated by numerous tiny pores which, together with the branches of the dentinal tubules, facilitate the movement of fluids and other matrix components across the peritubular dentine in all directions (Pashley, 1985; Mjör and Nordahl, 1996). Furthermore, peritubular dentine has an organic component called calcium-phospholipid-proteolipids (Gotliv and Veis, 2007). Similar proteins have been shown to have vital roles in brain neurological actions (Turner *et al.*, 2005). Thus, peritubular dentine may have a potential role in active transport of ions and signalling between the odontoblast and the intertubular dentine or regulating the actions that help in maintaining the dentine as a live and vital tissue (Gotliv and Veis, 2007).

The main bulk of dentine is composed of intertubular dentine, which fills the spaces between the rings of peritubular dentine. About half of its composition is organic, mainly made up of collagen fibres that run circumferentially around each tubule. Because of this organic matrix, intertubular dentine is usually preserved after pathological or laboratory decalcification (Beniash *et al.*, 2000). The intertubular dentine is less mineralised and different from peritubular dentine both structurally and

mechanically however, they both have similar crystal alignment and size (Weiner *et al.*, 1999).

1.8 Dentine sclerosis

This is a phenomenon of increasing thickness of peritubular dentine due to continuous mineral deposition on the inner wall of the dentinal tubules, leading to decrease diameter or complete obliteration of the dentinal tubules. There are two types of dentine sclerosis depending on the cause of its formation which could be either physiological or reactive (pathological) (Stanley *et al.*, 1983; Tjäderhane *et al.*, 2012). Physiological sclerosis is recognised as one of the pulp-dentine complex reactions to age and environmental irritation (Linde and Goldberg, 1993). It is more prominent in older teeth especially in the peripheral dentine and decreases towards the pulp (Stanley *et al.*, 1983). The sclerotic tubules appear to be totally occluded (Mendis and Darling, 1979b) and this possibly reduces the permeability of dentine, pulp irritation, and tertiary dentine formation (Tjäderhane *et al.*, 2012). This form of sclerosis can be recognized in areas without carious irritation such as the floor of the pulp chamber and root canals (Mendis and Darling, 1979a). Within intact dentine surfaces, this sclerosis can be present in some dentinal tubules while the rest remain normal. The mechanism or the trigger for such sclerosis is still not understood (Tjäderhane *et al.*, 2012).

Alternatively the reactive dentine sclerosis is considered the main dentine response under carious lesions and restorations. It appears as a translucent zone due to its higher mineralization content (Frank, 1990; Pugach *et al.*, 2009) and seems to represent a physiochemical precipitation of hydroxyapatite rather than a vital process (Smith *et al.*, 1995). Reactive sclerosis occurs either deep or superficial within the dentine (Tjäderhane *et al.*, 2012). The deep sclerosis is totally dependent on the odontoblast processes. However, in areas under the carious lesion where the dentinal tubules are devoid of cellular content, the presence of reactive sclerosis suggests it is a non-vital defensive process. The calcium phosphate that was extracted from the hydroxyl-apatite crystals within the carious lesion usually dissolves and is redeposited more deeply to the adjacent dentinal tubules (Daculsi *et al.*, 1987; Frank, 1990). It has been proposed that the calcium required for deep sclerosis is usually taken from the pulp through the odontoblast process, while in superficial sclerosis the source of calcium is mainly from the carious lesion and saliva

(Tjäderhane *et al.*, 2012). In the same way, reactionary sclerosis was also reported in dentine hypersensitivity which could be associated with attrition or abrasion (Addy, 2002). In radicular dentine, the exposure of dentinal tubules hypersensitise the pulp to occlude the dentinal tubules with intratubular crystals, resulting in reduced fluid exchange and dentine hypersensitivity (Yoshiyama *et al.*, 1989; Yoshiyama *et al.*, 1990).

1.9 Tooth innervation

The histological examination of nerve fibres entering the tooth reveals both myelinated and unmyelinated types. The majority of these nerves are nociceptive sensory fibres, myelinated A-delta and unmyelinated C fibres. The cell bodies of these fibres are mainly located in the Gasserian (semilunar) trigeminal ganglion. The unmyelinated fibres have also shown some minor quantities of both sympathetic and parasympathetic axons (Byers, 1984; Abd-Elmeguid and Yu, 2009). Almost all nerve fibres enter the tooth in bundles through one or more apical foramina. These bundles pass through the radicular pulp in association with blood vessels as neuro-vascular bundles. Very few nerve fibres appear to be terminated within the root and these fibres may reach the radicular Od layer. However, the rest of the nerve fibres terminate within the tooth crown (Byers and Matthews, 1981).

In the crown pulp, nerve bundles diverge and run toward the pulp-dentine border. The diverged nerves usually run in a relatively straight route until forming the subodontoblast nerve plexus of Raschkow. The exact function of this nerve plexus is still unknown. Within this plexus, the nerve fibres loop and form a complex network. The density of this nerve plexus is varied according to the tooth region. It is more dense in the cusp and lateral walls of the crown, then decreases in density gradually toward the cervical region of the tooth until disappearing within the coronal portion of the root (Johnsen, 1985). From the plexus, plenty and small nerve fibres are derived and run through the Ods into predentine and dentine with terminals showing bead-like structures. Within dentinal tubules about 30-70% of the OPs are accompanied by nerve fibres and this percentage seems to be higher under the cusp and decreased gradually toward the cervical tooth region (Carda and Peydro, 2006).

During tooth development in rat molar samples, very few nerve fibres appear within the basal region of the tooth germ during the advanced bell stage. After crown formation, beaded nerve fibres are present in the pulp core in association with blood

vessels, and the formation of a subodontoblast nerve plexus also commences within the cusp. After tooth eruption and during root development peroid, the density of nerve fibres within coronal Ods and dentine increases gradually, and the subodontoblast nerve plexus extend up to the cervical region (Fristad *et al.*, 1994). Neuronal development continues and axonal density gradually increases until the end of tooth maturation, which represents the time of complete root formation and development of a mature apical foramen (Byers, 1984).

Histochemical nerve markers have identified: i) sympathetic unmyelinated axons containing vasoactive intestinal peptide, ii) cholinergic, sensory or parasympathetic axons, iii) small sensory axons reactive to substance P and calcitonin gene related peptides (CGRP) (Luthman *et al.*, 1992). Both sympathetic and parasympathetic axons are primarily associated with the pulp vascular system (Luthman *et al.*, 1992; Fristad *et al.*, 1994). The CGRP-IR fibres are mainly sensory and run in association with the neuro-vascular bundles within pulp core and then ramify within the subodontoblast plexus, Ods and dentine. These axons appear with varicosities, represented by many vesicles along their courses containing neuropeptides. These neuropeptides have an important effect on circulatory regulation, inflammatory and allergic reactions and on wound healing (Taylor and Byers, 1990).

Due to their role in neurogenic inflammation, the effect of cavity preparation on CGRP nerves has been widely investigated, including different cavity sizes: dentine micro-abrasion (Taylor *et al.*, 1988), moderate cavity (Taylor and Byers, 1990), deep cavity with pulp exposure (Kimberly and Byers, 1988), and pulpotomy (Zhang and Fukuyama, 1999). In all cases, nerve sprouting was identified within pulp cells during period of inflammatory, with increasing nerve density, followed by a return to normal innervation patterns when inflammatory signs subside. This possibly indicates the role of CGRP in inflammation and wound healing.

1.10 Odontoblasts, and nociception

If the Ods are located at a strategic spatial relationship with the dentinal tubules to play a pivotal role in the defensive mechanism against injury, they are also the first to be targeted by external stimulation such as thermal variation and mechanical forces (Bleicher, 2014). Ods carry different structural and morphological properties which promote their sensing role within Od-dentine complex. The presence of OPs and their spatial relationship within dentinal tubules and intradentinal fluid is the most

important factor. The complexity of these processes with different terminal and lateral branches could facilitate the communication between these processes and with the external environment (Sigal *et al.*, 1985). In addition, the presence of primary cilia has been described in ultrastructural studies from the basal sides of Ods. This could promote the structural ability of the Ods in sensing pulp microcirculation (Thivichon-Prince *et al.*, 2009).

Although there is a dense network of sensory fibres in the pulp and unmyelinated afferent fibres engaging the Od layer (Corpron and Avery, 1973; Dahl and Mjör, 1973), no evidence for synaptic structures or gap junctions has been detected between the Od and these nerve fibres (Ibuki *et al.*, 1996). However, the expression of specific neural proteins (semaphoring and reelin) has been reported as a large mass of extracellular glycoprotein between the Ods and nerve fibres, which could promote intimate adhesion between them (Maurin *et al.*, 2004; Magloire *et al.*, 2009).

Odontoblasts also appear to express several classes of ion transporter which could be involved in nociception and signal propagation. These cells have been reported to express all nine voltage gated Na^+ channels in specific patterns and in different locations depending on tooth maturation stage. Channels such as $Na_v1.4$, and Na_v 1.7 are more expressed by immature Ods, while others are increased in mature Ods such as Na_v 1.3, Na_v 1.5, Na_v 1.6, and Na_v 1.8 (Byers and Westenbroek, 2011). The presence of Na^+ channels indicates that the Od is an excitable cell which can produce all or no spike (action potential) in response to depolarising current. This demonstrate that these cells are able to transduce and integrate somatosensory signals which could elicit nociceptive responses similar to nerve fibre (Allard *et al.*, 2006).

Additionally, the odontoblasts are identified to express several members of the transient receptor potential (TRP) superfamily. These ion channels play an important role in sensory physiology as transducers for thermal, mechanical and chemical stimuli. Different thermal sensing channels including heat-sensing TRPV1, TRPV2, and TRPV3 and cold-sensing TRPM8 and TRPA1 are all reported to be expressed by Ods (Son *et al.*, 2009; El Karim *et al.*, 2011). Other mechanosensitive receptors such as TRPV4, TRPM3, TRPP1 and TRPP2 also reported to be present within Ods (Son *et al.*, 2009; Thivichon-Prince *et al.*, 2009). These TRPP1 and TRPP2 are

shown to act in combination with the primary cilia of the Ods (Thivichon-Prince *et al.*, 2009).

As described in 1.5.2, the presence of acid sensing ion channels which belong to the degenerin/epithelial Na^+ channel superfamily are also identified within human Ods. These proteins express mechano-sensory functions in addition to their possible role in sensing a wide range of pH fluctuation during normal physiological and pathological conditions (Solé-Magdalena *et al.*, 2011).

Different types of K^+ channels are expressed by Ods. High conductance of Ca-activated K^+ channel (K^+_{Ca}) is observed within cultured human Ods. The membrane stretching of cultured Ods activates these channels, which suggests their mechano-transductive role turning mechanical stimuli into electrical signals (Allard *et al.*, 2000). The mechanosensitive TREK-1 potassium channels have also been detected within Od cell membranes (Magloire *et al.*, 2003). In mammals, these channels are activated in resting potential and gated during different chemical and physical stimuli such as cellular stretching, intracellular acidosis and heat (Patel and Honoré, 2001). These channels are expressed by coronal Ods and are absent in the root, which could speculate their spatial relationship to the afferent sensory nerve fibres (Magloire *et al.*, 2003). This could further propose that stretch activation of the Od could stimulate these channels to transduce signals to the afferent nerve ending (Magloire *et al.*, 2009).

Therefore, the Ods are not only involved in formation of dentine, but also in the maintenance of this tissue to provide protection and preserve vitality of the pulp tissue. Better knowledge in Od homeostasis and physiology may possibly help in developing new hypotheses and therapies for the management of dental pain and tooth sensitivity (Bleicher, 2014).

1.11 Tertiary dentinogenesis

This is the process of forming of tertiary dentine at specific loci of the pulp-dentine interface by Od or Od-like cells as a result of pulp irritation. If the primary Ods survive after such irritation, the formed dentine is called reactionary dentine. If these cells die due to extensive irritation, the newly differentiated pulp (Od-like) cells will form reparative dentine (panel B, Figure 1.2) (Smith *et al.*, 1995). Another type of tertiary dentine is called pulp stone or fibrodentine. This form is merely defensive, non-

specific production of mineralised tissue formed in regions of the pulp chamber or root canals which may cause difficulties or failure of root canal treatment (Tziafas, 2010).

The presence of chronological information is essential to identify whether the secreted tertiary dentine is regarded as reactionary of reparative. This is possibly important in the determination of the secretory cells which could be the guide for such dentine (Lesot *et al.*, 1993). In clinical conditions of tertiary dentine, where different stimulations could be involved within the causes, it becomes more difficult to distinguish between reactionary and reparative dentine within the same foci. However, due to the episodic nature of the dental caries, it is more likely to consider that both reactionary and reparative could be superimposed upon one another beneath such lesions (Smith *et al.*, 1995).

1.11.1 Reactionary tertiary dentinogenesis

Reactionary dentine formation is caused by mild irritation of the tooth (slow progressive caries, shallow cavity, wear), which stimulates primary Ods to increase secretion rate of dentine in comparison to secondary dentinogenesis. This results in increasing dentine thickness to protect the pulp. In most of the literature, the formed reactionary dentine is indistinguishable from the already present secondary dentine with more or less tubular continuity (Tjäderhane *et al.*, 2012; Tjäderhane and Haapasalo, 2012; Bleicher, 2014). Only one review article mentioned that, after stimulation of primary Ods, these cells will form irregular secondary dentine (reactionary dentine) (Tziafas, 1995). However, no experimental evidence or references are presented within this paper to support this idea.

The matrix of tertiary dentine was reported to have differences in its extracellular macromolecules which are involved in dentinogenesis (Smith *et al.*, 1995). A study by Moses *et al.* (2006), identified different small integrin-binding ligand, N-linked glycoproteins (SIBLING) in different aged rat molars (12, 18, 24, and 36w) within the tertiary dentine region caused by cusp attrition. They found that dentine matrix protein, and dentine sialoprotein show marked age-dependent decreases within tertiary dentine matrix in comparison to primary dentine matrix. Whilst the expression of the bone sialoprotein and osteopontin was absent in primary dentine, it was observed clearly in the tertiary dentine of 36 week old animals. This suggested that there were two different mechanisms of dentine formation within the tertiary dentine

region. In younger ages the tertiary dentine matrix was similar to primary matrix, because they were possibly formed by the primary Ods which formed reactionary dentine. With age and wear process progression, this possibly caused depletion of primary Ods which may be replaced by Od-like cells which commenced the formation of reparative dentine with a more bone-like matrix. Similar observations were also made in a rat incisor study which confirmed that Od-like cells resemble osteoblast in the formation of osteopontin within reparative dentine matrix (Cajazeira Aguiar and Arana-Chavez, 2007).

Reactionary dentine formation was targeted by numerous studies; however, the controlling mechanisms for the onset and intensity of reactionary dentine formation are still uncertain (Smith *et al.*, 1995). Most of these experiments used a controlled model of cavity preparation which presents a situation different from clinical reality (Turner *et al.*, 1989; Chiego Jr, 1992; Turner, 1992). There are several factors which could affect the formation of reactionary dentine, such as: sample species (whether human or animal), trauma model used (cavity, wear, caries), extension and dimensions of the dentine injury, duration of the trauma, type of restorative material, and time interval for laboratory measurements (Tjäderhane and Haapasalo, 2012). A confounding factor lacking in many laboratory studies is the presence of microbial biofilm.

Several immediate cellular changes have been detected within the remaining Ods and other pulp cells in response to mild cavity preparation (Turner *et al.*, 1989; Chiego Jr, 1992; Turner, 1992). These initial responses include breaking down of the junctional complexes between the injured Ods associated with changes of the intracellular organelles such as swelling mitochondria and dilated rough endoplasmic reticulum (Chiego Jr, 1992). In addition, there is dilation of pulp capillaries and invasion of the pulp by macrophages and dendritic cells (Ohshima, 1990). This is associated with the infiltration of macromolecular reparative compounds from the pulp toward the exposed dentinal tubules. One of these reported macromolecules is fibrinogen which could induce a fibrin clotting cascade to primarily occlude the exposed dentinal tubules (Chiego Jr, 1992). Nevertheless, the mediator for such cellular responses still unclear. Differences in the growth factors released from the injured pulp cells may mediate these responses (Byers *et al.*, 1992). Neuronal stimulation could also release CGRP neuropeptides which could also act as

mediators to promote the onset of neurogenic-inflammation within the injured region (Taylor *et al.*, 1988).

After the initial pulp inflammatory responses subside, which could take several days, the Od layer re-establishes. The apical junctional complexes between the Ods and the cytoplasmic organelles within these cells return their normal appearance (Chiego Jr, 1992). NGF and NGFR restored their normal expression (Byers *et al.*, 1992), and pulp innervation is also reported to be reversibly recovered (Taylor *et al.*, 1988).

Due to the variability between different experimental models, none of the previous studies take all these factors into consideration and examine them in one controlled experiment to identify their possible interactions. Furthermore, there is no previous link between the hard and soft tissue responses during the process of reactionary dentinogenesis.

1.11.2 Reparative tertiary dentinogenesis

With greater or more sustained dental injury, Ods may die. The fate of the primary Ods is not completely understood, but it is believed that these damaged cells degenerate or go through apoptosis to be phagocytosed by macrophages (Ohshima, 1990; Mitsiadis *et al.*, 2008). Other pulp cells which normally occupy the SOd region and pulp core that have no direct role in primary dentine secretion, may provide newly differentiated Od-like cells to compensate for the death of the original Ods. The progenitor cells of the Od-like cells were reported to be present within the SOd cell layer that can be directly stimulated after the death of the original Ods (Kitamura *et al.*, 2001). On the other hand, fibroblasts, perivascular cells, or undifferentiated cells of the central part of the pulp were also reported to have the ability to differentiate into Od-like cells (Shi and Gronthos, 2003; Téclès *et al.*, 2005). *In vitro* these cells can be differentiated into Od-like cells secreting mineralised matrix similar to dentine (About *et al.*, 2000). It remains an open question whether the Od-like cells originate from undifferentiated ectomesenchymal cells of the pulp, from other cells that represent the mature pulp population, or may be both of these cell types (Tziafas, 1995). The dedifferentiation and transdifferentiation of mature pulp cells would mean re-assessing the regeneration in the repair process. The possibility of the presence of all these derivatives from progenitor cells makes the term ‘Od-like cell’ inappropriate to describe any pulp cells capable of mineralised matrix deposition as a result of injury (Goldberg and Smith, 2004). The primary Od could be defined by its

morphology, the matrix it secretes and specific gene expression (Smith and Lesot, 2001). In comparison to Od-like cells, very few cells could fulfil all these requirements. Therefore, it must be recognized that these cells are capable of repair rather than regenerative processes (Goldberg and Smith, 2004; Simon and Goldberg, 2014).

The cellular responses to severe trauma associated with the reparative dentine are said to be much more extensive inflammatory process which may contain signs of pus with more inflammatory cells infiltrating the injured region (Bleicher, 2014). Od-like cells could be observed lining the dentinal bridge that formed after the resolution of inflammatory signs. These new cells were reported to ultrastructurally resemble the primary Od with large nuclei, high numbers of mitochondria and increased rough endoplasmic reticulum (Chiego Jr, 1992).

There is a controversy about the morphology of reparative dentine between completely dystrophic atubular matrix (Ricucci *et al.*, 2014), and tissue that started as atubular before changing to a tubular structure with complete differentiation of the Od-like cells into spindle-shape with the clamming appearance of cytoplasmic process (Tziafas, 1995; Magloire *et al.*, 1996). However, most consider it to be completely atubular form (Tjäderhane *et al.*, 2012; Ricucci *et al.*, 2014).

The goal of the tertiary dentine deposition, in addition to increasing dentine thickness, is to decrease dentine permeability beneath an injury, and thus to isolate the irritated pulp area from further stimulation (Ricucci *et al.*, 2014). The atubular characteristic and the differences in matrix composition make reparative dentine able to act as a protective barrier against trauma caused by dentinal tubule exposure (Tjäderhane *et al.*, 2012). It can also be argued that this impermeable barrier may decrease pulp sensitivity to the external stimulation. In addition, the presence of sensory nerve fibres extending in the pulpal third of the dentine (Byers, 1985), is reported to be lost in cases of reparative dentine (Taylor *et al.*, 1988; Tjäderhane *et al.*, 2012). All these suggest that the impermeable junction between the tubular dentine (primary and/or secondary) and reparative dentine may produce a barrier against further stimulation and this may decrease tooth responses to vitality test (Tjäderhane *et al.*, 2012). If a second injury occurs such as a carious lesion, the presence of reparative dentine possibly decreases the pulp’s response and the defence reaction after repeated insults (Johnson, 2004).

1.11.3 Pulp stones

Pulp stones are dystrophic calcified depositions that can be classified depending on structure and location (Nanci, 2012). Structurally, they can be divided according to their morphological distinction into true and false pulp stones. The structure of true pulp stone is merely dentine and could be lined by Ods or Od-like cells. Whereas false pulp stones are composed of atubular dentine and possibly fromed by degenerating cells of the pulp that can form mineralised material (Goga *et al.*, 2008). However, the differentiation between true and false appears to be artificial, because both tubular and atubular dentine is most frequently present within single pulp stone (Tjäderhane *et al.*, 2012). Depending on location, pulp stones can be divided into embedded, adherent, and free. The embedded type is believed to be formed with the ongoing physiological dentinogenesis so that the pulp stone becomes enclosed within dentine wall. This type is more frequently seen in the apical portion of the tooth. The adherent type is less attached to dentine wall, whereas free pulp stones are the most common type and found entirely within pulp tissue. The latter type is most commonly observed within the pulp chamber, and sometimes more than one stone or different types can be present within the same tooth (Goga *et al.*, 2008).

The formation of pulp stones is still incompletely understood. It is believed that external irritation such as caries or attrition enhance pulp stone formation. However, there are some present with no apparent cause (e.g. impacted 3rd molars) (Goga *et al.*, 2008). In addition, pulp stones have also noticed in relation with genetic conditions such as dentine dysplasia (Parekh *et al.*, 2006).

The organic matrix component of human pulp stone has been investigated. Type I collagen is the major component of free pulp stones. The non-collagenous matrix component is mainly osteopontin, which is similar to the matrix component of reparative dentine (Cajazeira Aguiar and Arana-Chavez, 2007). Osteopontin is also found within dental calculi (Kido *et al.*, 1995), and urinary stones (Kohri *et al.*, 1993), and is absent in primary and reactionary dentine (Moses *et al.*, 2006).

1.12 Animal models for the study of dentine/pulp

The host response to an injurious agent sustains a high degree of complexity which makes it impossible to be *in vitro*. The associated inflammatory and reparative processes are multifactorial, and in order to study these processes from all perspectives, a suitable experimental model is required. However, it is important to

address the fact that there is no universal animal model that is ideal for all research needs. Therefore, clinicians and researchers must be aware of the relative strengths and weaknesses of the diversity of the available animal models.

Nevertheless, animal models assist science and scientists to obtain new knowledge and better understanding of various physiological and pathological conditions.

Rodents models comprise the majority of animal studies in pulp biology, mainly due to the well-defined physiological parameters. They are easy to handle and house for long periods, are relatively low cost which enhances the possibility of large sample sizes, adaptable to the lab environment, have low social and ethical concerns compared to primates makes them a good choice (Saghiri *et al.*, 2015). In addition, most commercially available antibodies for cellular and molecular techniques are available for rats. In dentistry and despite the differences, rats presented a suitable model to study various fields.

Two different developmental models can be obtained from rat teeth. The continuous growing model is represented by incisors and limited growth (human-like) model by molars. Continuous growth makes the rat incisor a valuable model to investigate tissue structure and function within a single organ that may represent the whole life cycle of cellular activity from formation to maturation and repair after injury (Harada *et al.*, 1999; Harada *et al.*, 2002; Harada and Ohshima, 2004; Cajazeira Aguiar and Arana-Chavez, 2007). In addition, rat incisors provide the researcher with appreciable amounts of pulp tissue suitable for tissue cultures (Sloan *et al.*, 1998), and enough to provide a sufficient quantity of RNA even from a single pulp tissue (McLachlan *et al.*, 2003).

Rat molars are considered as a valuable tooth model and with greater similarity to human teeth in their mode of development. This model has been widely used in dental *in vivo* and *in vitro* studies (Sloan *et al.*, 1998; Woodnutt *et al.*, 2000). It is also widely used during cavity preparation experiments trying to simulate human dental preparation (Taylor and Byers, 1990; Murray *et al.*, 2008). However, care should be taken to consider species differences and interpreting the translation of tissue responses to the human situation. Working difficulties in controlling the experimental procedures are important considerations to be taken (Goldberg and Smith, 2004), in addition to ethical requirements. Other studies used the physiological occlusal attrition of rodents as a model of dental trauma (Kuratate *et al.*, 2008). The use of

such model is definitely overcome all experimental variables which could present during cavity preparation procedure in cavity-models (About *et al.*, 2001; Goldberg and Smith, 2004). The progress of tooth wear with time also allows the responses to different stages of injury to be investigated.

1.13 Aims of this study

- To develop structural and functional approaches to investigate pulp-dentine complex.
- To understand the complex physiology and pathophysiology of the pulp due to dentine exposure.
- To translate these ideas toward human tooth physiology and pathophysiology.

1.14 Objectives

- To use rat teeth as models to study the pulp-dentine complex.
- To understand changes in odontoblasts, odontoblast processes and other cellular elements of the pulp during development and in response to dentine exposure.
- To investigate the complex cellular interactions between these tissues.
- To link structural and functional understanding of the pulp response to dentine exposure following mechanical cavity preparation and natural tooth wear.
- To formalize these observations into new concepts of tooth physiology, repair and pathology that may be relevant in translational research to study human dental tissues.

Chapter 2 **Material and Methods**

2.1 Immunohistochemistry (IHC)

2.1.1 Animal culling regulations

All animals were administrated according to Schedule 1, UK Home Office guidelines (*Consolidated version of ASPA 1986*, 6 May 2014). The animals were either euthanizing in a CO_2 chamber (Smart box, Auto CO_2 System, Euthanex), or by intra-peritoneal injection with a lethal dose (0.7ml/Kg) of 200mg/ml of pentobarbiton. All procedures were conducted by appropriately licensed staff at Newcastle University.

2.1.2 Sample collection

Male Wistar rats of different ages: one day, 1 week, 2 weeks, 3 weeks, 4 weeks, 6 weeks, 8 weeks, 9 weeks, 12 weeks, 13 weeks and 24 weeks were included in this work. These ages were chosen according to the life cycle of rat mandibular first molar tooth development (Farris and Griffith, 1949). This includes cellular differentiation and tooth morphogenesis (one day), crown formation (1-2 weeks), tooth eruption (3 weeks), commencement of occlusal wear (4 weeks), repair following tooth wear (6-9 weeks), mature tooth (12 weeks), and ageing process (24 weeks). All ages were left on adlib food of type called RM3 (P) pellets (Special Diet Service, UK) to ensure similar dietary conditions during the entire work. This type is used as a routine diet for breeding, lactating, and growing young rats; however it is still considered that hard pellets promote tooth wear (Pang *et al.*, 2016). Details of animal ages and numbers were specific to each of the investigations described in results chapters. Depending on the experiment, sample consisted of:

1- Whole mandibles: dissected carefully before sectioning each half jaw into 3 pieces: apical containing the apical part of the mandibular incisor with the apical bud, middle containing the middle part of the incisor and the 3 molars, and incisal third containing the incisal portion of the incisor (Figure 2.1, A). Sections were made with a diamond coated disc mounted in a low speed straight handpiece under constant water cooling. The dental structures in one of the section pieces is illustrated in Figure 2.1, B. In the younger rats (one day, 1 week and 2 weeks) each half mandible was either left without cutting or cut

into two halves, the incisal containing the incisal half of the incisor and the apical half for the rest of the jaw.

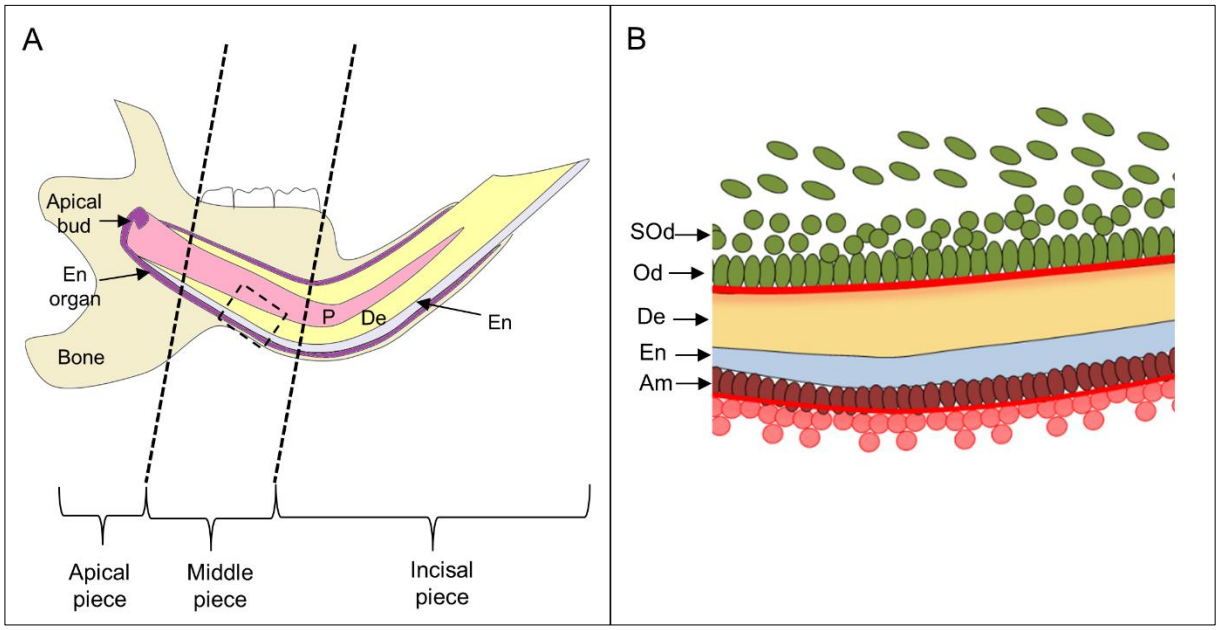

Figure 2.1: Diagram showing rat mandible sectioning (A), and different dental structures (B). Important elements of the mandibular incisor labelled as follows: apical bud, pulp (P), dentine (De), enamel (En), enamel organ, subodontoblast (SOd), odontoblast (Od), and ameloblast (Am). The two dotted lines in A represent the sectioning positions dividing the mandible into 3 pieces: apical, middle and incisal. Region of interest in A is shown in higher magnification in B.

2- Mandibular incisors: surgically extracted after removing the overlying mucosa and bone to remove the tooth gently with artery forceps. The extracted teeth were cut into two or three pieces by using a diamond coated disc mounted in a slow-speed straight handpiece under constant water cooling.

3- Mandibular incisor pulp: after extraction of the mandibular incisors, the pulps were dissected carefully by grooving the tooth longitudinally with high speed diamond burs under water cooling and operating microscope (DP Medical systems, UK). Care was taken to avoid exposure of the pulp and to minimise any trauma. Teeth were then readily split with a scalpel before carefully lifting the pulp tissue free with tweezers.

2.1.3 Sample fixation

All collected samples were fixed either before or after jaw dissection with freshly prepared 4% paraformaldehyde (PFA) in phosphate buffer saline (PBS) (Sigal *et al.*, 1985; Gage *et al.*, 2012). Fixation was important to preserve tissue morphology and

its antigenic immunoreactivity (Berod *et al.*, 1981). Fixation by specimen immersion and perfusion by cardiac infusion were employed in this work.

1- Immersion fixation: after surgical dissection, samples were immersed in 10 ml of 4% PFA for 24 hours at 4ºC (Fox *et al.*, 1985; Sigal *et al.*, 1985). Most of the samples used in this work were fixed by this method.
2- Cardiac perfusion: The rats were first anaesthetised with a ketamine/xylazine mixture (up to 80 mg/kg body weight ketamine and 10 mg/kg body weight xylazine) via intraperitoneal injection. After opening the rib cage, an incision was made in the posterior part of the left ventricle and the animal was perfused with physiological saline before using 4% PFA fixative. Another large incision was also made in the right atrium to create as large an outlet as possible for the perfused fluid. The perfusion of the fixative fluid continued until complete stiffness of the rat (Gage *et al.*, 2012). After complete fixation, the mandible was dissected and sectioned as previously described, the samples were then post fixed with 4% PFA for 4 hours at 4ºC (Sigal *et al.*, 1984a). All procedures were again performed by appropriately licenced and trained staff.

After completing the fixation process, the samples were washed in PBS twice for about 10 min each with continuous agitation to remove any excess fixative solution from the sample before starting the demineralisation procedure.

2.1.4 Demineralisation

Samples of hard tissue were demineralised with ethylenediaminetetraacetic acid (EDTA). This binds to the calcium minerals and removes them gently without damaging the antigenic properties of the examined tissue (Mori *et al.*, 1988; Cho *et al.*, 2010). As the samples used were pieces of mandible containing teeth, this required an extended period of demineralisation. To determine which concentration of the EDTA could be used in this work without possible harm to the antigenic properties of the sample, the following pilot experiment was undertaken. Firstly, different concentrations of EDTA, 4.3% (Cho *et al.*, 2010), 12% (Sigal *et al.*, 1984a), and 17% (Serper and Çalt, 2002) with pH 7.4 were used, in combination with the non-demineralised samples of extracted pulp to identify differences in the expression of all of the antibodies and fluorescent staining. After observing similar immunohistochemistry results using different concentrations of EDTA (see Appendix A) and in order to save time during sample demineralisation, the decision was made

to use 17% EDTA (pH 7.4) (Serper and Çalt, 2002) at 37°C with continuous agitation on a temperature controlled shaker (Environ-shaker, Lab-line, Jencons Scientific Ltd).

Each sample was stored in 15ml of 17% EDTA solution, which was renewed daily. The teeth were examined radiographically in addition to the use of a surgical blade to check the demineralization by assessing cutting resistance. This was performed every week during demineralisation process. The total period required for complete demineralisation depended on the age of the rat and ranged between one day and 4 weeks.

After completion of the demineralisation process, the samples were washed twice in PBS, for about 10 min each with continuous agitation to remove any excess demineralising material from the sample before starting the freezing procedure.

Isolated pulp samples did not require demineralisation. They were only washed after fixation, preparing for the next process of freezing and sectioning.

2.1.5 Freezing and sectioning

Demineralised samples or the non-demineralised fixed pulps were transferred into graded sucrose solutions for cryoprotection (10%, 20%, 30%) each for 24 hours at 4ºC before starting the freezing process (Peters, 2010). Samples were then dried gently on tissue paper in a petri dish. The required alignment and direction of the sample within the frozen block was performed under the dissecting microscope (Kyowa, Tokyo). The samples were then embedded in optimal cutting temperature medium (OCT) (Sakura Finetck Europe B.V. Netherlands) over a piece of laboratory paraffin thin film (Parafilm M, Bemis flexible packaging, USA) as a base. Care was taken in the alignment of each sample within the OCT gel. Only one piece of the cut mandible (apical, middle or incisal, see Figure 2.1) was placed in each prepared block. Samples with OCT were snap frozen using isopentane cooled in liquid nitrogen. The frozen samples were then removed from the isopentane to be sectioned immediately or stored at -80ºC freezer in separate labelled containers.

To section the frozen samples, they were transferred to the cryotome (Shandon Cryotome FSE, Thermo Fisher scientific, USA), mounted on serrated discs using OCT and cut using new blades (MX35 Premier +Microtome Blade, Thermo Scientific, USA). In sagittal sectioning, the sections were taken parallel to the long axis until all

cusps of the required tooth were visible. From this point about 20 to 25 sections of 8-15 µm thickness were obtained from each block in order to standardise the sections to be within the same orientation. The prepared sections were mounted on polysine slides (Thermo Scientific, USA), numbered, dated and allowed to bench dry for 24 hours. Resulting slides were either to be used immediately after drying, or were wrapped with cling film, avoiding any touch or damage to the tissues, and stored in a -80˚C freezer for later use.

2.1.6 Antibody staining procedure

After removing from the -80˚C freezer, the slide packs were allowed to equilibrate to room temperature for about one hour before unwrapping. In each slide, the position of the section was encircled with a hydrophobic barrier pen (PAP pen) before washing the slides with TBS (Tris buffer saline), TBS-T(Tris buffer saline-tween), and TBS in a Coplin jar for 5 minutes each with agitation over a 3D rocking platform (Stewart Scientific, UK). The primary antibody, either single or combination of two, was applied to each section before incubating slides in a humid environment at 4°C for 24 hours. These antibodies were diluted with triton in phosphate buffer saline (PBS-T) to enhance tissue penetration. Sections were stained with one or two of the primary antibodies listed in Table 2.1. These antibodies have been characterised by the manufacturers and validated in numerous peer reviewed reports (see respective manufacturers data sheets). Antibodies were chosen according to the following criteria: (i) Suitable for immunohistochemistry on frozen sections, (ii) the detection of epitope in control tissue, (iii) the detection of band of appropriate molecular weight with western blotting and (iv) the removal of antibody binding using the appropriate blocking peptide.

Antibody	Abbr.	Conc.	Cat#	Company
Mouse monoclonal anti-vimentin	vim	1:5000	MU074-UC	BioGenex, Launch Diagnostics
Rabbit monoclonal anti-α smooth muscle actin	actin	1:200	Ab32575	Abcam
Rabbit polyclonal anti-α tubulin	tub	1:1000	GTX102078	Gene Tex
Rabbit monoclonal anti-NaK-ATPase	NaK-ATPase	1:500	Ab76020	Abcam
Rabbit polyclonal anti sodium hydrogen exchanger-1	NHE-1	1:500	sc-28758	Santa Cruz Biotech
Rabbit monoclonal anti-Ki 67	Ki 67	1:500	RMAB 004	Diagnostic Biotech
Mouse monoclonal anti-calcitonin gene related peptide	CGRP	1:500	sc-57053	Santa Cruz Biotech
Rabbit monoclonal anti neurofilament heavy	Nf	1:1000	Ab40796	Abcam
Rabbit polyclonal anti nerve growth factor	NGF	1:500	sc-548	Santa Cruz Biotech
Goat polyclonal anti nerve growth factor receptor p75	NGFR	1:100	sc-6188	Santa Cruz Biotech
Mouse monoclonal anti-RT1-B (OX-6) Anti-MHC class II atibody	OX-6	1:200	GTX76190	GeneTex

Table 2.1: Primary antibodies employed in this work.

The following day, slides were washed in a three stage cycle (TBS, TBS-T, and TBS) for 20 minutes each before staining with one or two fluorescence (secondary) antibodies (Table 2.2) depending on the primary used. If two secondary antibodies were required, the first secondary should be selected in accordance with the species of the first primary antibody with green colour (488 Alexa Fluor), while the selection of second secondary should coincide the species of the second primary antibody but with different colour (red for 594 Alexa Fluor). The secondary antibodies were diluted in PBS. After removing the excess washing material from the slides, they were incubated with the first secondary antibody in a humidifier in darkness at room temperature for one hour. Subsequently, the slides were washed again with TBS, TBS-T, and TBS for 20 minutes each. The second secondary antibody, which targets the second primary antibody was then applied before incubation in darkness in the

humidifier for one hour. Finally, the slides were washed again with TBS, TBS-T, and TBS for 20 minutes each before applying Vectashield hard set mounting medium with dapi (nucleic acid molecular probe stain) (Vector Laboratories Inc, Burlingame, USA) which has the ability to fluoresce when bound to DNA and is usually used as a chromosomal or nuclear stain. One minute after applying dapi, a drop of glycerol in PBS was applied before placing a glass cover slip and sealing with nail varnish around its margins.

Fluorescent Antibody	Conc.	Cat#	Company
Donkey anti-mouse IgG Alexa Fluor 488	1:500	A21202	Molecular Probes®, Invitrogen
Donkey anti-goat IgG Alexa Fluor 488	1:500	A11055	Molecular Probes®, Invitrogen
Donkey anti-rabbit IgG Alexa Fluor 594	1:500	A21207	Molecular Probes®, Invitrogen
Donkey anti-goat IgG Alexa Fluor 594	1:500	A11058	Molecular Probes®, Invitrogen

Table 2.2 Secondary antibodies included in this work.

2.1.7 Staining Controls

Positive and negative control samples were included with each staining run, according to protocols reported by Sigal *et al.* (1985) and Sigal *et al.* (1984a). Positive controls usually consisted of other tissue in the same sample such as enamel organ, gingival tissue and bone. Tissues from other sources have also been used in this study to identify the expression of a specific antibody e.g. bladder tissue.

For negative controls, several methods were used as follows:

1- Use of blocking peptide: these peptides were specially manufactured for particular antibodies to block their active binding sites before incubation in the tissue. An example was the human alpha smooth muscle actin peptide (ab 211918) which was specifically manufactured by Abcam as the blocking peptide for anti-alpha smooth muscle actin antibody [E184] (ab32575). The concentration of actin blocking peptide was 10:1 of the anti-alpha smooth muscle actin according to the manufacturer instructions. The mixture was kept overnight with continuous agitation at 4ºC, before applying to the slides in a similar technique to the primary antibody application (mentioned previously). After 24h incubation with this mixture, the slides were washed and the

secondary fluorescence antibody (anti-rabbit IgG, Alexa Fluor 594) staining was performed (as described in section 2.1.6).

2- Use of the isotype controls: Isotype controls are a type of negative control designed to measure the level of non-specific background signal caused by primary antibodies, based upon the tissue type of the sample. The isotype controls used with this work were: rabbit IgG monoclonal (EPR25A) isotype control (1:500 Abcam cat# ab172730), and normal mouse IgG1 (1:500 Santa Cruz Biotechnology cat# sc-3877 UK). These isotype controls were used either singly or in combination with each other in each experiment, similar to any normal antibody protocol as negative controls. The slides were incubated for 24h before washing and staining with the secondary conjugated fluorescent antibodies.

3- Use of only PBS to incubate the slides instead of the primary antibodies, before staining with the secondary antibodies only, or the slides were incubated with PBS only without any staining.

2.1.8 Examination and analysis

The stained slides were examined at X10, X20, and X60 objectives with an Olympus BX61 microscope (Olympus Corporation, Tokyo Japan) using Alexa Fluor 488 and 594 fluorochromes. These fluorochromes were detected via the microscope light source and dichroic mirror to split excitation and emission light wavelengths. Relevant images were captured with a microscope-mounted Olympus XM10 monochrome camera and examined using ImageJ software (Java- based image processing program- National Institute of Health (USA)).

In addition, and in an attempt to obtain better images details, z-stack images were captured and analysed with AutoQuant x (Media Cybernetics Inc) which had 2D and 3D deconvolution algorithms available. Approximately 80 slides were examined to confirm the accuracy and consistency of the staining technique and to reveal constant staining phenomena (Gillespie *et al.*, 2006).

2.2 Rhodamine-phalloidin staining procedure

This is a fluorescent stain to label filamentous F-actin. The procedure for preparing slides was described in section 02.1.5. The slides were incubated with rhodamine-phalloidin stain (Molecular Probes®, Invitrogen), 1:500 in PBS at room temperature for 30 minutes in a humidified environment before washing them with TBS, TBS-T

and TBS for 10 minutes each. Following this, the Vectashield hard set mounting medium with dapi was applied to the slides with drop of glycerol in PBS before placing the cover slip and sealing the margins with nail varnish.

The slides were examined with a fluorescence Olympus BX61 microscope and images were captured as described in section 2.1.8.

2.3 Haematoxylin-eosin staining (H&E)

H&E staining (Goldberg, 2014) was performed by the Cellular Pathology Department in Royal Victoria Infirmary, Newcastle.

2.3.1 Sample preparation

The same sample size and ages were as described in section 2.1.2. The teeth were dissected, fixed, demineralised, and sectioned as previously described. Two out of ten sections were stained with H&E.

2.3.2 Staining examination and analysis

The slides were further fixed by immersion in formol calcium 40% for one hour at room temperature before the staining. The sections were rinsed in tap water before staining in Harris's haematoxylin for 5 minutes, followed by rinsing in tap water before differentiation in 1% acid alcohol. The sections were then rinsed again in tap water before staining with eosin for 5 seconds. The slides were finally rinsed in tap water before dehydrating, clearing and mounting. The stained slides were examined by Olympus BX51 light microscopy mounted with a Q-Imaging Micropublisher 3.3 RTV camera and Improvision Openlab 5.0.2 image analysis software.

2.4 Ground sections

Ground sections were used in order to identify the shape and complexity of the dentine tubules and to differentiate between the tubular and atubular dentine (Stanley *et al.*, 1983). Thanks to Hard Tissue laboratory in Oral Biology Department in Newcastle University for their help to do these ground sections.

2.4.1 Samples collection and preparation

Two male, Wistar rats of different ages (2, 4, 6, 9, 12 and 24 week) were used. The rats were culled in a CO_2 chamber before carefully dissecting the mandibles. The mandibular incisors were extracted, then the bone segment containing the three mandibular molars were trimmed out. The samples of either mandibular incisors or

molar segments was then stored in 0.5% chloramine-T for 48 hours. Ground sections were then prepared from both the incisors and molar bone segment.

After marking the correct plane for the required face with proper alignment, the tooth sample was adhered on a glass slide with sticky wax. The samples were then lapped gradually with Logitech (PM2A, Glasgow) lapping machine and 3µm calcined Aluminium oxide powder (Logitech, Glasgow). For the incisor sample, the lapping process was continued until nearly the central part of the sample was reached. In molar samples, the lapping continued until the whole pulp chamber of the 1st molar was exposed. The section was then thoroughly cleaned and polished to ensure a scratch free surface. The samples were finally polished with a polishing microcloth (Buehler) and liquid diamond solution 1µm, then thoroughly cleaned in an ultrasonic path with distilled water to remove surface lapping compound. Specimens were then dehydrated through graded alcohol then dewaxed with xylene in a fume cupboard before mounting over the slides. The thickness of the ground sections ranged between 90 to 110 µm.

2.4.2 Examination and analysis

The slides were examined by Olympus BX51 light microscopy mounted with a Q-Imaging Micropublisher 3.3 RTV camera and Improvision Openlab 5.0.2 image analysis software. Polarized light with filters which were available in the microscope ware also used depending on the thickness of the observed section.

2.5 Polymerase chain reaction (PCR)

2.5.1 Sample collection:

Details of sample collection are described in Ch 6, section 6.2.

2.5.2 RNA extraction:

Extraction of total RNA from the pulp tissues was accomplished using RNeasy mini kit (Cat. No. 74104, Qiagen, Germany) (Table 2.3). Before using the kit, four volumes of ethanol (96-100 %) were added to Buffer RPE and 10 µL β-mercaptoethanol (M7154, Sigma, Germany) was added to every 1 mL of the Buffer RLT to prepare a working solution according to the manufacturer instructions.

Material	Supplied volume/ quantity
Buffer RLT	45 mL
Buffer RW1	45 mL
Buffer RPE (Concentrate)	11 mL
RNase-free water	10 mL
RNeasy mini spin column	50
Collection tubes (1.5 ml)	50
Collection tubes (2 ml)	50

Table 2.3: The contents of RNeasy mini kit.

The protocol was as follows:

- Prior to RNA extraction, the tools were sterilised and the surrounding area was thoroughly cleaned with 70% ethanol or RNaseZap solution (Ambion, cat# AM9780). Additionally, in all steps the solution tubes were kept in an ice box because the RNA is easily broken down and contaminated by the atmosphere.
- The pulp was gently taken from the RNAlater solution with forceps, before drying with piece of sterile tissue and weighting by sensitive balance. The average weight of the pulp used was about 14.5 mg. The pulp then put within sterile petri dish before cutting into small pieces using a new scalpel for each sample. The sample was then immersed in a micro centrifuge tube containing 600 µL of the Buffer RLT with β-mercaptoethanol. Additionally, the tissue was disrupted further while being immersed in the Buffer RLT using Pellet Pestle motor and autoclaved plastic tips.
- Homogenisation was achieved using TissueLyser LT (Qiagen, Germany) at maximum speed for 5 minutes. The supernatant was then pipetted and transferred to a genomic DNA (gDNA) eliminator spin column placed in a 2 ml collection tube and centrifuged (SLS 4600, Scientific Laboratory Supply, UK) for 30 seconds at ≥8000 x g. The column was then discarded and the flow-

through saved. This step is very important because it helps to remove the insoluble materials and gDNA that may interfere with DNA removal.

- 600 µL of 70% ethanol was added to the saved flow-through solution before thoroughly mixing by pipetting.
- 600 µL of the mixture was then transferred to an RNeasy mini spin column, placed in a 2 mL collection tube supplied by the manufacturer. The lid of the collection tube was closed tightly and the tube centrifuged for 15 seconds at ≥8000 x g. The flow-through was discarded. This step was repeated until all the initial mix was fully used.
- 700 µL of Buffer RW1 was added to the RNeasy spin column, lid closed, centrifuged for 15 seconds at ≥8000 x g and the flow-through was discarded.
- 500 µL of Buffer RPE was added to the RNeasy mini spin column, before centrifuging for 15 seconds at ≥8000 x g and the flow-through was discarded.
- The RNeasy mini spin column was centrifuged for 1 minute at ≥8000 x g, for further drying of the column membrane.
- The RNeasy mini spin column was placed in a new 1.5 recovery tube supplied by the manufacturer. 30 µl of RNase-free water was directly added to the column spin membrane before centrifuging for 1 minute.
- The previous step was repeated to end with 60 µl flow-through RNA solution with the tube saved in an ice container for the next step.

2.5.3 RNA quantitation:

The total RNA products yields from both RNA isolation protocols were tested with NanoDrop ND-1000 spectrophotometer (ThermoFischer Scientific, USA) with the NanoDrop 1000 specific software (NanoDrop 1000 Version 3.8.1). The protocol was as follows:

- The software initialised, the sampling arm opened and the measuring pedestal cleaned using a soft laboratory wipe.
- 1 µL of autoclaved distilled water or elution buffer was used to create the blank measurement, pipetted carefully into the pedestal, the arm closed and the blank measurement made.
- Upon completion, the sampling arm was opened, the pedestal cleaned thoroughly, 1 µL of the sample RNA (according to the manufacturer's

instructions) was pipetted onto the pedestal and the spectral measurements made for each sample.

- The pedestal was cleaned thoroughly following every measurement and a blank measurement was made before each sample measurement.
- For every sample quantified by NanoDrop, the ratio of absorbance at 260-280 nm should be between 1.8 - 2.1 to show minimal amount of protein contamination present. Additionally, the ratio of absorbance at 260-230 nm should be greater than 1.8 to show minimal ethanol and salt contamination.

Due to inherent inaccuracy in quantifying total RNA using absorbance with NanoDrop (Aranda *et al.*, 2009), the amount of RNA added to an RT-PCR from each sample was more accurately determined by normalising against the housekeeping gene.

2.5.4 Reverse transcription (RT) and complementary DNA quantitation:

1 µg of total RNA was used in the synthesis of complementary DNA (cDNA) using High-Capacity cDNA Reverse transcription kit (Cat No. 4368814, ThermoFisher Scientific, USA). The contents of the kit are listed in Table 2.4.

Component	Quantity
10X RT Buffer	1 tube x 1mL
10X Random Primers	1 tube x 1mL
25X dNTP Mix (100 nM)	1 tube x 0.2 mL
MultiScripe Reverse Transcriptase (50U/µl)	2 tubes x 1 mL
RNase Inhibitor	2 tubes x 200µL

Table 2.4: Components of High-Capacity cDNA kit.

To synthesize a single-stranded cDNA from total RNA using this kit, the following protocol was employed:

- All the components of the kit were allowed to thaw on ice, then 2X RT master mix was prepared according to the manufacturer's instructions as illustrated in Table 2.5, always kept on ice and mixed gently. This master mix was for 20 µl yield reaction.

Component	Volume
10X RT Buffer	2 µL
10X Random Primers	2 µL
25X dNTP Mix (100 nM)	0.8 µL
MultiScripe Reverse Transcriptase (50U/µl)	1 µL
RNase Inhibitor	1 µL
Nuclease-free water	3.2 µL
Total volume per reaction	10 µL

Table 2.5: Volume components needed to prepare reverse transcription master mix.

- 10 µL of the 2X master mix was pipetted into a PCR tube followed by the addition of 10 µL of sample RNA of 1 µg concentration, pipetting up and down two or three times to mix the contents.
- PCR tubes were labelled, dated and the lid closed tightly. Tubes were then centrifuged for 15 seconds at 8000 x g to spin down the contents and eliminate any air bubbles and always kept on ice.
- To create negative controls (RT –ve), we included RT reaction tubes containing the same components of Table 2.7 excluding the MultiScripe enzyme. To create no template –ve control (NTC), all the components in Table 2.7 were included without the addition of RNA, but the same volume of nuclease free water was added instead.
- The tubes were then transferred to the thermocycler (T100 Thermal cycler, BIO-RAD, USA) using a special program suggested by the manufacturer as shown in Table 2.6.

	Step 1	Step 2	Step 3	Step 4
Temperature (˚C)	25	37	85	4
Time	10 min	120 min	5 sec	∞

Table 2.6: The program used with thermal cycler.

- The cDNA products were tested with NanoDrop ND-1000 following the same protocol as previously described for RNA quantitation in section 2.5.2.
- The synthesised cDNA product was either kept on ice for immediate use or stored in a -20˚C freezer for later use.

2.5.5 Primers:

Primer design was performed using Primer 3 input http://primer3.ut.ee/ (Rozen and Skaletsky, 1999), before checking all primers for specificity using UCSC In-Silico PCR https://genome.ucsc.edu/cgi-bin/hgPcr . The primers were designed to create amplicons of up to 200 base pairs (bp), have GC content of 40-60%. Primers with long runs of a single base were avoided as they can misprime. Then, primers were synthesised by Metabion (Metabion International AG, Germany), purified by desalting and with an annealing temperature of 58˚C. A full list of primers used in this work and their nitrogen bases sequences are listed in Table 2.7.

Type	Sequence name	Sequence	bp length
DNA	GAPDH forward primer	GCGGAGATGATGACCCTTTT	99
DNA	GAPDH reverse primer	GTGCTGAGTATGTCGTGGAG	
DNA	α-actin forward primer	CAGTTGTACGTCCAGAAGCA	71
DNA	α-actin reverse primer	CTTCAATGTCCCTGCCATGT	
DNA	α-tubulin forward primer	TGGGTTCCAGGTCTACGAAC	153
DNA	α-tubulin reverse primer	AGCTCTACTGCCTGGAACA	
DNA	Col 1a1 forward primer	GCAAAGATGGACTCAACGGT	189
DNA	Col 1a1 reverse primer	GGCCACCATCTTGAGACTTC	
DNA	Col 1a2 forward primer	TAACCCTGGCAGTGATGGTC	130
DNA	Col 1a2 reverse primer	CAGGACCCACAGAACCATGA	
DNA	NaKATPase a1 forward primer	GGTGGATGAAGTGCTCGATT	192
DNA	NaKATPase a1 reverse primer	TCACAAACGAGAACCCCTTG	
DNA	NHE-1a1 forward primer	GGCCTGCTTTTACCTCTGTT	187
DNA	NHE-1a1 reverse primer	GACTATTGCACGATCCTGGG	
DNA	NCX a1 forward primer	CTTTCTCATATTCCTCACGGTCA	101
DNA	NCX a1 reverse primer	ACCTTCTTCATTGAGATTGGAGA	
DNA	PMCA1 forward primer	TCAGCTCGTAGTGGTCTTCA	110
DNA	PMCA1 reverse primer	AATGGTGTAGTGCTCTGACG	
DNA	SERCA1 forward primer	CCATGATGTCCAGGTCAGGT	180
DNA	SERCA1 reverse primer	AAGCAGTTCATCCGCTACCT	
DNA	Na_v 1.6 forward primer	TGGCATGTCCAACTTCGCATA	145
DNA	Na_v 1.6 reverse primer	GTTCAGGATTGGCAGCAGCA	
DNA	Na_v 1.7 forward primer	ATGAGCATGTTCAGTGTGGG	130
DNA	Na_v 1.7 reverse primer	AGCCTAATTGTGACGCTGAG	

Table 2.7: List of primer pairs used in this study and their product size.

2.5.6 End point (qualitative) Polymerase Chain Reaction (PCR):

PCR reaction was accomplished using GoTaq Green Master Mix (Cat. No. M7122, Promega, USA). The protocol used was as follows:

- GoTaq master mix was thawed at room temperature, vortexed briefly and centrifuged for 15 seconds.
- The reaction mix was prepared in PCR tubes on ice as shown in Table 2.8:

Component	Volume	Final concentration
GoTaq green master mix, 2X	12.5 µL	1X
Forward primer (10 µM)	1 µL	0.4 µM
Reverse primer (10 µM)	1 µL	0.4 µM
Sample cDNA (10 ng)	1 µL	NA
Nuclease-free water	9.5 µL	NA

Table 2.8: End point PCR reaction mix/ 25 µl.

- The PCR tubes were transferred to the thermal cycler using a specifically designed program according to the manufacturer instructions as shown in Table 2.9.
- The yielded PCR products were immediately detected by gel electrophoresis.

Cycles	Temp	Time	Notes
1	95˚C	2 min	Polymerase activation
40	95˚C 58˚C 72˚C	30 sec 30 sec 30 sec	Denaturation Annealing Extension
1	72˚C	5 min	Final extension
	4˚	∞	Holding until usage

Table 2.9: End point PCR reaction mix/ 25 µl.

2.5.7 Post PCR detection and gel documentation system:

2% agarose gel was prepared by dissolving 2 gm of agarose (MB1200, Melford laboratories, UK) in 100 mL of 1X TAE buffer and completely dissolved by heating the mix in a microwave oven for 5 minutes. The mixture was then allowed to cool down for few minutes but not solidify, followed by the addition of 10 µL of GelRed Nucleic Acid Gel Stain 10000x (Cat 41003, Biotium, UK) to allow visualisation of nucleic acid bands. The solution was poured into a suitable gel tray, with the associated comb in place. After complete setting of the gel (around 30 minutes), the comb was removed, the tray transferred to the electrophoresis tank and more 1X TAE buffer added until it reached a specified level marked on the side of the tank. 3 µL Ladder (Hyper Ladder IV 100bp, Bioline, UK) was mixed with 5 µl gel loading buffer (5X DNA loading buffer blue, Cat. Bio-37045, Bioline, UK) followed by the addition of 3µL autoclaved distilled water, and loaded in the first well to the left. The samples did not need to be mixed with that stain, because the GoTaq master mix already contained two dyes (blue and yellow) that allowed monitoring progress during electrophoresis. 10 µL of each sample was loaded in the specified well. Negative controls for each gene were prepared following the same technique as with the samples but without cDNA and loaded in other wells.

Gel electrophoresis was subsequently performed by running TAE gels at 85 volts and 400 mAmp for 1-2 hours, until separation of DNA fragments were achieved using BIO-RAD Power Pac 300 device (BIO-RAD, UK).

After completion of the electrophoresis process, the gel was transferred to the Electrophoresis Documentation Analysis System (G:Box, Syngene, UK) for exposure to ultra violet light. Relevant images were captured with GeneSnap software (Version 7.08, Syngene, UK), saved and finally printed with a digital monochrome printer (P93D, Mitsubishi, Japan). The size of PCR products was subsequently determined by correlating the size and location of each sample band with the known size bands of the ladder.

2.5.8 Quantitative Reverse Transcriptase Polymerase Chain Reaction (q-RT-PCR):

q-RT-PCR was achieved using 2X SensiFAST SYBR No-ROX kit (BIO-98005, Bioline, UK), where all PCRs were prepared in 96 well optical reaction plates (RT-PL96-op, Eurogenetics, UK). All the reagents were taken out of the freezer and allowed to thaw on ice. All the work was accomplished on ice, using disposable filtered tips (StarLab, UK) and special pipettes with the SensiFAST kept protected from light. The contents of each well are shown in Table 2.10.

Reagent	Volume	Final Concentration
2X sensiFAST	10 µL	1X
10 µM Forward primer	0.6 µL	400 nM
10 µM Reverse primer	0.6 µL	400 nM
cDNA (Template)	1 µL (10 ng)	NA
Nuclease free water	7.8 µL	NA
Final volume	**20 µL**	

Table 2.10: Contents of each individual well for q-RT-PCR reaction.

In all the reactions, 10 ng/µl of cDNA was used in each well and a house keeping gene was included (GAPDH) as a positive control and to ensure that all data were expressed in close relation to an internal reference. All samples were tested in duplicate plus a negative control (NTC and RT-ve). Adhesive seals (Microseal B, cat. No. MSB 1001, BIO-RAD, UK) were fitted firmly over every reaction well plate, to avoid the samples evaporating during the thermal cycling. Subsequently, the prepared and sealed 96 wells reaction plates were loaded into the thermal cycler (Opticon Monitor software, Version 3.1, BIO-RAD, UK). A plate layout was required

for every reaction plate then the amplification conditions and protocol were determined. A three-step protocol was used with all reactions, with details of the protocol shown in Table 2.11 according to the manufacturer's instructions and the annealing temperature of the primers used in this study.

Cycles	Temperature	Time	Notes
1	95˚C	2 minutes	Polymerase activation
40	95 ˚C	5 seconds	Denaturation
	58 ˚C	10 seconds	Annealing
	72 ˚C	10 seconds	Extension

Table 2.11: Details of protocol used in q-RT-PCR.

At the end of each reaction, the data were collected by the system and graphically displayed. The files were saved containing all the specific details of the reaction including a melting curve, amplification curve and Ct values. The threshold was also set at the linear part of the amplification curve and the number of cycles needed to reach it was calculated. The Ct value is defined as the number of cycles required for the fluorescent signal to cross the threshold (i.e. exceeds background level) and this is the value which used for statistical analysis.

2.5.9 Results, analysis (real time) and absolute quantification

Relative mRNA levels for each gene were determined by use of a standard curve and by further normalisation to the reference gene to adjust for uncontrolled variabilities between the samples.

Calibration of the q-RT-PCR system was accomplished by including a standard curve prepared from gradual dilution of the cDNA template in each reaction. This can also serve as an internal positive control for primer function.

The melting curve analysis was performed by the system upon the completion of the cycles and was used to determine the specificity of each primer set. Melting curve allows the confirmation of specific PCR products and the absence of non-specific products which also help to determine the purity of the sample detected (see appendix B image II).

Following each reaction, the system presented the data in a numerical and graphical manner. All the data were then moved to an excel spread sheet where they were assembled from all experiments. The data was then categorised and initially analysed using excel in which mean, standard deviation and standard error values were calculated. To determine the level of significance, ANOVA and *post hoc* analysis was used for the different incubation group and student *t* test for control and treated groups using SPSS software.

Chapter 3 **The complexity of Odontoblast process and response to injury**

3.1 Introduction

Odontoblast processes are cytoplasmic extensions of the cell body, which reside within the tubular structure of dentine. The intimate relationship between the soft tissue of the pulp and its surrounding dentine, thus forms a spatially and functionally related pulp-dentine complex (Luukko *et al.*, 2011). Within this complex, the OPs are primarily responsible for dentinogenesis, whilst their presence within the dentinal tubules make the dentine a vital and responsive tissue (Holland and Botero, 2014) with a range of sensory and defensive roles throughout life.

At the ultrastructural level, TEM studies in human and animal models, reported the presence of intermediate filaments mainly of vimentin (10 nm in diameter), and microfilaments or actin fibres (5-8 nm in diameter) within odontoblasts and their processes. The intermediate filaments are believed run centrally within the core of the OP, whilst microfilaments are abundant peripherally in the form of bundles or networks (Nishikawa and Kitamura, 1987; Yoshiba *et al.*, 2002). These insoluble cellular proteins have also been reported in immunofluorescence studies (Sigal *et al.*, 1985; Nishikawa and Sasa, 1989; Byers and Sugaya, 1995) and are believed to have instrumental roles including structural and cytoskeletal support, cellular movement and secretion (Pollard and Cooper, 2009; Gunning *et al.*, 2015).

The OP plays a central role in dentinogenesis, a key element of which is the active transport of Ca^{2+} ions into the extracellular spaces and Na^{+}/Ca^{2+} exchange employing chemical energy derived from tissue with a high extracellular Na^{+} concentration (Guerini, 1998). NaK-ATPase is expressed widely in cellular systems, including dental tissues, where it is instrumental in maintaining cell membrane potentials (Obrien *et al.*, 1994). In the enamel organ, NaK-ATPase has been linked to transport activity of the sub-ameloblast cells (Josephsen *et al.*, 2010). NaK-ATPase has also been reported within the cells of the pulp, especially within subodontoblast, and odontoblast cells (Alhelal *et al.*, 2016; Mahdee *et al.*, 2016). It is proposed that detecting the presence of structural intracellular proteins (vimentin and actin), and cell membrane active enzyme NaK-ATPase within odontoblasts and cellular

processes may provide helpful insights on the anatomical complexity of the pulp dentine complex which may reflect its likely functions.

The presence of the immunocompetent cells i.e. macrophages and dendritic cells has been reported within the odontoblast cell layer during tooth development. This suggests that they may have a role in supporting dental development, in addition to their primary immune-surveillance function (Tsuruga *et al.*, 1999). Because dendritic cells can extend cellular processes into dentinal tubules (Kawagishi *et al.*, 2006), these must be identified during studies on OP complexity.

It is well known that the odontoblast cell layer shows remarkable morphological, structural, and functional changes during tooth development. This is seen both in continuous growing rodent teeth (Ohshima and Yoshida, 1992) and in teeth with limited growth (Couve, 1986; Yoshida and Ohshima, 1996). The degree of extension of the OP remains contentious with a number of groups identifying full extension to the dentino-enamel junction, provided that the tooth surface remains intact (Gunji and Kobayashi, 1983; Sigal *et al.*, 1984a; Sigal *et al.*, 1985; Grötz *et al.*, 1998; Kagayama *et al.*, 1999; Tsuchlya *et al.*, 2002). Less information is available on the morphological complexity of OP changes during stages of tooth formation.

Similarly, studies have shown changes in pulp innervation (Taylor *et al.*, 1988), growth factor expression (Byers *et al.*, 1990), presence of immunocompetent cells (Kawagishi *et al.*, 2006), and pulp cell apoptosis (Kitamura *et al.*, 2001) following dental cavity preparation, but the effects on odontoblasts and their processes are less well understood.

Odontoblast process is an active element during dentinogenesis in dentine secretion and mineralisation (Tjäderhane *et al.*, 2012) and their spatial sensing relationship within the pulp-dentine complex triggers inflammatory and reparative activities (Okumura *et al.*, 2005). The balance between secretory and defensive roles may suggest morphological and functional heterogeneity within the odontoblast population or changes in cells as they predominate in different duties. Specific objectives of the current work are:

1- To explore the development of OPs and their complexity in a rodent incisor tooth model.

2- To examine the response of OPs to trauma induced by cavity preparation into dentine.

3.2 Methods

3.2.1 Non-cavity samples:

About 10 male Wistar rats, 12-13w age (about 400-500g weight) were killed in a CO_2 chamber. Mandibles containing incisors were carefully dissected free and divided centrally into two halves. These half mandibles (n=20) were cut to divide incisors into apical, middle and incisal thirds (Figure 2.1 A), with a high-speed diamond bur under constant water cooling. Fixation, demineralisation, freezing and sectioning were done as described in Ch 2 sections 2.1.3, 2.1.4, and 2.1.5 respectively. Sections were placed on polysine coated slides. Approximately 20 sagittal, 10µm thickness sections were obtained from each block.

Sections from each animal were stained either with rhodamine phalloidin (Molecular Probes®, Invitrogen) (see section 2.2) or IHC antibodies (see section 2.1.6).

Immunohistochemical staining included either one or a combination of two of the following antibodies: mouse monoclonal anti-vimentin (vim) (1:5000), rabbit monoclonal anti-α smooth muscle actin (1:200), rabbit monoclonal anti-NaK-ATPase enzyme (1:500), and mouse monoclonal RT1-B antibody [OX-6], a dendritic cell marker, (1:200). Details about these antibodies were shown in table 2.1

Negative controls for IHC staining included blocking peptides and isotype controls for each experiment was described in section 2.1.7.

Fluorescent microscopy was conducted as described in section 2.1.8.

3.2.2 Cavity samples:

Similar number of male Wistar rats with similar ages were used in this experiment. After animal killing in CO_2 chamber, the mandibular incisors were extracted. The teeth (n=15) were divided into thirds as previously described, with only the relatively mature tissues of the incisal regions included in this investigation. One groove-like cavity was prepared on the labial surface, about 3 mm from the incisal edge, of each incisal specimen with high speed diamond bur No 009 (head diameter 0.5mm) (Kerr Dental, Switzerland), under constant cooling from a syringe containing Dulbecco's Modified Eagle's Medium (DMEM) solution (Sigma, USA), to overcome the osmotic

pressure changes that may have occurred under traditional water cooling. From our ground section archives of the rat mandibular incisor, the thickness of enamel at that region was estimated to be 200µm. Insertion of the bur to half-thickness therefore resulted in a cavity of approximately 50 µm depth in dentine. This depth of penetration was considered shallow given the typical thickness of dentine in this area in the range of 600-700µm. Work was conducted under a Global Operating Microscope (DP Medical Systems, UK). After cavity preparation, teeth were divide into 3 groups (n= 5). Group A was immediately fixed with 4% PFA solution for 24 h at 4 ºC. The working time for one cavity preparation was 60sec or less, and this group was referred to as the 60sec or group A within this study. The other groups were incubated in a CO_2 incubator (Sanyo, Japan) at 37°C with 5 ml DMEM solution supplemented with fetal calf serum (1% Sigma) and penicillin-streptomycin (50 IU/ml-µg/ml Sigma) for 3h (Group B) or 24h (Group C). After incubation, samples were fixed, demineralised and sectioned as described in sections 2.1.4 and 2.1.5. Tooth cross-sectional sections were prepared (10 µm, 20 serial sections from each sample). Only the mid sections from these series were used for staining in order to ensure the best section location within each cavity. These sections were stained with rabbit monoclonal anti-alpha smooth muscle Actin antibody (1:200) and mouse monoclonal anti-vimentin (1:5000) (same as described previously). Negative control sections were also obtained as described in Ch 2 section 2.1.7. Images were captured at X100, X200, and X600 magnification.

Depths for all cavities were verified as being in the range of 40-60 µm.

Measuring OP length:

Only images showing α-actin staining were used to measure the length of odontoblast processes, because, depending on the results of the first section, this stain was labelled within the full length of OPs. Measurements were performed on X100 magnification images to allow the whole thickness of dentine to be seen. Measurements of OP process were made from intact or cavity surfaces. Therefore, each group was subdivided into two sets of measurements: intact OP length ratios as “control” measurements and traumatised OP length ratios as “experimental” measurements. Groups A1, B1 and C1 were controls and A2, B2, and C2 were experimental groups. Measurements of OP lengths were performed using Cell F imaging software (Olympus). Figure 3.1 illustrates the process.

1- To measure OP length within cavity zone:
    a- A curved line was drawn between the two edges of each cavity to represent the position of the original DEJ before cutting (dotted line in Figure 3.1).
    b- To identify the cavity measurement zone (CMZ), two lines (blue lines in Figure 3.1) were drawn from the pulp margin to the curved line on the two boundaries of the cavity. These 2 lines should be parallel to the flow of OPs.
    c- The measurement lines were drawn (red line 1, Figure 3.1), which should be parallel to each process within the measurement zone and similar to the boundary lines. Each measurement line was used to measure:
        i- length of the odontoblast process (OP) from pulp margin to its terminal end.
        ii- Thickness of dentine before cutting (L), which is represented by the estimated curve line (dotted line in Figure 3.1). All measurements were done in micrometres.
    d- The ratios of OP/L were used to calculate the differences in OP length after cavity preparation in relation to the original dentine thickness.
2- Similar measurement lines were also used to quantify OP length ratios within intact tooth regions adjacent to the cavity (red line 2, Figure 3.1). These lines were outside cavity zone. The length ratios for control tooth surfaces were OP/DL.

In this preliminary investigation of proof of concept, only one section was analysed for each group of samples. About 25-50 OP measurements were performed in each section within and outside the cavity zone. Both controls and experimental groups were analysed using Kruskal Wallis test to identify statistically significant differences within groups for cavity or intact OP measurements. If significant differences were observed, multi comparison *post hoc* test was performed.

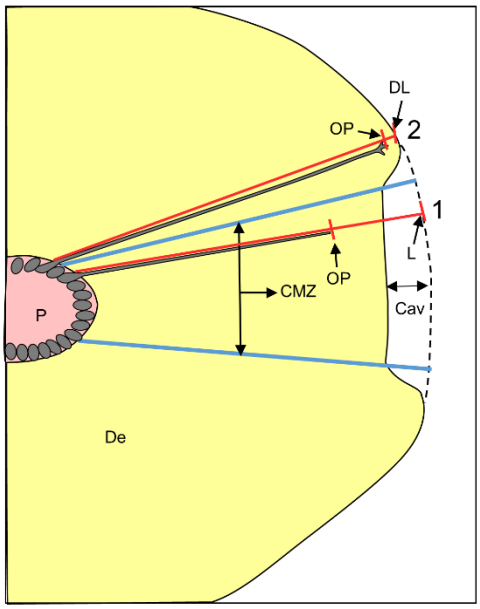

Figure 3.1: Cavity measurement diagram.
Cross section of the rat mandibular incisor for cavity region identifying measurements within and outside the cavity zone (CMZ) for traumatised (1) and normal (2) OPs respectively. The length of the OPs were normalised either with control dentinal tubule thickness (DL) in control surfaces or with estimated length (L) for dentine surface before cutting on cavity side. P= pulp and De=dentine.

3.3 Results

3.3.1 Non-cavity samples:

Structural proteins:

All images shown in this part of the work were demineralised longitudinal sections from the labial side of the apical, middle and incisal thirds of rat mandibular incisors. The apical third, which contains the apical bud (proliferation region) of the tooth and the newly differentiated Ods secreting the initial dentine (mantle dentine), is expressed in Figure 3.2. The apical bud contains an epithelial component (Figure 3.2 A, B *) which includes inner enamel epithelium (IEE) and outer enamel epithelium (OEE). Another component (mesenchymal origin) is clearly represented by proliferating cells of the dental papilla (DP). The latter cells appear with regular distribution of vim and actin within their cell bodies. Moving further, cellular differentiation results in formation of pre-ameloblast (PAm) cells which face the pre-odontoblasts (POd) (differentiating cells of the dental papilla). The PAm cells are not yet polarized, in comparison with the POds which appear as a single cell layer of low columnar shape with basally-located nuclei. The presence of actin represented by alpha smooth muscle actin (α-actin) (Figure 3.2 images A and a1), or the rhodamine phalloidin (RP) binding to F-actin (Figure 3.2 image B), is apparent in the junctional

region between POds and PAm cells i.e, the apical pole for these two developing groups of cells. However, the vim-IR is only present within the POds in the apical region above their nuclei and slightly basal to the apical actin pole (Figure 3.2 a1). After the start of predentine (PD) deposition, the differentiated Ods appear as a single polarised cell layer of about 45µm in thickness, with multiple cellular processes in their apical region (Figure 3.2 C). The α-actin seems to be more concentrated in the apical region of the Ods and within their processes. Additionally, F-actin is seen within Od cell bodies (Figure 3.2 D). The highest expressions of α and F-actin are still present within cells of the enamel organ, especially the Tome's processes (TP) of the ameloblasts (Am), followed by pulp blood vessels (arrows in D). Vim-IR becomes more concentrated within the Od cell bodies apical to their nuclei and within OPs (Figure 3.2 C). In higher magnification images (Figure 3.2 E, F, and G), this region is illustrated by the very complex appearance of OPs which clearly identify two different immuno-reactive (IR) processes (Figure 3.2, E): actin tree-like processes (*) (as also shown in image F) and vim-IR (▲ in E). These actin processes extend to about 20µm in front of the Ods. By use of an α-actin blocking peptide, no signs of this protein are seen within treated sections (Figure 3.2 image H).

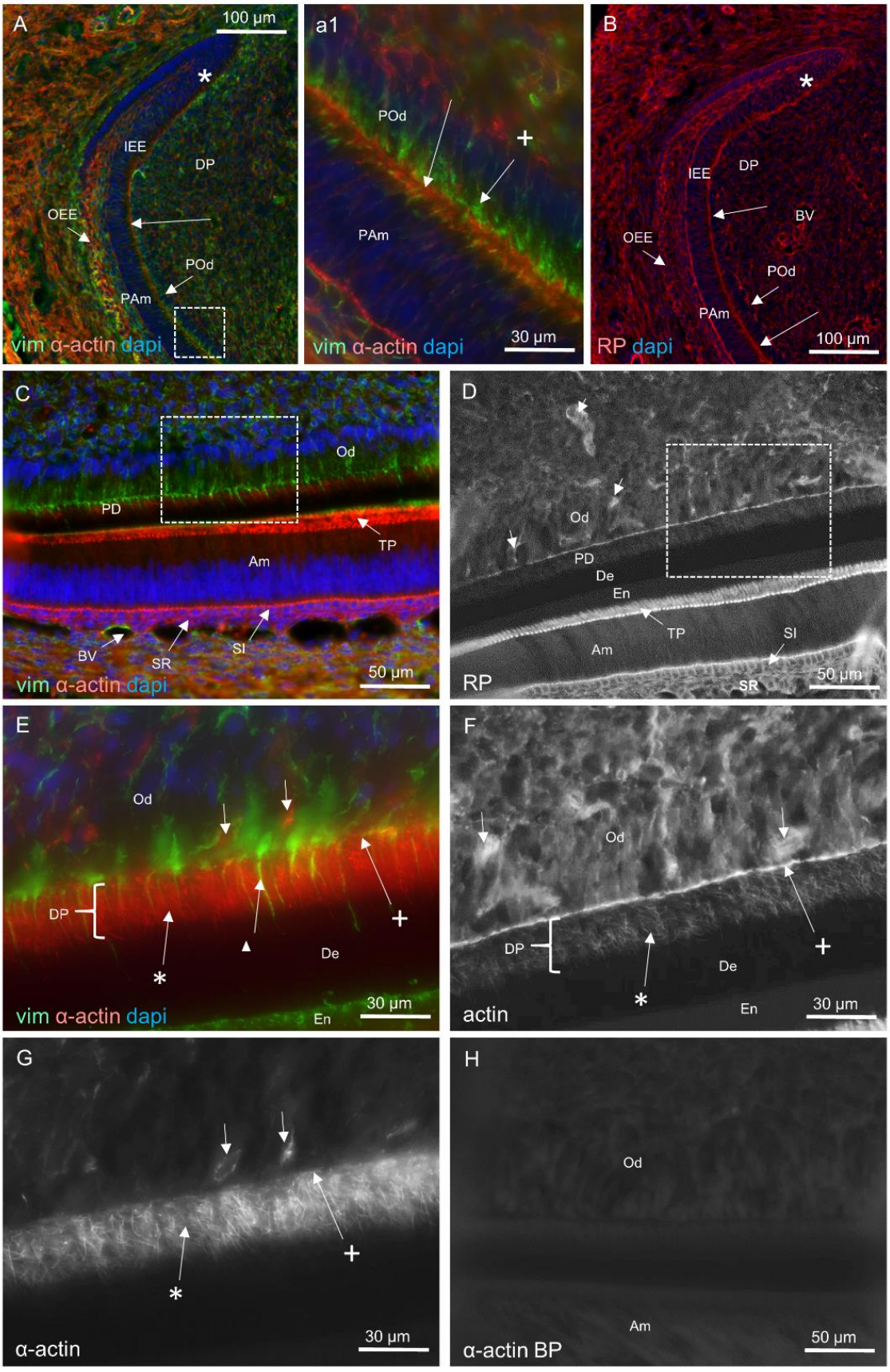
A
100 µm
IEE
DP
OEE
POd
PAm
vim α-actin dapi
a1
POd
PAm
vim α-actin dapi
30 µm
B
IEE
DP
BV
OEE
POd
PAm
RP dapi
100 µm
C
Od
PD
TP
Am
BV
SR
SI
vim α-actin dapi
50 µm
D
Od
PD
De
En
TP
SI
Am
RP
SR
50 µm
E
Od
DP
De
vim α-actin dapi
En
30 µm
F
Od
DP
De
actin
En
30 µm
G
α-actin
30 µm
H
Od
Am
α-actin BP
50 µm

Figure 3.2: Vimentin, α and F actin expressions in demineralised sections from the apical third of rat mandibular incisors of 12w rat.
Images A, a1, C, and E are stained for vim (green), α-actin (red) and dapi (blue), B for RP (red) and dapi (blue), D, F for RP, G for α-actin and H for α-actin + α-actin-blocking peptides. Images A, region of interest a1, and B show the apical bud region (*) with the following structures: inner enamel epithelium (IEE), outer enamel epithelium (OEE), dental papilla cells (DP), pre-odontoblasts (POd), pre-ameloblast (PAm), and blood vessels (BV). α-actin and RP expressions are seen in the junctional interface between POd and IEE (arrows), OEE cells and the BV of the pulp. Highly magnified image a1 shows the junctional interface between POd and PAm is α-actin-IR (arrow) and the apical region of the POd is vim-IR (+). Panels C and D show the region of hard tissue dentine (De), enamel (En) deposition with the following structures: odontoblasts (Od), ameloblasts (Am), Tomes' processes (TP), predentine (PD), stratum intermedium (SI), stellate reticulum (SR), and blood vessels (BV). Regions of interest in C and D are seen in higher magnification in E and F respectively and the component image G, which show two different OPs: actin processes (*), vim-IR processes (▲ in E). Actin expression also presents in the apical cell region of the Od (+) and pulp capillaries (arrows). No α-actin-IR could be detected in image H after using α-actin blocking peptides.

In the middle region of the tooth (Figure 3.3), the thickness of dentine (De) and Od layer increase. This is associated with a more specific SOd cell layer which becomes clearly recognised between Od and central region of the pulp. The Od layer appears as a pseudo-stratified layer of columnar cells with apically located nuclei, about 80μm in thickness. It is highly vascularised, with numerous capillaries both in between and on the apical region of Od (Figure 3.3, A). There is high actin expression in the apical pole of the Od layer associated with tree-like actin processes which extend within the predentine region (images A and D respectively). The extension of these actin processes is similar to that in the apical part of the tooth. The SOd is thinner compared to Od (short and long double sided arrows respectively in image A), but more densely packed. It has different cellular orientations and represents the region of blood supply passage from central pulp cells (CPC) toward the Od layer.

A very complex structure of OPs and their branches is clearly identified within all regions of dentine (Figure 3.3), extending from PD toward the DEJ. α-Actin within the PD region labels two different types of OPs: either vertical without division or horizontal with multidivisional shape processes (images B and C Figure 3.3). The straight vertical processes are short non-divided spikes (+ in image B and its component images), parallel to the main vim-IR OPs (▲), and do not extend further than the PD region. The horizontally actin-IR processes appear longer than the vertical processes and with tree like divisions (*). The main OPs which labelled vim-IR (▲) also have α-actin-IR in their circumferences (●) both with their branches (^). Similar complex actin processes are also labelled with RP stain (* in image D) in the

PD region. This F-actin marker is also expressed by the main OPs and their lateral branches in the inner dentine region (▲ and arrows in image D Figure 3.3 respectively). Similar observations are also present in the middle dentine. The lateral branches emerge at an acute angle from the main processes and directed distally toward DEJ. However, the outer dentine region, which represents the first deposited dentine (mantle dentine), shows much more complex detail. This region has intense staining due to the huge branching of the OPs. Firstly, the OPs are divided between 2 to 3 major branches (* in image E Figure 3.3) within outer dentine and these branches terminate into many terminal and lateral side branches reaching close vicinity to the DEJ (thick arrows in image E).

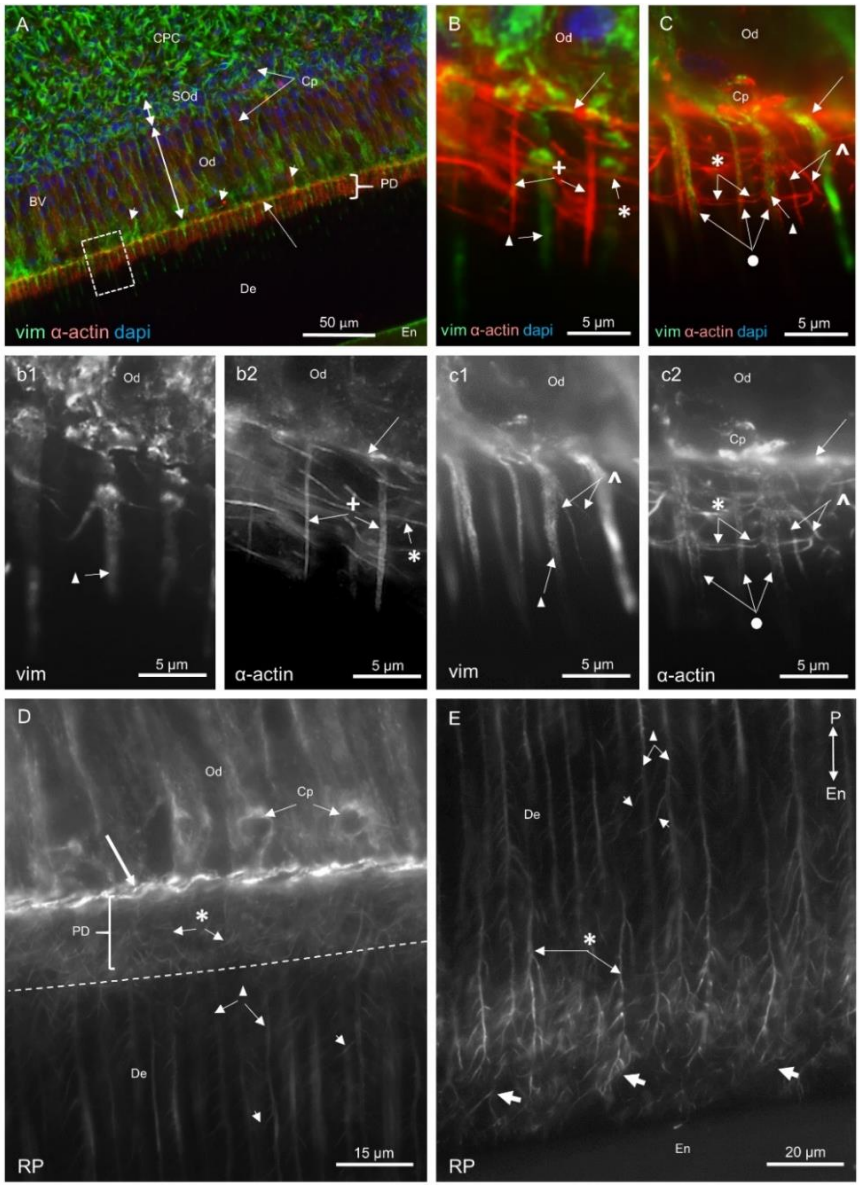

Figure 3.3: Vimentin, α and F actin expressions in the demineralised sections for the middle third of rat mandibular incisors.
Images A, B, and C are stained for vim (green), α-actin (red) and dapi (blue), b1, c1 for vim, b2, c2 for α-actin, D and E for RP. An overview of pulp region in middle tooth third is seen in image A with the following structures: odontoblasts (Od), sub-odontoblasts (SOd), central pup cells (CPC), odontoblast layer capillaries (Cp), predentine (PD), apical part of the odontoblasts cell layer (long arrow), and dentine (De). The box in A highlight the region for the high magnification images B and C and their component images b1, b2, and c1, c2 respectively. In these images the following structures are shown: two types of actin-IR processes are seen: vertical processes (+) parallel to the vim-IR main processes (▲), and horizontal processes (*). Actin-IR also presents in the boundary (●) of vim processes (▲) and their branches (^), Od apical membrane (arrows), and capillaries (Cp). Image D shows actin processes (*) of the main OPs (▲) in PD region. The apical part of the OPs (thick arrow) shows intense staining compared to other regions within Od. The dotted line marks the mineralising front region of the OPs. Lateral branches of OPs (short arrows) are numerous within the inner dentine. The mid and outer dentine regions are seen in image E with long lateral branches (short arrows) of OPs (▲) within mid dentine and major (*) and terminal (thick arrows) branches within the outer dentine region close to enamel (En).

In the incisal region of the tooth (Figure 3.4), the Od layer appears thicker with a heavily packed pseudo-stratified layer of cells (about 100µm in thickness). Similar to the middle region of the tooth, apically located vascular capillaries (arrow heads) are also seen within the apical region of the Od layer. This cellular pole still shows richness in actin and vim-IR (thick arrows in images A, a1 Figure 3.4 and A, B images Figure 3.5). At the same time similar vascular details are also observed with numerous capillaries (Cp) within the SOd running in different directions, which originate from the large blood vessels (BV) within CPC. The complexity of the OPs within PD region is still present with two types of processes, IR to actin and vim (* and ▲ respectively in Figure 3.4 a1). However, the actin tree-like processes decreased in extension to about 14.5µm and are noticeably less dense in comparison to the apical and middle regions of the tooth (Figure 3.2 and Figure 3.3 respectively). Moving toward the the dentino-enamel junction, the OPs show different regions of protein IR within different depth of dentine. Although α-actin is expressed within OPs through its entire thickness (Figure 3.4), vim-IR varies in different regions within their paths, dividing dentine into 4 different regions of expression. Working from the pulp, the first region is described here as region I, shows the highest vim and actin IR and may represent the predentine and inner dentine (Figure 3.4 images B and b2). Moving toward the DEJ, the IR for vim seemed to disappear in the inner part of the middle dentine. This is described as region II in the present study. Continuing outward, region III was characterized by a return of vim-IR within the bulk of the middle dentine (Figure 3.4 images C and c2). Finally, region IV was represented near to the DEJ, with the odontoblast processes appearing to lose their vim-IR.

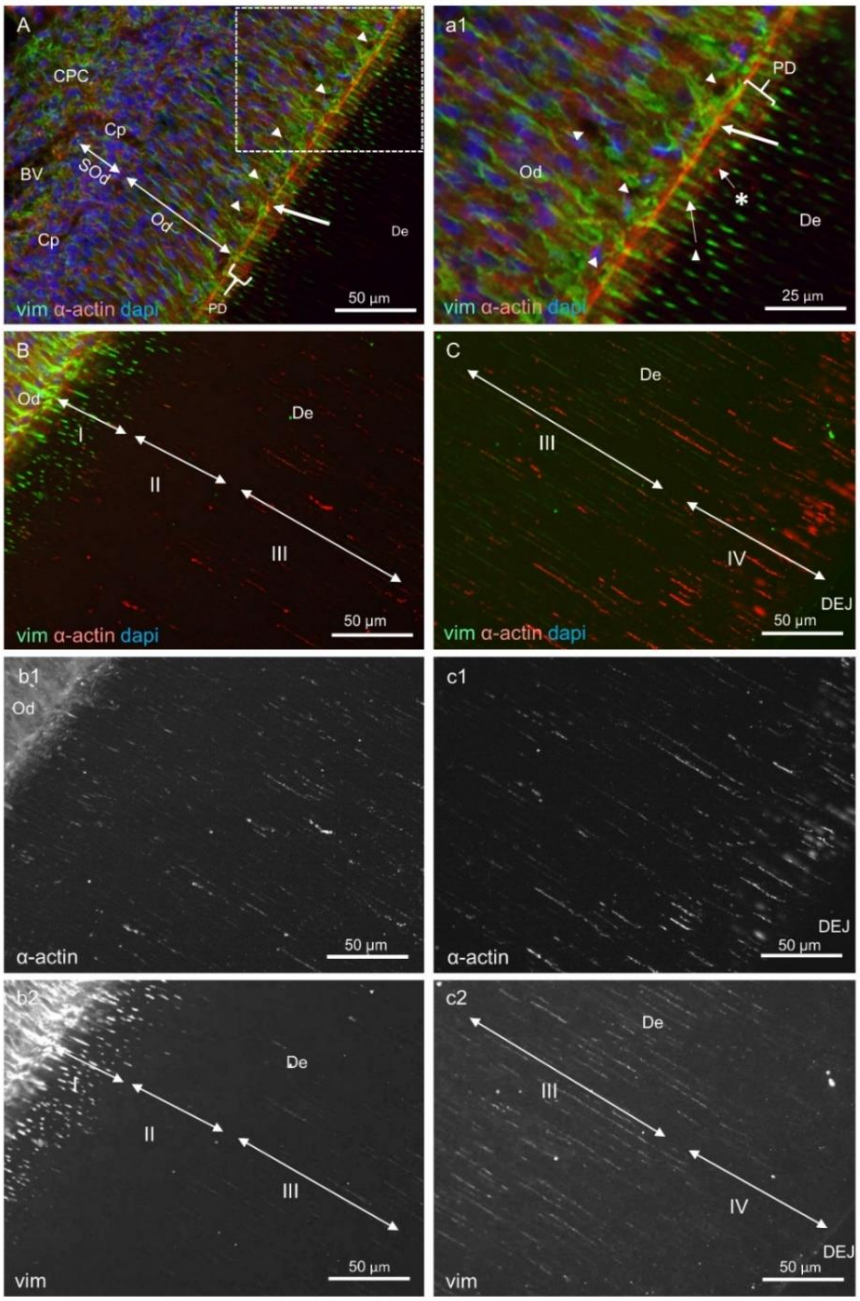

Figure 3.4: Vimentin, α-actin expression in demineralised sections from the incisal third of rat mandibular incisors.
Images A, a1, B and C are stained for vim (green), α-actin (red) and dapi (blue), b1, c1 for α-actin, and b2, c2 for vim. The pulp region in incisal tooth third is seen in image A with the following structures: odontoblasts (Od), subodontoblasts (SOd), central pup cells (CPC), blood vessels (BV) capillaries (Cp), odontoblast layer capillaries (short arrows), predentine (PD), apical part of the odontoblasts cell layer (long arrow), and dentine (De). Double sided arrows marked the thickness of the Od and SOd regions. A region of interest is highlighted in image a1 which shows both vim (▲) and α-actin (*) OPs. Image C is continuous to B (with their component images c1, c2 and b1, b2 respectively). As dentine is thicker in the incisal tooth part, it necessitated the presentation of two sequential images for adequate resolution, rather than one low magnification image. These images show different regions within dentine thickness according to vim-IR of the OPs (I, II, III, and IV in images b2 and c2), although, all these regions express similar α-actin-IR (images b1 and c1).

The complexity of the OPs at different depths within dentine is expressed clearly with RP staining in Figure 3.5. In the inner dentine and after passing the PD region, the OPs have numerous lateral branches which run in a forward direction between the main processes (1 and 2 in image B Figure 3.5). Similar complexity of the OPs is also identified in the middle dentine (Image C Figure 3.5). At higher magnification (as seen in image c1 Figure 3.5), there are two OPs (1 and 2) sending many lateral branches (a-f) which emerge about 45º from the main processes in a distal direction and directed toward adjacent processes (3-6). Some of these lateral branches (a and b) extended far away from their original OPs to about 4 to 5 processes distant. Other lateral branches are evident (d and e), where the origin process for them is not clear in this section, but they seem either to connect adjacent OPs (4 and 3 respectively) in a proximal direction or to be overlapped by these processes. In the outer dentine (Image C and higher magnified region in image c2 Figure 3.5), complex terminal branches of the OPs are also seen with numerous terminal branches for each process as mentioned previously in middle tooth part in Figure 3.3.

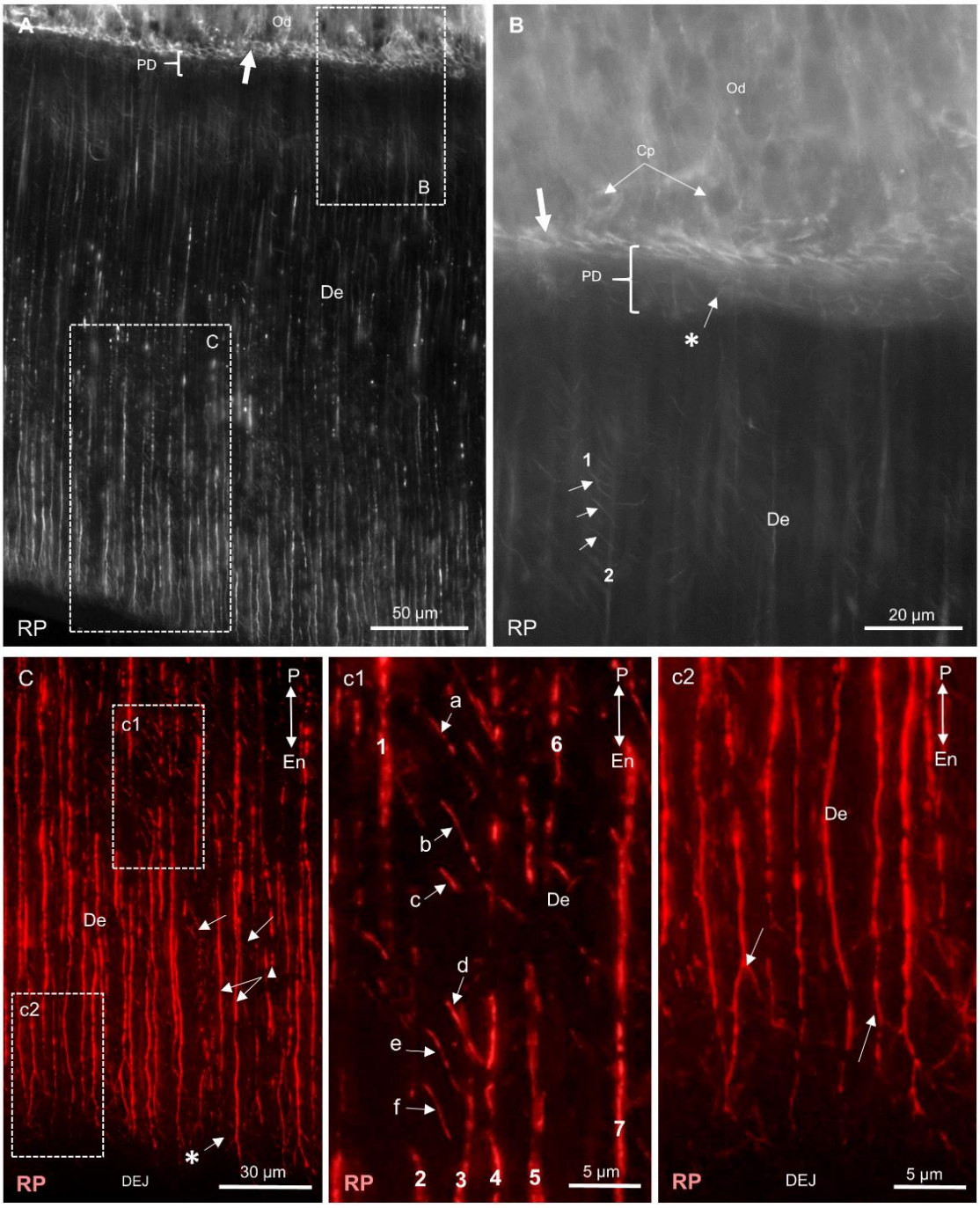

Figure 3.5: F-actin expression in the incisal third of rat mandibular incisor.
All images are stained for RP. Image A, shows De region with following structures: odontoblasts (Od), predentine (PD) and apical region of the Od (thick arrow). The two regions of interests are shown in images B and C. Image B shows the Od, predentine (PD) and inner region. The actin tree processes (*) in PD are fewer in number. Two OPs (1 and 2) and their three lateral branches (arrows) are highlighted. The mid and outer dentine are shown in image C. The OPs (▲) give many lateral branches (arrows) directed distally toward DEJ. Two regions of interest for mid and outer dentine are shown in higher magnifications in images c1 and c2 respectively. In c1 image, seven processes have been numbered (1-7) in addition to five lateral branches (a-f). The complexity of the OPs terminal branches (long arrows) are seen in image c2. Double sided arrows in images C, c1 and c2 are for orientating the pulp and enamel sides of the images.

NaK-ATPase:

A house keeping marker, NaK-ATPase, is not expressed in the pulp-side within the apical tooth region before hard tissue deposition commences (Figure 3.6 image A). However, NaK-ATPase-IR can be recognised within the outer cells of the OEE. After starting dentine deposition and moving toward middle and incisal regions of the tooth (Figure 3.6 image B and D respectively) this marker becomes more specific in the SOd region and to a lesser extent in Od cell layer. In higher magnification images of the PD region (Images C and its component images c1 and c2 Figure 3.6), the main OPs (▲) and their branches (+) show vim-IR. At the same time, the NaK-ATPase-IR also appears in a faint expression in the perimeter of these processes, because it may label their cell membrane. Additionally, there are some processes which shows only NaK-ATPase-IR and no vim-IR. This could be the labelling of the NaK-ATPase to the cell membrane of some α-actin tree-like processes which previously presented in Figure 3.2 and Figure 3.3. In the incisal tooth section and with increase thickness of deposited dentine (Figure 3.6 image D), NaK-ATPase-IR is only detected in the inner half within the OPs, while no observed NaK-ATPase-IR is seen within the external dentine half (images D and G Figure 3.6). In regions were NaK-ATPase-IR still working, it does not only label the main OPs (▲), but also the lateral (arrows in images E and Figure 3.6) and major branches (* in image F) of the OPs.

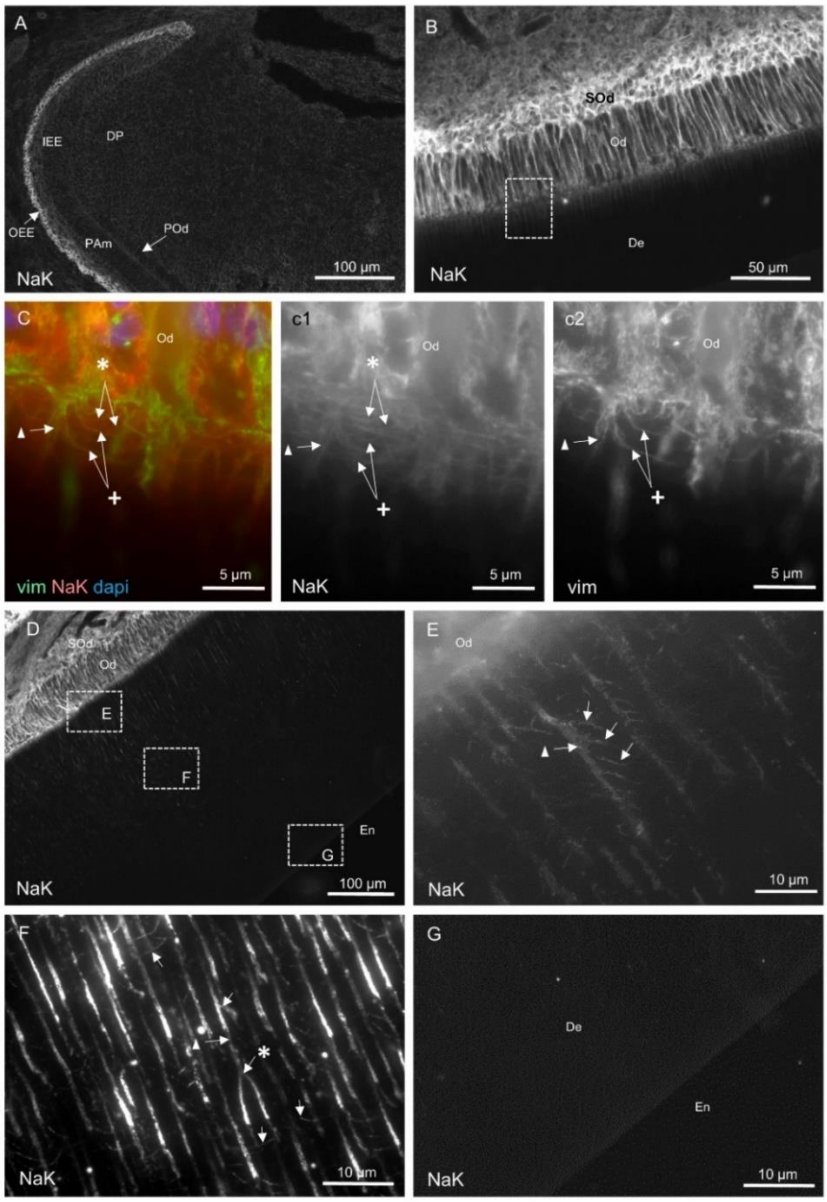

Figure 3.6: NaK-ATPase expression in demineralised sections from different portions of the rat mandibular incisors.
All panels are stained for NaK-ATPase, except image C for vim (green), NaK-ATPase (red), and dapi (blue), and c2 for vim. An overview image A of the apical bud shows the following structures: outer enamel epithelium (OEE), inner enamel epithelium (IEE), dental papilla cells (DP), pre-ameloblasts (PAm) and pre-odontoblasts (POd). Image B shows a demineralised section from the middle part of the tooth showing subodontoblast cells (SOd), odontoblast (Od), and dentine (De). Region of interest in B is shown in higher magnification in image C and its component images c1 and c2. These images show the main OPs (▲) and their branches (+), and other NaK-ATPase-IR processes (*). An overview image of the pulp and dentine in incisal tooth part is shown in image D. There are three regions of interest which are presented in higher magnifications in images E F and G. The inner dentine is seen in image E showing one of the OPs (▲) with many lateral branches (arrows). Mid dentine region is seen in image F identifying one OP (▲) which has many lateral branches (arrows) and one major branch (*). In outer dentine region (image G) no NaK-ATPase-IR has been identified within OPs.

OX-6:

The dendritic cell marker (OX-6) was used in combination with α-actin in order to exclude other cellular components within the Od cell layer and their possible relationship to the actin processes within PD region. In the apical part of the incisor (Figure 3.7 A), no positive OX-6 cells were identified either in the pulp or in enamel organ cellular components. The only positive cells present are in the connective tissue surrounding the tooth apical bud (arrows). After dentine deposition has commenced, (Figure 3.7 B), some OX-6-IR cells are seen in between the cells of Od associated with the capillaries within this cell layer (arrows in image B). No OX-6-IR processes for these cells have been identified in association with α-actin-IR OPs in PD region (* in image B). The number of the OX-6-IR cells increase in the middle and incisal third of the tooth within all regions of the pulp especially in SOd and CPC (arrow heads in Figure 3.7 image C) and in association with the BV. In higher magnification (image D Figure 3.7), the OX-6-IR cells are seen within the Od layer, either in between cells (arrow) or associated with the apically located capillaries (+) within Od cell layer, but the cellular processes within predentine region (*) are only α-actin-IR OPs.

Tissue sections that had been incubated in isotype controls, rabbit IgG monoclonal (EPR25A) and normal mouse IgG1, show a complete absence of immunoreactivity.

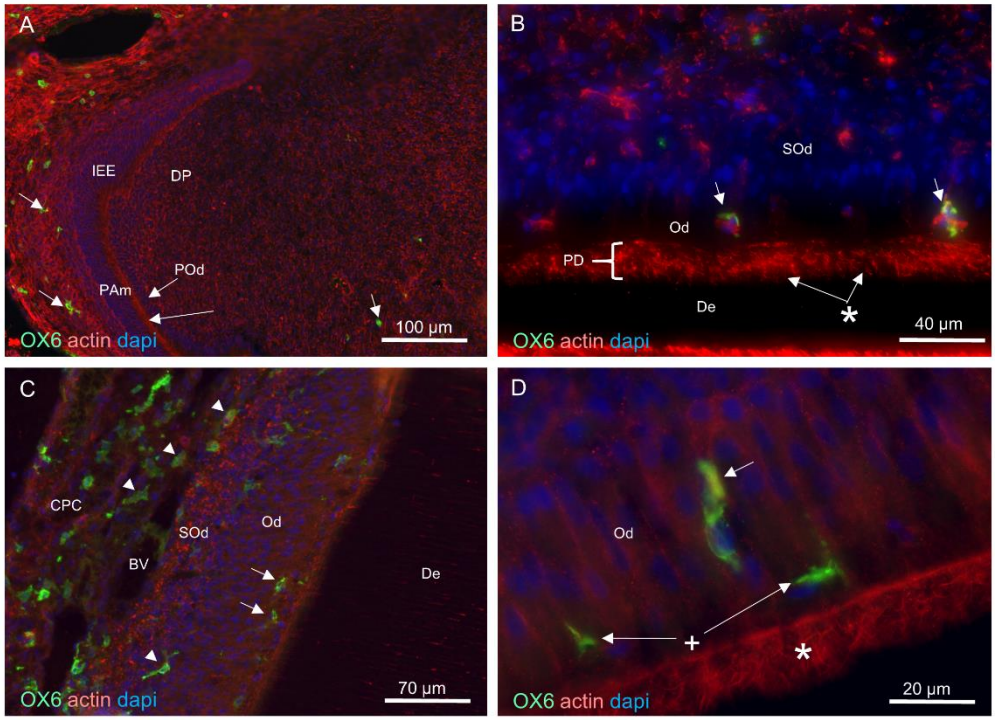

Figure 3.7: Dendritic cell marker (OX6) expression in demineralised sections of rat mandibular incisors.
Images A, B, C, and D are stained for OX6 (green), actin (red) and dapi (blue). An overview image for apical bud region in image A with following structures: dental papilla (DP), inner enamel epithelium (IEE), pre-odontoblast (POd), pre-ameloblasts (PAm), junction between POd and IEE (long arrow) and dendritic cells (short arrows). Image B shows OX-6-IR cells within Od region, and (*) symbol highlight the α-actin-IR OPs in predentine region (PD). Image C shows a highly developed region of the tooth containing more OX-6-IR cells. In higher magnification (image D), 2 dendritic cells lie within Cp of the Od region (+), while one big dendritic cell (arrow) is seen between the Od cells.

3.3.2 Cavity samples:

The work in this section was done on demineralised cross sections for cavity region in the incisal third of the rat mandibular incisor. Three controls and experimental reading groups are available depending on the incubation time: immediate fixation (A1, A2), 3 hours (B1, B2) and 24 hours (C1, C2) incubation before fixation. Each group shows images and quantitative values for the length ratios of OPs.

Control surfaces:

The non-cavity, intact, or normal surfaces, as control groups, confirm the first result section about the extension of OPs across the entire thickness of dentine. α-Actin-IR is identified along the entire length of OPs within different groups of the study. Vim-IR shows regional variations with the deficiency in the outer region of dentine (IV) as shown in Figure 3.8 and Figure 3.9. The terminal branches of the OPs also show

similar complexity in the outer dentine regions with many branches terminating within the DEJ (Figure 3.8 images F and Figure 3.9 image B and C).

Measurements of the length ratios OP/DL for control groups are shown in Figure 3.10 A, B, C and Table 3-1. Values for all groups range between 0.95 and 1. This means that in control surfaces (non-cavity surfaces) the OPs extend fully across the dentine thickness. The Kruskal Wallis test was used instead of ANOVA to identify the statistical significant differences between these groups because the data in these groups were not normally distributed as tested by Shapiro Wilk test ($p<0.05$). There was no statistical significant difference between 3 control groups (A1, B1, and C1) by Kruskal Wallis test ($p>0.05$).

Experimental (cavity) surfaces:

60sec group A2:

The traumatised OPs, labelled with α-actin, are seen close to the cavity margin (dotted line in Figure 3.8). Some show immediate retraction as a result of cutting (arrows in Figure 3.8 Images A). Actin labelled the full length of OPs (image C in Figure 3.8). Although, the traumatised and retracted OPs lost their lateral branches (image E Figure 3.8), most of the unretracted processes still preserved these lateral branches (image F Figure 3.8)

Measurements of the length ratios (OP/L) for group A2 are shown in Figure 3.10 A and Table 3-2. These indicate that some OPs retracted immediately after cutting (values range from 0.7-0.925). However, most of the processes persist in their original places after cutting (ratios between 0.925-0.975). The presence of differences between none responding OPs and the control group (A1) which illustrated in Figure 3.10 A (between 0.975 to 1) is due to the cut amount of dentine. In order to measure the instance speed of retraction for the furthest retracted processes within group A2, the values between 0.725-0.8 were chosen (about 24 processes). The average retraction distance for the processes was 122µm. If the actual cutting time required for preparing one cavity is considered to be 1 min (60sec), the retraction speed of these processes will be as fast as 122µm/min (2.03µm/sec).

3 hour group B2:

After 3h of incubation, the traumatised OPs show different levels of pulpal-ward retraction leaving empty dentinal tubules behind (2 arrows in Figure 3.9 image A).

However, several processes remained in their old positions close to the cavity margin (thick arrow). Under higher magnification (Figure 3.9 images b1), these processes show two different profiles: either preserving their lateral branches (arrows), or appearing without branches as straight processes (arrow heads). Only α-actin labels all these retracted processes, while vim-IR appear in some (Figure 3.9 b2). Measurements of OP/L ratios (Figure 3.10 B) shows a varied range of frequencies from 0.95 for the processes which still reside within original sites to the half distance of the retracted processes (0.45-0.55). The median value is 0.687 (Table 3-2) with maximum frequencies for length ratios between 0.65-0.675. Therefore, most of the traumatised OPs have managed to retract toward the pulp. To calculate the retraction speed, the maximum frequency range was chosen which consisted of 22 processes with average retraction distance about 198.87µm to give nearly 1.1µm/min (0.02µm/sec) which is less than about 100 times the immediate retraction speed calculated in group A2.

24 hour group C2:

In the 24h incubation group, more OPs retracted toward the pulp leaving more empty space behind within dentinal tubules (* in images C Figure 3.9). Almost all of the retracted OPs appeared without lateral branches (arrows in images D, d1 and d2 Figure 3.9) and labelled both α-actin and vim-IR within middle dentine region. OPs labelled with the former, appear more in number than those labelled with latter antibody. With α-actin (arrows in image d2 Figure 3.9), some OPs show globular ends after retraction. Measurements of length ratios in group C2 (Figure 3.10 C) shows increased numbers of retracted OPs compared to group B2 (image B Figure 3.10). This can also be identified in Table 3-2 by inverted skewness values between these two groups. However, the higher frequency values of OPs retraction are still between 0.65- 0.675, but with a narrower whole frequency range (between 0.45-0.8). This means the number of OPs which didn't manage to retract or those which showed minimum retraction at 3h incubation period (ratios larger than 0.675 in Figure 3.10 B) become more retracted at 24h. The chances of processes still residing in their old places within dentinal tubules become less. However, no process retracting below the ratio of 0.45 has been identified in group C2 (Figure 3.10 C) which is similar to the lower ratio in group B2. It is worth mentioning here that no cellular changes have been noticed within Od cell bodies in all incubation groups.

Although groups B2 and C2 were normally distributed according to Shapiro Wilk test ($p>0.05$), they showed no homogeneity of variances according to Levene test ($p<0.05$). Therefore, to identify the presence of statistical differences within ratios of OP/L for experimental groups (A2, B2, and C2), the Kruskal Wallis test was used. This test shows a high significant difference ($p<0.001$) present between these groups. To compare between them, a Pairwise Comparison test (Table 3-3) shows highly significant differences ($p<0.001$) between all of these groups.

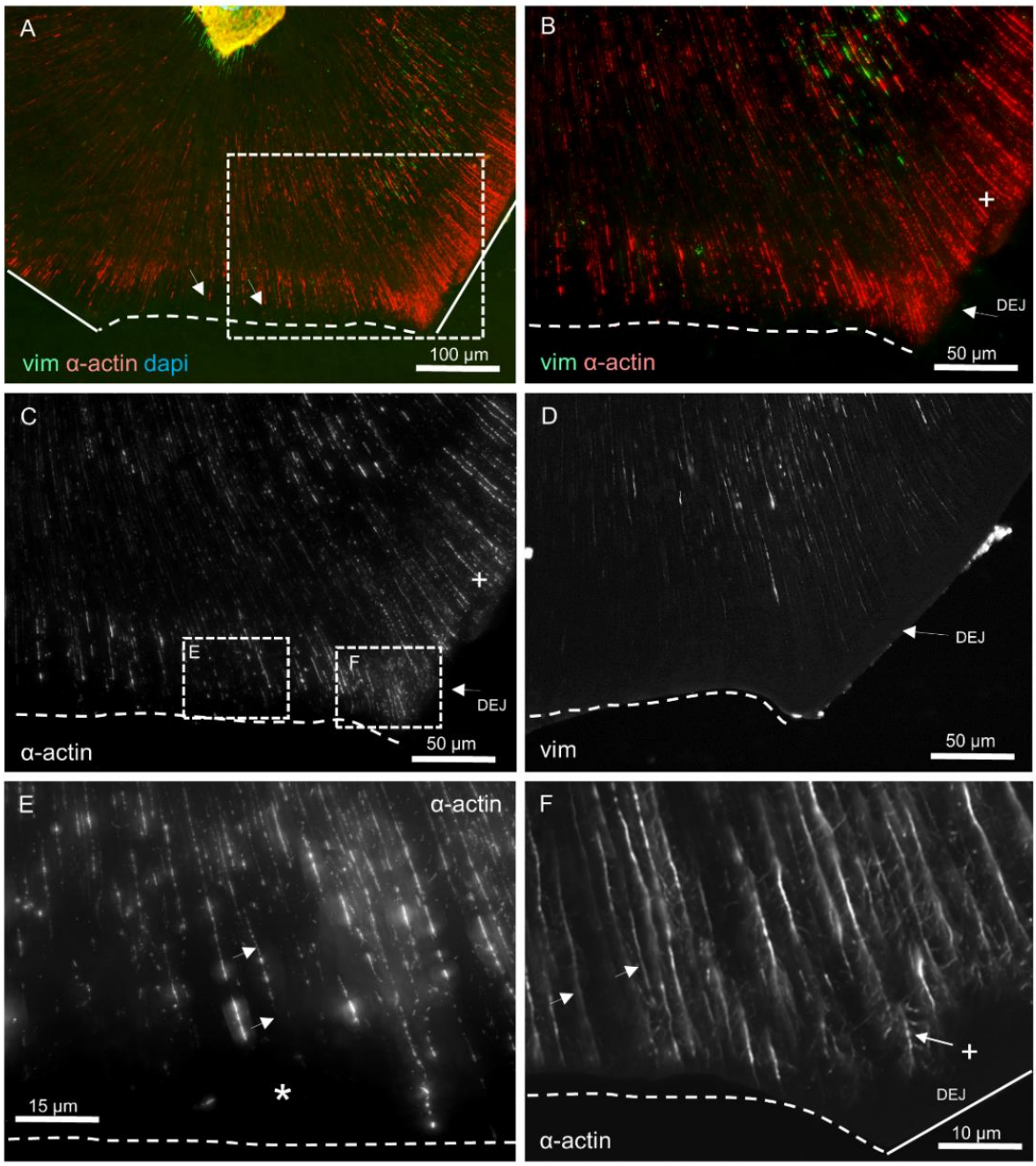

Figure 3.8: OPs in group A (60sec) samples.
Images A, B were stained for vim (green), α-acin (red), dapi (blue), D stained for vim and the rest images stained for α-actin. Overview of the tooth section is shown in image A containing cavity surface (dotted line), intact tooth surfaces (solid lines) and some retracted OPs (arrows) which also appear in component image C. Region of interest in A is shown in B and its component images C and D. In B and D, the OPs have vim-IR in the middle and inner part of the outer dentine while the α-actin-IR appear within the full thickness of the OPs as seen also in image C. The two regions of interest in C are represented in higher power in images E and F. In image E, the traumatised and retracted OPs (arrows) are seen without lateral branches and leaving empty dentinal tubules behind (*). The other region in image F shows that most of the traumatised and unretracted OPs still have their lateral branches (arrows) similar to the intact OPs (+) beyond DEJ.

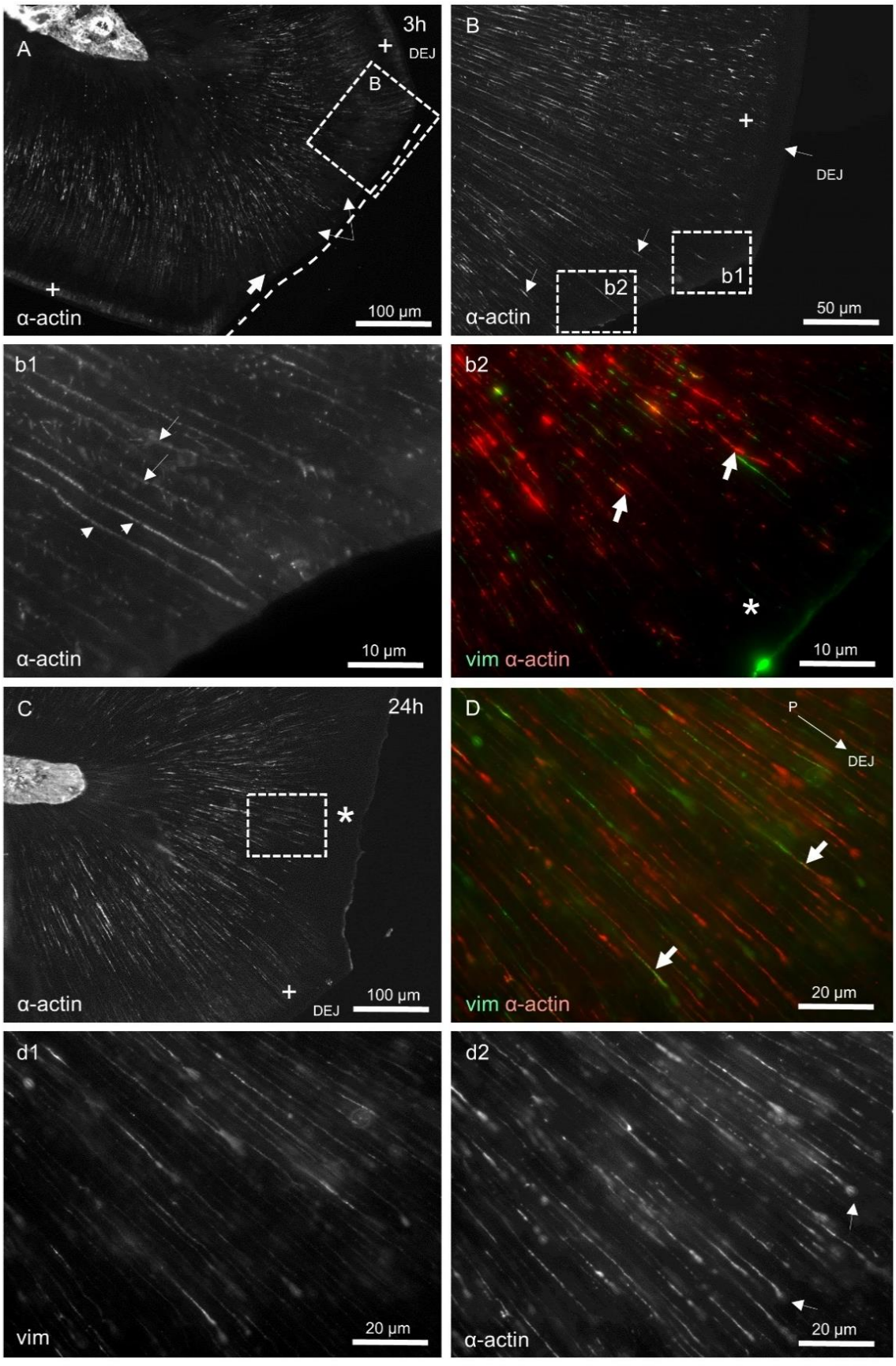
A
3h
DEJ
B
α-actin
100 µm
B
DEJ
b1
b2
α-actin
50 µm
b1
α-actin
10 µm
b2
vim α-actin
10 µm
C
24h
α-actin
DEJ
100 µm
D
P
DEJ
vim α-actin
20 µm
d1
vim
20 µm
d2
α-actin
20 µm

Figure 3.9: OPs in groups B and C (3h and 24h respectively) samples.
Images b2 and D were stained for vim (green), α-acin (red), dapi (blue), d1 stained for vim and the rest images stained for α-actin. In 3h incubation sections (Image A), the intact dentine surface still has complex terminal branches of the OPs (+) similar to 24h sample in image C. Region of interest in A is shown in higher magnification in B which illustrate the edge of the cavity in order to compare between intact OPs (+) and those under cavity surface (arrows). Two regions of interest are also shown in higher magnification in images b1 and b2. In image b1, some OPs are still not retracted. These processes either lose their lateral branches (short arrows) or still preserve them (long arrows). The other region in image b2 shows that almost all of the retracted OPs lost their lateral branches and have α-actin and some vim-IR. The region of empty dentinal tubules marked with (*). More OPs retraction is seen in 24h incubation sections (in image C) under the cavity surface. A region of interest is shown in higher magnifications in images D and its component images d1 and d2. An oblique arrow in D orientates the directions of tooth pulp and DEJ. The retracted OPs (arrows in d2), terminated with globular shape due to retraction within the dentinal tubules (arrows in image d2).*

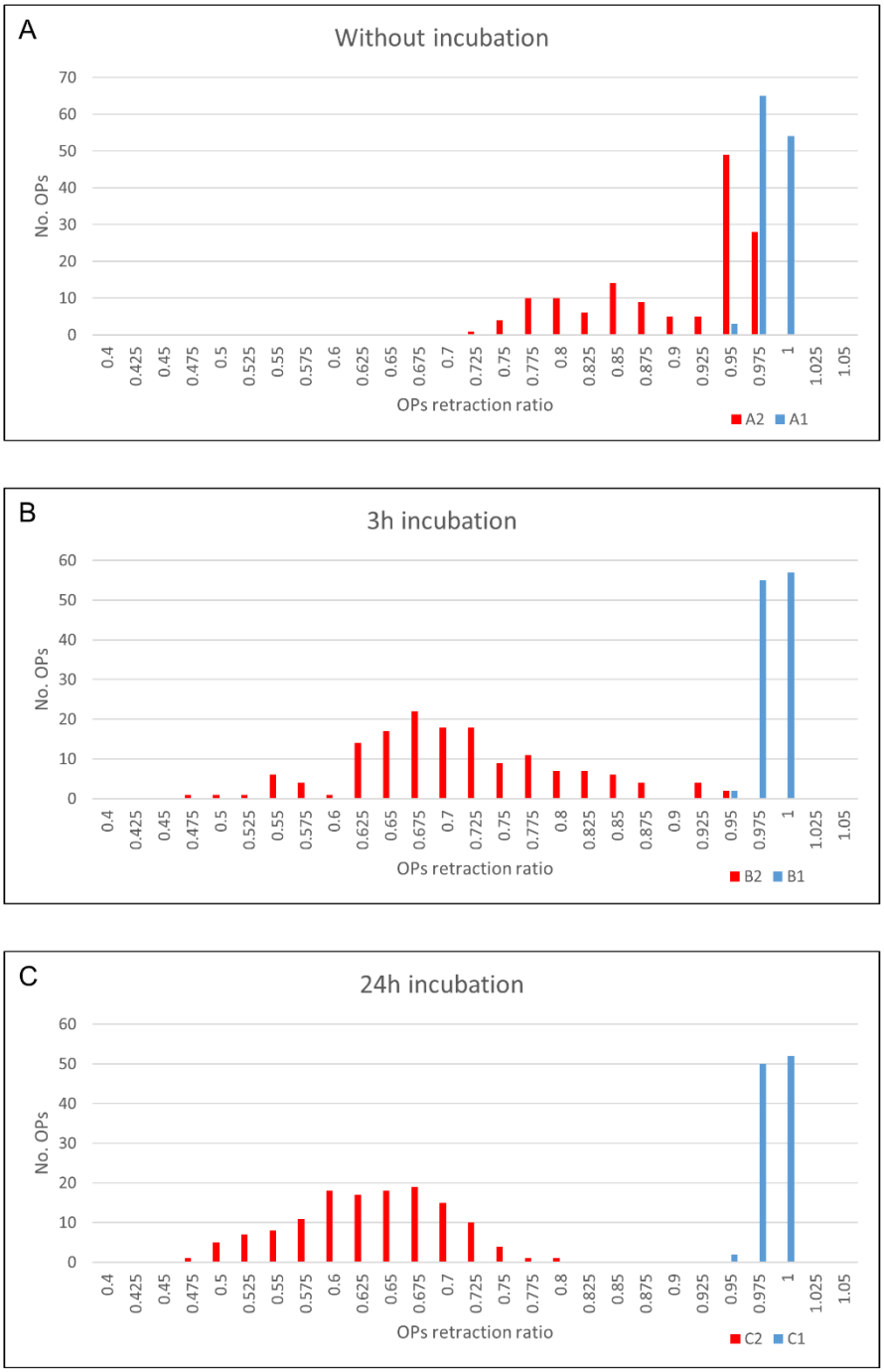

Figure 3.10: Frequency amplitude distribution of the OP length ratio measurements. A shows groups without incubation (A1, A2), B shows groups with 3h incubation (B1, B2), and C shows groups with 24h incubation (C1, C2). The OPs length ratio for the control groups (A1, B1, and C1) is OP/DL, while for the cavity groups (A2, B2, and C2) is OP/L.

Groups	Mean	Min	Max	Median	Interquartile range	Skewness
A1	0.973	0.938	0.987	0.974	0.008	-1.665
B1	0.974	0.949	0.998	0.975	0.01	-0.613
C1	0.973	0.942	0.990	0.974	0.013	-0.461

Table 3-1: Descriptive statistics for control surfaces (ratio OP/DL) of the three time period groups.

Groups	Mean	Min	Max	Median	Interquartile range	Skewness
A2	0.890	0.714	0.963	0.935	0.115	-0.792
B2	0.697	0.467	0.948	0.687	0.112	0.28
C2	0.622	0.468	0.777	0.625	0.095	-0.16

Table 3-2: Descriptive statistics for experimental surfaces (ratio OP/L) of the three time period groups.

groups	p-value
A2 vs B2	0.000
A2 vs C2	0.000
B2 vs C2	0.000

Table 3-3: Multi-comparison test (post-hoc) test ($p<0.05$) for OPs length ratios for three time periods of experimental groups.

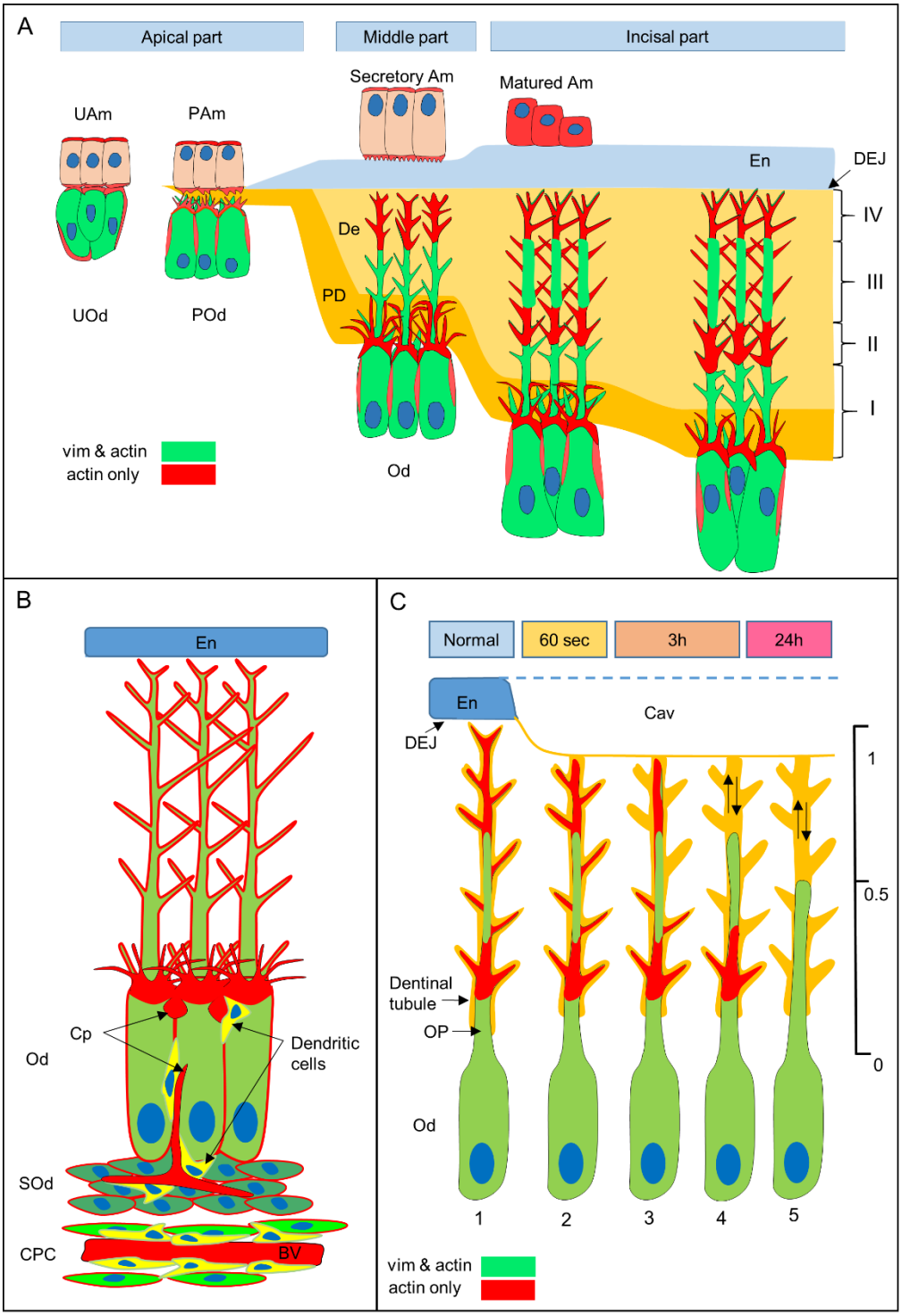
A
Apical part
Middle part
Incisal part
Secretory Am
Matured Am
UAm
PAm
En
DEJ
De
PD
IV
III
II
I
UOd
POd
Od
vim & actin
actin only
B
En
Cp
Od
Dendritic cells
SOd
CPC
BV
C
Normal
60 sec
3h
24h
En
Cav
DEJ
1
0.5
0
Dentinal tubule
OP
Od
1
2
3
4
5
vim & actin
actin only

Figure 3.11: Diagrammatic summery of key findings.
A and B depict observations beneath intact surfaces, while C illustrates events beneath exposed surfaces. In A, the apical portion of the tooth shows cells of undifferentiated ameloblast (UAm) contacting the undifferentiated odontoblast (UOd) cells. After withdrawal from cell division cycle both pre-ameloblast (PAm) and pre-odontoblast (POd) cells polarise and the latter cells develop both actin and vim processes as they secrete PD matrix. In the middle portion, Ods appear longer and columnar in shape with polarised nuclei. The PD region contains complex tree-like actin OPs in addition to the main OPs which express both actin and vim and extend fully across the full thickness of dentine. These processes show complex lateral and terminal branches. In the incisal portion, the Od layer is pseudostratified, and the main OPs present 4 distinct regions of vim-IR. These regions become wider with increased dentine thickness and are accompanied by decreased density of tree-like actin OPs within PD. Panel B shows the position of the dendritic cells within Od, subodontoblast (SOd), and central pulp region (CPC) in association with the blood vessels. Panel C shows time dependant retraction of OPs beneath exposed dentine surfaces. OP #1 is the control, #2 is 60sec after cavity preparation with maintained position. OP #3 and 4 (3h), show two types of OPs response either maintaining its original position or retracted. OP #5 (24h) shows OPs retracted to half dentine thickness.

3.4 Discussion

3.4.1 Non-cavity samples

This part of the study investigated the complexity of Ods and their cellular processes during different stages of development in continuous growing rodent mandibular incisor. The complexity of SOd and CPC has also been identified. The continuously growing incisors of rodents have provided a valuable model for investigating physiological processes within the dental organ, including epithelial-mesenchymal correlated induction processes, cellular differentiation mechanisms (Ohshima and Yoshida, 1992; Arana-Chavez and Massa, 2004), and other studies on cellular function (Yu and Abbott, 2007). Almost all previous research that deals with the extension, density and complexity of the OP has been conducted on teeth with a limited growth period including human (Kubota et al., 1969; Thomas, 1979; Gunji and Kobayashi, 1983; Sigal et al., 1985; Grötz et al., 1998; Goracci et al., 1999; Kagayama et al., 1999; Yoshiba et al., 2002; Carda and Peydro, 2006) and other animal species (Sigal *et al.*, 1984a; Byers and Sugaya, 1995; Tsuchlya *et al.*, 2002) . One frequently highlighted benefit of the continuously growing tooth model is the opportunity to study physiological processes such as dentinogenesis from the early stages of mantle dentine formation until complete dentine mineralization in the same tooth. It has been reported that after formation of the mantle dentine and an increase in the thickness of dentine, the OPs start to retreat and reside in the inner third of the dentine (Luukko *et al.*, 2011). In an effort to model the human tooth crown situation, investigations in the current study were limited to the enamel-covered, labial side of the rat incisor (Beertsen and Niehof, 1986).

Structural protein (vim and actin)

Intermediate filaments and microfilaments have been demonstrated in previous studies to be major components of OPs and their branches which extend from the Od cell body (Lesot *et al.*, 1982; Thomas and Carella, 1983; Thomas and Payne, 1983). In this study, microfilaments (actin fibres) were investigated by fluorescent staining with rhodamine phalloidin and immunohistochemistry α-smooth muscle actin. Vimentin antibody was used as a marker for intermediate filaments. In their filamentous derived form, these proteins are essential cytoskeletal scaffolding elements which participate in ordering and shaping the compartments and organelles to their appropriate physical locations (Gunning *et al.*, 2015). A second property of some polymers is that there is a directed polymerization or depolymerisation ability.

This can provide pushing or pulling forces that can be integrated into biological processes when movement is a necessary component (Pollard and Cooper, 2009).

During early cellular differentiation, a rich actin apical pole of POd and PAm is associated with apical accumulation of vimentin within POd cell bodies were clearly identified (Figure 3.2). The presence of reciprocal transmembranous epithelio-mesenchymal communications between these cells has been reported to control cellular differentiation and their re-structural modification (Thesleff, 2003). The redistribution of the structural filaments from a uniform distribution in the undifferentiated cells of the dental papilla, into accumulation of these filaments in the apical pole of the POd was suggested to be responsible for polarization of these cells prior to their terminal differentiation (Lesot *et al.*, 1982; Nishikawa and Kitamura, 1986).

After predentine deposition commences, the cellular polarity of the Ods is evident with concentrated apical actin pole associated with the appearance of multiple processes of two different types: actin and vimentin. The apical concentration of actin filament bundles is associated with the plasma membrane and is in a direction parallel to the long axis of the tooth. This has been reported to provide essential contractile isomeric form to keep the Ods in a single layer despite the pressure applied by accumulative dentine deposition (Nishikawa and Sasa, 1989). Although, it has been published that the newly differentiated Ods have more than one apical cellular process (Couve, 1986; Ohshima and Yoshida, 1992), this is the first study to identify the presence of more than one type of OP, with IR to structural proteins actin and vimentin, within the predentine region (Figure 3.2). It is uncertain from the current investigations what could be the function of the actin processes. It can be hypothesised that these processes are part of the cellular stabilizing system of the Od cell layer in combination with the presence of apical rich actin pole (Nishikawa and Sasa, 1989). These processes with their different orientations could provide better support for the Od cell layer against lateral forces that could be generated from the centripetal pressure of accumulative dentine formation. Another suggested role is that these processes could be associated with dentine matrix deposition, since the density and length for these processes within the predentine region reduced toward the incisal edge (Figure 3.4 and Figure 3.5). It also has been reported that nerve endings were seldom observed within the Od cell layer of the rat incisors (Nishikawa, 2007). The role of Ods as mechano-sensory cells (Magloire *et al.*, 2009) has been

established. This can be evidenced by the excitable properties of these cells (Allard *et al.*, 2006), the concentration of mechanosensitive mediator (calcium-activated potassium channel-KCa and mechanosensitive TREK-1 potassium channels) (Allard *et al.*, 2000; Magloire *et al.*, 2003) and thermos-sensitive (TRPV1) ion channel (Okumura *et al.*, 2005) preferentially in the apical cell part (terminal web). In addition, the cytoskeleton is part of the system that senses both external forces applied to the cell and the mechanical property of the cell's environment. This could alter different aspects of cell function, including gene expression and cellular differentiation (Pollard and Cooper, 2009). Therefore, the presence of the actin processes emerging from the Ods terminal web toward the predentine region could contribute to the sensing tools of these cells.

In the middle and incisal thirds of the tooth, the thickness of the Od layer has been increased as a thick pseudo-stratified layer and is associated with a persistent apical rich actin region (Figure 3.11 B). The increase in thickness of the Od layer could reflect the increase in its activity in dentine deposition in these parts of the tooth with numerous capillaries evident (Ohshima and Yoshida, 1992). On the other hand, continuing dentine deposition in an inward direction limits the total surface area of the dentine-forming face. The presence of actin filament bundles as well as myosin in the Od apical region associated with the plasma membrane may help in centripetal cellular movement (Nishikawa and Sasa, 1989). The contractile ability of these proteins could be the cause for this type of movement (Pollard and Cooper, 2009). In addition, it may also help to resolve cell crowding by shifting of the cellular configuration from simple single into a more complex, pseudostratified layer (Ohshima and Yoshida, 1992). In addition, the cell membrane of the mature Od displays αvβ3 integrins which are suspected to be involved in continuous reorganization of actin that accompany process elongation and cell body movement toward the pulp core (Lucchini *et al.*, 2004; Staquet *et al.*, 2006).

In the current study, OPs were observed by fluorescent labelling to extend to the DEJ. This was through the expression to rhodamine phalloidin stain and different antibodies which were different at different depths within the dentine (Figure 3.3 and Figure 3.11 A). The IR to vimentin was greatest in region I and lowest in regions II and IV. By contrast, the expression of α and F-actin was consistent in all regions within the entire thickness of the dentine. The increase in the thickness of deposited dentine requires the present of actin as a structural element responsible for OPs

elongation (Pollard and Cooper, 2009; Gunning *et al.*, 2015). In addition, ultra-structural studies found the localisation of actin filaments within the OP as a network of bundles beneath the cell membrane running along the long axis of the process (Nishikawa and Kitamura, 1987). All the above support the current study findings that actin is expressed within the full length of the growing OPs. On the other hand, the presence of intermediate filaments (vim-IR) in particular regions, named I and II in the current study, could reflect the special job allocated for these two regions within the OPs. The highest intensity was observed in the basal part of the OPs. These filaments are abundant in the core of the processes and run in singular filaments unlike the actin filament bundles (Nishikawa and Kitamura, 1987). In addition to their role in maintaining the cell shape, they act as an active tensional bearer and a resistant element for the mechanical forces (Pollard and Cooper, 2009). Intermediate filaments in this study are present only in certain areas, possibly due to specific structural or functional requirements not present over the entire length of the process. Alternatively, the current observation of lower vimentin-IR in the distal regions of OPs may reflect imperfect fixation of these proteins deep within the tissue specimens.

Two previous immunofluorescence studies have reported differences in the IR to different structural proteins (vimentin, actin and tubulin) within the OPs of humans (Sigal *et al.*, 1985) and rat molars (Sigal *et al.*, 1984a). In common with current findings, they reported actin-IR to be more concentrated in the pulpal third of the process, but their observation of vimentin and tubulin throughout the length of the OP was at variance to current findings. This variation could be due to differences in samples used (continuous growing vs limited growing teeth), age of the sample, or techniques (fixation, demineralisation, sectioning or staining). Regional differences in the structure of the OP i.e. certain protein filaments may only be present in certain regions within the process were also identified within these studies.

Studies have also reported the possible presence of a tubular lining membrane that remained after decalcification of the peritubular dentine and appeared as an electron dense structure in TEM (Thomas, 1984). This membrane is termed the lamina limitans and could be artifactually observed as OPs (Holland, 1985). In contrast, the observation of intracellular proteins, vimentin, and actin, and to a certain extent, membrane located enzyme NaK-ATPase in the present, and other immunohistochemical studies (Sigal *et al.*, 1984a; Sigal *et al.*, 1985; Tsuchlya *et al.*, 2002), the identification of processes with microfilaments in TEM studies in the outer

dentine of human samples (Frank and Steuer, 1988), and the presence of real process reported by SEM (Kelley *et al.*, 1981; Gunji and Kobayashi, 1983) support the assertion that OPs may fully traverse mature dentine.

The side branches of the OPs showed a huge number of the lateral processes in different regions of the dentine. These commonly forked off at an acute angle and were orientated toward the DEJ. Lateral branching was also observed, with long extensions crossing more than 4 primary processes (Figure 3.5). In addition, lateral processes seemed to contact adjacent processes in a proximal direction. Although most of the previous studies have shown branching of the OPs only within the middle region of dentine and near the DEJ, a variety of shapes and sizes have been reported (Sigal *et al.*, 1984a; Grötz *et al.*, 1998; Tsuchlya *et al.*, 2002). SEM studies have revealed lateral branching that appeared to bridge between OPs and connect them (Thomas, 1979; Gunji and Kobayashi, 1983). Similar complex systems of dentinal tubules with multiple side branches have been reported by others in human teeth (Mjör and Nordahl, 1996; Schilke *et al.*, 2000). The primary roles for these lateral branches is to ensure full mineralization of the dentine matrix (Tjäderhane *et al.*, 2012). However, their spatial existence within the dentinal tubules of mature dentine regions reveals their fundamental activity in preserving vitality for this mineralized tissue.

Furthermore, the outer dentine contains very complex terminal branching of the OPs. This is the first dentine secreted by the odontoblasts (mantle dentine). This dentine part is the outer most part for this mineralized tissue, the closest to the outer tooth surface and the first which is affected by external stimulation or trauma. Therefore, the presence of such complex terminal branches may suggest their involvement in detecting the integrity or flexion of surfaces during functional and parafunctional activity, acting as a receptor field. Any stimulation, mechanical or chemical, could be transmitted along OPs to the cell body of the Ods. The stimulated Od triggering a cascade of events that includes retraction of OPs, stimulating Ods to start reactionary dentinogenesis and possible signalling to afferent nerve fibres underpinning inflammation, sensation or pain (Femiano *et al.*, 2014). This could reflect the massive numbers of the lateral and terminal branches of the OPs to maintain the vitality of this region (Figure 3.3 and Figure 3.5 images C and c2 respectively).

It is uncertain whether, in an intact system, OPs fill the entire cross sectional volume of the dentinal tubule (Thomas, 1979; Yoshiba *et al.*, 2002; Carda and Peydro, 2006), however, the remaining space within the tubules in the presence of OPs and their side branches is reported to be extremely limited (Carda and Peydro, 2006). This spatial limitation of the OPs with this complex structure may raise questions about the validity of hydrodynamic theory, with very minor spaces available within the dentinal tubules.

NaK-ATPase:

NaK-ATPase is a cellular homeostasis element involved in ion transport, fluid movement and the maintenance of membrane potentials (Josephsen *et al.*, 2010). Although, the presence of the NaK-ATPase has been recognised within the SOd cells of rat molars (Mahdee *et al.*, 2016), it's precise role in the pulp environment is not currently known. In the present study, the limited expression within undifferentiated cells of the dental papilla suggested limitation in its action during the cellular differentiation process. Alternatively, it showed high expression in the SOds, followed by Ods, and the least in the inner half of the OPs as soon as dentine deposition has started (Figure 3.6). This may reveal its active transport role associated with dentine matrix deposition. The rich vascularization and massive abundance of NaK-ATPase in the papillary layer was reported as the pumping activity of these cells which play a pivotal role in the function of the enamel organ (Josephsen *et al.*, 2010). The abundant vascularisation of the SOds may allocate similar ion pumping function to support dentine matrix deposition and mineralisation by the Ods (further discussion is seen in Ch5 section 5.4.6). However, it can be speculated that it plays a central role in the signalling systems operating within OPs.

Dendritic cell marker (OX-6):

Another marker, dendritic cell marker (OX-6), was used in this study to check other elements of the Od layer, dendritic cells, and the possibility of their cellular processes interacting with OPs during development and primary dentinogenesis. Although no signs of dendritic cells have been detected in the dental papilla region, they appeared within the Od layer in early period of dentine deposition in association with capillaries. This confirms with previous studies (Okiji *et al.*, 1996; Tsuruga *et al.*, 1999) which reported delay in the appearance of immunocompetent cells in the pulp during early stages of tooth development. Even after dentine thickness increased in the middle and incisal third of the tooth, the number of the OX-6 positive cells within Od layer is

still few in comparison to other regions of the pulp (Figure 3.7). In addition, none of these cells appeared to send processes to predentine. It can be speculated that this region of the tooth is apparently intact and not affected by bacterial antigens which challenge the tissue and facilitate the migration of immune cells (Okiji *et al.*, 1996). In addition, the temporary appearance of the dendritic cells on the dental pulp border sending their processes into the dentinal tubules was only reported after 12 to 24h following dental trauma (Ohshima *et al.*, 2003; Kawagishi *et al.*, 2006).

3.4.2 Cavity samples:

The results of this section support the hypothesis that the OPs are not static structures, but rather have a dynamic capacity to retract in response to dentine surface trauma (Figure 3.11 C). Since the presence of actin was confirmed within the structural framework of the OPs and its possible role in cellular process elongation during dentinogenesis, the results of this section suggest that these microfilaments could be involved in OP retraction as a result of trauma from shallow cavity preparation. A second protein involved in cellular mobility is myosin (Gunning *et al.*, 2015). The presence of myosin in association with actin filaments in the apical pole of the Ods was reported (Nishikawa and Sasa, 1989). During cellular locomotion, myosin interacts with actin filaments to alter cellular shape, in this case to produce cellular processes contraction, working as structural elements with myosin motor proteins (Pollard and Cooper, 2009).

Immediate response (60 sec):

Within immediate fixation groups, there are two phenomena involved in OPs responses: traumatised retracted and traumatised unretracted processes (Figure 3.11 C, Od no. 2). Because actin is present in both main OPs and their side branches, it could be the cause for this protective cellular response resulting from direct bur cutting. However, this immediate and very fast retraction could occur in two ways. Firstly, these processes manage to pull back their side branches as fast as the OP retraction. The second hypothesis is that the main OP retraction was so fast and unexpected, that it could rip off the numerous side branches. This may intensify the trauma for the retracted process. However, only a minority of the OPs retracted immediately, while the majority appear to be unaffected; even their side branches (Figure 3.8). The absence of an immediate response could be due to the duration of cavity preparation (maximum 60 seconds) being insufficient to initiate a retraction response for these processes. Alternatively, what appears to be a slower retraction

may be a part of programmed retraction to enable initial plugging of the dentinal tubules as a defense mechanism. The presence of a clear sequence of events includes immediate OP retraction with or without side branch withdrawal, in addition to unretracted OPs. This suggests a programmed withdrawal of the OPs within exposed dentinal tubules.

3 hour response:

The complexity of retraction for the OPs starts to be apparent after 3 hours, which raises the possibility of what might be a programmed sequence of events. It involves first the retraction of the side branches, a maintenance of single core process, then retraction of the modified processes (Figure 3.11 C processes 3&4). Examining of Figure 3.10 B, the values on the right side of the median for group B2, represent OPs without side branches and not yet retracted. This indicates a slower process, a part of program almost certainly not involving cell damage but reorganization of the cellular architecture. Although, some processes are still not retracted, the majority of the processes respond to trauma after 3h incubation which suggests a time dependent response of the OPs. However, the most retracted processes did not pass 0.5 their original length with the majority of the withdrawn processes retreating no further than 0.675 (Figure 3.10 image B, group B2).

24 hour response:

After 24 hours, none of the OPs in the cavity zone remained near the cavity surface, but all of the processes retracted toward the pulp. This means that all OPs responded within 24h from the time of cavity preparation. However, the maximum retraction distance is still similar to that in the 3h response, although the majority passed the 0.675 of original dentine thickness (Figure 3.10 C), i.e. inverted skewness values between B2 and C2 groups (Table 3.2). This means that even though all processes responded by retraction, their response within 24h remained within a certain distance limitation. This can be explained either mechanically or structurally. The former (as illustrated in Figure 3.11 C) depends on the tight space available within the lumen of dentinal tubules (Yoshiba *et al.*, 2002; Carda and Peydro, 2006). This may limit the retraction of processes and could explain the presence of globular appearances at the end of retracted processes (Figure 3.8 image H). These globules may be formed due to folding of the retracted process components which could be impacted within the lumen of the dentinal tubules (Figure 3.11 C, Od 5). Another question raised here is, whether the fluid movement inside the tubules occurs in normal physiological

conditions, when the OPs possibly occupy most of the tubule space, or if it is more applicable after OPs have withdrawn pulpward after pathological, physiological or iatrogenic opening of dentinal tubules.

The second explanation, depends on the structure of the processes in the mid dentine region. There is a presence of vim in addition to actin within the OPs in this region. This delay in retraction could be due to the presence of intermediate filaments within the structure of OPs to reduce tensions and mechanical forces on the structural framework (Pollard and Cooper, 2009) of processes which could result from continuous retraction. Therefore, this guarded way of retraction of the OPs within 24 hours confirms the programmed sequence of events which aims to preserve cellular vitality of the traumatised dentine/pulp complex.

It should be mentioned that due to limitation in the incubation technique used in this study and the concerns about tooth sample vitality that could be affected if the incubation time extended further than 24h, no extra groups with longer incubation time were included. The question here is whether OPs will stop retraction on the 24h limit or it they will continue to retract toward the pulp. In vivo preparations showed disappearance of OPs within 4 days and appearance of tertiary dentine during 14 days after cavity preparation (Byers and Sugaya, 1995). Another study reported empty dentinal tubules beyond worn dentine surfaces associated with region of tertiary dentine near the pulp in rat molar. The tubules under intact dentine surfaces still preserve their OPs (Mahdee *et al.*, 2016). The present study used in vitro technique and was limited to 24h because of limitations on tissue vitality. A third possible model may extend the investigation to investigate responses to tooth wear model in the rat molar. Natural tooth wear produces damage similar to our cavity and up to 24 weeks. This model is explored in Chapter 5.

3.5 Conclusions

1- In the intact, enamel-covered dentine of the rat mandibular incisor, OPs extended all way to the DEJ.
2- OPs are complex morphologically and have a large number of side branches along the entire length of the process.
3- OPs show heterogeneity in their cytoskeleton in relation to distribution of vimentin. The functional significance of this is not known at present. The experiment in response to cavity preparation (see below) suggested that this

cytoskeletal arrangement may set limits on programmed retraction of the processes triggered by damage.

4- The initial response to cavity preparation (up to 24h) can be seen to involve both rapid and slow events: initial fast retraction and a slower programmed phase involving withdrawal of the side branches, stabilizing of the process, and final retraction up to 50% of the initial process length. This limited contraction may be due to the distribution of structural elements vimentin and actin in the outer third of the OPs.
5- These observations highlight the complexity of structure and function of the OPs that may play a role in early patho-physiological responses induced by trauma.

3.6 Clinical Implications

1- Based on this animal model, without any underlying pathological condition or microbial contamination, drilling into intact dentine may trigger the defense mechanism of the OPs.
2- Retraction of OPs and filling of the vacated tubule space with fluid allows hydrodynamic forces to come in to play and possibly link to tooth sensitization. The prevention, slowing or reversal of OP retraction could have a therapeutic role in the management of tooth vitality and sensitivity. An appreciation of this cellular molecular mechanism and complexity can give a fundamental insight into potential new pharmacological and therapeutic intervention in dental practice.

Chapter 4 **Complex cellular responses to tooth wear in the rodent molar**

4.1 Introduction

The dental pulp shares intimate spatial and functional relationships with dentine, and is commonly described within a pulp-dentine complex (Yu and Abbott, 2007). Ods perform a range of formative, supportive, sensory and defensive functions throughout life (Ricucci *et al.*, 2014), and the comparison of regions within the same tooth that have been subjected to or spared from injury provides one means of understanding important cellular and hard-tissue responses.

Recognised age-related changes in the pulp-dentine complex include reduced cellularity, particularly within the Od and SOd layers (Morse, 1991; Burke and Samarawickrama, 1995; Murray *et al.*, 2002), and changes in volume, structure and permeability of dentine (Moses *et al.*, 2006; Tjäderhane *et al.*, 2012). Much understanding has derived from rodent molar studies, which have shown a reduction in Od size and cytoplasmic volume with age (Lovschall *et al.*, 2002), along with physiological occlusal tooth wear, which is apparent within 4 weeks and consequent hard and soft tissue changes (Lovschall *et al.*, 2002; Kawashima *et al.*, 2006), including reactionary dentine deposition beneath worn cusp tips (Moses *et al.*, 2006).

Dentine exposure by cavity preparation has revealed a reduction of Od numbers, probably resulting from apoptosis (Murray *et al.*, 2000; Kitamura *et al.*, 2001), but with newly differentiated odontoblast-like cells appearing within 7 days (Ohshima, 1990). Cellular responses may be age-related, since the presence of dendritic like cells in the SOd cells, with processes extending into the predentine is more prominent after cavity preparation in aged than in young rats (Kawagishi *et al.*, 2006).

The degree of OP extension within dentine remain contentious (Luukko *et al.*, 2011), with the suggestion that they are limited to the inner third of dentine (Byers and Sugaya, 1995; Goracci *et al.*, 1999; Yoshiba *et al.*, 2002; Carda and Peydro, 2006), whilst others have demonstrated OPs reaching the DEJ (Gunji and Kobayashi, 1983; Sigal *et al.*, 1984a; Sigal *et al.*, 1985; Kagayama *et al.*, 1999; Tsuchlya *et al.*, 2002). In the rat molar, it has been reported that the OPs fully traverse the dentine throughout life in cusp areas, while in the cervical regions, they retract to the inner

third as teeth mature (Tsuchlya *et al.*, 2002). In Ch 3, we have demonstrated the extension of OPs to the rodent incisor DEJ with regional variations and complex branching along their path, especially near the DEJ.

The arrangement and roles of the Od and its process in sensing and responding to injuries such as tooth wear are incompletely understood. This report presents evidence from the rat molar that dentine-exposing tooth wear triggers a discrete and hitherto undescribed series of structural and functional changes that aim to protect deep connective tissues from the oral environment.

4.2 Methods

In order to investigate tooth changes associated with dentine exposure due to the wear process, this study used ground sections to characterise hard tissue changes and decalcified sections with immunohistochemistry to identify pulp cellular differences.

Ground sections: Six lower first molars were extracted from freshly culled male Wistar rats (age 8 weeks; weight 240-300g). Ground sections (100-105µm thickness) of the largest, mesial cusp, were examined by light microscopy using objectives X20 and X40 to identify variations in tubular arrangement associated with the wear process.

Immunofluorescence technique: Ten lower first molars were extracted as previously, with immediate fixation in 4% paraformaldehyde in PBS for 24 hours at 4°C, demineralisation in 17% EDTA (pH 7.4) for 4-6 weeks at 37°C. This was followed by freezing and sectioning as described in Ch 2, section 2.1.5. Ten micrometre thickness sagittal sections were divided randomly into different staining groups (approximately 50 slides for each group) and stained as follows, using either single or a combination of two antibodies:

- Monoclonal mouse anti-vimentin structural protein (vim) (1:5000).
- Monoclonal rabbit anti-α smooth muscle actin (actin) (1:200).
- Monoclonal rabbit anti-NaK-ATPase enzyme (1:500).
- Polyclonal rabbit anti-α tubulin (tub) (1:1000).
- Polyclonal rabbit sodium hydrogen exchanger-1 (NHE-1) (1:200). Both NaK-ATPase and NHE-1 are enzymes present in the cell membrane and they were used in the present study to detect the cell membrane of the OPs.
- Monoclonal mouse anti-calcitonin gene-related peptide (CGRP) (1:500) for afferent sensory nerve fibres.

The secondary antibodies; donkey anti-mouse Alexa Fluor 488 and donkey anti-rabbit IgG, Alexa Fluor 594, were applied in accordance to the species of the primary antibody used.

The immunohistochemistry staining procedure was described in detail in Ch 2, section 2.1.6.

Control samples were included. The slides were either incubated with PBS instead of the primary antibodies, before staining with the secondary antibodies, or incubated with PBS only.

To standardize the region of interest for all the teeth, this study examined only the mesial cusp of the first mandibular molar (Figure 4.1). The stained sections were examined as previously described in Ch 2, section 2.1.8. Approximately 50 slides were examined for each group to confirm the accuracy and consistency of the staining technique and to reveal consistent staining phenomena (Gillespie *et al.*, 2006).

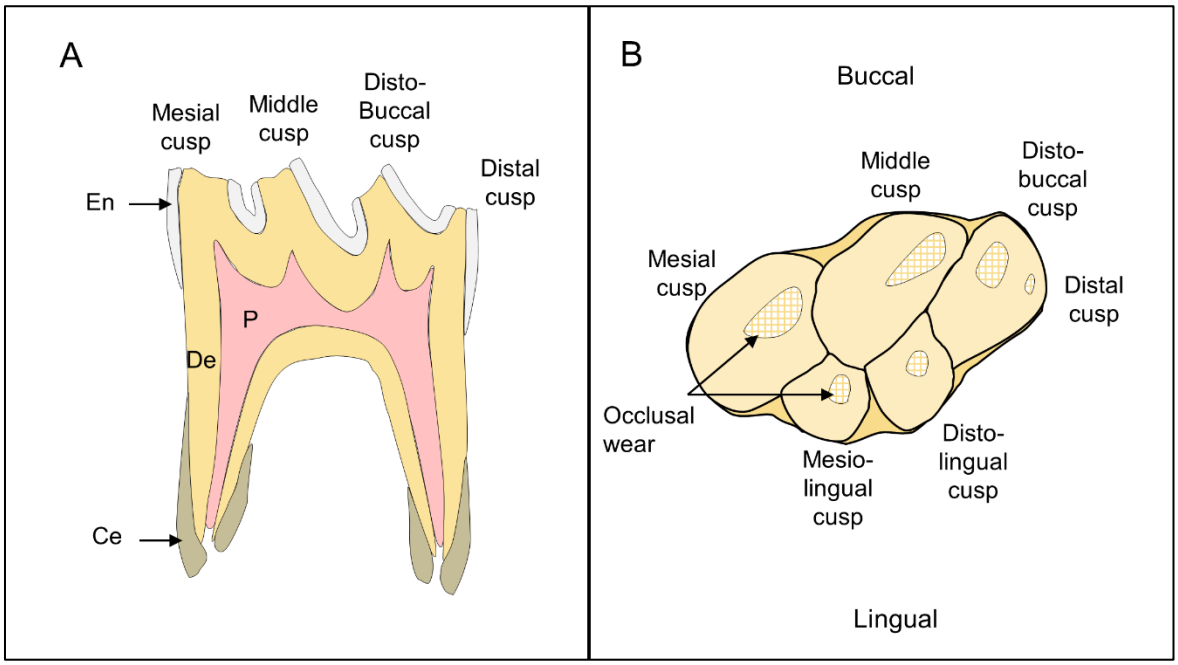

Figure 4.1: Diagram represents the rat mandibular 1st molar cusps viewed in sagittal plane (A) and occlusal surface (B).
The following structures have been identified: enamel (En), dentine (De), pulp (P), cementum (Ce).

4.3 Results

All images illustrated in this chapter are for the mesial cusp of the rat mandibular 1st molar (Figure 4.1). These images are illustrated in a way that the mesial side is always displayed on the left side of the image and vice versa for the distal side. To identify time-dependent changes in the mesial cusp as a model for tooth wear, the following descriptions of tooth wear were used (Figure 4.2):

Stage 0 (S_0) tooth regions under unworn dentine surface (lateral and central walls of the mesial cusp).

Stage 1 (S_1) tooth regions close to worn dentine surface (at the angle of the cusp from the unworn cusp side).

Stage 2 (S_2) tooth regions of minor worn dentine surface (near the angle of the cusp from the worn cusp side).

Stage 3 (S_3) tooth regions of severe worn dentine surface.

All the ground sections observed in this study showed worn occlusal dentine, associated with an underlying area of tertiary dentine close to the pulp space (big panel in Figure 4.2). In S_0 regions, the complexity of the dentinal tubules could easily be recognized in the outer dentine with abundant lateral and terminal branching (image S_0, Figure 4.2). The terminal branching seemed to terminate within the DEJ. A

similar pattern of dentinal tubules is also illustrated in S_1 region which is located close to the worn dentine surface at the cusp angle (image S_1-S_2, Figure 4.2). In the same image, it is apparent that in S_2 region, the dentinal tubules were worn and had lost their outer branching region. In the S_3 region (image S_3, Figure 4.2), the dentinal tubules appeared shorter with the proximity of the worn dentine surface to the pulp space becoming apparent. Considering the region of tertiary dentine deposition near the pulp (image R, Figure 4.2), there was no continuity of the dentinal tubules between the primary dentine and the newly-formed tissue, which appeared to present tubules with a meandering pattern.

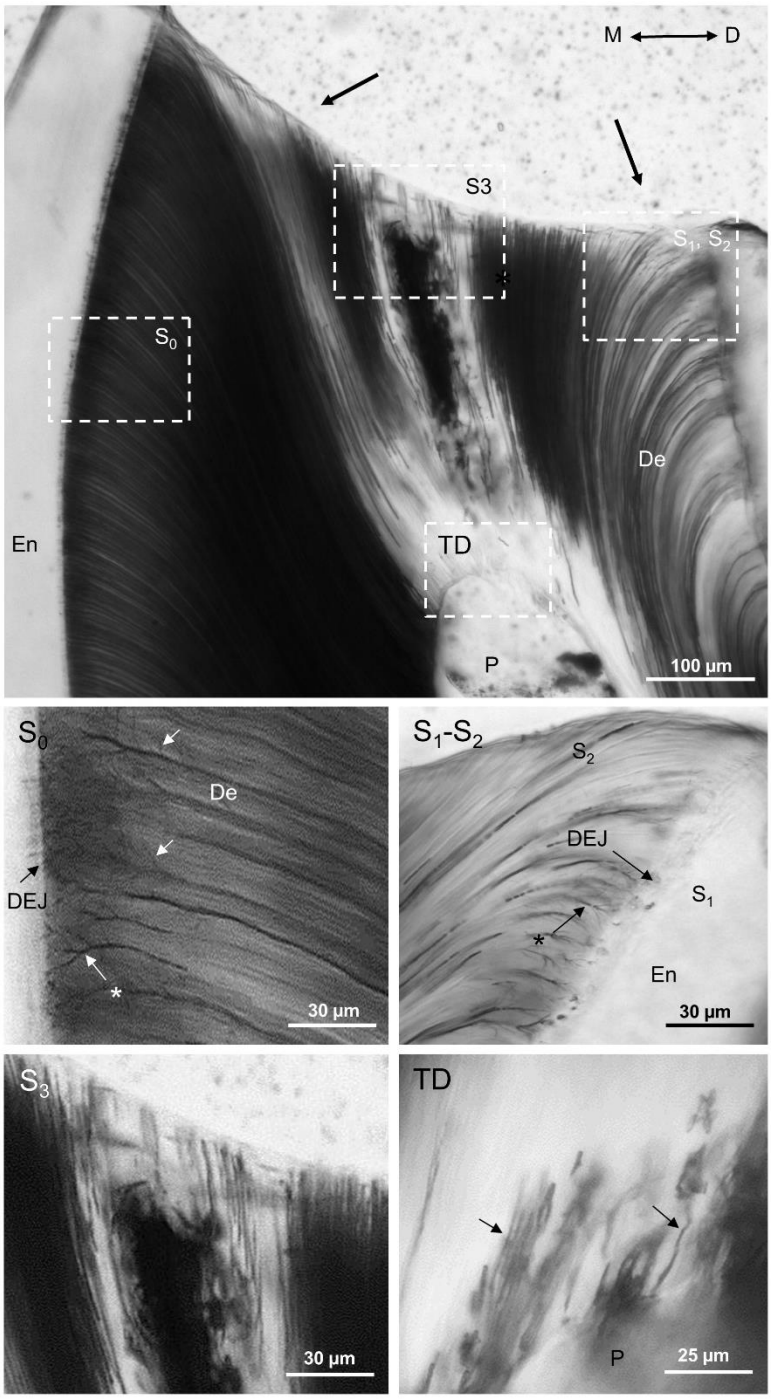

Figure 4.2: Ground sagittal section of rat mandibular 1st molar mesial cusp. The following structures were identified, P; pulp space, De; dentine, En; enamel, DEJ; dentine-enamel junction. The big panel shows the worn occlusal dentine (arrows). An orientation double sided arrow points to the mesial (M) and distal (D) sides of the image. Four regions of interest are highlighted (S_0, S_1-S_2, S_3 and R). Image S_0 shows a region of intact tooth surface with complex lateral branches (arrows) appearing in the outer third of the dentine associated with complex terminal branches (*) of the dentinal tubules. S_1-S_2 image shows the cusp angle with S_1 region on the top and in which the dentinal tubules still possess complex terminal branches (*) near DEJ. In S_2 regions, the dentinal tubules appear to be worn to a minor degree. The S_3 image identify the severely worn dentine surface. In R panel, an area of tertiary dentine with meandering tubules (arrows) is illustrated.

In decalcified sections, the extension of the OPs to the outer region of the dentine was demonstrated with NHE-1 (first panel, Figure 4.3). The intensity of labelling was relatively uniform throughout the full dentine thickness in S_0, S_1, and S_2 regions and this labelling also followed a linear course along the primary curvature of the dentinal tubules (Figure 4.2). In S_3 region, the odontoblast processes were limited to the inner dentine while the rest appeared to be devoid of any specific fluorescence labelling (image A, Figure 4.3). The OPs showed vim immunoreactivity (IR) in the region between the cell body and into inner dentine (image B, Figure 4.3). This IR changed to be more NHE-1 within the remainder of the dentine, indicating a heterogeneity of antibody expression within the same OP.

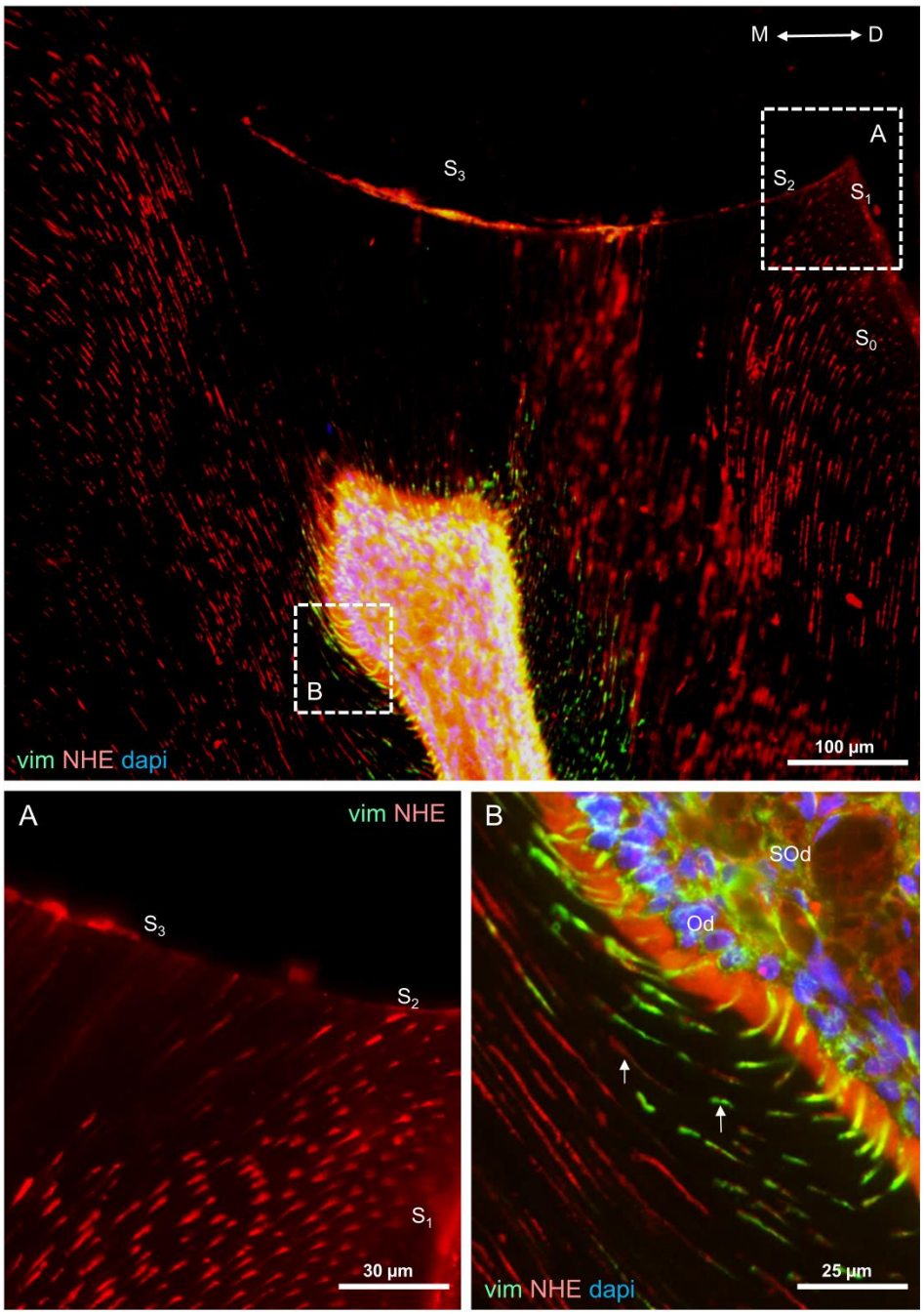

Figure 4.3: Decalcified sagittal section of the mesial cusp of rat mandibular 1st molar. All images were stained for NHE-1 in red, vim in green and dapi in blue. The large panel shows the extension of OPs to the dentine surface in S_0, S_1, and S_2 regions, while in S_3 region, the processes are limited to the inner region of the dentine. A double sided arrow provides orientation for the mesial (M) and distal (D) sides of the image. In A panel, the continuity of NHE-1-IR for the OPs in the outer dentine in S_1 is apparent and partly in S_2 region. In S_3 the outer dentine is devoid of NHE-1-IR. B image shows a region of the pulp-dentine area with odontoblasts (Od) and sub-odontoblast cells (SOd). The OPs show vim-IR near the Od cell body, then change to NHE-1-IR when the process extends further within the dentine (arrows).

The antibody to α- tub, also labelled the OPs throughout the full thickness of the dentine. The OPs showed very complex lateral and terminal branches in the outer region of the dentine near the DEJ in S_0 regions (images A and a, Figure 4.4). Some of these processes showed more than 4 terminal branches (image a, Figure 4.4), indicating great complexity in the outer dentine. In region S_3, tub-IR (images B and b, Figure 4.4) was also absent in the outer dentine and was limited to the inner third of the dentine, similar to the pattern observed with NHE-1. In S_2 region the OPs that reached to the outer dentine appeared to be thicker than the ones observed in S_0 regions, and without lateral branching (image b, Figure 4.4).

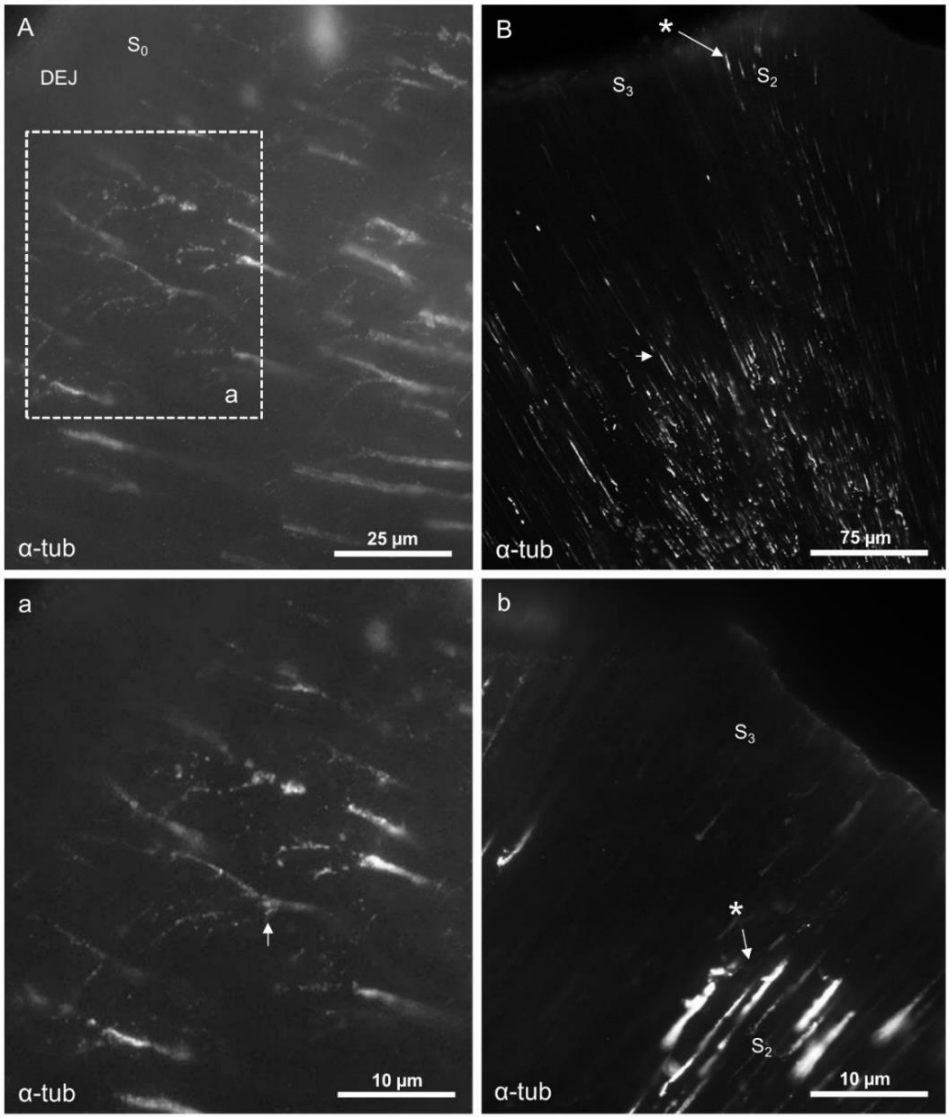

Figure 4.4: Decalcified sections from S_0 compared to S_2 and S_3 regions in the mesial cusp of rat mandibular 1st molar.
All images were stained for α-tub. A shows the extension of OPs in the outer dentine in an area of intact enamel (En) on the lateral wall of the cusp (an S_0 region). The region of interest in A is delineated by the box which clearly shows complex terminal branching of the OPs (arrow). Panel B shows no OPs extending to outer dentine in an S_3 region and some processes extending to outer dentine in an S_2 region (*). The higher magnification image in panel b shows some of the OPs labelled with α-tub extending close to the outer dentine surface in S_2 region but these processes have no branches.

IR to α-actin and NaK-ATPase was limited in the inner third of the dentine with no immunofluorescent labelling detected in the external dentine in any region of the mesial cusp, as shown in Figure 4.5 images A and B. A notable observation for these two antibodies was the cellular heterogeneity of the odontoblast cells expressing these antibodies in comparison to vim (images C and D, Figure 4.5).

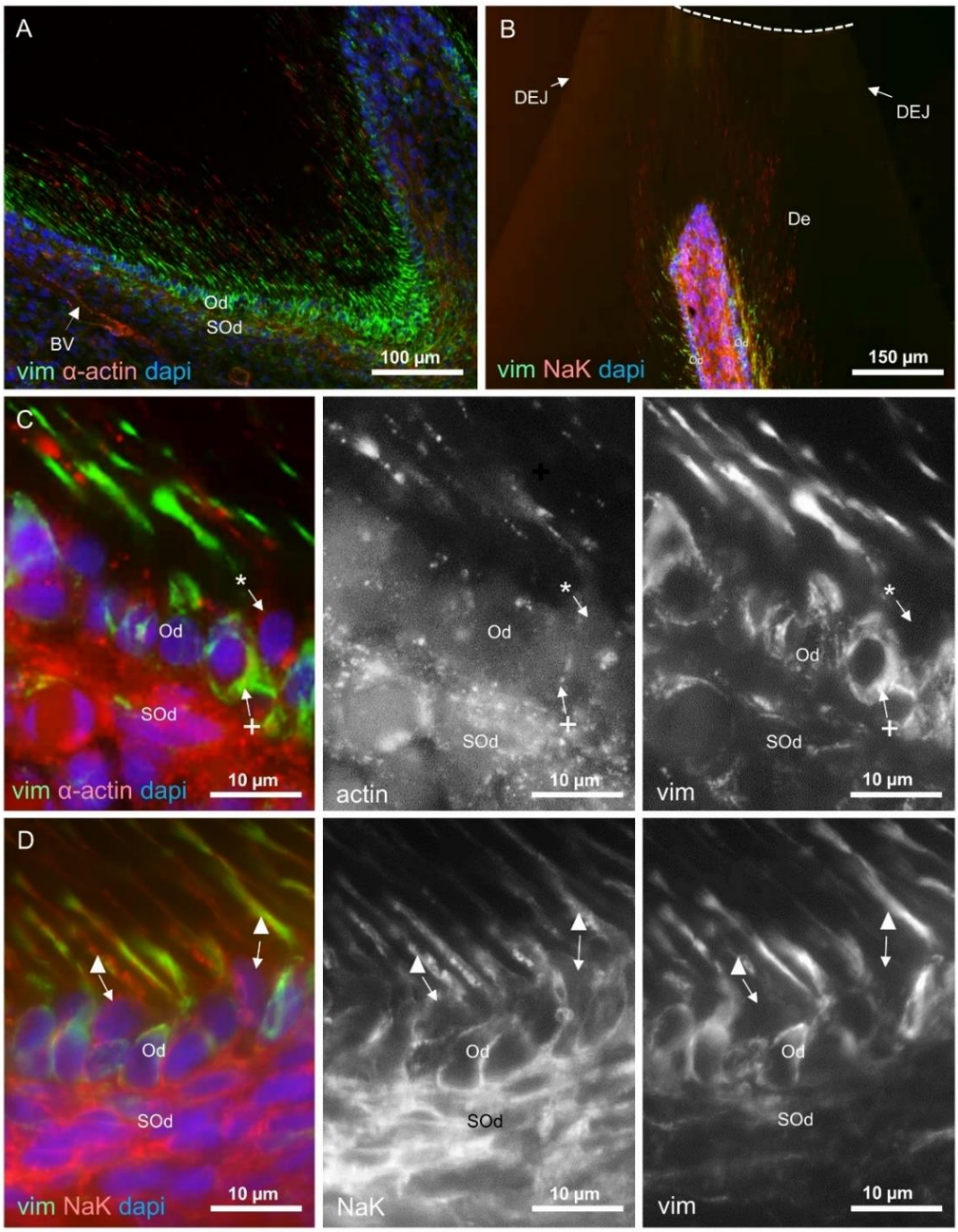

Figure 4.5: Decalcified sagittal sections of rat mandibular 1st molar from groove region (A) and mesial cusp (B) to identify dentine/pulp regions beneath intact tooth surface (S_0). Sections were either stained for vim (green), α-actin (red), dapi (blue) in panels A and C, or vim (green), NaK-ATPase (red), dapi (blue) in panels B and D. The following structures were identified: Od; odontoblast cell layer, SOd; sub-odontoblast cells, BV; blood vessel, De; dentine, DEJ; dentino-enamel junction. In panels A and B, the OPs show IR for vim, α-actin, and NaK-ATPase only in the inner third of the dentine. The dotted arrow in B demarcates the worn dentine surface. C and D are high power images of Od and SOd in S_0 regions. In C and its component images (actin and vim), some Od cells show actin-IR (*) with no vim-IR and others have only vim-IR (+) with no actin-IR. Panel D and its component images (vim and NaK-ATPase) show most of the Od cells labelled both vim and NaK-ATPase-IR, but some have no vim-IR (▲).

The dentinal tubules and OPs showed differences in their pattern between S_0 in one side and S_2 and S_3 regions on the other side. There were other differences related to the cellular elements within the pulp. In S_0 region, the Ods appeared as a single cell layer, with their cellular processes extending into the dentine. They were morphologically distinct from the SOds (image A, Figure 4.6). Cellular heterogeneity was also identified within the Ods between vim and tub antibodies (images a1 and a2, Figure 4.6). Moving to S_2-S_3 regions, the Ods were arranged in a pseudostratified or stratified layer of 2-3 cells thickness (image B, Figure 4.6). Some cells from the second line of Ods were also observed, sending processes into the predentine (image b1, Figure 4.6). Some SOd cells in this region showed modification in their cellular morphology to be similar to the Ods. However, no cellular processes were recognized in these cells (image b2, Figure 4.6).

Finally, the distribution of afferent sensory nerve fibres was identified with antibodies to CGRP. These fibres appeared with punctate staining and did not extend further than the inner dentine (image C, Figure 4.6). The varicosities of CGRP-IR fibres gave rise to this punctate staining, whilst the axons between these varicosities were very weakly detectable. These sensory nerves showed a complex distribution in between the SOds and the Ods and they ran with the odontoblast process (Figure 4.6, images c1 and c2).
None of the control groups showed any specific fluorescent labelling within the pulp, dentinal tubules, or DEJ.

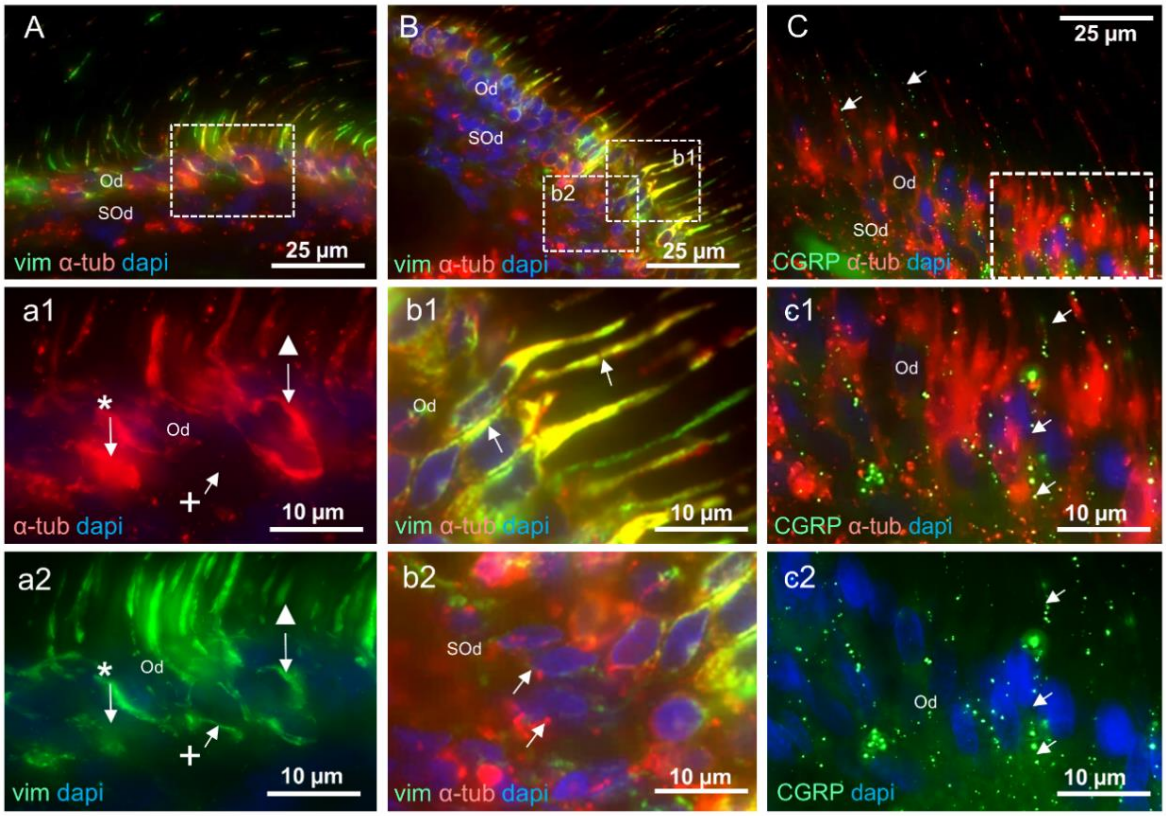

Figure 4.6: Decalcified sections from mesial cusp of rat mandibular 1st molar to compare between S_0 and S_2-S_3 pulp regions.
Images A, a1,a2, B, b1, and b2 were stained for vim (green), α-tub (red), and dapi (blue), and images C, c1 and c2 for CGRP (green), α-tub (red), and dapi (blue). A shows the single layer arrangement of the Od cells in S_0 region. The two panels below a1 and a2 represent region of interest in image A and identify three types of Od cells: vim-IR (+), tub-IR (*), and vim-tub-IR cells (▲). Panel B shows the arrangement of Ods in a pseudo-stratified layer of 2 to 3 cell thickness in S_2 and S_3 regions of the pulp. Two regions of interest are shown in image B. The first one appears in image b1 with cells (*) in the second line of the thick Ods cell layer sending processes (arrows) to the predentine (Pd). The second region is identified in image b2 which shows the SOd cells heading toward the proximal cells of the odontoblasts. Image C from S_2-S_3 region shows nerves stained with CGRP running from the pulp and terminating in the inner part of the De (arrows). A region of interest is shown in image c1 and the component image c2, which clearly identify nerve fibres running between Ods (*) and then into the inner De (small arrows).

4.4 Discussion

This study is among the first to present evidence from the rat molar that dentine-exposing tooth wear triggers a discrete and hitherto undescribed series of structural and functional changes that aim to protect deep connective tissues from the oral environment. Although rat molars have enamel-free areas on their cusps, they remain covered with bone and gingival tissue until eruption, with tooth wear commencing soon after, and certainly within 4 weeks for the rat mandibular first molar (as seen in different age groups in chapter 5). The largest cusp (the mesial) was examined in all cases for consistency.

Antibodies for structural proteins vim, α-actin, and α-tub were used since intermediate filaments, microfilaments and microtubules have been reported as major components of the odontoblasts cytoskeleton and have not been shown to exist extracellularly in viable cells (Lesot *et al.*, 1982; Thomas and Carella, 1983; Thomas and Payne, 1983). The other antibodies used were for cellular homeostatic elements indicative of living cells; NaK-ATPase and NHE-1. NaK-ATPase is expressed widely in the cellular systems of the dental pulp (Duan, 2014), where it is instrumental in maintaining the ionic gradient cross cell membranes. NHE-1 is an isoform of the sodium/ hydrogen exchanger, which is a membrane protein primarily responsible for maintaining the intracellular pH (Duan, 2014). Josephsen *et al.* (2010) found both NaK-ATPase and NHE-1 in cells of the rodent enamel organ and linked them with cellular pumping activities. Pulp cells, especially odontoblasts, have also been reported to contain both of NaK-ATPase and NHE-1 in their cell membrane (Duan, 2014). Another antibody, CGRP, was used as a marker for sensory nerve fibres (Mori *et al.*, 1989).

An illustration of the changes from normal undamaged surfaces to a situation of significant wear is shown in Figure 4.7. In normal physiology (A in Figure 4.7), OP and their complex branches occupy the full tubular space (Carda and Peydro, 2006). The current study confirms that the OPs extend the full thickness of the dentine and terminate within an intact DEJ through the function of either structural (α-tub) and ion transporter (NHE-1) markers. However, the other antibodies including vim, α-actin, and NaK-ATPase were labelled only in the inner third of the dentine. This could reflect regional differences in the structure of the OPs i.e. certain protein filaments may be present only in defined regions depending on the function of the OPs in these

regions. Previous studies have also reported the α-tub-IR of OPs throughout the thickness of the dentine, whilst vim and α-actin-IR were limited to the inner dentine in human (Sigal *et al.*, 1985) and rat molars (Sigal *et al.*, 1984a). These findings are supported by the current study. By contrast, our previous work (Ch 3) on the rat incisor found α-actin-IR in OPs throughout the entire thickness of the dentine, and this may reflect the greater concentration of that protein in continuously growing teeth compared with rat molars and human teeth. Additionally, using earlier age samples (up to eruption time in 3w old rat, further discussion in Ch 5) gave similar observation to rat incisor sections. This could reveal that there is also an age-dependent factor which could cause these differences in OPs labelling behavior. Therefore, it would appear that OPs beneath intact molar surfaces are complex and show regional variations in protein expression that may reflect structural and functional specialization. Furthermore, this is the first report to identify NHE-1-IR within the full length of intact OPs. The role of this ion transporter within OPs is still unknown. However, it could be one of the homeostatic elements that maintain vitality of the OPs by regulation of the intracellular pH. On the other hand, it could also play a role in controlling the intratubular pH of the tubular fluid to regulate ion transportation and mineral deposition within peritubular dentine (see Ch 5 section 5.4.6 for further discussion).

In normal physiology, OPs terminated with complex branches within the DEJ. The function of this complex branching is not known, but may suggest its involvement in detecting the integrity of that region, acting as a receptor field. Any stimulation, mechanical or chemical, could be transmitted along OPs to the cell body of the Od, the stimulated Ods triggering a cascade of events that could include retraction of OPs. The primary aim for such events are possibly to initiate pulp inflammation and defense mechanism in the face of injury to prevent further tissue destruction and promote healing and regeneration (Tjäderhane and Haapasalo, 2012). Additionally, the presence of voltage gated sodium channels (Allard *et al.*, 2006), and mechanosensitive potassium channels (Allard *et al.*, 2000) were also reported within the Od. This could reveal the ability of Od to sense the external environment possibly through its process and generate an action potential to transduce this stimuli as an electrical signal to the other pulp cells or adjacent nerve fibres (Allard *et al.*, 2006).

It was observed that after exposing of the dentine surface to the oral environment, there was an initial loss of side processes in S_2 regions (B in Figure 4.7). However, in

areas of minor or perhaps slower wear, the OPs still extended to the end of the dentinal tubules. The trauma within this region could be transient which gave more time for the OPs to react in a slower and programmed retraction process. Similar observations were also detected in the cavity experiment in Ch 3. Additionally, the persistence of OPs within their dentinal tubules for longer periods of time may promote further mineral deposition or accumulation for internal obliteration and sclerosis of the exposed tubules. Hyper-mineralization lumens of hypersensitized dentinal tubules was also reported (Yoshiyama *et al.*, 1989; Yoshiyama *et al.*, 1990), and this may also support the possible function of these non-retracted OPs.

Further retraction of OPs, could leave more space within the tubules for intratubular fluid movement (C in Figure 4.7). This hydrodynamic fluid movement could stimulate either the remaining part of the OPs or persisting afferent sensory nerves within the tubules as suggested by the hydrodynamic theory (Ciucchi *et al.*, 1995). This may also contribute to altered sensation including pain in damaged or worn regions of the teeth. This hyper-stimulation of the exposed tubules due to hydrodynamic fluid movement, response to microbial or other external noxious stimuli could all stimulate OPs for further retraction toward the pulp and the Od cell body to deposit reactionary atubular dentine matrix (D in Figure 4.7). This atubular matrix possibly blocks the inner part of the dentinal tubules, in addition to increasing the distance between the pulp tissue and the exposed area (further discussion in Ch 5 section 5.4.1). The afferent fibres in the pulp express CGRP (Mori *et al.*, 1989), and in other systems where CGRP afferent fibres are found, it can be released during nerve activation to initiate neuro inflammatory reactions (Assas *et al.*, 2014). This raises the possibility that the nerves may feedback to stimulate the Ods. Collateral branches of such axons almost certainly exist, in addition to the electrical coupling between Ods (Ikeda and Suda, 2013). This has an effect on triggering Ods some distance away from the injury (Kimberly and Byers, 1988). Thus, the effect of damage may be spread to Ods over a considerable area.

Changes in the pulp cellular population were also noticed in regions undergoing dentine exposure i.e. S_2 and S_3 regions in the present study (Figure 4.6). The first change was the increase in thickness of the Od layer to 2-3 cells which could reflect more activity of the Ods in this region as they are involved in the formation of reactionary dentine. However, this could be the normal distribution of the Ods in this region as these cells tend to be more crowded in areas under the cusps (Lovschall *et*

al., 2002). At the same time, differences were also noticed SOd cell populations as the most distal cells in this region become more odontoblast-like. These cells could be supportive to the remaining Ods or recruited to replace extensively damaged Ods. However, and under the conditions of this study, all the cells present at the border of the pulp-dentine complex contained processes. These border Ods were associated with meandering processes which form similar shape dentinal tubules (E in Figure 4.7). This could be the second part of the reparative procedure for the remaining Ods, to reestablish the tubular pattern of the dentine. However, more severe trauma such as deep cavity preparation, can be suggested for further studies to investigate pulp cell reaction to such trauma (hypothesis in Figure 4.7, panel F).

Another important observation from the current study is the heterogeneity of the Ods, both in intact and worn regions of the tooth (Figure 4.6). This could either suggest the presence of another cell type within Ods layer such as dendritic cells as seen in Ch 3. Another speculation could be that the Ods themselves could possess different functions within the same layer. These duties may include the primary function of Ods as a dentine-formative cell, in addition to possible sensing, nutrition and inflammatory functions (Luukko *et al.*, 2011).

In summary, this study provides novel observations about the pulp-dentine complex, and suggests a new explanation for the role of OPs in maintaining dentine surface integrity following exposure by tooth wear. New insights have also been given about the roles of cellular complexity within the pulp-dentine complex and possible roles in sensing, defense and repair. Furthermore, two possible sensing approaches for the pulp-dentine complex have been suggested depending on the integrity of the dentine surface. The examination of rats of varying ages and degrees of tooth wear (see Ch 5), will shed further light on the pulp-dentine complex reactions associated with exposing dentine. This may advance understanding of pulp physiology in health and disease, and provide opportunities for therapeutic intervention.

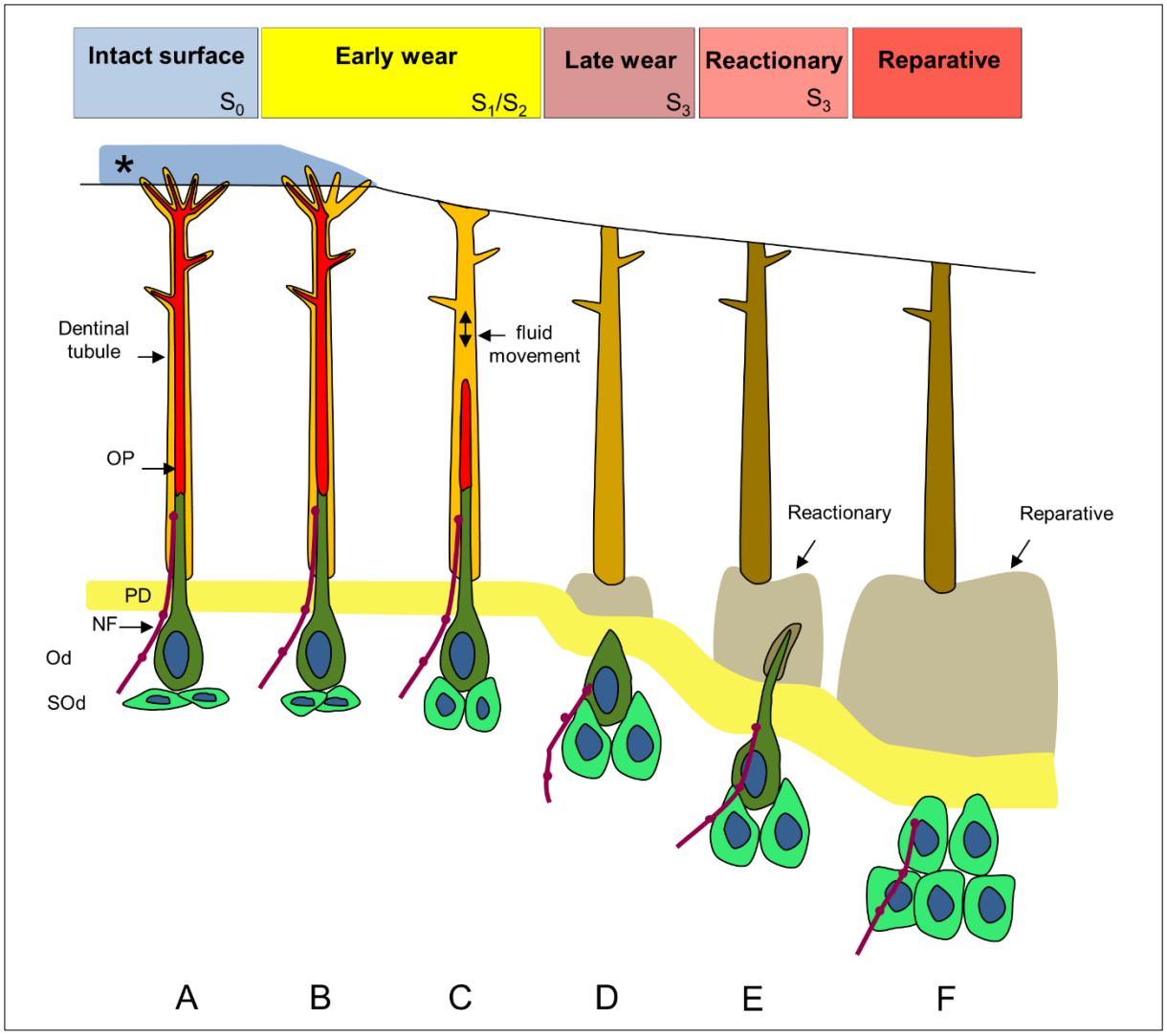

Figure 4.7: Schematic illustration representing the hypothesis of this chapter. The following abbreviations have been used: OP odontoblast process, PD predentine, NF nerve fibre, Od odontoblast, SOd subodontoblast, and (*) the covering tissue. Reading from the left, it illustrates the presentation of an odontoblast within a healthy unworn dentine surface (A), followed by early (B and C) to late pathological changes (D) resulting from the opening of dentinal tubules, and finally the development of defensive reactionary (E) and reparative responses (F). (Note: F is speculative and was not observed in the results of this chapter).

Chapter 5 **A longitudinal investigation of formative and reactionary changes in the dentine/pulp during the life of the rodent molar**

5.1 Introduction

Odontoblasts are highly specialised and polarised cells, arranged in a continuous layer of tall columnar cells with clear epithelioid appearance on the pulp boundary (Arana-Chavez and Massa, 2004). The fundamental function of these cells is their ability to lay down dentine during and after tooth eruption. This includes primary and secondary physiological dentine respectively, with dentinal tubular continuity between them (Tjäderhane *et al.*, 2012). After primary dentinogenesis, there is an obvious decrease in cellular activity, which is evidenced by morphological and functional changes within the Od cell layer (Murray *et al.*, 2002; Magloire *et al.*, 2009). However, most of these cells survive for the life of the tooth unless subjected to injury (Murray *et al.*, 2002). Various injurious stimuli (wear, cavity, or caries) trigger cellular responses to form a structurally different tertiary dentine which could be reactionary (formed by the same Ods) or reparative (formed by new Od-like cells) (Tjäderhane *et al.*, 2012). Generally, and in most of the previous reviews, reactionary dentine is reported to have more or less structural continuity with the secondary dentinal tubules. Alternatively, reparative dentine with it's a tubular organisation shows significant structural and mineral variations (Smith *et al.*, 1995; Smith *et al.*, 2008; Tziafas, 2010; Tjäderhane *et al.*, 2012; Femiano *et al.*, 2014). In the case of reactionary dentine, the primary function is to isolate the pulp from external stimuli, by reducing the permeability of dentine overlying the pulp. This isolation cannot be proposed if the dentinal tubular continuity between this dentine and the original dentine is still maintained. To investigate such response, it is important to follow a trauma stimulus (tooth wear in the current model) and the response to it over time.

NGF, is a member of the neurotrophin family, promoting neuron development, maintenance and repair, through its action on tyrosine kinase receptors (trkA) (Chao, 2003). It also reported to be involved in the epithelial-meshenchymal induction associated with tooth development, by its action on p^{75} neurotrophin receptors (Mitsiadis *et al.*, 1992). NGF is also present in mature tooth tissue and is involved in pulp tissue inflammatory reaction and repair after trauma (Byers *et al.*, 1992). However, its role within tooth development and tissue repair is not well known.

Dental pulp, particularly the cusp region, is a highly innervated tissue. The vast majority of this is sensory innervation such that the primary sensation perceived is pain (Abd-Elmeguid and Yu, 2009). In normal conditions, there is no stimulation above their nociceptive threshold, therefore, no pain is sensed. In pathological conditions, these nerves become hypersensitive to simple thermal, mechanical, or osmotic stimuli which can cause severe pain (Byers and Narhi, 1999). We include the trauma caused by wear in the present study model which is associated with tissue insult and inflammation. It becomes necessary to record the reaction of the pulp neurons to this trauma and to determine how this could affect nerve distribution and sprouting during inflammation and after repair.

Very few previous studies used an animal tooth attrition model to study the impact of dentinal exposure on the OPs, vitality of the Ods, sensory nerve morphology, and the associated repair mechanisms (Mahdee *et al.*, 2016). The use of such a model could possibly avoid all the experimental variables in the cavity preparation models that could not be overcome during surgical procedures (About *et al.*, 2001; Goldberg and Smith, 2004). Equally, the roles of pulp cells in sensing danger from wear, tooth flexion, and microbial challenge are incompletely understood. There is no recorded information about the initial response of the pulp cells to the exposure of dentinal tubules, or the late reaction of these cells after the deposition of reparative dentine, which was suggested to be a barrier to isolate the pulp from the external stimuli. In addition, if these findings proceeded by earlier tooth developmental records and normal tissue structure before the surface wear took place. This would probably help to follow the whole story from its early phases to give a broader understanding about the changes that could occur in response to the stimuli. Therefore, the overarching aim of this chapter is to identify possible complex cellular interactions of the major pulp elements including Ods, OPs, SOds, blood vessels and nerves during different stages of tooth of development and response to dental injury. The rat mandibular first molar was chosen as the model in this chapter, because it is a validated model for human teeth. Additionally, this model allows the phenomena of occlusal wear to be investigated, providing a valuable trauma tooth model. This is expected to give novel insights about the early and late tooth responses to occlusal wear.

5.2 Methods

Male Wistar rats of different age groups: zero day (0d), 1, 2, 3, 4, 6, 9,12 and 24w (5 or 6 of each) were killed as follows. After the birth of the 0d pups, they were killed by intra-peritoneal injection with lethal dose (0.7ml/Kg) of pentobarbitone. The remaining age groups were killed by using a CO_2 chamber. Mandibles were carefully dissected and divided centrally into two halves. Right and left halves were sectioned into three pieces as described in 2.1.2 and Fig 2.1. Only middle pieces, which contain the bone segment with 3 molars, were utilised in this experiment. In 0d and 1w samples, the half mandibles were kept without sectioning in a one-piece sample because they were small in size.

Three samples from 2, 4, 6, 9, 12, 24w aged rat were used in ground sections. The ground section preparation protocol and method of slide examination was described previously in section 2.4.

The rest of the samples were fixed immediately in freshly prepared 4% PFA solution for 24h. The samples were washed thoroughly in PBS and demineralised 17% EDTA (pH 7.4) (see 2.1.3 and 2.1.4 respectively) except 0d and 1w samples which were used without demineralisation. Samples were then frozen and sectioned as described in section 2.1.5. Twenty to thirty slides of 10µm sections (each slides have 2 sections on) were obtained from each block and stored in -80ºC freezer.

Three different staining procedures were performed: hematoxylin and eosin (H&E), fluorescent staining with rhodamine phalloidin (RP), and immunohistochemistry staining (IHC) using various antibodies. The H&E and RP staining protocols were described in 2.3 and 2.2 respectively. Different antibodies were used in IHC staining which included the following:

- Structural framework antibodies: vim (1:5000), α-actin (1:200) and α-tub (1:1000).
- Cell division marker (Ki 67) (1:500)
- House-keeping proteins: NaK-ATPase (1:500), and NHE-1 (1:500).
- Nerve growth factor (NGF) (1:500) and nerve growth factor receptors (NGFR) (1:100)
- Nerve markers: calcitonin gene related peptide (CGRP) (1:500), and neurofilament (Nf) (1:1000).

All details for the above antibodies were described in table 2.1. Either a single or a combination of the two antibodies were used in each staining experiment. The staining protocol for IHC was also described thoroughly in 2.1.6.

The negative controls for the IHC staining were previously described in section 2.1.7. This included:

- Blocking peptide (BP) for anti-alpha smooth muscle actin antibody [E184].
- Use of the isotype controls including rabbit IgG monoclonal (EPR25A) isotype control and normal mouse IgG1.
- Use of PBS to incubate the slides instead of primary antibodies or both primary and secondary antibodies.

Other oral tissue within the same samples served as internal positive staining controls. Examples included the use of gingival tissue as a positive control for nerve staining, the apical bud region of the mandibular incisor as a positive control for cell division marker Ki 67, and the use of the enamel organ cells as a positive staining for α-actin, NaK-ATPase, and NHE-1. Other tissue organs were also used as positive controls including rat bladder and skeletal muscle.

For each staining, samples from different animals (4-8 rats) in each age group were examined to confirm the accuracy and consistency of the staining technique and to reveal constant staining phenomena.

For nerve staining with CGRP, nerve counting was made for nerve fibres within the Od layer of the mesial cusp region for 3, 4, 6, 9, 12 and 24w sections. The procedure for qualitative nerve counting was as follows (see Figure 5.1):

- The region for nerve counting was determined within 200μm from the cusp margin of the pulp. Only nerve fibres within Od layer were counted.
- The Od layer within the counting zone was divided into two regions; mesial and distal of the cusp. The trauma region due to wear, which occurs from 4w and older samples, was included within the distal side measurements of each age.
- Within each mesial and distal Od regions, the number of CGRP fibres and Od layer surface area was calculated.
- To measure nerve fibre density within the surface area (nerves/1000μm^2) the following formula was used:

Nerve density= (nerve number / Od surface area) * 1000

Therefore, in each sample there was a mesial nerve density (M-Den), distal nerve density (D-Den) and total nerve density (T-Den) for the whole cusp.

Between 4-6 images from each age group were measured and these measurements were analyzed by ANOVA and Bonferroni *Post Hoc* test to find the statistically significant differences between each nerve density within different age groups. Unpaired T-test was also used to compare between M and D-Den within the same age group.

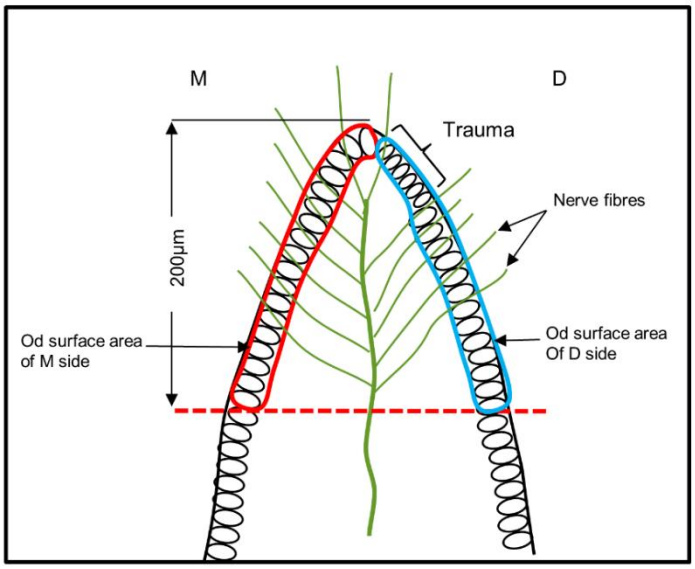

Figure 5.1: Illustration of the CGRP nerve counting procedure within mesial cusp. M is for mesial, and D is for distal side, and the latter includes the trauma site within it.

5.3 Results

For consistency, and because the examined piece of the mandible contained 3 molars and each molar had a different number of cusps, only the mesial cusp of the first molar (the largest cusp within the largest molar) was focused on during this work (see Figure 4.1). However, the image archive for this experiment contains many images of other cusps of the 1st molar or within other 2 molars which confirm the same story details in each cusp.

There are several regions within the mesial side of the tooth are focused on during the presentation of the figures. These regions include (see Figure 5.30): the mesial cusp (cusp tip and lateral wall), groove region (which is mainly between mesial and middle cusp), mesial cervical region, and mesial root. Additionally, all images for

mesial cusps in each figure were arranged to show the mesial side of mesial cusp to be on the left hand side of the image and vice versa for the distal side.

5.3.1 Ground sections

The ground section for 2w molar shows no enamel covering the cusp tip (image A Figure 5.2). The tooth is still not yet erupted with unbroken cortical bone covering the mesial cusp. The dentinal tubules above the pulp horn region appear as dark tubules which represent the peritubular dentine. These tubules are highly condensed to each other with very limited white spaces in between them, even under higher magnification (image a Figure 5.2). No clear branching of the dentinal tubule is evident in the inner dentine compared to the many lateral and terminal branches within outer dentine (images A and a Figure 5.2).

In 4w age sections, the occlusal wear of the mesial cusp surface is apparent. It appears more severe on the distal side of the mesial cusp which looks shorter than mesial side (image B Figure 5.2). This wear has resulted in the cutting off of the terminal branches of the dentinal tubules and hence exposing them to the oral cavity. There is a region of atubular dentine evident near the pulp and marked by a dotted curved line in image B Figure 5.2. This region at higher magnification shows an atubular dentine pattern which contains a few irregularly shape tubules (white arrows in image b Figure 5.2). This atubular dentine region seems to obliterate the proximal opening of primary dentinal tubules (black arrows in image b Figure 5.2).

In 6, 9 and 12w sections, more occlusal surface wear is observed, which progressively increased with age. The cusp attrition affects not only the central region of the cusp in 6 and 9w sections (images C and D Figure 5.2), but also includes the whole cusp depth in 12w sections (image E Figure 5.2). This can be identified by comparing the depth of the occlusal groove between different age groups (double sided arrow in images D and E respectively in Figure 5.2). There is also an associated retraction of the pulp space due to increased deposition of atubular dentine. This changes the profile curvature of the occlusal boundary of the pulp (images C, D and E Figure 5.2). Under higher magnifications, new dentinal tubules appear from the proximal side of the reactionary dentine region (images c and d Figure 5.2). These tubules have large areas of atubular dentine between them, short in length, meandering in shape, and extending only into the inner part of the

reactionary dentine. The number and length of these new tubules increases with age (image e Figure 5.2).

In 24w sections, the wear continues to progress to reach the atubular part of the reactionary dentine (x_1 in image F Figure 5.2). The mesial cusp becomes much shorter in its distal side compared to other ages. Additionally, the dentine on the sides of the cusp is severely worn and is shorter than the adjacent enamel (2 arrows in image F Figure 5.2). An important observation at this age is the tubular pattern of the inner half of the reactionary dentine. Although these tubules run in meandering style, which looks different to the pattern of the primary dentinal tubules, they appear more packed with each other and the white atubular spaces disappear. This is due to progressive surface wear which could expose new dentinal tubules near the distal side of the mesial cusp presented in thick arrow in image F Figure 5.2. This resulted in the appearance of a new region of atubular dentine on the distal margin of the pulp space ($\times_2$ symbol in image f Figure 5.2).

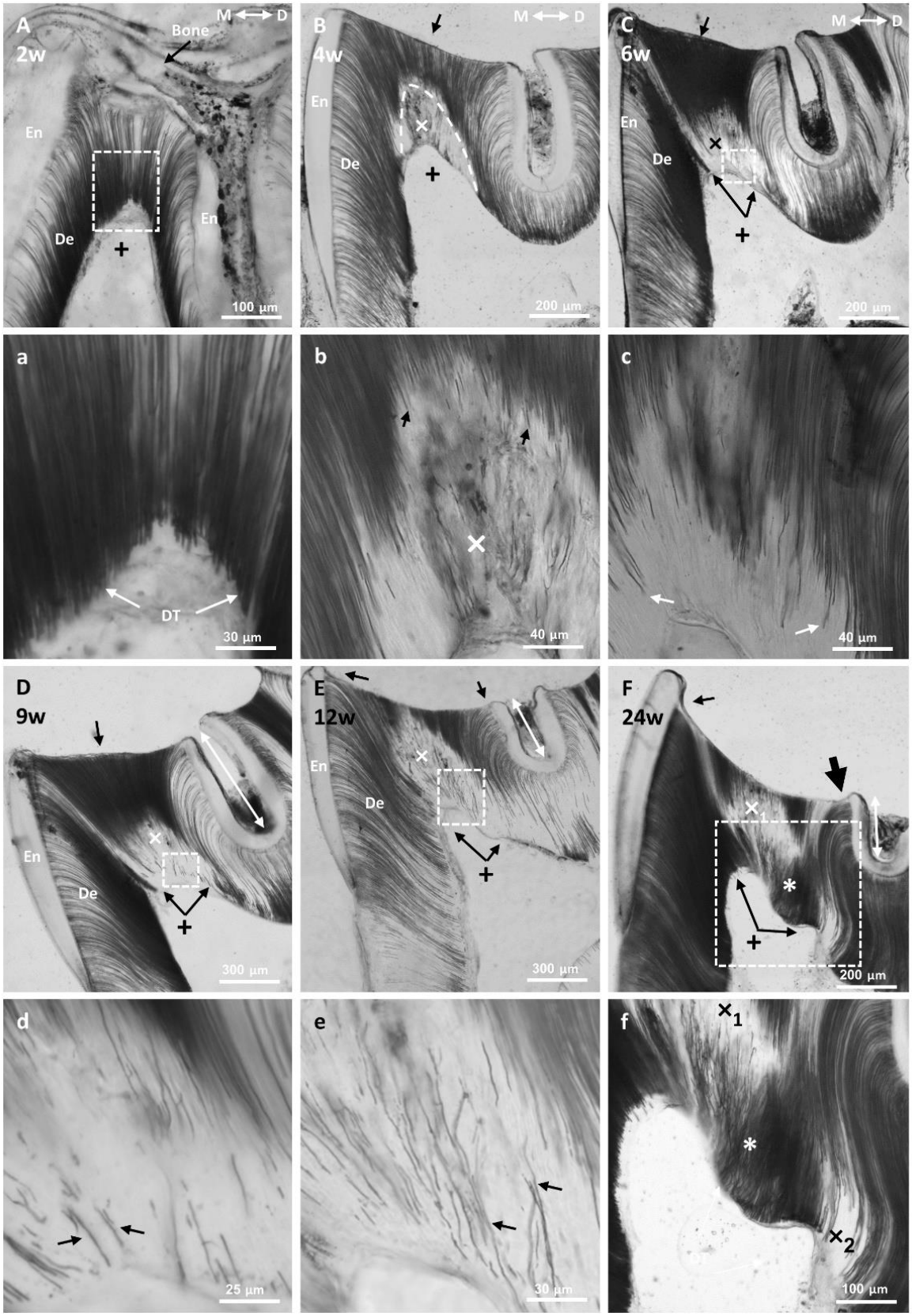
A
2w
M
D
Bone
En
De
En
100 μm
B
4w
En
De
200 μm
C
6w
En
De
200 μm
a
DT
30 μm
b
40 μm
c
40 μm
D
9w
En
De
300 μm
E
12w
En
De
300 μm
F
24w
200 μm
d
25 μm
e
30 μm
f
100 μm

Figure 5.2 Ground sections for different age of rat mandibular 1st molar (mesial cusp). The six panels of interest from A, B, C, D, E, and F are labelled a, b, c, d, e, and f respectively. Panel A shows the unerupted tooth of 2w aged rat, with mesial cusp still covered by cortical bone and there is no enamel (En) covering the dentine (De) on the tip of the cusp. The (+) symbol in images (A, B, C, D, E, and F) points to the changes of the occlusal outline of the pulp space within different age group samples. The dentinal tubules near the pulp space (arrows in image a) are compact. Panel B shows worn occlusal De (arrow) of mesial cusp at 4w rat, associated with a region of atubular tertiary dentine (×) near the pulp and its margin is marked by a curved dotted line. Image b at higher magnification shows atubular dentine region (×) which block the proximal ends of the primary dentinal tubules (black arrows). The wear increases (arrows) at 6 and 8w (images C and D), but the region of atubular dentine (×) shows few signs of short dentinal tubules near pulp (arrows in images c and d respectively). In 12w section (panel E), the occlusal surface is affected by more wear which is obvious both in the centre and sides of the cusp near En margins (arrows). The tubules become apparent near the pulp space (arrows in image e). The 24w section shows progressive signs of cusp wear at the distal and mesial side of the cusp dentine (thick and thin arrows respectively). Two forms of the tertiary dentine have been distinguished: atubular ($\times_1$ and $\times_2$), and tubular dentine (*). In higher magnification (image f) the tubular tertiary region (*) shows more compacted dentinal tubules. The double sided arrows in images D, E and F refer to the depth of the groove between the mesial and middle cusp.

5.3.2 Demineralised sections

Structure

This part of the report includes sections stained for H&E, RP, and IHC. The latter include cytoskeletal proteins (vim, α-actin, and α-tub). In most of the figures, the H&E image used is an overview and navigating image for the regions of interest for the other staining images.

0d and 1w:

In 0d, the mandibular 1st molar is still in the bell stage with no signs of dentine or enamel deposition (image A in Figure 5.3). Cellular differentiation is more recognised on the tip of the mesial cusp where the POd cells appear as a single cell layer, columnar in shape with apically retreated nuclei. These cells are vim-IR with higher staining intensity on the apical part of the cells (image B in Figure 5.3). Both α-actin and RP (F-actin) show more reactivity in the cusp region with the highest on the contact region between UOd and IEE cells (images B and C in Figure 5.3) including the basement membrane. In higher magnification, this region shows both actin and vim-IR processes of the POd (+ and * respectively in image D Figure 5.3), actin-IR is in the apical region of the POd (thick arrow in image D Figure 5.3), and intense actin-IR is seen in the basement membrane of the IEE cells (arrow image D in Figure 5.3). Cells in the sides of the cusps show less differentiation characteristics in which the region of UOd still have similar morphology to the other cells of the dental papilla (image E in Figure 5.3) with the highest F-actin expression within basement membrane region of the IEE. Additionally, no evidence of cellular processes are observed within the UOd, and all cells of the dental papilla express faint RP staining in their cytoplasm.

In sections from rats 1w after birth, both dentinogenesis and amelogenesis have already begun in the mesial cusp (image F Figure 5.3). The ameloblasts appear fully differentiated, long columnar cells with intense α-actin and RP staining in their Tome's processes. The Ods appear as a single cell layer, and are more vim-IR than α-actin-IR, but sending both actin and vim-IR OPs (+ and * respectively in image G Figure 5.3) into the PD region. Additionally, the apical region of Ods express both α-actin and vim-IR (thick arrows in image G and its component images). In higher magnification, the Ods show peripherally located F-actin staining within their cell bodies, and these send actin tree-like processes to the PD from their intense F-actin apical pole (image I Figure 5.3).

The α-tub seems not to specifically label UOd, POd (image A Figure 5.8) or even secretory Od during these early ages of development.

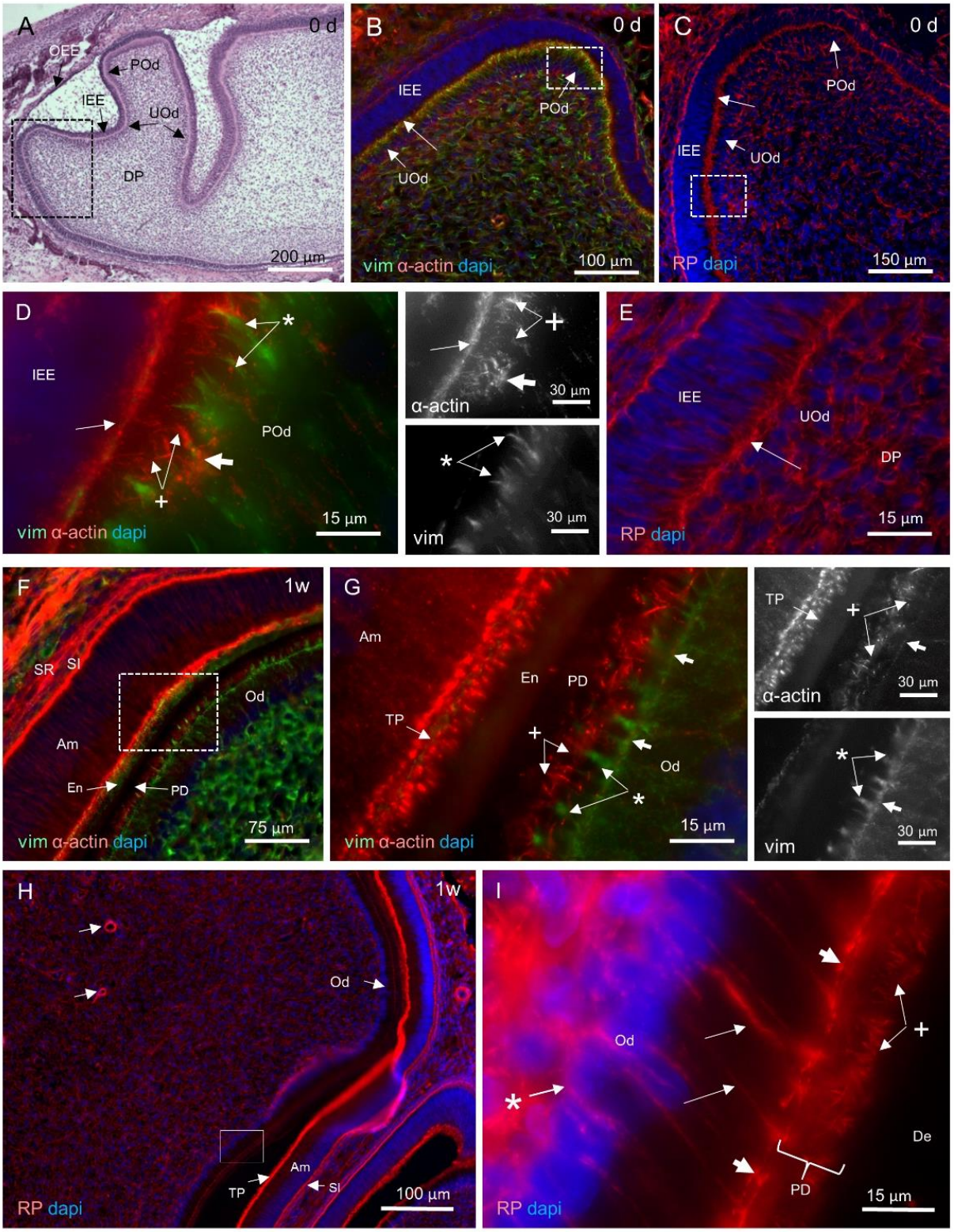
A
0 d
OEE
POd
IEE
UOd
DP
200 µm
B
0 d
IEE
POd
UOd
vim α-actin dapi
100 µm
C
0 d
POd
IEE
UOd
RP dapi
150 µm
D
IEE
POd
vim α-actin dapi
15 µm
α-actin
30 µm
vim
30 µm
E
IEE
UOd
DP
RP dapi
15 µm
F
1w
SR
SI
Od
Am
En
PD
vim α-actin dapi
75 µm
G
Am
En
PD
TP
Od
vim α-actin dapi
15 µm
TP
α-actin
30 µm
vim
30 µm
H
1w
Od
Am
TP
SI
RP dapi
100 µm
I
Od
De
PD
RP dapi
15 µm

Figure 5.3: Undemineralised sections for mesial cusp of rat mandibular 1st molar at day zero (0d) and 1w after birth.
Images B, D, F, and G were stained for vim (green), α-actin (red), and dapi (blue), images C, E, H, and I were stained for rhodamine phalloidin (RP) in red and dapi in blue. Images A-E are for 0d. Panel A is an overview H&E section of the advanced bell stage showing outer enamel epithelium (OEE), inner enamel epithelium (IEE), undifferentiated odontoblasts (UOd), pre-odontoblasts (POd) and dental papilla cells (DP). The highlighted region of interest in A is shown in B, which identifies the intense actin interface between pulp and IEE cells (long arrows). Similar observation is shown in panel C. Image D is a highly magnified region of interest in B which shows the two types of POd processes: actin (+) and vim (*), and high actin apical region of these cells (thick arrow). The basement membrane of the IEE (arrow) also shows high actin-IR. This is clearly illustrated in the two component images (α-actin and vim). Panel E is a higher magnification of the region of interest from C which shows intense F-actin in the interface between IEE and UOd (long arrow) including the basement membrane region. Images F-I are for 1w aged rat. F panel shows fully differentiated odontoblasts (Od) and ameloblasts (Am) and other cells of the enamel organ, stratum intermedium (SI) and stellate reticulum (SR). Region of interest is shown in higher magnification in panel G, which clearly identifies high actin-IR of TP of Am extending within the early formed enamel (En), and presents two types of odontoblast processes extending to predentine region (PD), actin-IR (+) and vim-IR (*). This is shown clearly in two component images actin and vim. The thick arrows in these images point to the apical region of the Ods. Image H shows a large region of mesial cusp on the left side of the image, groove region between the cusps, and small region of the middle cusp in the right lower corner. Higher RP intensity in TP of the Am, SI cells and blood vessels of the pulp (arrows) than the remaining cells of the pulp including Od. At higher magnification (panel I), the Od clearly appear as unipolar cells with basally located nuclei. RP stain appears in apical (thick arrows) lateral (long arrow) and basal (*) regions of cells in addition to OPs (+).

2w:

In H&E staining (image A Figure 5.4), the crown morphogenesis seems to be finished, while the root is commencing growth. The dentine thickness decreases from cusp tip toward the cervical region, which indicates that the dentine deposition is still progressing on the lateral walls of the cusp and cervical tooth region. Additionally, the thickness of the Od cell layer also changes from a single cell layer on the cervical region of the tooth to a thicker pseudostratified layer on the tip of the cusp region of the pulp. At the same time, and in IHC sections, the α-actin tree-like processes also show variances in their density between different developing regions of the tooth. These variances include none to very few in cusp tip region, to plenty in the cervical and developing root regions (images B and G, H respectively in Figure 5.4). There are also several of α-actin tree OPs still present in the predentine of the groove region (image C Figure 5.4). The main OPs show vim-IR only in the inner third of the dentine, alternatively α-actin-IR appears through the full length of OPs (images D and E Figure 5.4). At the apical part of the root developing region, pulp cells are still undifferentiated to Ods. These cells are vim-IR but with intense α-actin apical poles,

which are in contact with the high α-actin-IR Hertwig's epithelial root sheath (HERS) cells (image I Figure 5.4).

Similar observations are also present in RP staining. With this staining, the actin expression of the apical pole region of the Ods are well represented along the full distance of the pulp perimeter (arrows image J Figure 5.4). The OPs express RP staining along their entire length (image K Figure 5.4). The cervical region of the tooth still shows actin tree-like processes which disappear from the cusp region (image L Figure 5.4). At higher magnification, the lateral branches of the OPs are only observed in the outer third of the dentine, before their terminal branches (long and short arrows respectively in image M Figure 5.4).

Although, α-tub-IR becomes more specific within Od cells in 2w sections, it is still limited to cell bodies and no signs of this protein label the OPs (image B Figure 5.8).

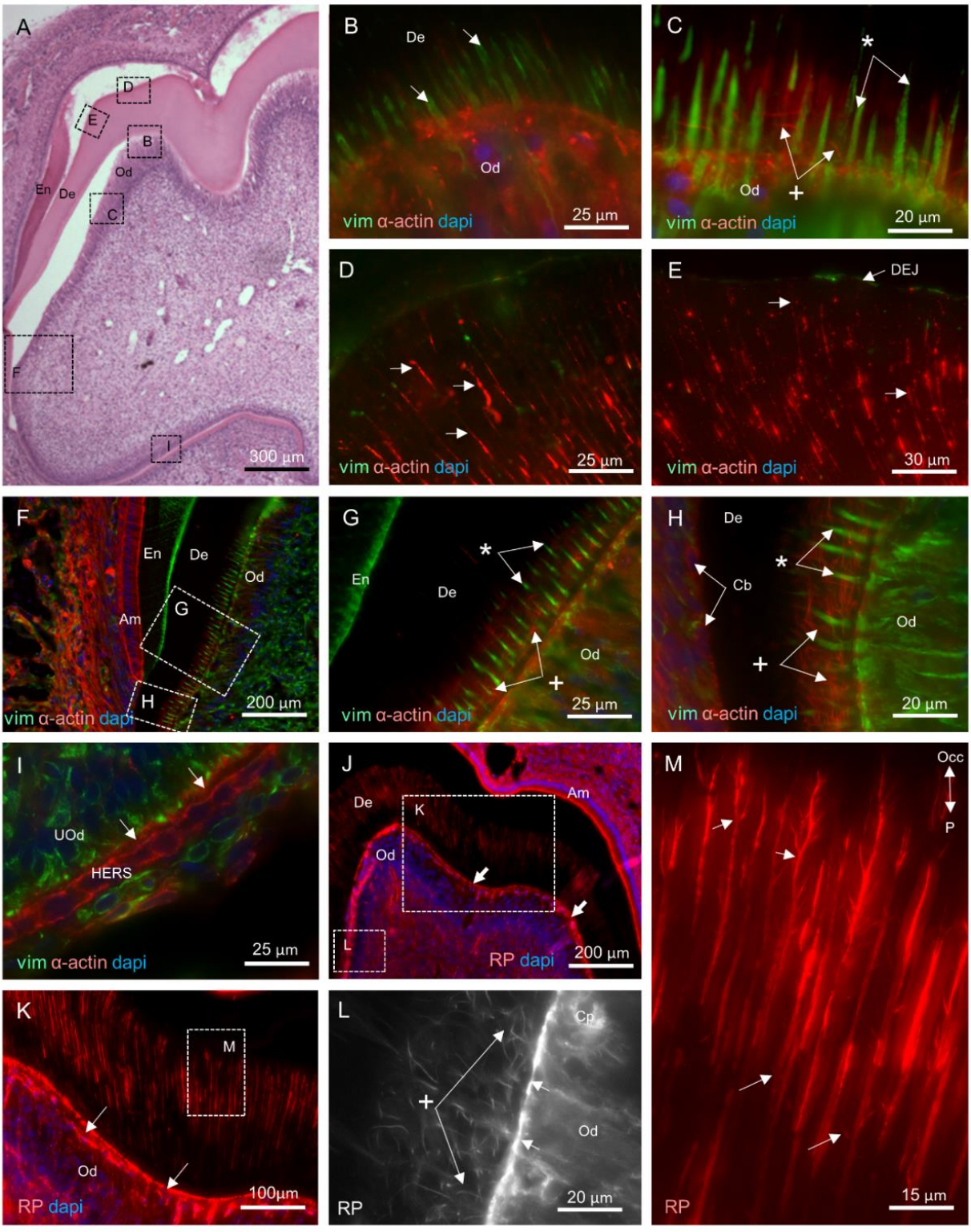
A
D
E
B
Od
En
De
C
F
I
300 µm
B
De
Od
vim α-actin dapi
25 µm
C
*
Od
+
vim α-actin dapi
20 µm
D
vim α-actin dapi
25 µm
E
DEJ
vim α-actin dapi
30 µm
F
En
De
Od
Am
G
H
vim α-actin dapi
200 µm
G
En
De
*
Od
+
vim α-actin dapi
25 µm
H
De
*
Cb
Od
+
vim α-actin dapi
20 µm
I
UOd
HERS
vim α-actin dapi
25 µm
J
De
Am
K
Od
L
RP dapi
200 µm
M
Occ
P
RP
15 µm
K
M
Od
RP dapi
100µm
L
Cp
+
Od
RP
20 µm

Figure 5.4 Demineralised sections for mandibular 1st molar mesial cusp in 2w old rat. Images stained for H&E in A, vim (green), α-actin (red), and dapi (blue) in B-I panels, and RP (red) and dapi (blue) in J and K, and just with RP in image L and M. A shows an overview image for the mesial side of the developing tooth with crown morphology almost complete and commencement of root formation. Following structures are identified: enamel En, dentine De, odontoblasts Od. Several regions of interest are highlighted in boxes in this image and are shown in the following panels: B shows Od layer in mesial cusp region with high actin-IR Od and only vim-IR OPs (arrows) extending toward De. The Od cells and their cellular processes in groove region are shown in panel C with two types of processes: actin-IR (+) and vim-IR (*). The outer region of the dentine is shown in images D and E for cusp tip and lateral wall respectively which shows rich actin-IR OPs (arrows). The cervical region of the tooth is shown in panel F which illustrates more actin-IR of the Am compared to Od. Two regions of interest are shown in higher magnifications in images G and H with greater and thicker actin-IR (+) processes in root Od (image H) compared to crown Od (image G). Also, the cementoblasts (Cb) in image H express actin-IR. Panel I presents the developing region of the root with high actin-IR in the apical region of undifferentiated Od (UOd) (arrows) and the Hertwig's epithelial root sheath (HERS) cells. The mesial cusp section is also presented in panel J, which shows high expression of RP in Am, apical region of the Od (arrows), Od processes within De and other pulp cells. The 2 boxes highlight regions of interest in cusp tip and cervical tooth region respectively. The Od have high RP expression in the apical part of the cells (arrows) and within entire length of OPs. Also, more lateral Od processes in PD appear toward the cervical region of the tooth (+ in Image L). The outer region of dentine in K is shown in higher magnification in image M, which identify the presence of OPs lateral branches close to their final termination.

3w:

The 1st molar is erupted at this age but still does not reach its functional occlusal contact (image A Figure 5.5). The appearance of the pulp horn is clearly observed as a thin conical extension of the pulp cells into the dentine. The Ods along pulp horn region express a higher intensity of RP stain, which indicates higher F-actin in their cytoskeleton in comparison to the adjacent pulp cells (images B and C Figure 5.5). A similar observation is present with α-actin in pulp horn region. The Od layer in the whole cusp appears as a thick, continuous, pseudostratified layer of cells which shows high α-actin-IR in the apical poles of Od (image D Figure 5.5). No actin tree-like processes are seen in the PD region and the main OPs express vim-IR in their inner third and actin along their entire length (image E Figure 5.5). The SOd cells also express a high α-actin and F-actin in comparison to the Od layer. There are also numerous capillaries present in the SOd, in between Od cells, and in the apical region of this cell layer.

Ods in the groove and cervical region still have actin processes in their apical side (images F and G respectively Figure 5.5), but the density of these processes is much higher in the root. The root is still growing and shows α-actin-IR in the HERS cells in its apical part (image H Figure 5.5).

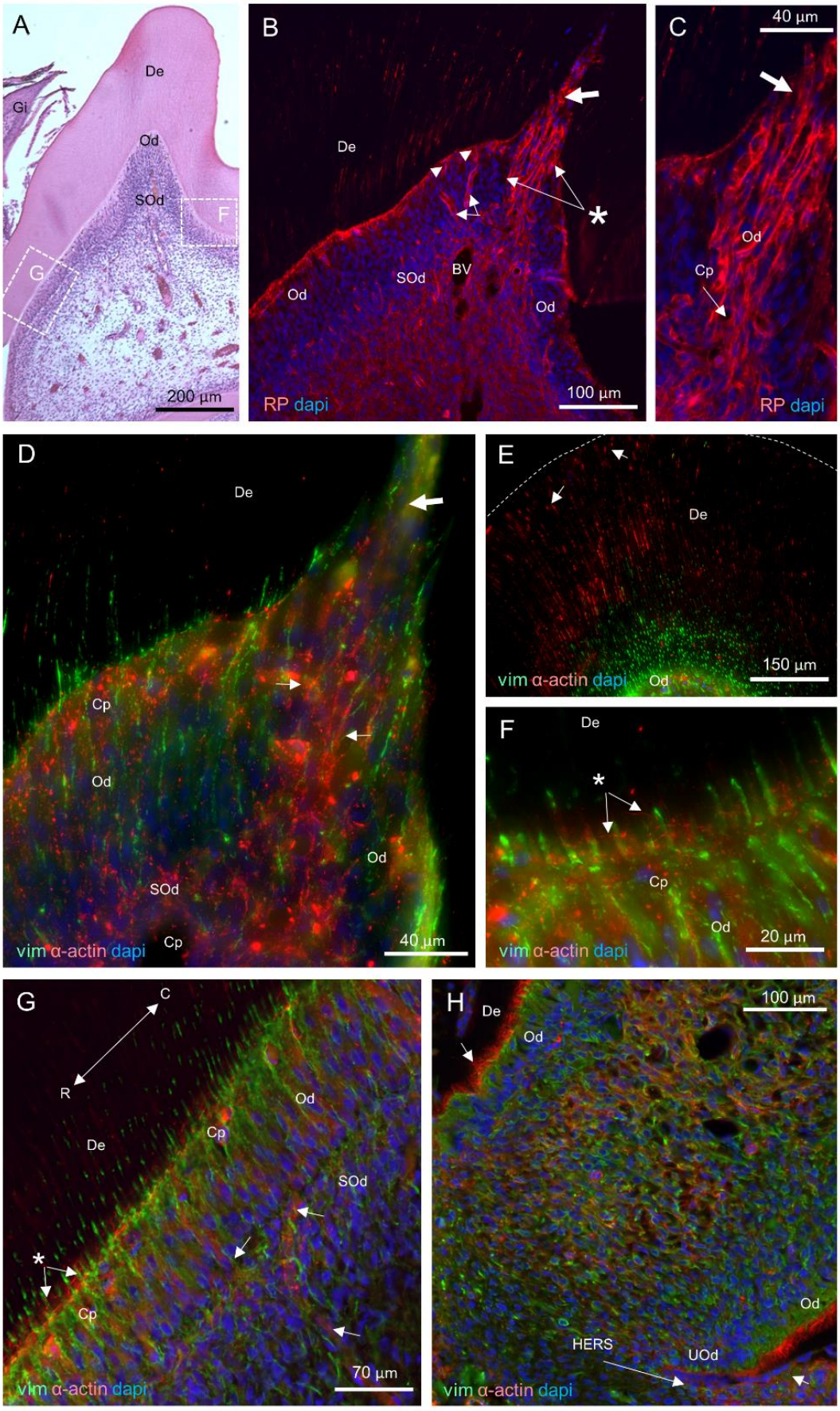
A
De
Gi
Od
SOd
F
G
200 µm
B
De
Od
SOd
BV
Od
RP dapi
100 µm
C
40 µm
Od
Cp
RP dapi
D
De
Cp
Od
Od
SOd
Cp
vim α-actin dapi
40 µm
E
De
150 µm
vim α-actin dapi
Od
F
De
Cp
Od
20 µm
vim α-actin dapi
G
C
R
Od
Cp
De
SOd
Cp
70 µm
vim α-actin dapi
H
De
Od
100 µm
Od
HERS
UOd
vim α-actin dapi

Figure 5.5: Mesial cusp sections of demineralised mandibular 1st molar in 3w old rat. A shows an overview H&E image for the mesial cusp identifying the following structures: odontoblasts (Od), sub-odontoblasts (SOd), dentine (De), and gingiva (Gi). Images B and C stained for RP (red), dapi (blue), D-H images stained for vim (green), actin (red) and dapi (blue). Panel B shows the pulp horn (thick arrow), odontoblasts (Od) and sub-odontoblast cells (SOd). Arrows with (*) showing the pulp horn cells, small arrows show capillaries running in Od cell layer, arrow heads illustrate small capillaries on the apical side of the Od, and (BV) large blood vessel in the SOd. Image C is a magnification from B to show the complexity of pulp horn Od cells (thick arrow). Panel D shows the mesial cusp with arrows pointing to the actin-IR Od cells of pulp horn which overlap each other. Capillaries (Cp) appear in both Od and SOd. The extension of the OPs (arrows), with actin-IR, toward the outer surface of the dentine (dotted line) is shown in panel E. Higher magnification image F shows the Od in groove region of the tooth. Arrows with (*) point to the lateral actin-IR OPs, with some Cp in Od cell layer. The cervical region is shown in panel G. The orientation is included by the two-sided arrow pointing toward root (R) and crown (C). Arrows pointing to large blood vessel which runs from the SOd and gives number of branches emerging the Od with some Cp in the apical region of the Od. The root apex is shown in image H, with actin-IR for OPs and less for the cells of the Hertwig's epithelial root sheath (HERS).

4w:

At this age, occlusal wear is evident on the mesial cusp, and it looks greater on the distal side compared to the mesial. The trauma effect of the wear is mirrored within Ods layer and SOd cells. This is apparent on the distal side in comparison to intact mesial side of the cusp pulp (images A and B Figure 5.6). The effect of trauma from wear can be summarised as follows starting from the dentinal surface:

- The worn dentine surface shows empty dentinal tubules in the central worn area (long arrow in image F Figure 5.6). Alternatively, the OPs still present in the dentinal tubules beyond the minor worn dentine surface, are labelled with α-actin, and devoid of any lateral branches (short arrows in image F Figure 5.6).
- Several cellular nuclei are obvious within the atubular dentine region (image B-E Figure 5.6). These nuclei show faint staining in comparison to other cells of the pulp, and seem to be separated from the pulp horn region and the distal side of the Od layer.
- The discontinuity of the pulp border Ods is apparent beyond the trauma region with high actin-IR (image C and D Figure 5.6).
- The traumatised Ods appear without OPs (image D and E Figure 5.6).
- The traumatised Ods lose their apical junctional contacts and look more separated in comparison to adjacent non traumatised Ods (image D and E Figure 5.6) with many dilated capillaries in between.
- The SOd beyond the trauma region express the highest actin-IR (images C and D Figure 5.6). These cells also seem densely packed with limited spaces in between them.
- Several dilated capillaries are illustrated within Od and SOd (image B Figure 5.6). No signs of pus have been distinguished between Od layer and newly formed atubular dentine.

The appearance of the non-traumatised region of the crown and developing root cells can be summarised as follows:

- The unworn dentine surface of the cusp still shows complex terminal branches of the OPs in the outer dentine region and OPs are fully labelled with actin (thick arrow in image F Figure 5.6).
- The tree-like actin processes are less within the predentine region of the crown (image G Figure 5.6).
- These processes are still evident within the root, especially the developing regions (image H Figure 5.6).
- α-tub-IR becomes more specific in Od cell layer. It also labels some large nerves running within the pulp core, and small nerve branches within SOd cells (image C Figure 5.8). This structural protein also marks the pulpal half of the OPs beyond intact tooth surface.

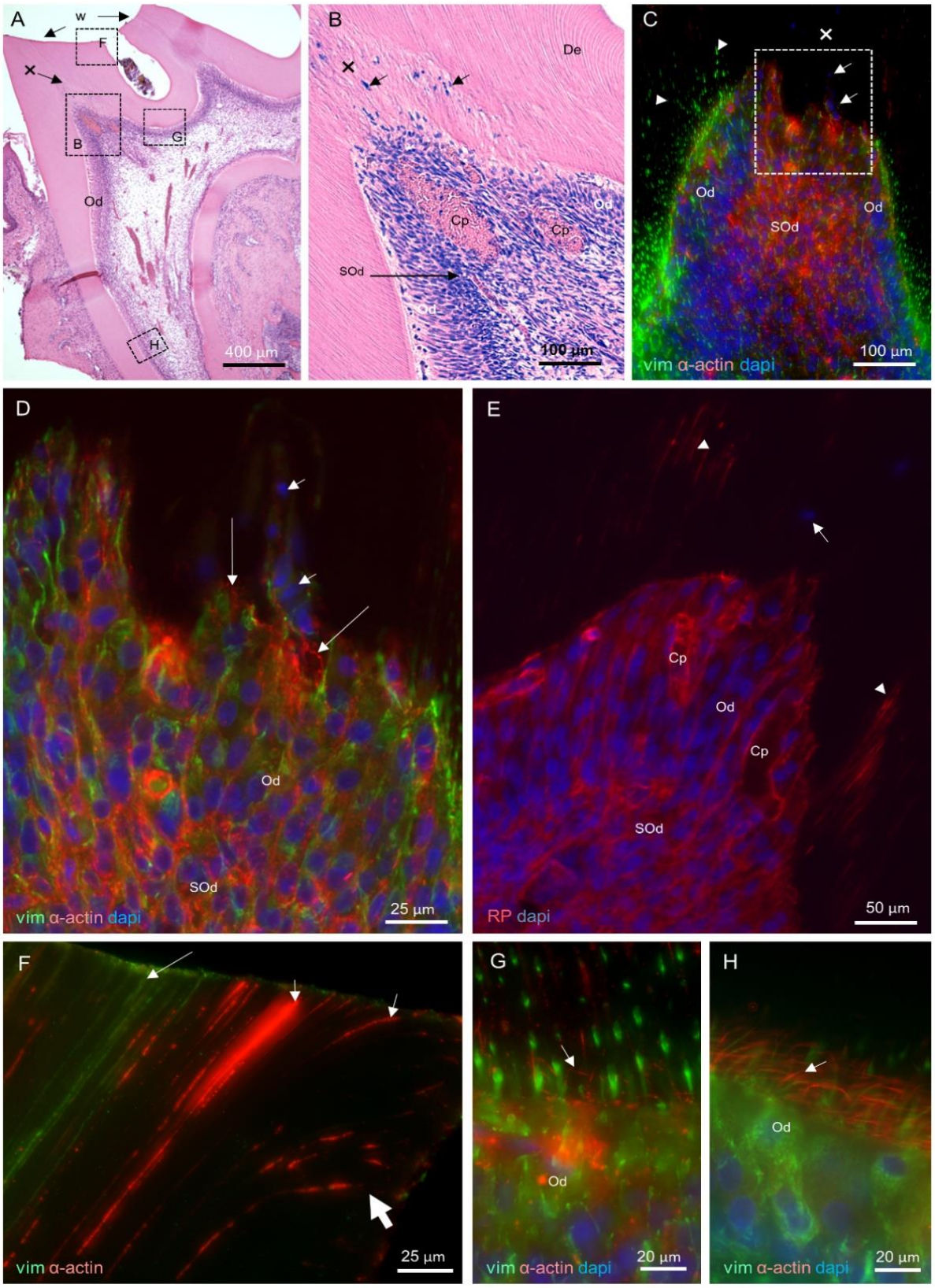
A
w
F
B
G
Od
H
400 µm
B
De
Od
Cp
Cp
SOd
Od
100 µm
C
Od
SOd
Od
vim α-actin dapi
100 µm
D
Od
SOd
vim α-actin dapi
25 µm
E
Cp
Od
Cp
SOd
RP dapi
50 µm
F
vim α-actin
25 µm
G
Od
vim α-actin dapi
20 µm
H
Od
vim α-actin dapi
20 µm

Figure 5.6: Effect of occlusal wear in 4 weeks old rat mandibular 1st molar in demineralised mesial cusp sections.
Images stained for H&E in (A and B), and panels C,D,F, G and H stained for vimentin (green), actin (red), and dapi (blue), and image E for RP (red) and dapi (blue). An overview image A shows mesial (left) and middle (right) cusps wear (w) associated with an area of tertiary dentine (×). Region of interest in A is shown in higher magnification in panel B, which identifies the tertiary dentine region containing nuclei (arrows) of some odontoblast cells (Od) and dilated capillaries (Cp) appear within Od and SOd. Same region in B is also presented in panel C and E but with different staining, shows the discontinuity in Od beyond tertiary dentine region (×). Od also have lost their cellular processes which are still present in the adjacent Od (arrow heads), where some nuclei merge into tertiary dentine region (arrows). Additionally, the highest actin intensity is identified within SOds. Region of interest in C is shown in higher magnification in panel D with actin-IR cell membrane (long arrows) of the separating cells (small arrows). The worn dentine surface is shown in panel F with some actin-IR OPs still reaching the outer dentine (short arrows). In the severely worn region, the dentinal tubules look empty (long arrow). In unworn side (right side of the image) the OPs still have complex terminal branches (wide arrow) near the outer surface. Panels G and H show the Od in groove and root regions respectively, with more actin-IR tree-like OPs in panel H compared to the thinner and dispersed pattern in panel G.

6w:

By this age, the overall pulp profile seems to be retracted in a pulpal direction in the region of tertiary dentine, beyond the cusp worn surface (two arrows in image A Figure 5.7). The structural morphology of the pulp cells in this region can be summarised as follows:

- The Ods in the trauma region return their apical junctional contacts which express both actin and vim-IR (images B Figure 5.7).
- The orientation of the Od cells in the trauma site appear in different directions (sometimes horizontally as seen in * image B Figure 5.7) in comparison to their orientation in non-trauma regions which look parallel to each other and perpendicular on their apical junctional region (+ in image B Figure 5.7).
- Short OPs start to extend into the PD region behind the atubular dentine as secondary OPs. These processes are meandering in shape and express both vim and actin-IR.
- The Ods have a higher IR of both actin and vim in comparison to SOds (images a1 and a2 Figure 5.7).
- No actin tree-like processes are evident within the PD region of the crown, although they are still apparent within root PD region of the tooth.
- As α-tub becomes more specific in Od from the 4w sections, it is more intense within OPs and starts marking the outer third of processes beyond intact tooth surfaces (+ in image D Figure 5.8). However, in the region of reactionary dentine, the newly formed OPs IR to α-tub is nearly similar to vim expression (images E and F Figure 5.8).

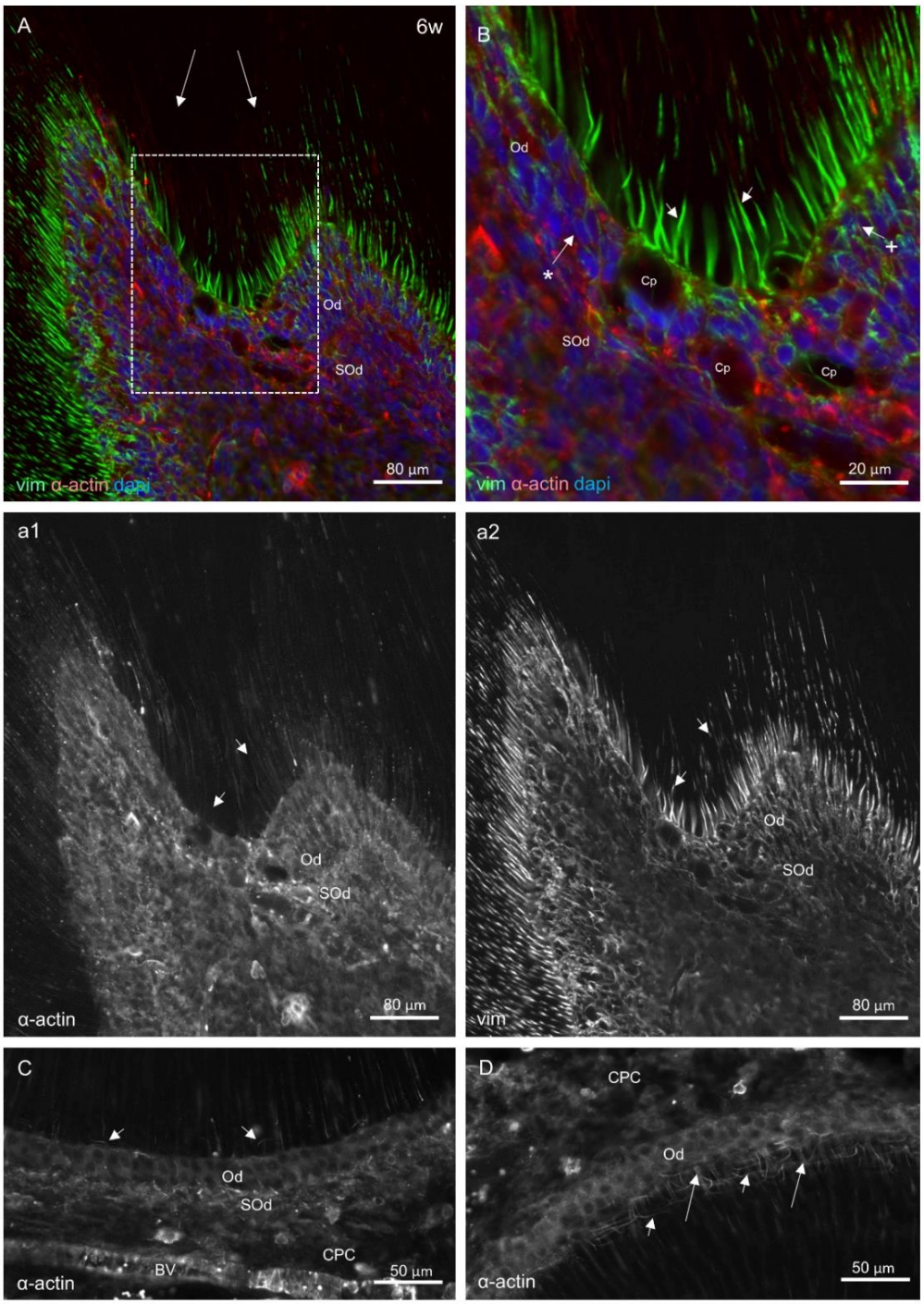

Figure 5.7: Demineralised sections of the 6w old rat mandibular 1st molar.
Panels A and B were stained for vim (green), α-actin (red), and dapi (blue), image a2 for vim and rest of the images for α-actin. Panel A shows the mesial cusp region with pulp receeded (arrows) following tooth wear. Region of interest is shown with higher magnification in B, with vim-IR OPs within the tertiary dentine region (arrows), and dilated capillaries (Cp) engaging the Od and SOd cells. The two component images a1 and a2 show vim-IR for the newly formed OPs is more than for α-actin (arrows). Panel C shows the groove region with a sparsity of actin-IR lateral process (arrows) of Od compared to the furcation region in panel D that have abundant actin-IR lateral process (arrows) of Od in addition to actin-IR in the basal part of the main OPs (long arrows).

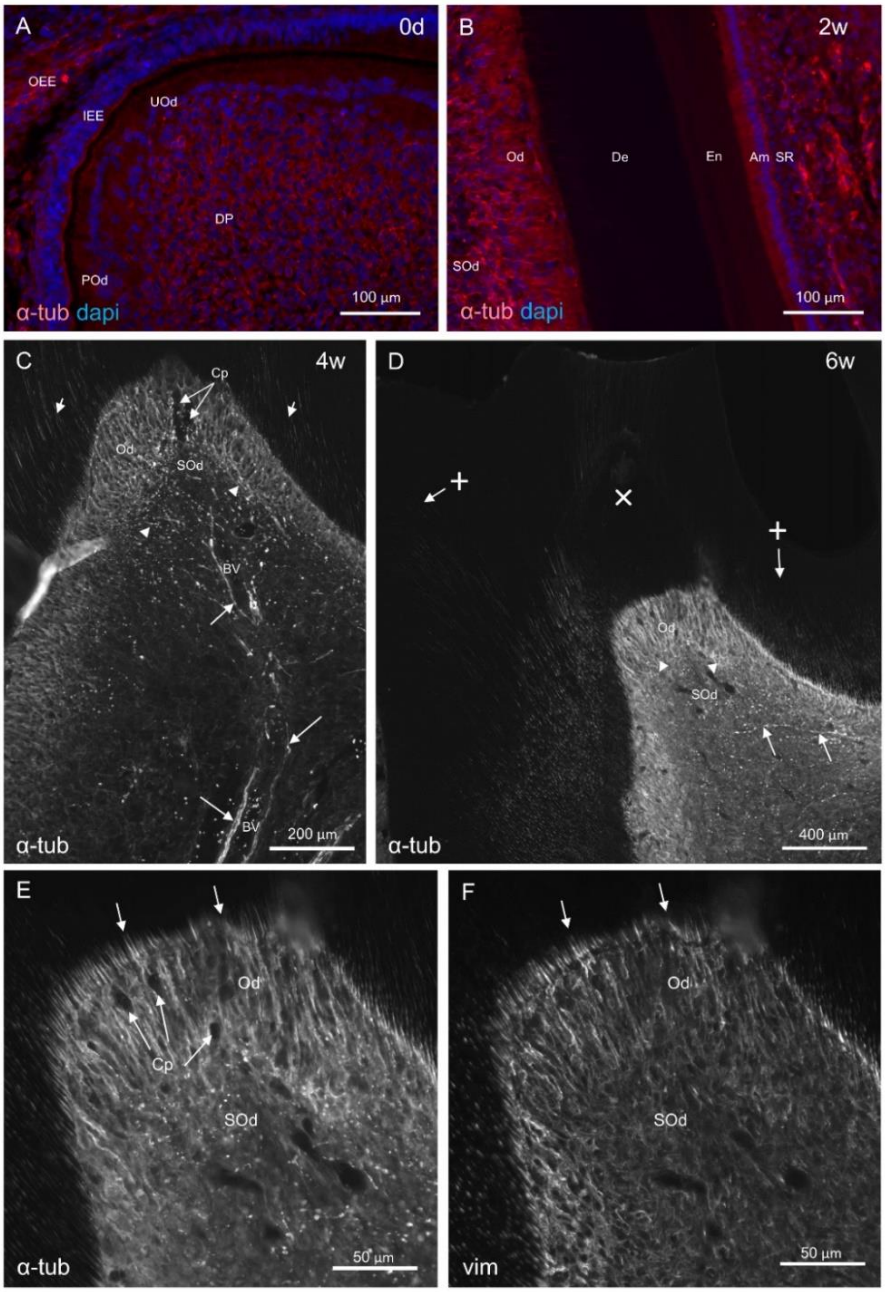

Figure 5.8: α-Tubulin (tub) expression in different age groups of rat mandibular 1st molar mesial cusp.
A and B images were stained for α-tub (red) and dapi (blue), C, D and E for α-tub and F for vim. Panel A of 0d rat section, shows more tub-IR in dental papilla (DP) and outer enamel epithelium (OEE) cells than in undifferentiated odontoblasts (UOd) and the inner enamel epithelium (IEE). The tub-IR increase in Od and SOd cells in 2w rat (image B), but there is no expression detected in OPs within the dentine (De). In 4w rat (image C), the tub-IR becomes more specific in the Od cells, their processes (arrows), large nerve fibres (long arrows) run within central pulp region in association with big blood vessels (BV). Small nerves (arrow heads) also labelled with tub are seen in SOd regions. Similar findings are presented in image D for 6w rat but with higher tub-IR in the outer region of the OPs (+) and no tub-IR detected in tertiary dentine region (×). Images E and F are higher magnification images for pulp region in image D which shows similar labelling of the OPs by α-tub and vim in reactionary dentine region. Capillaries in Od region are pointed to by arrows in image E.

9w-12w:

The signs of pulp responses to trauma start to subside with progressing age. The following morphological features are recognised:

- The reactionary dentine starts to express different profiles: atubular occlusally and tubular pulpally. Within atubular dentine some lacunae can be recognised. (images A and B Figure 5.9). These could be the site for trauma associated apoptotic pulp cells.
- The Od layer beyond the trauma region appears uniform, and the large capillaries seems to be more retracted in a pulpal direction toward SOd region (image C Figure 5.9).
- The meandering secondary OPs become longer and denser with time (images D Figure 5.9 and C, D Figure 5.10).
- OPs near outer worn dentine surface (image F Figure 5.10) show similar details as described previously in Chapter 4 section 4.3.

Within non-trauma regions, the following morphological features can be seen:

- The OPs start to express α-tub within their entire length (image G Figure 5.10). Actin is expressed in the inner half, and vim only the inner third of the entire OPs length (image C and D Figure 5.10).
- The root formation is fully accomplished at 12w of rat age with complete formation of the apical foramen. The signs of occlusal loading due to the wear process can also be manifested in the apical region of the root. The hypercementosis process is obviously recognised and the thickness of the deposited cementum appears more on the outer side of the root in comparison to the inner side (image A Figure 5.10).

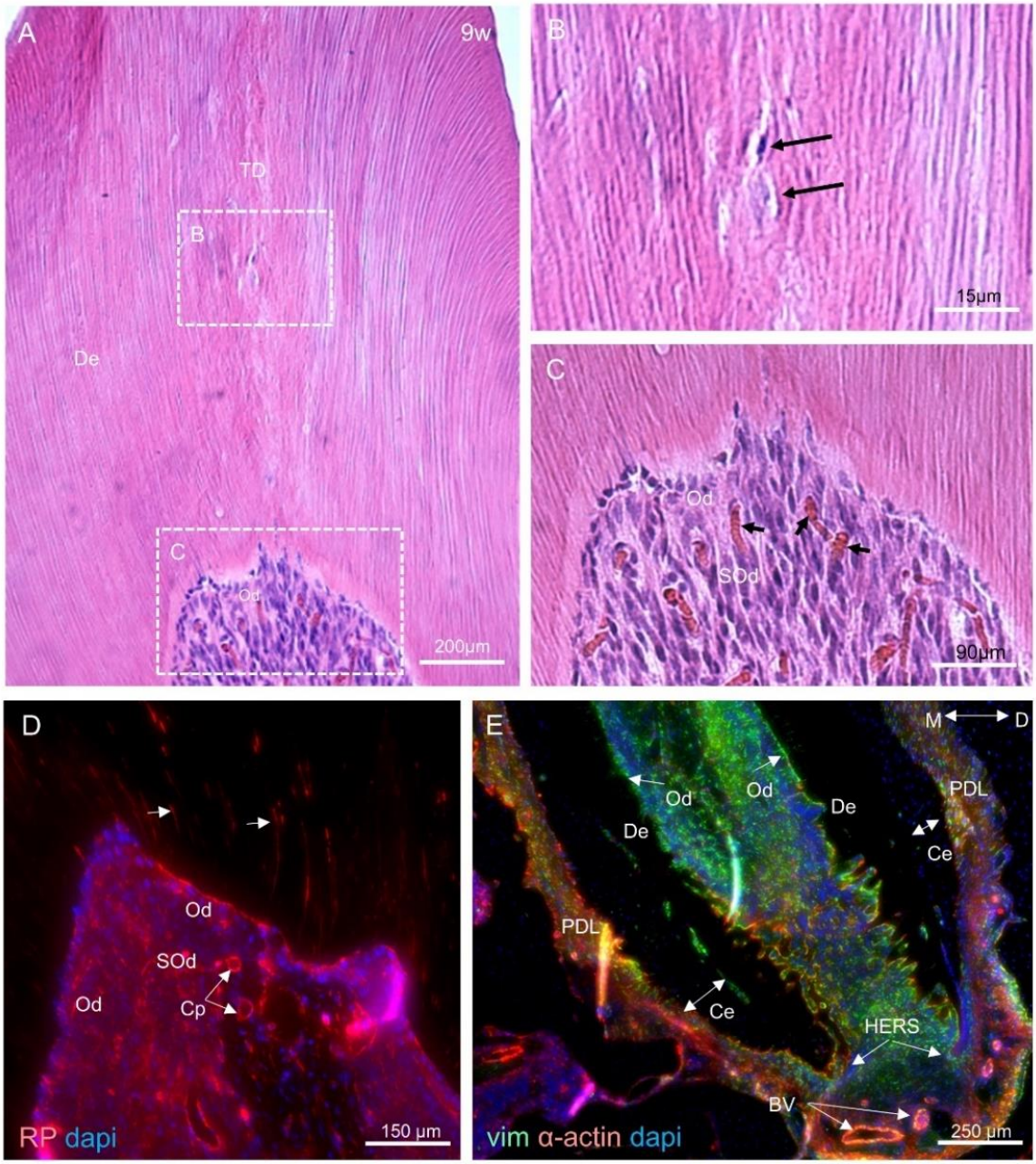

Figure 5.9: Demineralised sections of the 9w old rat mandibular 1st molar. Images A,B and C are stained for H&E, D for RP (red) and dapi (blue), and E for vim (green), α-actin (red), and dapi (blue). Panel A shows an overview image for the pulp and associated reactionary dentine region. 2 regions of interest are illustrated in higher magnifications in image B and C. Two arrows in Image B point to a lacuna-like structure within tertiary dentine. Several capillaries are identified in SOd region (arrows). Same details in C are illustrated by different stain in D, with arrows pointing to the newly formed OPs. The mesial root apical region is presented in panel E with wider cementum (Ce) thickness on the outer surface of the root (left double sided arrow) in comparison to the inner surface (right double sided arrow) with large blood vessels in the periodontal ligament (PDL) near the root apical region, which still contains the cells of HERS. Double sided arrow at the top of the image is orients the mesial (M) and distal (D) sides of the root.

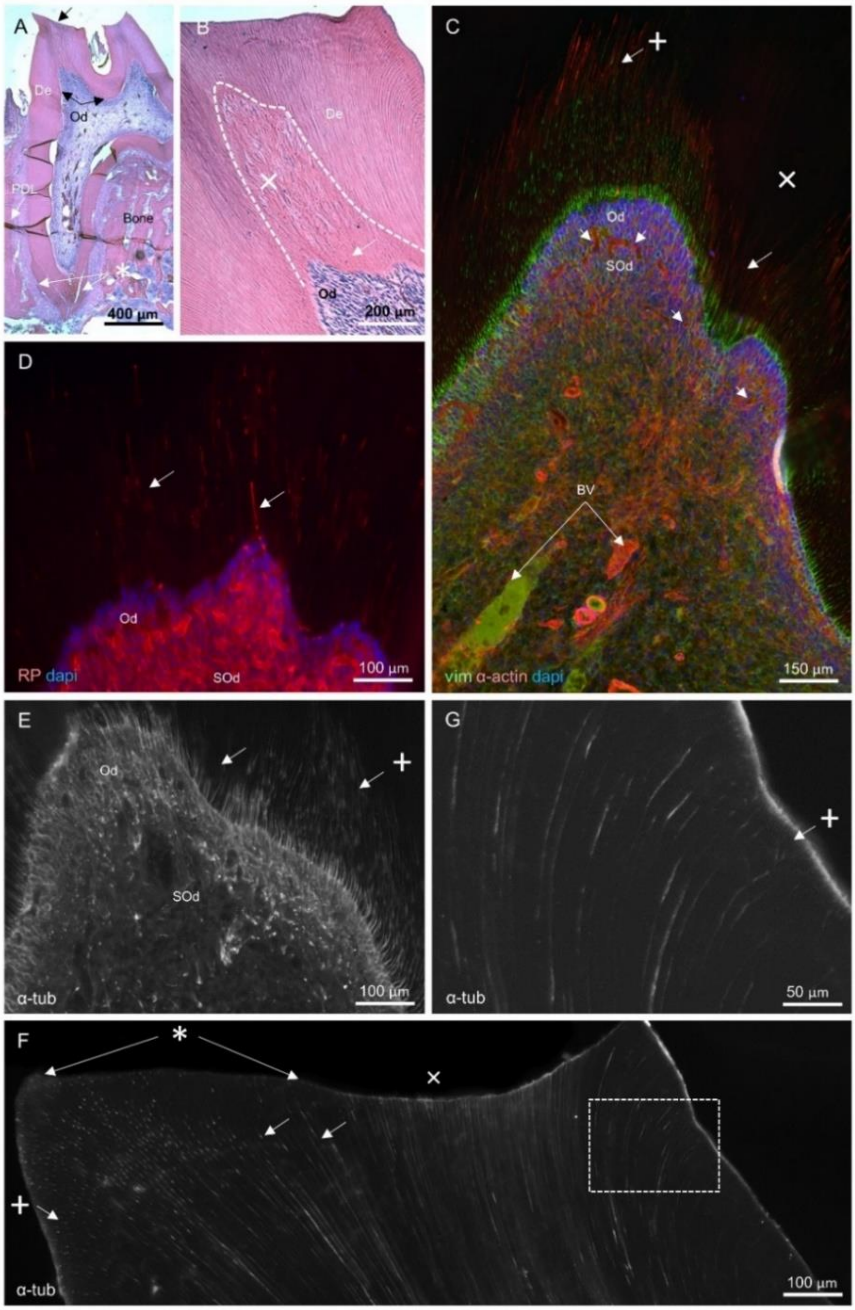

Figure 5.10: Demineralised sections of 1st mandibular molar of 12w old rat mesial cusp. Images A, B stained for H&E, C for vim (green), actin (red) and dapi (blue), D for RP (red) and dapi (blue), and E, F, and G for tub. A is an overview image for mesial cusp and root with following structures: dentine (De), periodontal ligament (PDL), odontoblasts (Od), bone, hypercementosis of the root apex (*), and wear of the occlusal surface of the cusp (arrow). In higher magnification, the region of tertiary dentine (dotted line) show two different dentinal tubule arrangements: atubular (x) and tubular (arrow) closer to the Od. This atubular dentine region (x) shows no signs of OPs in image C, while many OPs run parallel to each other in dentine region closer to the pulp (arrow) similar to other part of the dentine (+). Large blood vessels (BV) and small capillaries (arrows) are also detected. The same OPs arrangement is detected in both RP and tub (image D and E respectively), but with more tub-IR within OPs in the outer dentine under the unworn tooth surfaces (+ in image F and at higher magnification in G). Panel F also shows no OPs detected under severe worn tooth surface (x), while there are OPs (arrows) reaching to the outer De under minor worn De surface (*).

24w:

The limitation in the remaining pulp space due to continuous secondary and tertiary dentine deposition is quite obvious in 24w sections. This causes difficulty in getting the pulp chamber and pulp canal in one section together (image A Figure 5.11) in most of the presented figures. Similar to the ground section observations (image F Figure 5.2), the H&E sections also confirm the differences in dentine tubular pattern from atubular occlusal to tubular pulpal parts of the tertiary dentine region (image B Figure 5.11).

In IHC and RP staining, the number and length of the newly formed secondary OPs in the reactionary dentine are increased (long arrow in images C, D and E in Figure 5.11). These secondary processes express actin within their entire thickness and vim and α-tub within their pulpal third. However, in image C, a new region of atubular dentine (x_2) shows an absence of the primary OPs in the adjacent, more distal region of the Od cells. This indicates a new trauma site as a result of progressive wear. The SOd cells beyond the new trauma region also show high actin expression similar to the reaction to the first trauma in 4w sample. In non-trauma surfaces, the OPs shows similar labelling for actin, vim and tub that has been described previously in 12w rat sections (images C, D, and E Figure 5.11 and image G Figure 5.12)

The signs of ageing can be identified by an increase of secondary dentine deposition in the non-traumatised region of the tooth. This can be illustrated in the groove region of the tooth by comparing the differences in pulp width between 12 and 24w sections (images A and D respectively in Figure 5.12). The pulp width in 24w sections is reduced to less than half its size in 12w sections which indicate continuous secondary dentine formation during this period. Additionally, the furcation and root of the tooth lose their actin tree-like OPs in their PD region (image F Figure 5.12), which was present in 12w sections (image C Figure 5.12). Furthermore, the ageing signs could be easily identified in the root apex region. This region shows increase in thickness of the accumulated hypercementosis on the outer and inner side of the mesial root increasing the root length (two double sided arrows in image H Figure 5.12).

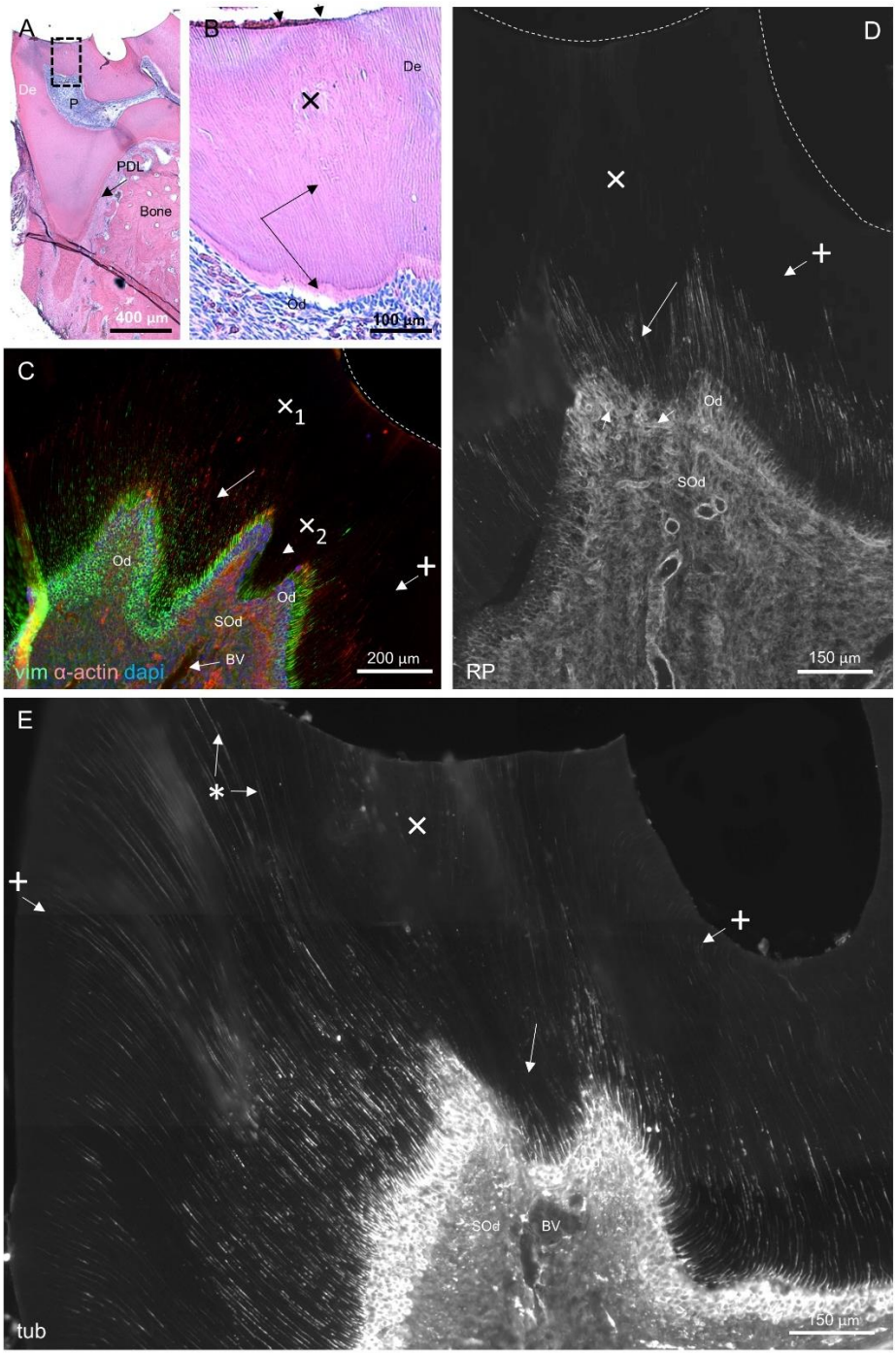

Figure 5.11: Demineralised sections of 1st mandibular molar of 24w old rat mesial cusp. Images A and B are stained for H&E stain, C for vim (green), actin (red) and dapi (blue), D for RP, and E for tub. A is an overview image of mesial cusp and root with following structures: dentine (De), limited pulp (P), periodontal ligament (PDL), and bone. Deep wear is shown on the occlusal surface of the cusp (arrow). In higher magnification (image B), the region of atubular tertiary dentine (×) reaches the worn surface (small arrows) and the region of tubular tertiary dentine (big arrows) become wider. The OPs near pulp become denser as shown in images C and D (long arrows), with no signs of OPs detected in atubular De region (x). At the same time, processes on the lateral walls of the cusp label actin-IR only in pulpal half of these OPs (+). Second region of atubular dentine is also detected in image C (×2). Similar observations are detected in panel E but with tub-IR expressed in the outer part of OPs both under unworn (+) and minor worn (*) dentine surfaces.

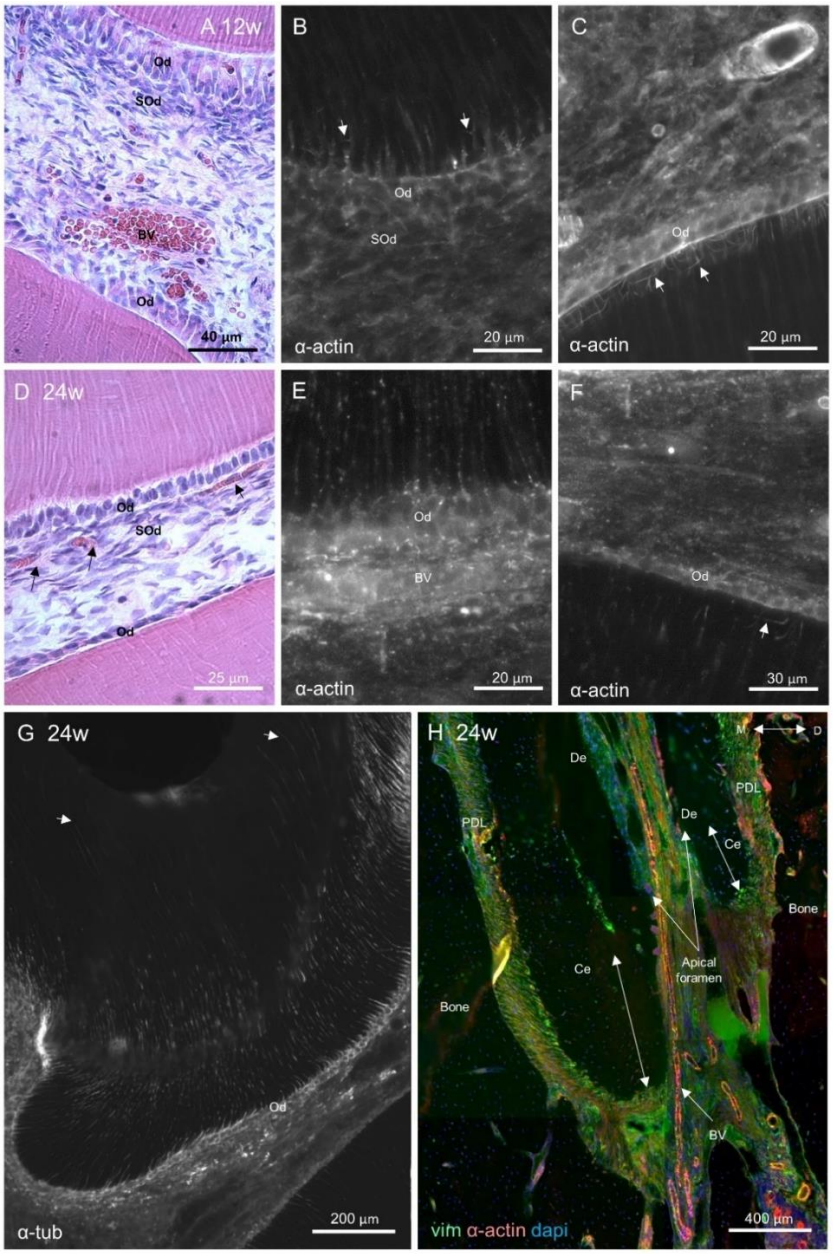

Figure 5.12: Demineralised sections of groove and root regions in 12 and 24w old rat mandibular 1st molar.
Images A, B, and C is for 12w while the rest are for 24w aged rat. Panels A and D, are stained for H&E, B ,C ,E and F for actin, G for tub, and H for vim (green), actin (red) and dapi (blue). The pulp space is larger in 12w in comparison to 24w as shown in images A and D respectively. Also large BV and small capillaries (arrows) have been identified. Comparing the groove and furcation regions, only small branches of the OPs are detected (arrows in image B), while numerous long lateral actin-IR OPs are still present in PD region of furcation area (arrows in image C). However, these two regions show no lateral actin-IR OPs in 24w (image E and F) except very few in furcation region (arrow). The extensions of the OPs to the outer dentine is detected with tub, as shown in panel G (arrows). Panel H shows the apical region of the mesial root with the region of hypercementosis (Ce) (double sided arrows) with triple its size on the mesial surface (left side of the image) compared to the distal (right side of the image). Also large blood vessels enter the tooth through its apical foramen. PDL= periodontal ligament. Double sided arrow at the top of the image is to orientate the mesial (M) and distal (D) directions of the root.

Cell division (expression of Ki 67)

During tooth crown morpho-differentiation stage of rat 1st molar at 0d, the cellular division for the whole tooth germ cells is apparent by Ki67-IR in nuclei of the differentiating cells (image A Figure 5.13). All cells of the DP, including regions of UOd, and enamel organ, including IEE and OEE, show Ki67-IR which indicate cellular division activity of these cells (images a1 and a2 Figure 5.13).

After cellular differentiation and commencement of hard tissue deposition in 1w sections, no Ki67-IR has been identified within all pulp cells of the tooth crown (images B and C Figure 5.13). The region of the tooth which still shows the Ki67-IR in their cellular nuclei is the developing root region, including both pulp and HERS cells, which indicates that these cells still show cellular division activity (image D Figure 5.13). These observations remain similar during all ages of the study where root development is still unfinished (Figure 5.14 and Figure 5.15). The signs of cellular division that are observed within fully differentiated tooth region are only located within the capillaries, which could be some dividing blood cells in these vessels (image a and d with their component images in Figure 5.14).

In the 4w old molar, the region of pulp trauma due to wear process has no detected signs of Ki67-IR neither within the traumatised Od nor within the adjacent SOd cells (image A Figure 5.15). The oldest age group within this study (24w) also confirms the absence of any signs of cellular division within all pulp cells (images D and E Figure 5.15). The positive controls for each group are sections of the apical bud for the mandibular incisors for each age, and one section is illustrated in image F Figure 5.15.

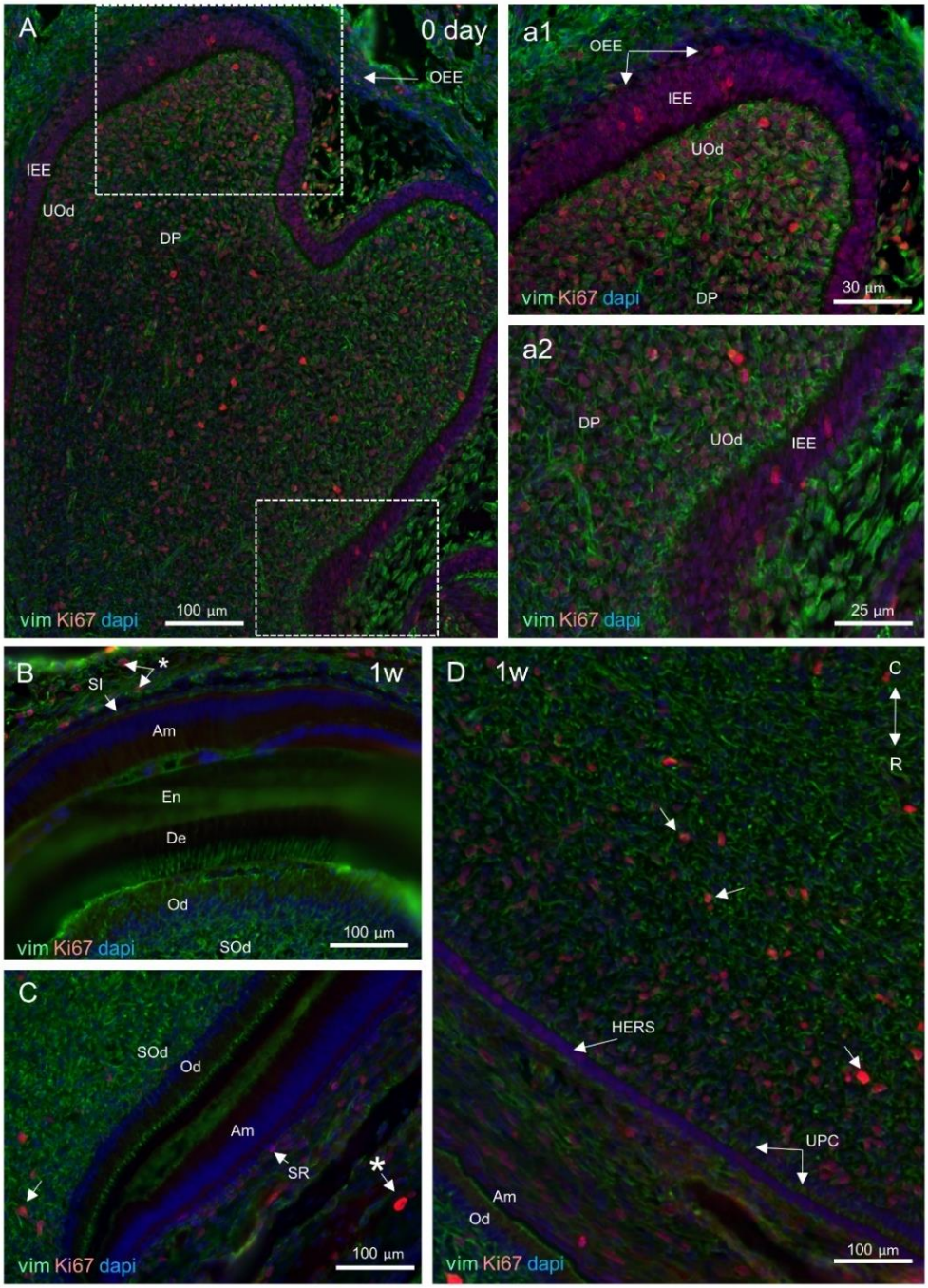

Figure 5.13: Cellular division in mesial cusps undemineralised sections of 0d and 1w rat mandibular 1st molar.
Images A, a1, and a2 is for 0d, B, C and D for 1w old rat. All images stained for vim (green), Ki67 (red), and dapi (blue). Panel A shows an overview of the developing mesial cusp with following structures: inner enamel epithelium (IEE), outer enamel epithelium (OEE), undifferentiated odontoblasts (UOd), and dental papilla (DP). Two regions of interest are shown in higher magnification in images a1 and a2. The majority of cells of IEE, OEE, DP, and UOd show Ki67-IR in their dividing nuclei. No Ki67-IR is shown in image B in Od, SOd, Am and SI cells but is still presented within outer cells of enamel organ (*). Similarly, no expression is seen in image C, except in some pulp cells toward the root (arrow) and in bone (*). Panel D shows most of the pulp cells toward the root (arrows), UOd, and HERS express Ki67-IR. This image also shows the Am and Od of the incisor tooth down in the image.

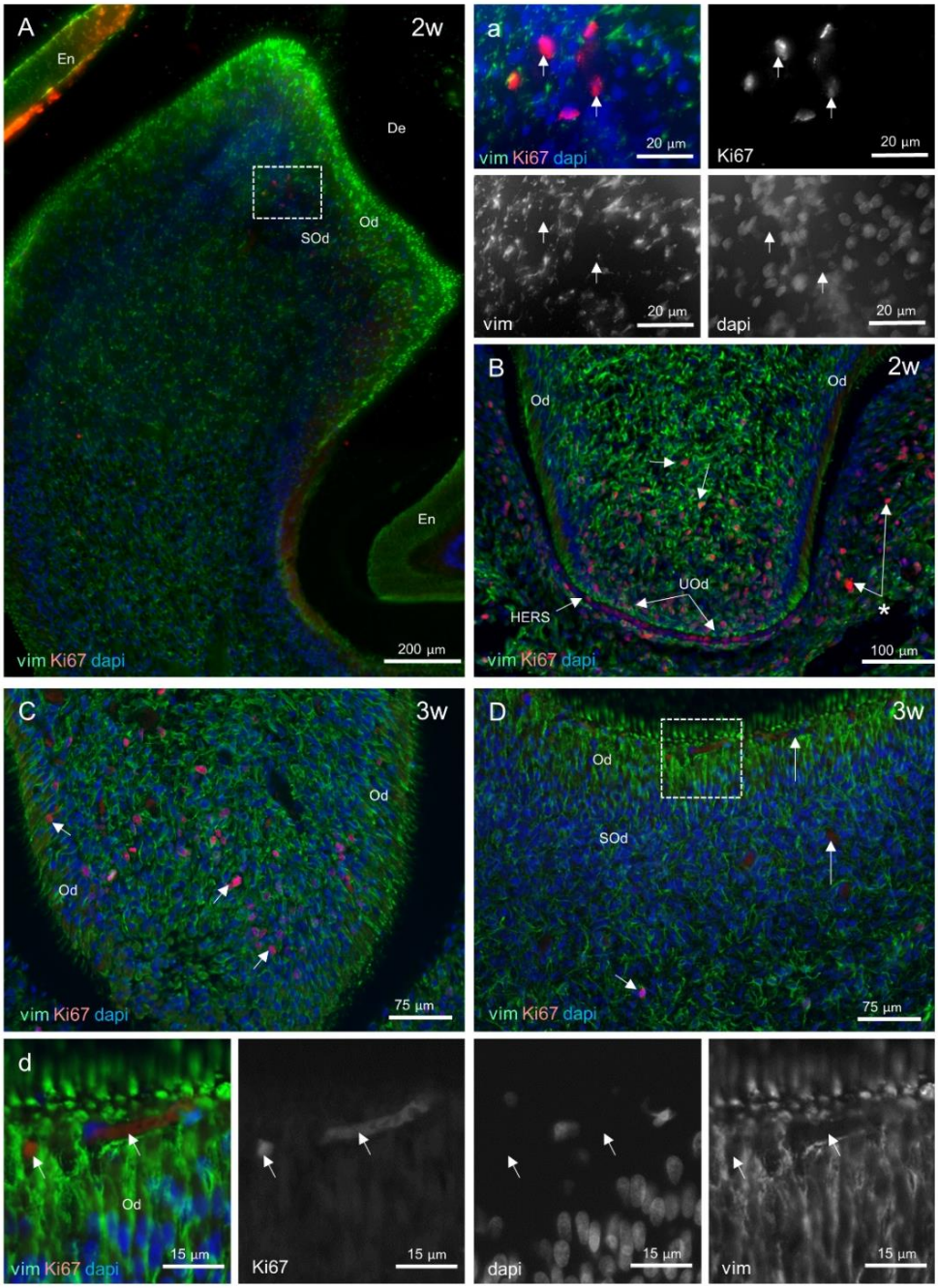

Figure 5.14: Cell division marker (Ki67) in demineralised sections of 2 and 3w old rat mandibular 1st molar.
A and B images are for 2w, while C and D for 3w old rats. Images stained for vim (green), Ki67 (red), and dapi (blue). Panel A shows the mesial cusp with no signs of Ki67-IR in any regions of the cusp except for one region of interest in SOd which is presented in (a) and its component images (Ki67, vim, and dapi). These images show cellular division occurring in blood vessels only. Panel B shows cellular division still active in developing root especially in UOd and HERS cells, in addition to other pulp cells (arrows) and PDL (*). Root region continues to show Ki67-IR in some of the dividing cells in Od and other pulp cells of 3w aged rat (image C). Panel D shows the groove region with faint Ki67 staining only in some capillaries (arrows) in Od and SOd regions. One of these capillaries is shown in higher magnification in image d and its component images, which identify some red blood cells (arrows) within this vessel.

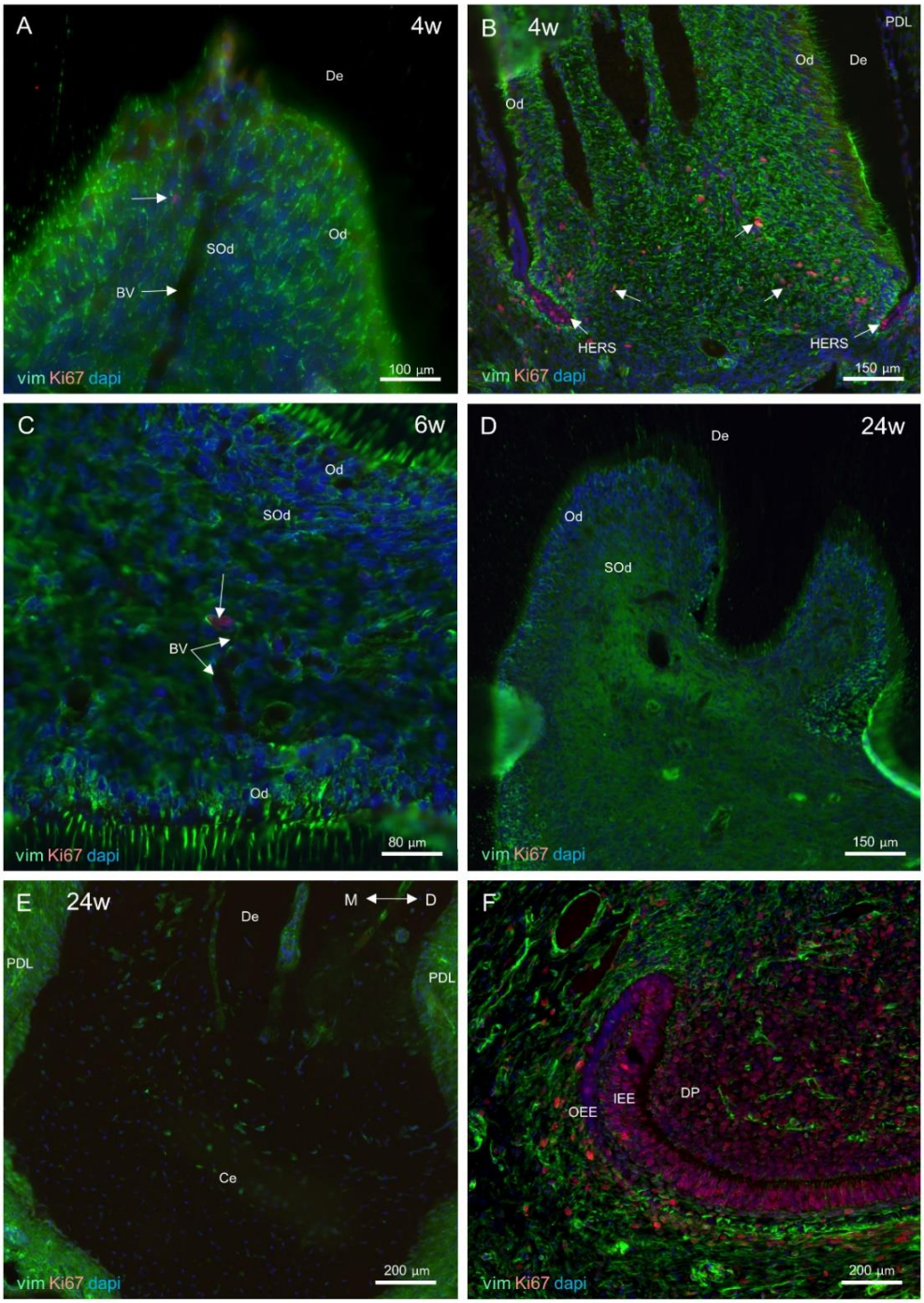

Figure 5.15: Cell division marker (Ki67) in demineralised sections of different ages of rat mandibular 1st molar and one positive control image.
Images A and B are for 4w, C for 6w, D and E for 24w, and F for apical bud region of mandibular incisor. Images stained for vim (green), Ki67 (red), and dapi (blue). No signs of Ki67-IR are shown in images A, C, D and E, except the developing root region which appear in image B, in which the Ki67-IR is still present in some pulp cells (arrows) and HERS cells. Arrows in images A and C pointed to cells with Ki67 evident which could be white blood cells. Image F is the positive control region for the Ki67-IR, which shows Ki67-IR cells in dental papilla (DP), inner enamel epithelium (IEE) and outer enamel epithelium (OEE) cells of the apical bud of rat mandibular incisor.

Ion transporter markers

NaK-ATPase:

In the 0d rat molar, NaKATPase-IR labels only the outer cells of the enamel organ including the developing SR and OEE cells. This antibody seems undetectable in both dental papilla and IEE cells (image A and B Figure 5.16).

After hard tissue deposition commences at 1w, NaK-ATPase-IR becomes evident in the Od and SOd region of the crown and within cells of the HERS of the developing root (image C and D Figure 5.16). The expression of NaK-ATPase becomes more apparent within SOd than Od cells in 2 and 3w sections (image E-H Figure 5.16). Additionally, faint labelling of NaK-ATPase is also evident in OPs. The highest expression is seen within SR cells of the enamel organ and it is used as a positive internal control for this antibody (image D and E Figure 5.16).

At 4w, when wear processes have started, the cells of SOd and basal part of Od cells beyond the region of trauma show the highest NaK-ATPase-IR in comparison to other region of the mesial cusp (image A Figure 5.17). The expression remains unchanged within adjacent non-traumatised Od, SOd and OPs (+ in image A Figure 5.17).

In the other age groups (6-24w), similar expression of the NaK-ATPase-IR is seen within their sections, in which SOd cells show higher NaK-ATPase-IR than Od cells (B-D Figure 5.17). However, only Od and some adjacent pulp cells, especially those in between Od cells and BV, express this marker in furcation and root regions of the tooth (E and F Figure 5.17). This is because there are no evident SOd cells that have been identified associated with Od within molar root canal pulps.

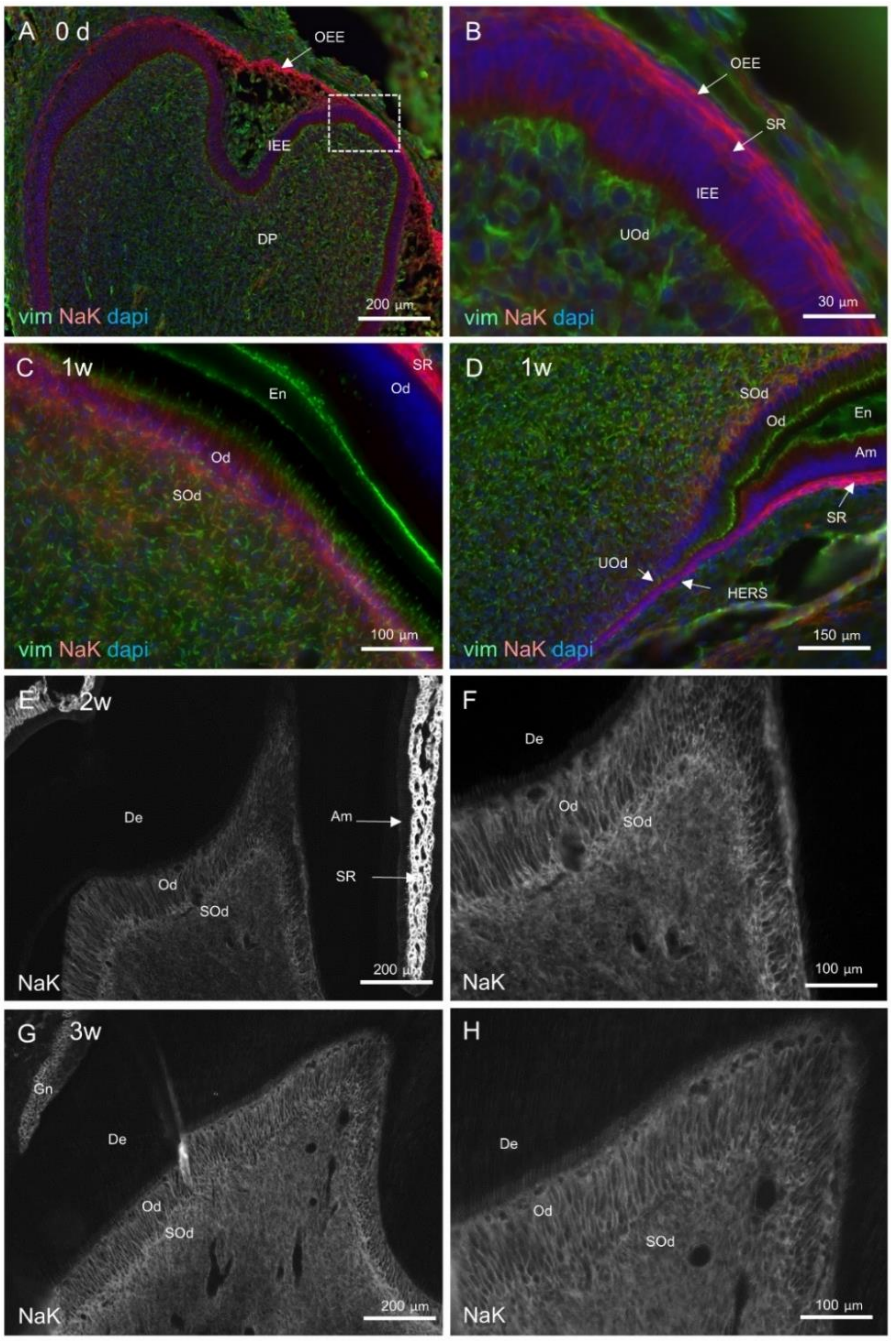

Figure 5.16: NaK-ATPase expression in mesial cusp regions during development and tooth eruption of rat mandibular 1st molar.
Images A, B is for 0d, C, D for 1w, E, F for 2w, and G, H for 3w. Panels A, B, C and D are undemineralised sections stained for NaK-ATPase (red), vim (green), and dapi (blue), and the remaining images are demineralised sections stained only for NaK-ATPase. Developing mesial cusp appears in image A, with no expression of NaK-ATPase within DP cells. NaK-ATPase-IR is clearly identified in the outer cells of the enamel organ (SR, and OEE) as shown in image B. In 1w both Od and SOd express NaK-ATPase-IR (image C) while the highest expression is present in SR cells. In cervical region and toward developing root side (base of image D), the UOd cells still do not express NaK-ATPase-IR which is clearly identified in HERS. Both Od and SOd cells express NaK-ATPase-IR in 2 and 3w aged rat (images E, F and G, H respectively). The highest NaK-ATPase-IR is still in SR cells (image E). Very low expression is identified in the OPs within De (image H).

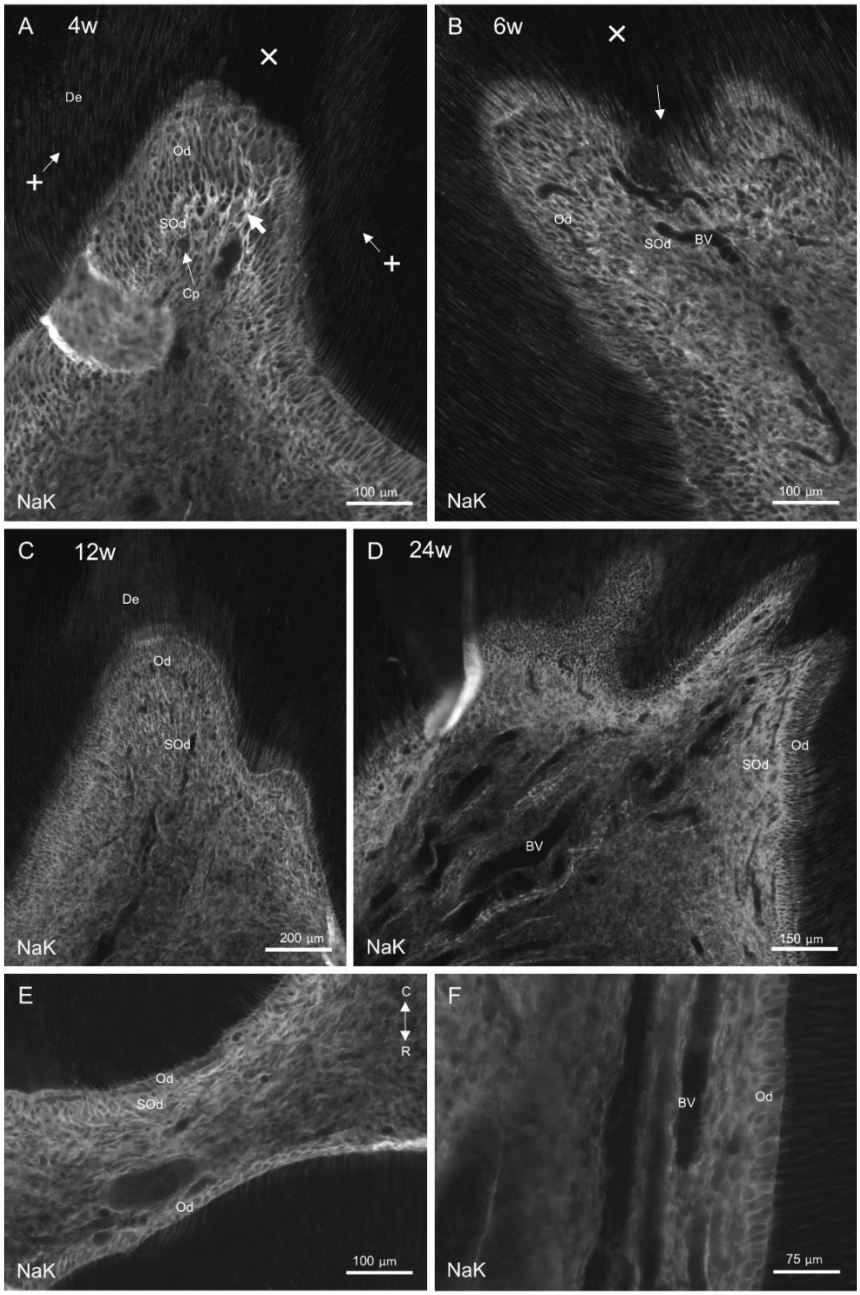

Figure 5.17: NaK-ATPase expression in different regions of mandibular 1st molar between 4 to 24w old rats.
Images A, B, C, and D are for mesial cusp sections for 4, 6, 12, and 24w rat respectively, and E, and F are for 24w rat groove and mesial root respectively. A shows higher NaK-ATPase-IR in SOds and basal part of Ods (thick arrow) beyond atubular dentine region (×), and the latter has no expression of the NaK-ATPase in the OPs compared to the adjacent dentine regions (+). The NaK-ATPase-IR looks similar in all regions of SOd along the cusp, and no expression within BV. The newly formed process (arrow) show NaK-ATPase-IR. Similar NaK-ATPase-IR is shown in images C and D with very low expression in the central region of the pulp (image D). In groove region (image E), the expression of the Od and SOd in the crown side (oriented to the top of the image) seems much higher than furcation side Od and adjacent pulp cells (bottom of the image), which also obvious in root Od cells (image F).

NHE-1:

In 0d sections, the expression of the NHE1-IR is only seen in OEE cells, junctional basement membrane between IEE and UOd cells and within capillaries in DP of the tooth germ (image A and B Figure 5.18). During 1 and 2w, which include the period of dentine deposition in rat 1st molar before tooth eruption, the NHE1-IR appears within pulp capillaries especially those present within Od and SOd cells (image C-F Figure 5.18). Additionally, faint staining is also present in Od cell cytoplasm and in the basal part of the OPs.

After 1st molar eruption at 3w, the expression of NHE1-IR become more apparent within Od cells and capillaries in addition to the OPs (images A and B Figure 5.19). The NHE1-IR starts to faintly label the entire length of the OPs.

After wear commences at 4w, the NHE1-IR is seen to a greater extent within SOds in comparison to the above traumatised Ods (image C Figure 5.19). This expression in SOd cells disappears within 6w sections and remains only within Ods and keep this form similar in all other ages of the study (images D and E Figure 5.19). The NHE1-IR within OPs also become apparent in older ages especially within the outer part of the OPs (image E Figure 5.19).

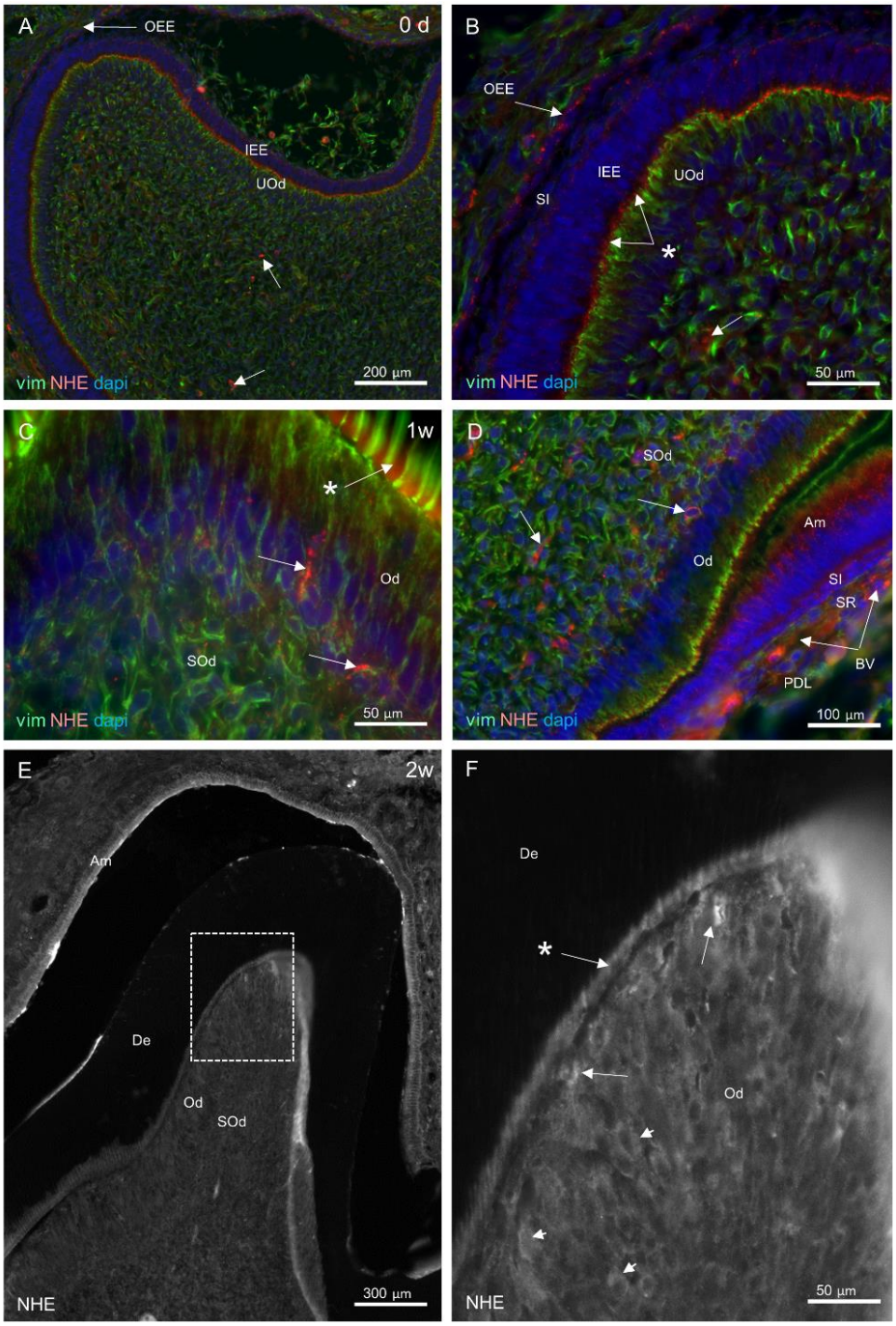

Figure 5.18: NHE-1 expression in developing rat mandibular 1st molar (mesial cusp sections). Images A, B are for 0d, C, D for 1w, and E, F for 2w rats. The coloured images are undemineralised sections stained for NHE-1 (red), vim (green), and dapi (blue) and images E and F are demineralised sections stained only for NHE-1. In 0d rat (images A and B) the expression of NHE-1 only presented in regions of the interface (*) between IEE and UOd, cells of OEE and several blood vessels (arrows) within DP region. In 1w rat sections (images C and D), NHE1-IR is seen in inner region of the OPs (*), BV of the pulp (arrows) and BV of PDL at the boundary of enamel organ (image D). In 2w rat sections (E and F images), there is no NHE1-IR in the OPs within De. NHE1-IR is observed to a greater degree in the BV of the apical regions of the Od (long arrows), also the initial region of OPs (*), in addition to low expression within Od cell bodies (arrow heads).

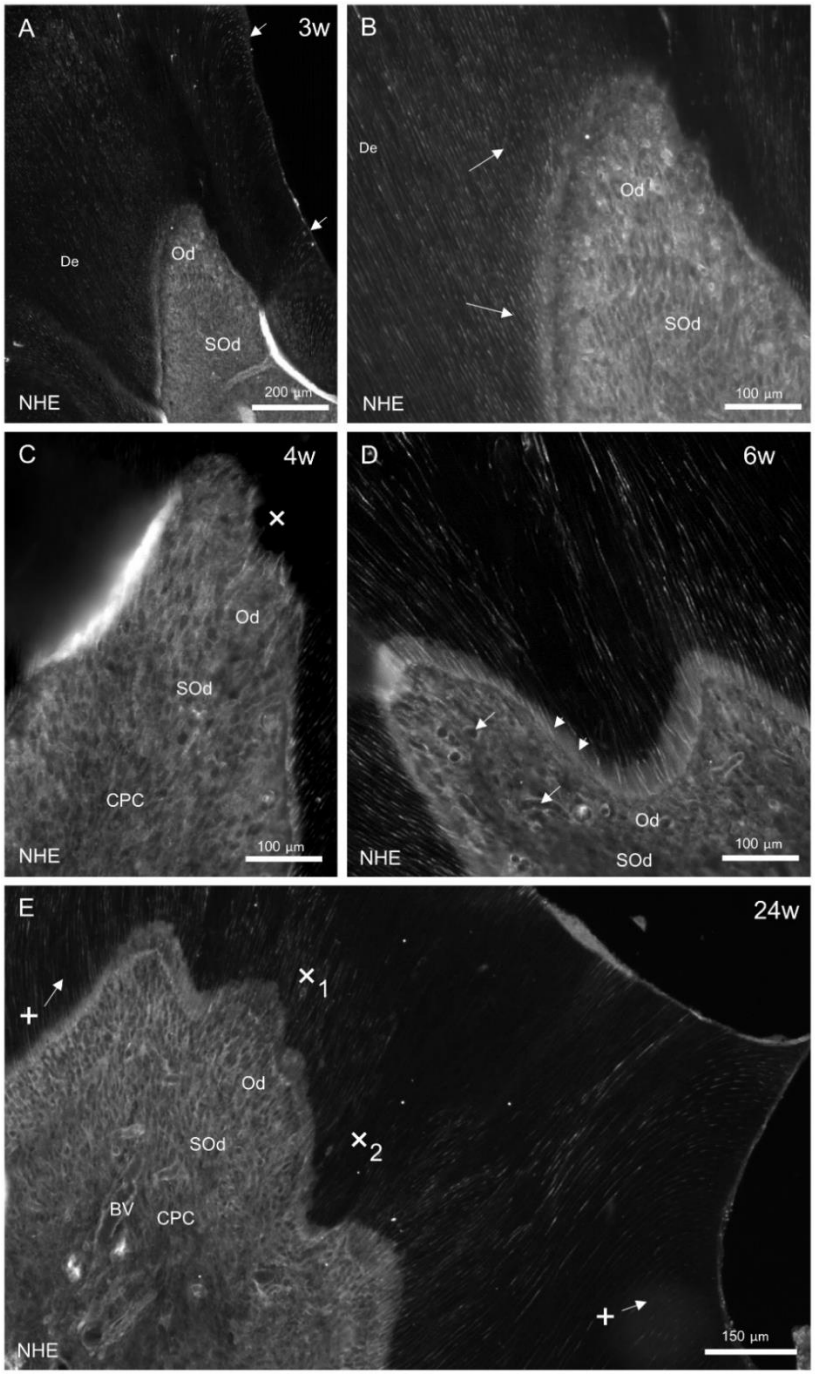

Figure 5.19: NHE-1 expression in demineralised sections of mesial cusp in different age rat mandibular 1st molars.
Images A, B for 3w, C for 4w, D for 6w, and E for 24w rats. In 3w sections (images A and B) the NHE1-IR is obvious in OPs within De, fine details of the terminal OP branches in the outer dentine (arrows in image A), in Od cells, capillaries in between (arrows in image B) and less extent in SOd. In 4w sections (images C) after wear started, SOds become more NHE-IR than Ods under trauma region (×). In 6w sections, the Ods return more NHE-IR than SOds and the same also seen in 24w (image E). In latter image, the old trauma ($×_1$) shows NHE-IR OPs which disappeared in second trauma region ($×_2$). In other unworn De regions, the OPs express NHE1-IR to the outer region of dentine (+).

NGF and NGFR

In 0d sections, the expression of NGF and NGFR varies according to the degree of cellular differentiation (image A Figure 5.20). In regions of the tooth germ, where the DP cells are close to differentiation to Od cells, the POd start to express NGR-IR in their cytoplasm in addition to faint staining to NGFR (image a1 Figure 5.20). The adjacent DP cells also express NGFR-IR while IEE cells have no evident expression for either of the previous antibodies. In region of the tooth germ that is further back from differentiation, the IEE cells and central region of the DP cells show NGFR-IR (image a2 Figure 5.20). However, the DP cells in between these two regions show no evidence of either antibody. The other component of the tooth germ which is OEE, shows intense NGFR-IR (image A Figure 5.20).

After the beginning of dentine formation in 1w old rats, the NGF-IR appears more specific in the apical region of the Ods and the basal part of OPs, while NGFR-IR is seen within SOd and the whole CPC of the cusp region. In 2w sections, with increased thickness of dentine deposition, the NGF-IR label the whole Od layer and NGFR-IR is expressed by SOd and the adjacent CPC of the cusp.

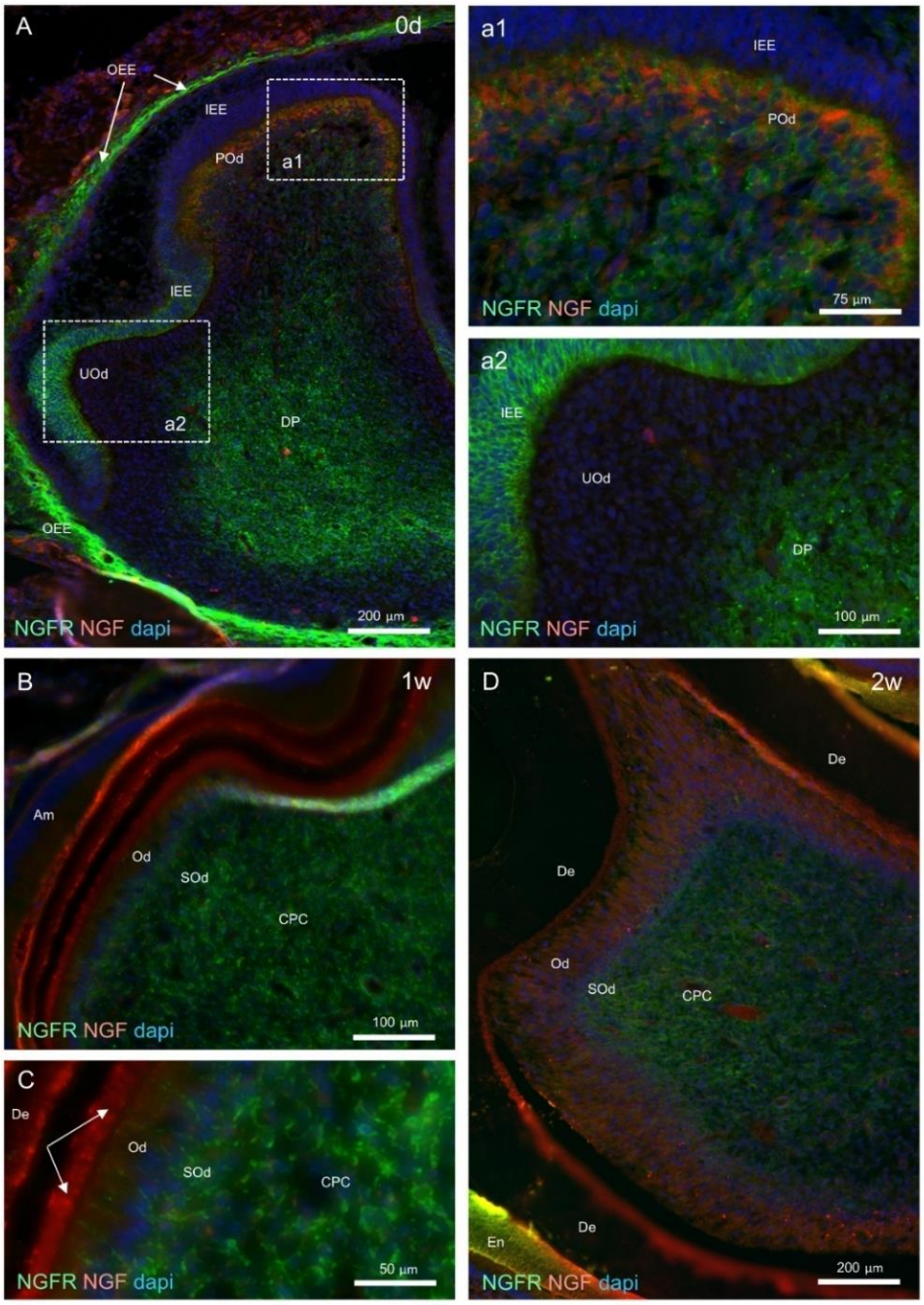

Figure 5.20: Expression of nerve growth factor (NGF) and nerve growth factor receptor (NGFR) in developing rat mandibular 1st molar.
Images A, a1, a2 are for 0d, B, C for 1w, and D for 2w rats. All images stained for NGF (red), NGFR (green), and dapi (blue). In Image A, an overview section for the mesial cusp in bell stage showing 2 regions: more developed upper part of the cusp, and less developed lower region. The NGF-IR is only seen in the POd (images A and a1). The NGFR-IR is more obvious in cells of the OEE of the whole tooth germ, IEE within the less developed region of the cusp (Image a2 in higher power), the central cells of the DP (image A), and less IR within mesenchymal cells near POd. In 1w sections (images B and C) the NGF-IR is more concentrated in the apical part of the Od and beginning of the OPs (arrows in C). Other pulp cells express NGFR-IR. In 2w sections, the NGF-IR appears in Od cells of the crown and decrease toward the root, while the NGFR is shown in SOd cells and adjacent CPC of the cusp.

In 3w sections, and after tooth eruption the cusp region shows high intensity for expression of NGF in Od cells and the basal part of OPs (images A, a1 Figure 5.21). The NGFR-IR is intensely evident in SOd, cusp CPC, including cells around large blood vessels, and less IR within Ods on the cusp peripheries. The expression of these two antibodies is reduced toward the tooth cervical region and disappears in the root (image B Figure 5.21). However, the Ods in the tooth cervix expressed both NGF and NGFR. In addition, NGFR-IR is also seen in small nerve fibre and nerve bundle within CPC region (small and big arrows respectively in image B and b2 Figure 5.21).

After commencement of cusp wear at 4w (Figure 5.21), NGF-IR is weakly labelled within Ods and associated SOds beyond trauma site (images C Figure 5.21). This clearly affected the distal side of the cusp much more than the mesial. The SOds also has no NGFR-IR except some nerve fibres within this region (small arrows in image D Figure 5.21). On the cusp peripheries, the mesial side shows higher IR than the distal for both NGF and NGFR within Ods and SOds respectively. Even the CPC, located mesially within the cusp, express higher NGFR-IR than those located distally. Additionally, only Ods on the mesial side (thick arrow) express NGFR-IR in comparison to those on the distal side.

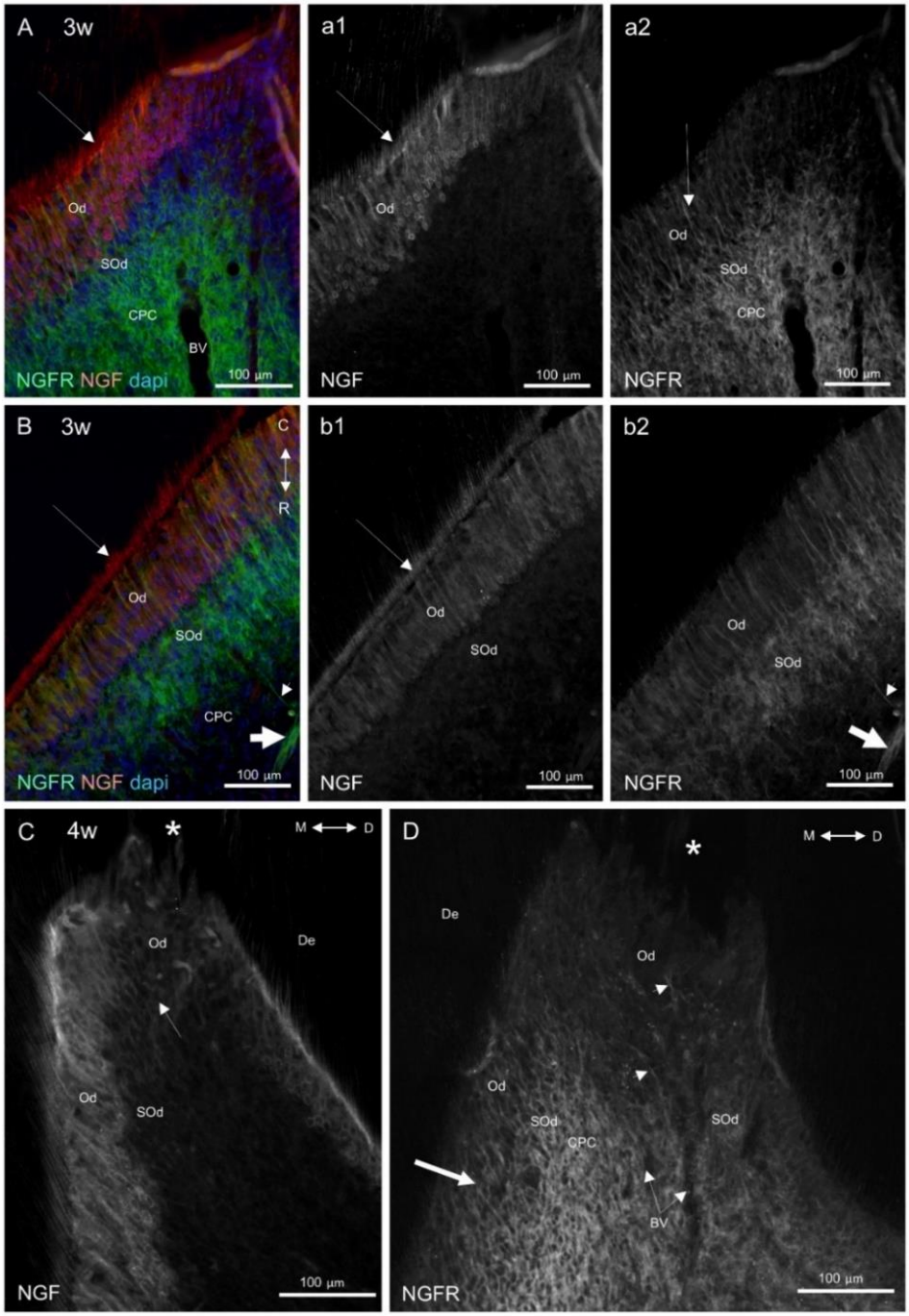

Figure 5.21: NGF and NGFR expression in demineralised sections of mesial cusp of 3, and 4w old rat mandibular 1st molars.
Images A, B (component images a1, a2 and b1, b2 respectively) are for 3w, and C, D for 4w rat sections. Images A, and B are stained for NGF (red), NGFR (green), and dapi (blue), a1,b1 and C for NGF, a2, b2 and D for NGFR. In 3w sections, NGF-IR is well recognised in Od and basal part of OPs (long arrow in A and a1), while SOd, adjacent CPC, and less in Ods (long arrow in a2) express NGFR-IR (Image A). These expressions are reduced toward cervical region and disappear in root (image B, b1, and b2). Also nerve bundle and small nerve fibre (thick and small arrow respectively) are shown to express NGFR. In 4w sections (images C and D) weak expression of NGF occur beyond trauma region (*) within Ods and SOds (arrow in C) respectively. Higher expression of NGF and NGFR appear within non-trauma of mesial side of the cusp more than distal side.

In 6w sections (Figure 5.22), within the trauma region (*) Ods return their NGF expression similar to the adjacent non-traumatised Ods. Additionally, the Ods cells in this region start to express NGFR-IR on the lateral region of the trauma (thick arrows in image b2, Figure 5.22) and on cusp peripheries (non-trauma regions). SOds underlying trauma region do not express NGFR, but still are labelled with NGF-IR and this expression appears more shifted toward the distal side of the cusp, which was more affected by trauma (arrow in images A, B and b1 Figure 5.22). However, the SOds of non-traumatised cusp peripheries expressed high NGFR-IR with the adjacent CPC on both sides of the cusp. Both NGF and NGFR expressions decreased gradually toward the root and only large bundles of nerves within root labelling NGFR (thick arrows). Similar observations were also obtained from 9w sections.

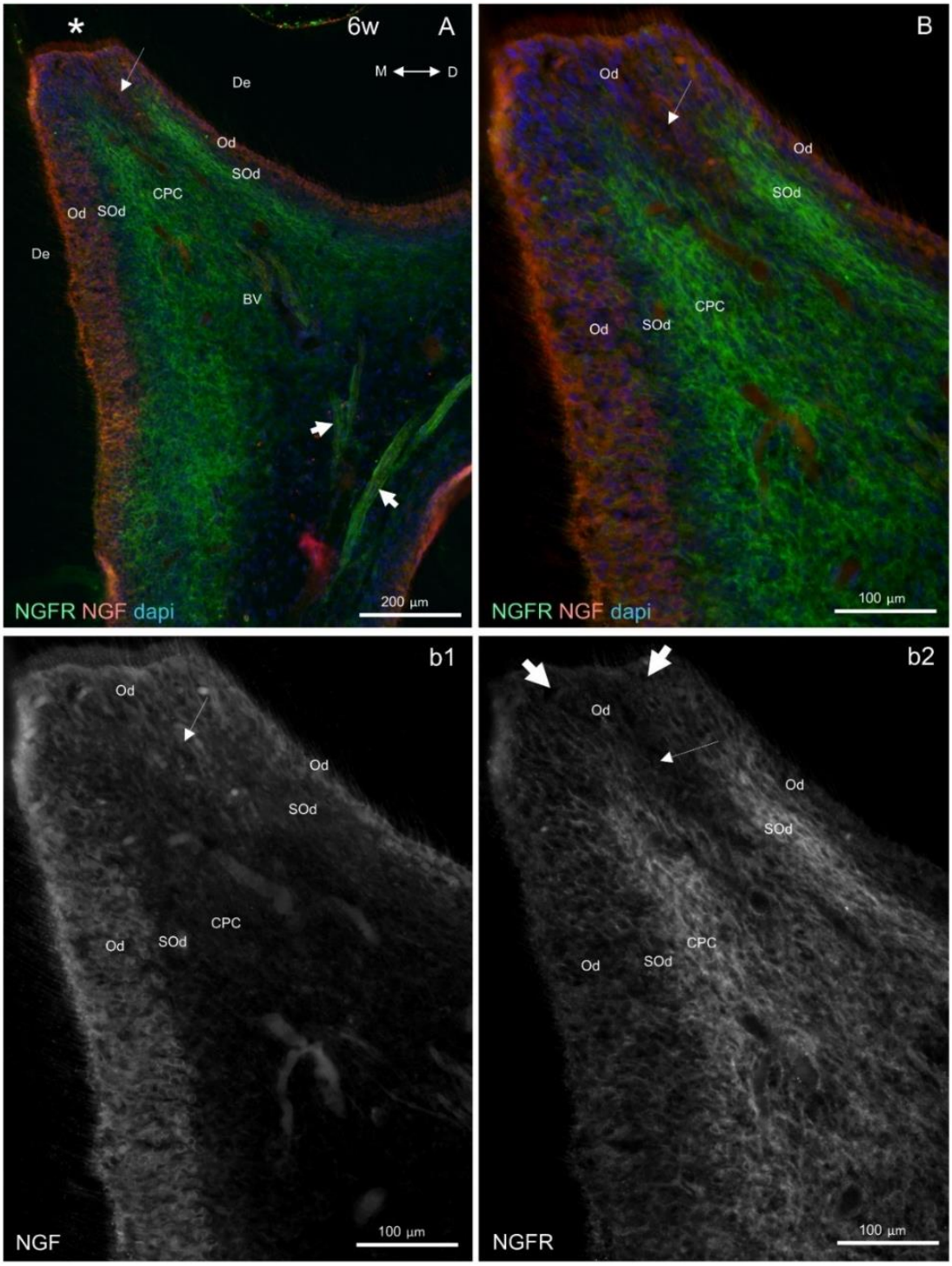

Figure 5.22: NGF and NGFR expression in demineralised sections of mesial cusp of 6w rat mandibular 1st molar.
The coloured images are stained for NGF (red), NGFR (green), and dapi (blue) and component images b1 and b2 are stained for NGF and NGFR respectively. In image A and at higher magnification in image B, trauma region (*) shows NGF staining in Ods and less in SOd (arrow) and the latter shows no expression to NGFR as shown in component images b1 and b2. Thick arrows in image A point to big nerve bundles express NGFR-IR. In component image b2, the thick arrows pointed to the traumatised Ods NGFR-IR.

In 12w sections, the trauma site shows relabelling of Od and basal part of the OPs by NGF and SOd cells by NGFR antibodies (images A and B Figure 5.23). However, the expression of NGFR becomes more localised within CPC cells which are adjacent to SOds, and decreasing gradually until disappearing in central region of the cusp. This means that only specific cells of CPC in cusp region express this marker. Additionally, some nerve fibres and bundles within central pulp region express NGFR-IR.

In 24w sections, the old trauma region (* in image C Figure 5.23) appears similar in expression to non-traumatised lateral sides of the mesial cusp. The Od cells label NGF-IR and SOd and adjacent CPC express NGFR-IR, while the central region of the cusp shows no NGFR expression. A new trauma site is also identified (arrow in image A and B Figure 5.23) with negative reaction to both NGF and NGFR in all their cells.

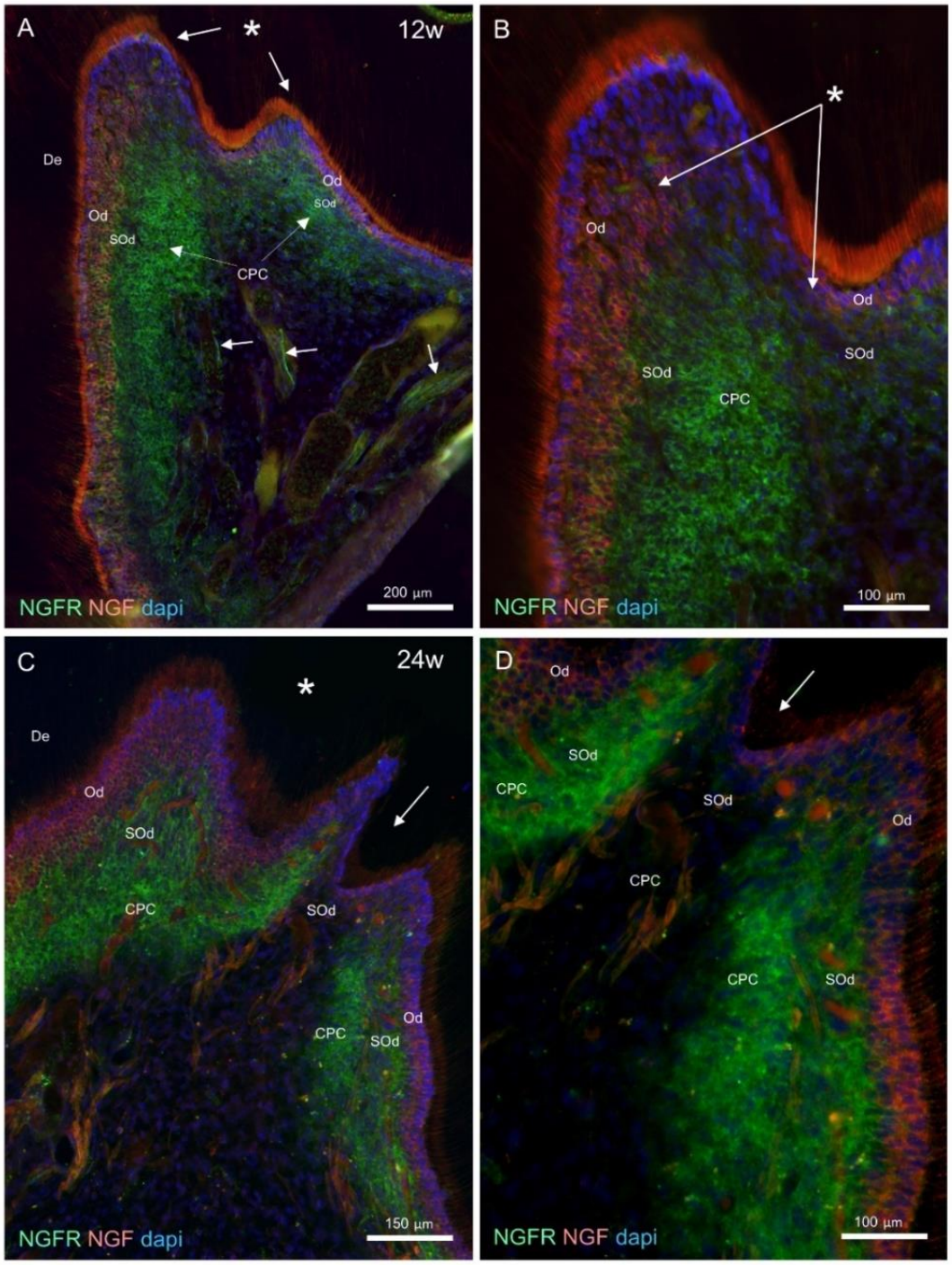

Figure 5.23: NGF and NGFR expression in demineralised sections of 12, and 24w old rat mandibular 1st molar.
All images stained for NGF (red), NGFR (green), and dapi (blue). In 12w sections (Images A and B), the NGF-IR is only localised to Od. The NGFR-IR is more specifically identified in SOd cells and the close adjacent pulp cells. This is gradually depleted toward central region of pulp. In addition, some singular or multiple nerve fibres (arrows in A) which run centrally within the pulp also express NGFR-IR. Region of repair also shows a return in NGF-IR in Od (*) and NGFR-IR in SOd (thick arrows). In 24w sections (images C and D), the expressions of NGF and NGFR-IR return completely in old repair region (*) but disappear in new trauma site (arrow).

Sensory nerve markers (CGRP and Nf)

0d to 2w:

No expression of CGRP and Nf marker has been identified within the cusp region before 2w. Very few nerves are present in 1w sections in the central tooth part and close to the apical side of the tooth which labelled with both CGRP and Nf antibodies (images A and B Figure 5.24). The CGRP fibres appear more in sections of 2w rat mesial cusp (image C Figure 5.24). These fibres are mostly present in CPC region and some of them pass along SOd into Od cell layer, but non are observed entering PD area. Very few Nf fibres are identified within central region of the tooth crown (image D Figure 5.24).

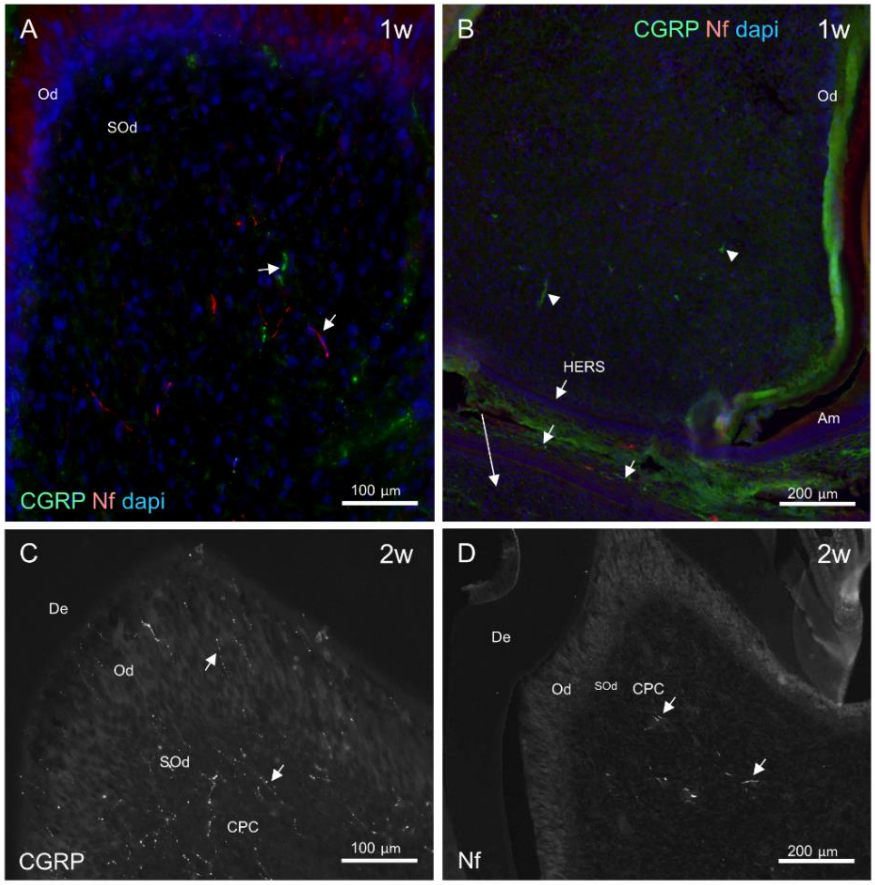

Figure 5.24: Developing rat (1 and 2w) mandibular 1st molar innervation.
Images A and B stained for CGRP (green), Nf (red) and dapi (blue), C for CGRP and D for Nf. In undemineralised sections of 1w aged molars (images A and B), few nerve fibres express CGRP and Nf-IR appears only in the central part of the pulp (arrows image A) and in the root side of the tooth (arrow heads in B). There are some nerves (short arrows) seen in region between molar root side (HERS) and the incisor tooth (long arrow). In demineralised 2w sections (images C and D), only CGRP-IR nerves shows several branches in CPC passing into SOd and few to Od regions (arrows in C), while the Nf-IR nerves are only present in the CPC of the pulp.

3w:

After tooth eruption, a large network of sensory afferent fibres is observed engaging different cell types of the mesial cusp in 3w sections (image A Figure 5.25). Two different types of nerves are observed: CGRP and Nf fibres. The nerve bundles of CGRP and Nf fibres (thick arrows in image a1 Figure 5.25) are present within CPC region and mainly run in association with big blood vessels. From these bundles major nerve branches emerge. The mean diameter for CGRP major branches is (1.3µm) and for Nf nerves is (1.8 µm) (* and + respectively in image a1 Figure 5.25). These branches run in SOd region and subdivide into minor branches which have smaller diameter (CGRP nerves 0.45 µm and Nf nerves 0.69 µm). The minor branches of CGRP pass through Od layer and into the inner region of the dentine (arrow heads in image a1 Figure 5.25) and can also be seen within Od cells of the pulp horn (image a2 Figure 5.25). The CGRP small fibres appear punctuated due to nerve fibre varicosities. They are distributed either intercellular, between Od cells, or perivascular to the Od capillaries (images a1 and a2 Figure 5.25). While the Nf minor branches mainly run within SOd cells (short arrows in image a1 Figure 5.25), few nerves are seen within Od layer (long arrows in image a2 Figure 5.25). These fibres appear uniform in their pattern as a straight fibre without apparent varicosities.

While, root formation continues during this period, nerve development within cervical region also occurs. CGRP axons start to engage the coronal SOds and Ods. The Nf fibres are still within CPC region in this stage. The root only contains nerve bundles passing centrally, with very rare branching into Od cells (image D Figure 5.25).

Comparing between groove and furcation regions, in both of them the actin short OPs are still present, only few CGRP fibres have developed within SOd and basal regions of Ods in groove region. None of these nerves are recognised near Od cell layer of furcation region (images B and C in Figure 5.25).

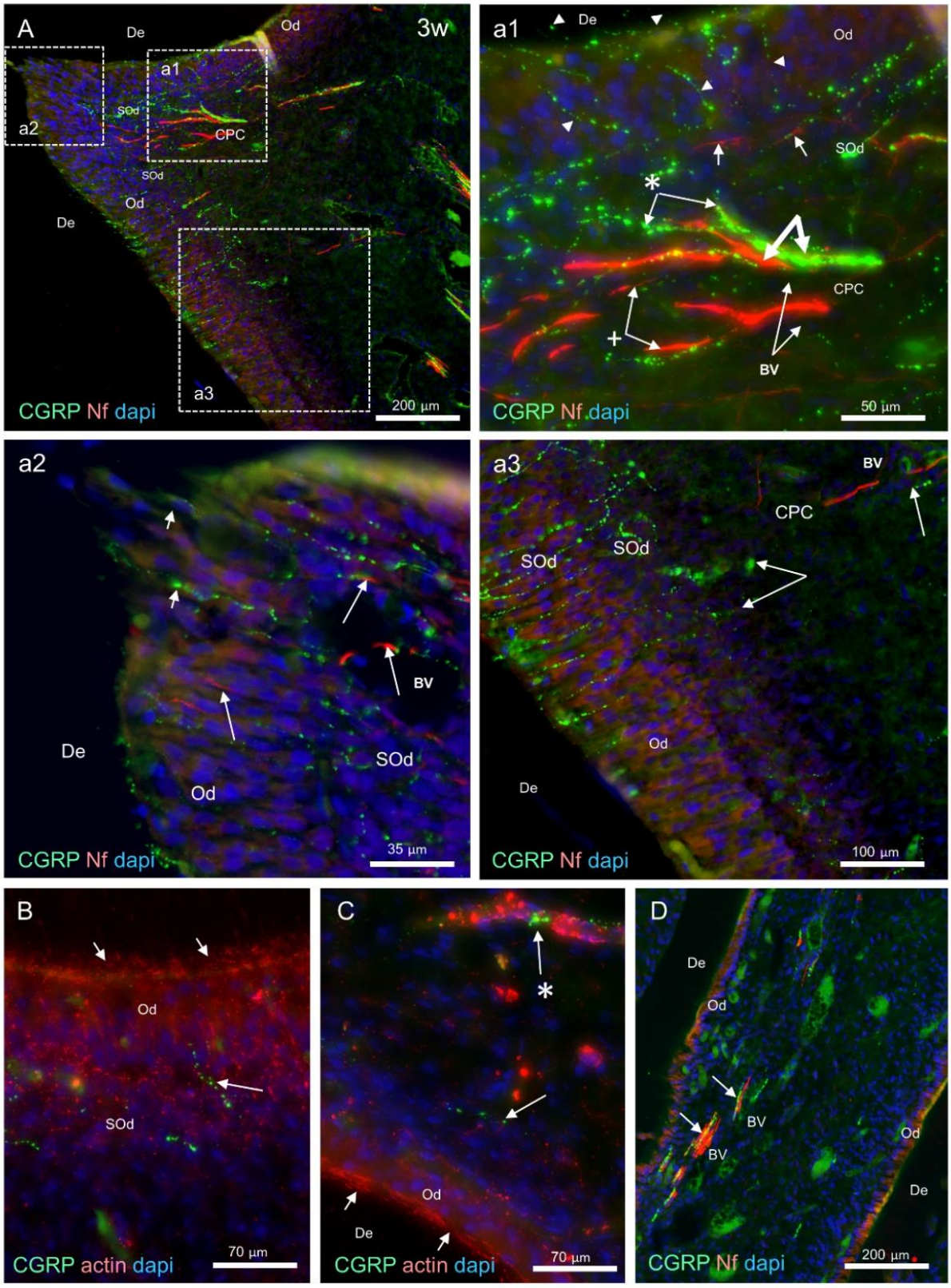
A
De
Od
3w
a1
a2
SOd
CPC
SOd
Od
De
a3
CGRP Nf dapi
200 µm
a1
De
Od
SOd
CPC
BV
CGRP Nf dapi
50 µm
a2
BV
De
SOd
Od
CGRP Nf dapi
35 µm
a3
BV
CPC
SOd
SOd
Od
De
CGRP Nf dapi
100 µm
B
Od
SOd
CGRP actin dapi
70 µm
C
Od
De
CGRP actin dapi
70 µm
D
De
Od
BV
BV
Od
De
CGRP Nf dapi
200 µm

Figure 5.25: Expression of CGRP and Nf nerve markers in demineralised sections of 3w rat mandibular 1st molar.
Images A, a1, a2, a3 and D are stained for CGRP (green), Nf (red) and dapi (blue), and B and C are stained for CGRP (green), actin (red) and dapi (blue). Overview image for mesial cusp section is shown in image A, with complex network of CGRP and Nf-IR nerve fibres. 3 regions of interest are presented in images a1, a2, and a3. Different bundles for main trunk nerves for both CGRP and Nf-IR nerves are shown in image a1 (thick arrows) which run in the central region of the cusp toward the SOd region. Major branches of CGRP-IR nerves (*) emerge from the previous bundle to give many small branches both in Sod, Od and inner De (arrow heads). Similarly seen in Nf-IR major nerve branches (+), but the minor branches mainly terminate within SOd region (short arrows). In pulp horn region (image a2), both CGRP and Nf-IR small nerves (short and long arrows respectively) run from SOd to Od regions. In cervical region (image a3) the CGRP-IR small branches are not present in Od region of the root side (downward in image) compared to many nerve fibres present in crown Od. Both Od cells in groove and furcation regions (images B and C respectively) still have actin-IR lateral processes (small arrows). Very few CGRP-IR nerves are noticed emerging Od in groove region (long arrow in B). Image C also identifies some CGRP-IR fibres either running as single nerve in central part of the pulp (arrow) or associated with the wall of BV (*). Only the main trunk of CGRP and Nf-IR nerves pass within the root (image D) and no branches to Od region have been identified.

4w:

After wear commences, the traumatised Od cells and underlying SOd show depletion from CGRP and Nf fibres (image A Figure 5.26). The nerve disappearance is on the distal side of the mesial cusp. However, one faintly stained CGRP fibre is seen in the same image (short arrows in image B Figure 5.26) engaging SOd and Od beyond trauma region. This CGRP fibre could be a new proliferating nerve. The mesial side shows a large network of CGRP fibres engaging Od layer to the PD and inner dentine. At higher magnification, two CGRP fibres are seen wrapping around either capillary or Od cell within the non-traumatised Od cell layer (▲ and + respectively in image B Figure 5.26). Major branches of CGRP and Nf are present in CPC region and run perivascularly to the present blood vessels. The CGRP-IR nerve fibres are only limited to the trauma bounded region (thick arrows in image B Figure 5.26),

Within the groove region, more CGRP and Nf axons have developed. Numerous CGRP fibres start to engage the Od layer (image C Figure 5.26) which shows reduction in number of the actin short processes within PD in previous images (image G Figure 5.6). Several Nf fibres are also seen, but do not extend further than SOd cells in this age group. No evident of CGRP or Nf fibres are recognised within furcation Od cells.

6w:

Nerve proliferation is apparent within trauma region of the cusp (image D Figure 5.26). Under higher magnification, CGRP nerve sprouting is also evident within

traumatised Od and passing toward PD (short arrows in image E Figure 5.26). The increase in number of Nf fibres become evident in SOd region of the traumatised site (long arrows in image E Figure 5.26). These fibres show big network of branches between cells of the SOd.

Returning to image D Figure 5.26, which shows the main nerve bundle that engages the mesial cusp (thick arrows). This bundle contains both CGRP and Nf nerve trunks in association with large blood vessel, and numerous major nerve branches arise from this bundle. These branches run peripherally toward the SOd region where they arborise into many small minor branches (long arrows). These small branches form a network of nerve fibres which innervate the whole cusp Od layer. This innervation is only limited with the cervical region of the tooth (+ in same image) and no nerve is seen within Od layer in the root side. Also one large capillary is present in the cervical region which passes through the Od layer at the cervical region in association with numerous CGRP fibres (image D Figure 5.26).

The groove (image F Figure 5.26) and furcation regions show similar innervation details to those described in 4w sections.

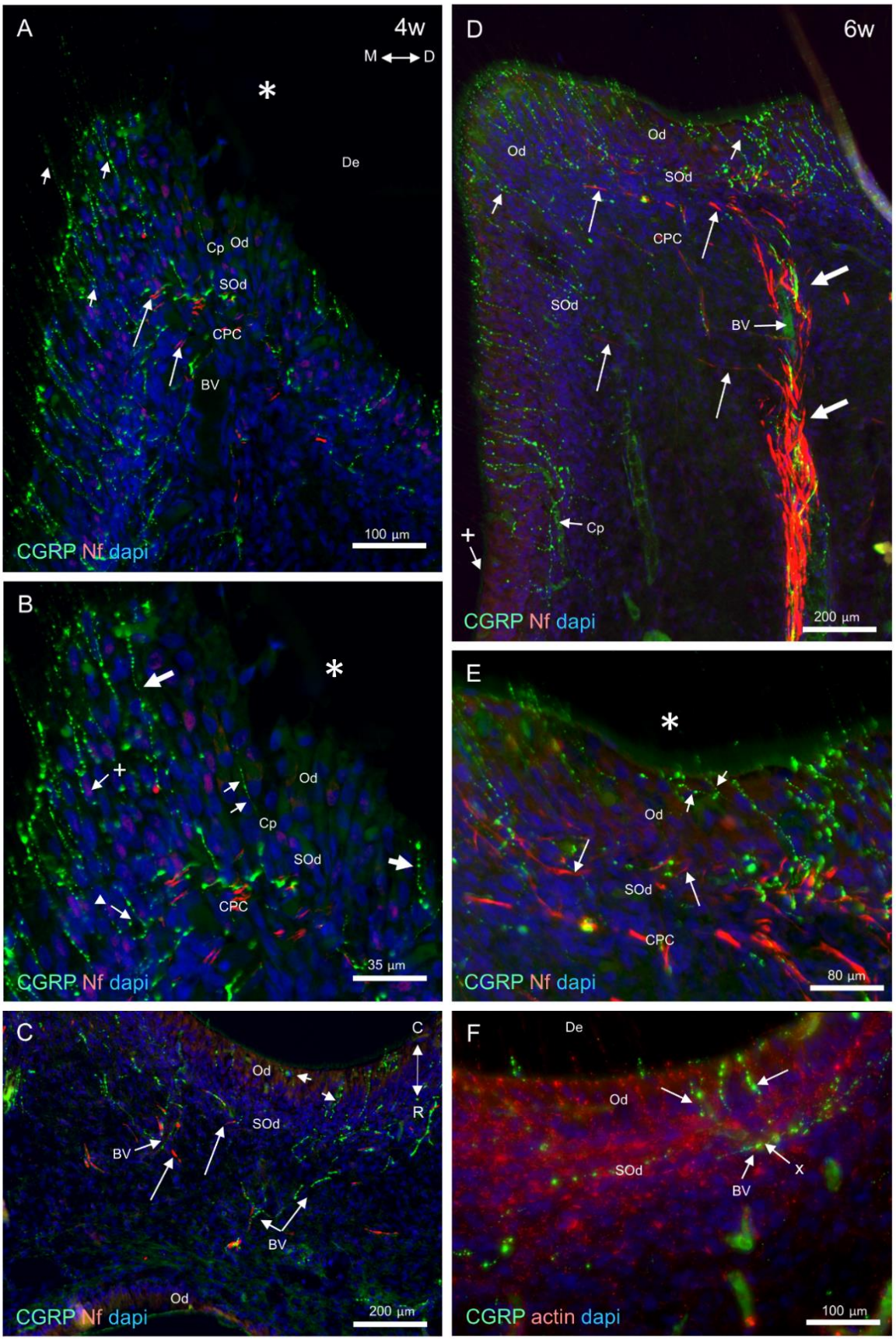
A
4w
M ⟷ D
*
De
Cp
Od
SOd
CPC
BV
100 µm
CGRP Nf dapi
B
*
+
Od
Cp
SOd
CPC
35 µm
CGRP Nf dapi
C
C
R
Od
SOd
BV
BV
Od
200 µm
CGRP Nf dapi
D
6w
Od
Od
SOd
CPC
SOd
BV
Cp
+
200 µm
CGRP Nf dapi
E
*
Od
SOd
CPC
80 µm
CGRP Nf dapi
F
De
Od
SOd
BV
X
100 µm
CGRP actin dapi

Figure 5.26: Expression of CGRP and Nf nerve markers in demineralised sections of 4w (images A, B, C) and 6w (images D, E, and F) rat mandibular 1st molar.
Panels A-E are stained for CGRP (green), Nf (red) and dapi (blue), and F is stained for CGRP (green), actin (red) and dapi (blue). Mesial cusp in 4w section (Image A) shows absence of CGRP and Nf nerve fibres from traumatised (*) Od and SOd cells. In adjacent non-traumatised region, the number of CGRP nerves on the mesial side of the cusp increases (short arrows). Also Nf-IR branches noticed only in CPC and SOd region beyond non-traumatised Od (long arrow). At higher magnification, the trauma region (*) is shown in image B. The CGRP nerves are limited to the traumatised region (thick arrows) with one nerve (short arrows) seen within this region. Additionally, two CGRP fibres wrap either capillary (▲) or Od cell (+) on mesial non-traumatised cusp side. Panel C compares between innervation in groove (upward in image) and furcation (downward in image) regions. There are many CGRP-IR fibres (short arrows) in SOd and Od regions, and Nf-IR nerves (long arrows) in Sod and central pulp regions only. However, the Od and other adjacent pulp cells in furcation region (downward in image C) are devoid of innervation. Mesial cusp section in 6w aged rat is presented in image D and its region of interest in image E. The main nerve bundle (thick arrows) of both CGRP and Nf-IR nerve trunks is clearly shown in panel D. Several Nf-IR branches (long arrows) from this bundle run peripherally toward Od layer. The CGRP-IR branches are also presented in whole SOd, and Od regions except below cervical line (+). Higher magnification of the region of interest is shown in E, which identify CGRP-IR nerve sprouting (arrows) in repair region of Od (*). The groove region of 6w rat sections (image F) shows no actin-IR short OPs and numerous CGRP nerves engaging PD region through Od layer which ramify from the main nerve (x) in SOd region.

9 and 12w:

The CGRP nerves appear denser within this period. The SOd nerve plexus become apparent specially within 12w sections. At higher magnification, higher density of CGRP fibres present in Od region of 12w in comparison to the same region in 9w sections (images D and B respectively in Figure 5.27). These CGRP fibres pass from SOd through Od into the inner dentine (short arrows in image D Figure 5.27). The Nf nerves still reside within the CPC and do not extended further than SOd region of the cusp (long arrows in image B and D Figure 5.27).

In the cervical region (E Figure 5.27), the end of the CGRP nerve branching within SOd and Od with level of cervical line (dotted line) is apparent. CGRP nerves cannot be detected within the Od layer of the root. Additionally, the CGRP nerves are also evident within the gingival tissue.

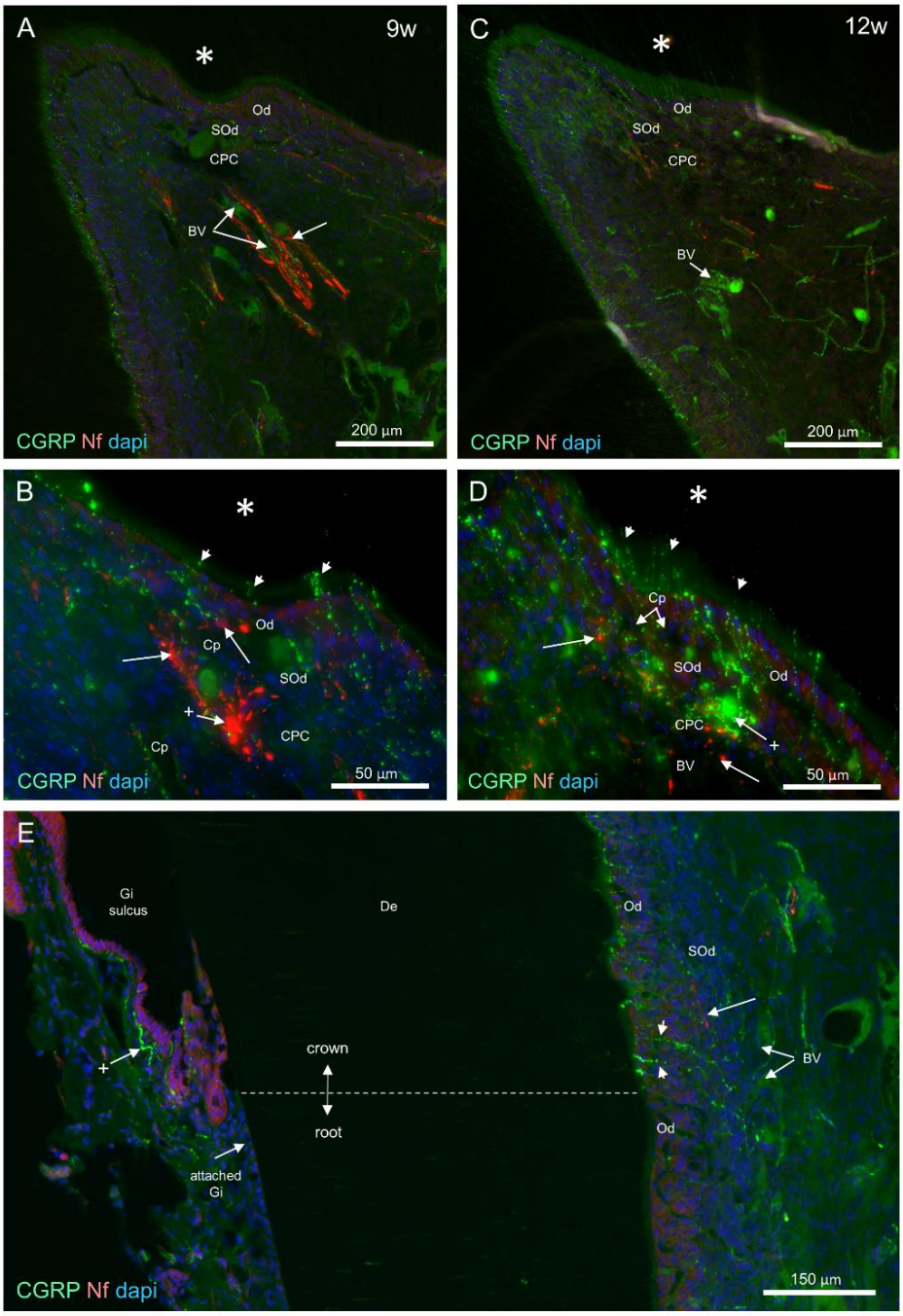

Figure 5.27: Expression of CGRP and Nf nerve markers in demineralised sections of 9 and 12w rat mandibular 1st molar.
All panels are stained for CGRP (green), Nf (red) and dapi (blue). Images A and C shows overview for the mesial cusp at 9 and 12w sections respectively and B and D are higher magnification for the trauma site (*) of the cusp. These clearly identify CGRP-IR nerve branches running between Od cells (small arrows) into PD and Nf fibres that do not pass further than SOd (long arrows). Nerve plexus (+) are observed for Nf (long arrows) and CGRP (short arrows) within SOd regions. The cervical region is shown in image E with dotted line highlights the level of the attached gingiva (Gi) on left side of the image and divided the Od layer into crown innervated Od and root non-innervated Od on the right side of the image. CGRP-IR nerve branches (short arrows) only identified incisally to the cervical line. At the same time the Nf-IR branches (long arrow) are only identified in crown SOd region. Some CGRP nerves (+) are identified within gingival tissue.

24w:

Although, the pulp innervation beyond trauma region appears similar to other non-traumatised regions, a new trauma site emerges which shows depletion of CGRP innervation within its Od layer (image A Figure 5.28). Under higher magnification, the new trauma site shows signs of CGRP nerve sprouting on the lateral margins of traumatised Od region (+ in image B Figure 5.28). The Nf fibres are also seen within SOd and CPC regions (long arrows in image B Figure 5.28). The innervation associated with one of the CPC blood vessel is shown in C Figure 5.28. This image clearly identifies the presence of 2 types of nerves, CGRP and Nf, running perivascularly to this vessel.

The Od layer within groove region also appears densely CGRP innervated (image D Figure 5.28). However, no evident of CGRP nerve fibre is seen within or close to the Od of the furcation region.

Considering the negative controls for all IHC staining, none of these slides show staining signs for the targeted regions.

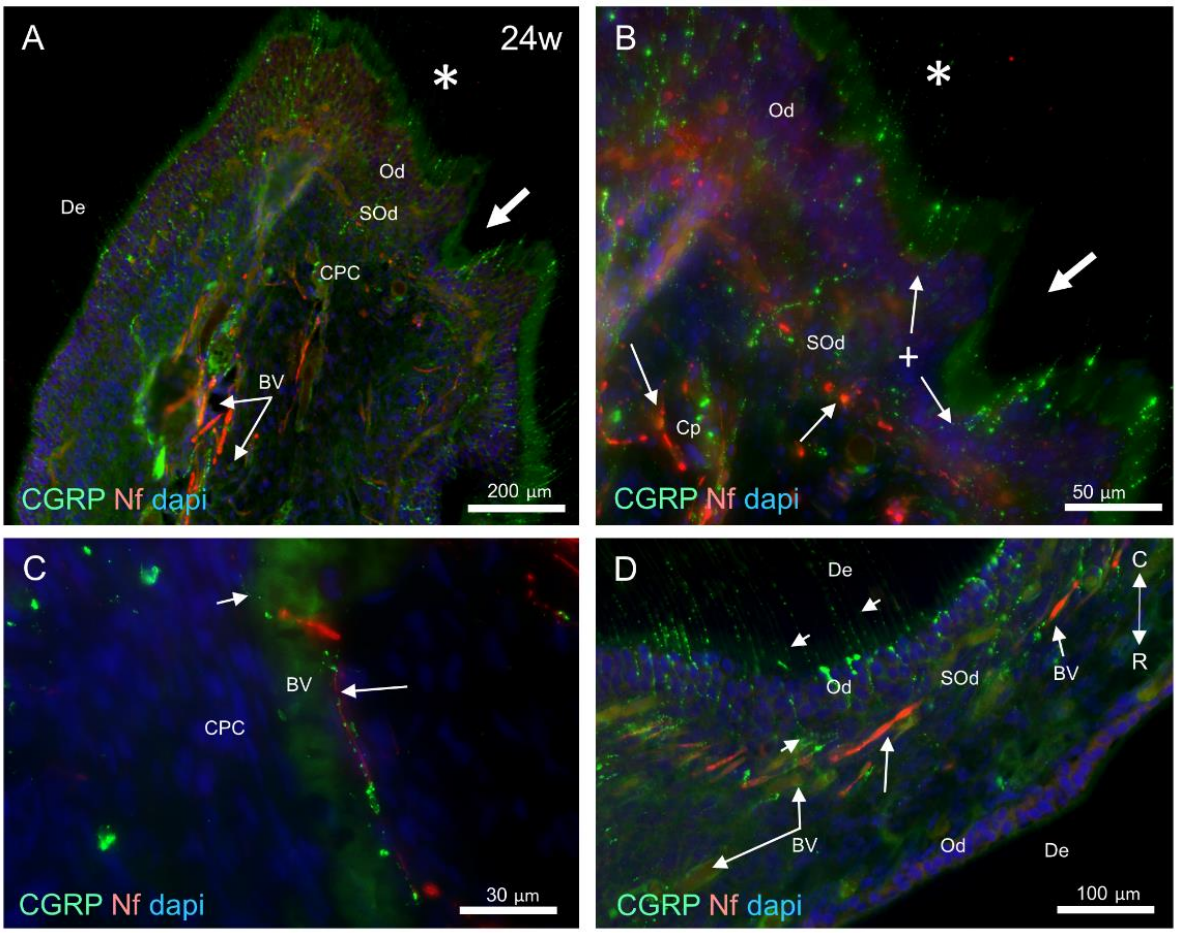

Figure 5.28: Expression of CGRP and Nf nerve markers in demineralised sections of 24w aged rat mandibular 1st molar.
All panels are stained for CGRP (green), Nf (red) and dapi (blue). Image A is an overview of 24w section of mesial cusp, a new region of no nerve is identified (thick arrow). In higher magnification (image B), this region shows new CGRP-IR nerve sprouting (+) in Od, and Nf-IR fibres (long arrow) only run in SOd. Image C identify a BV from cusp region associated with two different nerve: CGRP and Nf-IR (short and long arrows respectively). The groove region (image D) shows numerous CGRP-IR nerves (short arrows) which run from SOd to Od and inner De at the crown side (upward in the image). Also the Nf-IR nerves (long arrow) run only in SOd and central region of the pulp. The furcation side is depleted of nerves.

CGRP nerve density

M, D and T-Den of CGRP nerve fibres within Od layer of the mesial cusp for different age groups are illustrated in Figure 5.29. The M-Den increases gradually with age until 12w, which shows the highest value (4.23 ± 0.9). This increase shows no statistical significant differences until 12w age sections (Table 5-1). Followed by reduction in M-Den in 24w group, but it still high to give statistical significant differences with younger age groups (3,4, and 6 w). The D-Den shows the lowest value (0.92) in 4w sections due to the effect of wear and Ods damage that affected the distal side of the mesial cusp. Then D-Den shows remarkable increases after that especially at 9w group, and reaches the highest value in 12w group (4.8 ± 0.3). This is followed by reduction in 24w samples. The changes in D-Den are much more detected statistically which show differences between all groups except 3 and 4w (Table 5-1). The T-Den shows nearly similar statistical differences to D-Den. Additionally, in T-test, the statistical significant differences are only present between M and D-Den of 3, 4 and 9w age groups (Table 5-2).

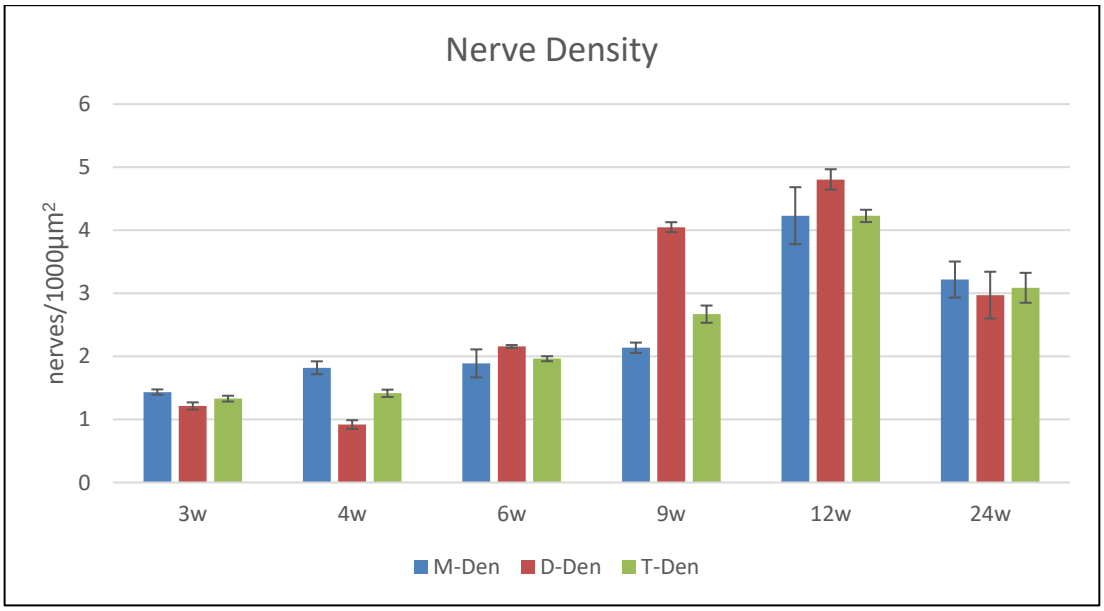

Figure 5.29: CGRP nerve fibre density (nerves/1000µm^2) within mesial cusp. It includes mesial (M-Den), distal (D-Den) and total nerve densities (T-Den) within mesial cusp of different age groups.

		M-Den	D-Den	T-Den
3w	4w	NS	NS	NS
	6w	NS	**	*
	9w	NS	***	***
	12w	***	***	***
	24w	***	***	***
4w	6w	NS	***	*
	9w	NS	***	***
	12w	***	***	***
	24w	**	***	***
6w	9w	NS	***	**
	12w	***	***	***
	24w	*	*	***
9w	12w	***	NS	***
	24w	NS	**	NS
12w	24w	NS	***	***

Table 5-1: Bonferroni Test (p<0.05) to compare between same nerve densities within different age groups.
*Non-significant (NS) is P>0.05, * is p<0.05, ** is p<0.01, *** is p<0.001.*

Groups	M-Des vs. D-Den
3w	*
4w	***
6w	NS
9w	***
12w	NS
24w	NS

Table 5-2: Unpaired T-test (p<0.05) to compare between M and D-densities within the same age group.
*Non-significant (NS) is P>0.05, * is p<0.05, ** is p<0.01, *** is p<0.001.*

5.4 Discussion

The developmental changes within Ods and OPs in the rat mandibular incisor, as a continuous growing tooth model, were reported in Chapter 3. In this work, the responses of OPs to simple cavity preparation were investigated. This was followed by studies on the rat mandibular first molar, as a limited-growing tooth in Chapter 4, and the effects of wear on OPs and the formation of tertiary dentine were described. It is now necessary to develop a broader project to follow the single tooth model from its early formation, including all developmental stages, maturation, eruption, trauma from occlusion, followed by reparative processes and ending with the ageing process. Because of our developing techniques in managing rat samples and the difficulties associated with acquiring appropriate human material, the rat mandibular first molar was chosen. This model offers many advantages in addition to pure convenience. One of these advantages is the presence of occlusal wear that provides a valuable dental trauma model. Tooth responses to such trauma may not be identical to those associated with cavity preparation or carious lesions. However, this particular model shows a rapid and progressive physiological tooth damage that could provide a novel insight into the early and late tooth responses to such trauma.

In order to guide the reader through the discussion of results in each section of the current study, schematic illustrations have been prepared (Figure 5.30 to 5-35). These will summarise results and introduce the hypotheses that have developed from this study.

5.4.1 Dentine structure (ground sections)

The effect of occlusal wear on molar dentine is quite evident within the different age samples presented in this study. Before wear commenced in 2w samples, high density and heavily packed dentinal tubules were observed within the inner dentine of the cusp. The highest density of dentinal tubules within cuspal regions has been reported before (Mjör and Nordahl, 1996). This could influence the regulation of the pulp defensive system within the cusp region against trauma from surface wear (Tjäderhane *et al.*, 2012).

After cusp wear commenced at 4w, tertiary dentine was recognised near the pulp. The primary aim for such dentine deposition is the protection of pulp from injury through exposed dentinal tubules (Tziafas, 2010). Although, part of the Od layer was traumatised as a result of occlusal trauma (Figure 5.6) (see later discussion), several

Od cells within the traumatised region persisted. As a result, this formed tertiary dentine is called reactionary dentine (Tjäderhane *et al.*, 2012). However, in 4w specimens, the reactionary dentine seems atubular and could act as a plug for the pulpal orifices of the primary dentinal tubules (images B and b Figure 5.2). Furthermore, and with age progression, the re-establishment of a tubular pattern within reactionary dentine became apparent, especially within 24w samples. This means that, in the present study reactionary dentinogenesis was divided into two stages: initial or responsive, occurring immediately after dentine surface exposure, to ensure pulp isolation by closing the pulpal ends of the dentinal tubules with atubular dentine. In addition, it increased dentine thickness between the pulp and the external dentine surface. This was followed by a second stage of re-formation of new dentinal tubules by the existing primary Ods. This pattern of reactionary dentine formation is not well supported in previous studies (Tziafas, 1995) (for more details see section 1.11.1). Most previous studies describing the reactionary dentine with a more or less structural continuity with existing physiological dentine (Stanley *et al.*, 1983; Tjäderhane *et al.*, 2012). This idea contradicts the primary purpose for such responsive dentine, to block the exposed dentinal tubules and provide effective isolation of pulp beneath the area of trauma. However, the newly formed tubular pattern of reactionary dentine presented in this study shows meandering arrangement, in comparison to the primary dentinal tubules. This could have resulted from the effect of dentine surface exposure on the arrangement of the traumatised Ods after repair and their ability to form a regular dentinal tubular pattern (this will be discussed in more details in the ‘Trauma region:‘ section).

Additionally, in 24w samples, a second region of atubular dentine was detected due to progressive wear process that extended trauma to another tooth part on the distal side of the cusp. Examining the Ods beneath this trauma region also reveals that some of these cells still survive. This could reflect the ability of the pulp to respond similarly to trauma even after age progression.

Finally, an important question can be raised: how could the same Ods switch in their ability to form two different patterns of dentine, i.e. atubular then tubular? Are these different patterns within reactionary dentine reflecting different stages of Od cell trauma response? The possibilities for answering these questions will be discussed later.

5.4.2 Pulp structure

Development (0d-2w)

This study revealed changes in the distribution of structural proteins associated with cellular differentiation. The vim changed from uniform in UOd into being more apically localised within the cell body of the polarised Od cell. Actin also became more laterally distributed within polarised Ods and concentrated in the apical region of the cells. This is in agreement with previous studies (Lesot *et al.*, 1982; Nishikawa and Sasa, 1989). The role of the basement membrane, separating epithelial and mesenchymal cells, is essential for the terminal differentiation of the Ods (Couve, 1986; Ruch *et al.*, 1995). Degradation of this membrane releases collagenous and non-collagenous glycoproteins in addition to glycosaminoglycans (Thesleff *et al.*, 2001). These in the presence of fibronectin surrounding the dividing POd, generate cell-matrix interactions which are possibly responsible for cellular mediating function. These cellular inductions possibly play a fundamental role in redistribution of the cytoskeletal components to accomplish Od polarisation and terminal differentiation (Thesleff *et al.*, 2001; Tjäderhane and Haapasalo, 2012).

After deposition of PD, two types of OPs were observed: actin and vim. These processes were associated with intense actin and vim IR in the apical region of the Ods. This is similar to Ch 3 observations within rat incisor samples. While the vim OPs were the main cellular processes, the actin OPs were different with a complex morphology and extending only within the PD region. The term actin tree-like processes is also used to identify these processes in this chapter. As discussed in Ch 3, the function of these actin tree-like processes is still unknown. One hypothesis is that they could play a role in the cellular stabilising system along with the actin immunoreactive apical region of the Od cells (Nishikawa and Sasa, 1989). Additionally, the disappearance of these processes when primary dentinogenesis is nearly finished in the tooth crown, may support the suggestion of their role in dentine matrix deposition. However, the persistence of these processes in the root region until older ages (till 12w age rats) may support the idea of a sensing function for these processes (this will be discussed further in section 5.4.5).

The Od cell layer morphology changes in relation to formation, maintenance, and repair of dentine (Linde and Goldberg, 1993). In cusp regions, because it is the region of thickest dentine deposited, the Ods change from a single cell layer into a pseudostratified layer. Dentine is accumulated in association with the centripetal

retraction of the Ods restricting the available space within pulp chamber. The Od cells tend to slide above each other (Ohshima and Yoshida, 1992). The abundance of microfilaments in the structural framework of Ods, especially within apical poles, aids such sliding movements. These microfilaments are also important to exert contractile pressure to keep the Ods in one layer, in addition to their relation to plasma membrane and the intercellular junctional contacts (Nishikawa and Sasa, 1989). In other tooth areas, such as the cervical region, the thickness of the Od layer decreases gradually toward the root, depending on the amount of the dentine deposited.

Eruption, maturation and aging (3w-24w)

Non-trauma regions:

These regions include lateral cusp walls, cervical region, groove, furcation and root (see Figure 5.30). With age progression, the thickness of the pseudostratified layer of Ods decreased. A programmed cellular apoptosis could be responsible for such changes, which not only affects Ods but also other cells within pulp (Mitsiadis *et al.*, 2008). Additionally, the total pulp space was decreased with age. After tooth eruption and commencement of secondary dentinogenesis, the activity of the Ods to produce dentine is remarkably reduced in comparison to the primary dentinogenesis period (Lovschall *et al.*, 2002; Murray *et al.*, 2002). However, Ods continue to form and maintain dentine during their life (Arana-Chavez and Massa, 2004). Furthermore, the presence of cusp wear and the continuous occlusal forces associated with the deposition of reactionary dentine has huge impact on the remaining pulp space. The effect of these forces was quite clear in the 24w samples, especially on the root apex which showed accumulations of hypercementosis (Figure 5.30). Therefore, it remains unclear whether the decrease in pulp size after 24w would be similar than if the pulp had no wear at all. In other words, is the decrease in pulp size in root canals of the mesial root one of the consequences of increased occlusal loading on the worn cusp, or is it part of the physiological secondary dentine formation or a combination of both?

Although the differentiated Od cells reacted positively to the three structural proteins used in this study (vim, actin, and tub), their responsiveness varied in intensity in different age groups. Ods were more intensely labelled with actin and vim in younger age groups before tooth eruption. After tooth eruption, the expression of tub within Od cell bodies became more apparent. Additionally, and with age progression, actin

and vim became more concentrated in the apical region of Ods and OPs. This is in agreement with a previous study which found reduction of vim and F-actin expression in Ods with age progression in rat molar samples (Moxham *et al.*, 1998). This age-dependent cytoskeletal changes within Ods possibly reflects changing in function. It has been reported that cellular organelles change when Ods altered from active secretory to mature cells (Ohshima and Yoshida, 1992). The secretory Ods have highly polarised nuclei and numerous supra-nuclear organelles, including large rough endoplasmic reticulum, Golgi apparatus and many mitochondria. After ageing, several changes occur within Od cells including decrease in cell length, reduction in the number and size of cytoplasmic organelles, and these organelles move to be infra-nuclearly located (Couve, 1986; Sasaki and Garant, 1996). Additionally, the appearance of tight junctions was reported to be more prominent between mature Od cells, which could reflect shifting in cellular function (Turner *et al.*, 1989). Therefore, the observed age related changes of Ods cytoskeletal components could reflect the alteration in dentine forming activity, turning these cells from active secretory to aged dentine maintaining cells.

Moreover, the OPs labelled fully within the whole dentine thickness; but this labelling was different according to age and position within dentine (see B in Figure 5.31). In younger age and before tooth eruption, the main OPs were fully labelled with actin and partly with vim. There was no evidence of tub labelling within these samples. This regional difference in the expression of these structural proteins was also observed in the incisor sections in Ch 3. Since primary dentinogenesis is still proceeding during this age, microfilaments are the essential structural element within developing OPs possibly facilitating process elongation (Pollard and Cooper, 2009). This coincided with the suggested function of the intermediate filaments within the pulpal third of OPs. These filaments could act as an active tensional bearer and resistant element for the mechanical forces, which could resolve the accumulated stresses within OPs due to their elongation (Pollard and Cooper, 2009). After tooth eruption, the expression of tub became more evident within the inner half of the dentine. In the older sample, tub became apparent within the entire length of OPs, while actin retreated to the inner half and vim only labelled inner third of the total OPs length (see B Figure 5.31). This change in labelling of these cytoskeletal markers suggests changes in the structure of the OPs during age progression and this could reflect a change in function. Microtubules were reported to be the major component

within OPs. They had a parallel arrangement and longitudinal flow within the trunk of the processes (Nishikawa and Kitamura, 1987). The elementary function for these cytoskeletal elements is the maintenance of cell shape, and to some extent, participation in cellular shape changes including extension and retraction. This is dependent on the rapid structural ability of these microtubules to assemble and disassemble (Garant, 1972). This could explain the detected structural changes within this study. After tooth eruption, the secretion of secondary dentine matrix commences, which is slower in comparison to primary dentine deposition (4 µm/day in compared to 0.5µm/day respectively). As a result, the amount of OPs elongation per day is also decreased. Therefore, in this stage more cytoskeletal support for OPs is expected to be obtained from microtubules rather than microfilaments, especially in the outer part of OPs. This possibly clarifies the changes in labelling of the outer part of OPs from actin to tub. Furthermore, another important function for the microtubules is intracellular transport, depending on their tubular structure and straight flow (Garant, 1972; Nishikawa and Kitamura, 1987). This gives remarkable support for the basic functions of the OPs after dentine formation which include maintenance and sensing activities (Tjäderhane and Haapasalo, 2012).

Although the level of OPs extension within the dentine of the crown is still a subject of controversy, the vast majority of the opponents agree with the idea of full extension in younger samples (Holland, 1985). This is quite important in this study because the wear occurs in the young rat sample. This means that, the consequences for such trauma could occur as a result of direct trauma to the OPs. The major controversy occurs after tooth maturation and ageing. The opponents still believe that the OPs retreat toward the pulp. They claim that the purpose for such physiological retraction is that the OPs cannot survive at such a distance away from the pulp (Byers and Sugaya, 1995; Goracci *et al.*, 1999; Yoshiba *et al.*, 2002). However, there are many studies supporting the remote vitality of the OPs away from the pulp (Yamada *et al.*, 1983; Sigal *et al.*, 1984a; Sigal *et al.*, 1984b; Grötz *et al.*, 1998). There are several technical problems including sample type, preparation, fixation, sectioning and viewing which could explain the differences between these observations. Furthermore, other studies reported closure of the terminal third of dentinal tubules with ageing as a result of physiological dentine sclerosis (Stanley *et al.*, 1983). This could be true, taking the age limit of this study into consideration. Therefore, either

older rat samples or even human samples could be suggested for further investigations.

Trauma region:

This section includes the trauma region starting from first detected signs of wear at 4w up to 24w samples (see A Figure 5.31). Although, occlusal attrition is a familiar process within study models such as the rat molar, this is the first study which looked in detail within different age groups to illustrate the effects of this process on the structure of OPs, Od, and adjacent pulp cells.

When wear commenced after tooth eruption, the first cell component to be affected was not surprisingly the OPs. Exposure of the dentinal tubules and direct trauma to the terminal branches of the OPs could be a possible interpretation. However, the direct contact of the cellular process with oral fluids, and bacterial contamination, is another existent traumatic factor. Regardless of the irritation mechanism, the visible effect of this trauma was empty dentinal tubules from their OPs beyond the worn surface. According to our previous work in Ch 3, cavity preparation caused a programmed retraction of the traumatised OPs toward the pulp. Therefore, the traumatised OPs in this experiment might also have undergone a programmed retraction. This was probably the initial response to trauma occurring in a period between the 3rd and 4th weeks of age. Additionally, there were some non-retracted processes in regions of minor wear (Figure 5.31). These processes were either in a preparation stage for retraction, the wear was still simple and not enough to stimulate retraction, or their roles were to plug their tubules to decrease the number of contamination routes toward the pulp cells (as discussed previously in chapter 4).

The second effect was identified within Ods and can be divided into two observations: Od cells of pulp horn, and pulp border Od cells beyond the trauma region. Because the pulp horn cells were the nearest to the worn surface, the responses of these cells were exaggerated. As observed in 4w sections in Figure 5.6, these cells were separated from the Od layer and their nuclei appeared within the atubular dentine region of the reactionary dentine. However, there was no evidence of cellular cytoplasm within these cells. At the same time, their nuclear staining was faint in relation to other pulp cells. This could reflect signs of cellular degradation (Mitsiadis *et al.*, 2008). Cavity preparation has also been reported to induce apoptosis within Ods and SOd cells (Ohshima, 1990; Kitamura *et al.*, 2001).

The border Od cells beyond the trauma region also showed remarkable morphological changes. These cells lose their apical junctions, appear more separated, have a large network of dilated capillaries evident near pulp border, and the cells became highly actin labelled both with the associated SOd cells. The junctions between Od cells are structures which can break and reform intermittently (Turner, 1992). Breakdown of the junctional complexes was also recognised within 24h of deep cavity preparation. This was associated with changes in intracellular organelles of the Od cells (Turner *et al.*, 1989; Chiego Jr, 1992). This could facilitate the passage of reparative compounds and associated ions from pulp to the overlying predentine as a first stage of the inflammatory response, which was boosted by the presence of dilated capillaries (Turner, 1992). Studies also show that the increase in permeability of the Od layer allows large macromolecules such as fibrinogen penetration through predentine into the dentinal tubules. Polymerisation of fibrinogen into fibrin can be activated via the clotting cascade and this possibly seals the pulpal opening of the occlusally exposed dentinal tubules prior to the formation of a calcified barrier (Chiego Jr, 1992; Pashley, 1996). Furthermore, evidence of microfilaments within cytoskeleton of Od and SOd cells possibly aids cellular movement and morphological changes within these regions induced by inflammation (Pollard and Cooper, 2009). In the same way, because actin was also intensely observed within secretory Ods in earlier age groups, the induction of such protein within traumatised cells could be the sign of an increase in dentine formation behaviour. The mechanisms possibly behind this cellular induction will be discussed later in sections 5.4.4 and 5.4.5.

The remarkable increase in actin expression within the SOd is a subject that should be considered. These cells also appeared highly packed to each other, under traumatised Ods, dissimilar to their loose arrangement beyond intact Ods. Within normal Ods, the microfilaments are always involved in keeping Od cells in one layer in addition to their junctional contacts (Nishikawa and Sasa, 1989). The highest expression of these microfilaments are within SOds in this stage and they possibly aid cellular movements to make these cells tightly packed with one another to provide cellular seal to direct extracellular fluid diffusion toward the traumatised pulp cells. This could help to localise the pulp responses within trauma region and prevent diffusion of the reparative material in the wrong direction. A repeated behaviour of these cells was also seen in the second trauma region in 24w samples (Figure 5.11).

A similar pulpal response was reported within the deeper cavity. This includes formation of a fibrous layer containing fibroblast like cells possibly to isolate the trauma region from other intact pulp regions (Taylor and Byers, 1990). Additionally, these highly actin IR SOds could also be preparing to be the precursors. This could occur when the whole Od cells within the trauma region die (Fitzgerald *et al.*, 1990). Other signs were detected within SOds in the trauma site in this study which included hyper expression of NaK-ATPase, and faint expression of NHE-1 (image D, Figure 5.34) and NGF (image D, Figure 5.32). These cellular changes will be discussed within each section and in the final homeostatic hypothesis for this study (Figure 5.35).

This stage of tissue response is possibly followed by a next step, including the formation of a calcified dentine plug. This atubular plug evident in 4w samples (Figure 5.6) is in the same location of the pulp horn cells in 3w samples (Figure 5.5). This may suggest the role of these cells in the formation of such stage-dependant dentine. Although these cells showed signs of apoptosis, they still labelled with dapi stain which reflects their vitality. After losing their OPs, these cells possibly separated from the entire pulp body due to trauma. This may stimulate these cells to start dentine matrix deposition to occlude the pulpal opening of dentinal tubules, i.e. acting as scarifying cells. At the same time, the pulp border Ods possibly deposit further dentine matrix in a pulpo-occlusal direction. This increases the thickness of this atubular plug for further pulp isolation. The evident dentine lacunae which were observed within this atubular dentine in later age group sections (as seen in Figure 5.9) could support this suggestion. There was also similar observation reported in previous studies of Ods sucked into the dentinal tubules immediately after cavity preparation (Ohshima, 1990; Mitsiadis *et al.*, 2008). The Ods that have been sucked could also participate in the formation of the impermeable barrier between pulp and exposed dentinal tubules. Another possible hypothesis is that the atubular reactionary dentine could only be formed by the border Ods and these degraded Ods were just dying cells because of the traumatic insult. Furthermore, the absence of OPs during this stage is the major cause of atubularity of this dentine. Whatever the depositing cells of this atubular dentine, its formation could be part of the initial inflammatory responses of the pulp cells to form a pulp isolator plug in front of exposed dentinal tubule contamination. The impermeability of this plug was also evident in this model because these trapped pulp horn cells after deposition of

atubular plug were degraded and only their calcified lacunae were apparent within older tooth section. This agrees with previous research which identified reduction of the dentine fluid diffusion after atubular dentine formation (Byers and Lin, 2003).

To summarise, the initial response to trauma which includes the morphological changes of pulp cells and initial reactionary dentine plug, aims to minimise pulp damage by: (i) enhancing pulpal permeability for reparative compounds and ions into the predentine region which accelerated healing of the injured pulp cells and boosted reparative dentine deposition (Turner, 1992). (ii) limiting dentinal tubule permeability by formation of an impermeable dentine plug to restrict harmful compound diffusion to the repair region and pulp tissue. (iii) structural and functional changes within SOds which aids pulp healing from the injury side and protects the involvement of the rest of the pulp from the other side.

After the pulp response subsides from the immediate trauma effect, the Od cells return their morphological characteristics, which include apical cellular junctions and OPs (Figure 5.7). The gap and tight junctions between Od cells, as well as the intracellular organelles, were reported to be re-established at five days after trauma from cavity preparation (Chiego Jr, 1992). The presence of an atubular plug within the reactionary dentine, possibly provides a good barrier for the pulp healing process and this led to gradual disappearance of the inflammatory signs. The new OPs, called secondary OPs in this study, appear similar in their structural protein labelling to the primary OPs during development. The secondary OPs were evidently labelled with actin along their entire length and vim and tub only in the inner region of the processes. However, these secondary processes appeared in a meandering style compared to the straightness and parallelism of the primary OPs. The reason for that is still unknown. It could be due to the effect of trauma, which possibly altered the Od cellular orientation within the re-established Od layer. Consequently, the orientation of the secondary OPs and the resultant reactionary dentinal tubules were possibly altered.

The model of this study showed the dynamic capacity of the pulp cells, especially Ods, to change their shape and function. This was not only during developmental stages but also in response to trauma and ageing. This capacity appeared recurrent, even with age progression. This can be recognised within 24w samples which showed similar reaction of the Ods and SOds to progressive trauma from wear.

Previous studies showed that repetitive, microbial, chemical or mechanical trauma possibly reduced the pulp healing ability (Johnson, 2004; Tjäderhane *et al.*, 2012). This could be due to depletion of the Od cells, which leads to differentiation of Od-like cells that will form structurally different reparative dentine (Smith *et al.*, 1995; Tjäderhane *et al.*, 2012). Therefore, samples from older ages of rat could be suggested for future work to improve our understanding about the repetitive trauma from progressive surface wear on the remaining aged pulp tissue.

The control that is responsible for the Od switching in their morphological and functional behaviour in response to trauma is still unknown. However, and according to the findings of this study, there were two switching patterns that should be taken into consideration. The first was the immediate response, which could be mediated directly by trauma itself and this was aimed at pulp protection. The second occurred after the success of the first aim, followed by a gradual termination of inflammation and return of Ods to their original morphology and function before trauma. Therefore, the stimulator causing the first Ods switching should subside to allow the stimulator of the second change to occur. Further discussion can be found in section 5.4.4.

5.4.3 Cell division

It became important in this study, which used a broad range of age groups (including the developmental, maturation, trauma, repair and ageing stages), to explore cellular proliferation. This aided the identification of the proliferation time, cell differentiation period, and the possible effect of trauma applied by wear on the affected pulp cell proliferation responses. Ki67 is a proliferation marker. Human Ki67 protein is strictly associated with cell proliferation. It reacts with nuclear structures present exclusively within proliferating cells (Scholzen and Gerdes, 2000). The Ki67 antigen is available in nuclei of cells in G_1, S, and G_2 phases of the cell division cycle as well as cell mitosis and absent in resting cell (G_0 phase) (Gerdes *et al.*, 1984). This marker is widely used as diagnostic evidence for different types of neoplasm (De Azambuja *et al.*, 2007) and in biological studies including continuously growing rodent teeth (Gomes *et al.*, 2010).

This study confirmed the presence of cellular proliferation only during the development stage (bell stage (0d)) of the tooth before terminal differentiation of the Ods and predentine deposition. The differentiated Od cells passed through the proliferation period followed by a cellular reorganisation of their cytoskeletal elements

and organelles, before commencement of dentine matrix deposition (Ruch *et al.*, 1995). Therefore, Ods are specialised post-mitotic cells that should continue living and being functional, as long as the tooth is kept intact and vital (Tziafas, 2010). Following tooth development and morphogenesis, neither Ods nor other pulp cells showed any proliferation signs within all age groups except the developing root region. After root completion, there was no evidence of Ki67 within pulpal cells, except very few cells within the pulp core and near blood vessels (which could be white blood cells).

The trauma model associated with this study showed evidence of cellular apoptosis within Ods of the pulp horn and some border pulp cells. However, no evidence for cellular proliferation has been detected within SOd or central pulp cells associated with the trauma region. As mentioned previously, the existing Ods, or part of them, within the trauma region, successfully survived after insult and returned to their normal morphology and function after the end of inflammation. Therefore, this trauma type is possibly not sufficient to activate adult mesenchymal cells within the pulp to differentiate into Od-like cells (Tziafas, 2010), as deep cavity or pulp exposure trauma may do (Fitzgerald *et al.*, 1990; Chiego Jr, 1992). On the other hand, this possibly questions the availability of these adult pulp stem cells which were reported to be either part of SOd cells, pericytes or fibroblasts of the pulp core (Shi and Gronthos, 2003; Téclès *et al.*, 2005). In Ch 4, the SOd cells, which were closely underlying the Ods beneath the worn cusp region, have been observed to change their morphology and be more Od-like cells but without detected cellular processes. We were expecting to see the cell division marker to be present within these cells especially during early trauma age (4w). The absence of this marker from these cells probably support the idea of dedifferentiation ability within these cells to change their morphology and possibly function in response to the stimuli (Simon and Goldberg, 2014). Additionally, the high actin-IR for these cells during early stage of trauma and then their ability to recover their original expression after passing this period could also support the above idea. However, the absence of severe stimuli within this study which possibly cause total degeneration of the Od layer within trauma region may require further investigations. Identifying cellular division markers and other structural proteins within the possible Od precursor cells possibly give new insights about the actual pulp response to be regeneration process or just tissue repair response.

5.4.4 NGF and NGFR

NGF was reported to regulate non-neuronal cellular function through its action on low affinity neurotrophic p^{75} (known as NGFR in this study) and high affinity trkA receptors. Its dual action on these receptors together was reported to enhance cellular differentiation and survival (Woodnutt *et al.*, 2000). Previous studies also reported the involvement of p^{75} receptors during tooth development, ageing and trauma (Byers *et al.*, 1990; Byers *et al.*, 1992). This study used IHC to explore the expression of NGF and its p^{75} receptor through a broad range of age groups of rat mandibular 1^{st} molar sections. Data collected from this section, associated with other sections of this chapter, could help to link information to improve understanding about the possible cellular induction which could occur during these different tooth stages. A marker for trkA receptors was not used in this study and could be suggested for further research.

Changes in the expression of both NGF and NGFR were introduced in this study during the morpho and cyto-differentiation stages of tooth development (image A Figure 5.32). These differences occurred between undifferentiated and more developed dental papilla cells within the tooth germ. This is in line with previous studies, which suggested the presence of sequential regulatory signalling between the epithelium and mesenchymal developing tissue, possibly with mediated timing and spatial differentiation during early morphogenesis. (Byers *et al.*, 1990; Mitsiadis *et al.*, 1992). Additionally, no sensory nerve fibres were evident in similar age group sections, which confirms the previous suggestion (Figure 5.24). The autonomous, nerve independent, mechanism of NGF synthesis within developing tissue was previously reported (Rohrer *et al.*, 1988). This indicated the ability of the developing dental cells to produce NGF and provide its membrane receptors by themselves, suggesting an autocrine or paracrine mode of action (Mitsiadis *et al.*, 1992). Therefore, the presence of this signalling mechanism within this stage of tooth development suggested its active implication on the cyto-differentiation changes occurring within Ods and other cells of the pulp. In addition to the effect of growth factors on cellular differentiation, the basement membrane derived substrates, such as fibronectin, were also reported to be essential in Ods differentiation (Lesot *et al.*, 2001). The presence of all these factors together promote Ods to withdraw from division cycles. This was followed by cytoskeletal modifications occurring in post

mitotic, polarised, Ods with apical redistribution of the structural cytoskeletal proteins (Tjäderhane and Haapasalo, 2012).

After commencement of primary dentinogenesis (images B and C Figure 5.32), NGF expression was specifically identified within Ods and the basal region of the OPs. The NGFR labelled SOd and nearby CPC. This is also in agreement with previous studies, which reported similar location of NGF and NGFR during period of primary dentine formation (Byers *et al.*, 1990; Mitsiadis *et al.*, 1992; Luukko *et al.*, 1996). This expression could hypothesis the maestro role of Ods in controlling associated pulp cells. This possibly related to several spatial and functional properties of the Ods which include: 1) they are the formative cells of the tubular dentine which control its calcification both before and after tooth eruption (Linde and Goldberg, 1993); 2) they are neural crest derived cells (Ruch *et al.*, 1995); 3) they form a special cellular barrier separating pulp from mineralised dentine and/or oral cavity, and cells within this layer are linked by numerous gap junctions (Turner *et al.*, 1989). As a result, we can suggest the coordination role of the Ods on other pulp cells acting as supportive cells during dentine formation. Additionally, the primary role of the NGF, as a neurotrophic factor, is an important regulator for survival, differentiation, and maintenance of nerve cells. This induces NGF-responsive neurones toward NGF source (Chao, 2003). This function was also recognised within the present study by NGFR labelling of the nerve bundles in the central pulp region and small nerve fibres in SOd region (Figure 5.21). Additionally, there was a high intensity labelling of both NGF and NGFR within Ods and SOds respectively. This could explain the growth direction of sensory nerve toward the Ods and OPs, especially after tooth eruption and accomplishment of primary dentinogenesis, represented in 3w sections (see Figure 5.21). To summarise, the unique properties of the Ods layer with their specific expression of NGF could suggest their controlling ability not only on the adjacent responsive cells, but also on the pulp nerve supply.

With trauma onset (image D Figure 5.32), there is an evident reduction of NGF-IR within injured Ods, and a weak expression within the underlying SOds, associated with the absence of NGFR-IR within latter cells. These injury responses agreed with the previous studies, which reported similar cellular reactions up to 9 days after trauma (Byers *et al.*, 1992; Woodnutt *et al.*, 2000). Additionally, a marked increase in the expression of NGF-IR in Ods was identified within adjacent, non-trauma regions, especially on the mesial side of the cusp. This was associated with increase in the IR

of NGFR within underlying SOds and CPC. This could be part of the inflammatory process within this cusp to support the injury region and repair mechanism in the pulp. These cellular responses were identified in normal and denervated teeth, indicating that these alterations were possibly nerve-independent (Byers *et al.*, 1992). The reduction in the NGF production by the traumatised Ods may also cause an increase in its formation by the underlying SOd and the adjacent non-injured Ods to compensate that lost within injured tissue. The lack of NGF mRNA within injured Ods was also reported, suggesting that NGF was transferred to these cells from adjacent SOd (Woodnutt *et al.*, 2000). This suggested the role of these NGF producing cells in mediating and regulating the injured Ods. By forming excess NGF, this might influence the reparative process by supporting Ods within the trauma region to perform reactionary dentinogenesis (Magloire *et al.*, 2001). This is in agreement with the results of this study suggesting the SOd fibroblasts may control the Ods function during trauma time (Byers *et al.*, 1992; Magloire *et al.*, 2001).

The NGF was reported to induce the invading leukocytes to the injured region by its non-neuronal paracrine receptors during the inflammation period (Woodnutt *et al.*, 2000). It also may induce significant morphological changes within Od cells, enhance production of cellular microfilaments within Ods and OPs, activate the nuclear transcription factor (NF-kB), induce formation of trk-A (Woodnutt *et al.*, 2000) and (Magloire *et al.*, 2001). The latter agrees with the present study finding, which showed the IR of NGFR was detected in the Ods close to the trauma region, and this continued within 9w samples (image E Figure 5.32). Therefore, the structural cellular changes which were detected within the worn cusp could be mediated by NGF and its paracrine or autocrine receptors. The presence of this signalling system between these adjacent cells possibly controls cellular inflammatory responses and tissue repair mechanisms. Furthermore, a returned IR of NGF within traumatised Ods associated with a prolonged expression within SOds was also recorded, persisting within 6 and 9w sections. The persistence of a large number of NGF formative cells within trauma region is possibly related to their role in tissue reparative mechanisms. This also could suggest the role of NGF on OPs elongation during reactionary dentinogenesis, because of its actin formation inductive activity (Magloire *et al.*, 2001). On the other hand, increase production of NGF could attract the CGRP nerve fibres within this region and this enhanced CGRP release which in turn accelerated

the healing process (Davies, 2000). This will be discussed in more detail in the next section.

The altered cellular expression of NGF and NGFR within the trauma region was continued until 12w sections, where the normal tissue expression returned (image F Figure 5.32). At this age, the injured Ods and OPs looked similar in their expression of NGF to other regions of the cusp. This is also true in the underlying SOds which NGFR-IR appeared continuous with the non-injured SOds. Because of the age group intervals included within this study, it was unclear whether the normal expression of these markers re-established exactly at 12w (about 8w period from the onset time of trauma) or between 9 to 12w. Therefore, to overcome this shortage, a period of within 8w is considered in the present study, as a time that is possibly required by the pulp tissue in this model to return to its normal expression.

Moreover, the NGFR-IR appeared less diffuse within CPC and became more limited to SOd and the close vicinity central pulp cells. This pattern of NGFR expression became apparent within 24w samples (image G Figure 5.32) and this agreed with previous studies which showed continuous reduction of NGFR-IR within older ages of rats (Swift and Byers, 1992). The reason for this is unknown, however, due to the restriction of the pulp volume with ageing, the number of the Ods was also reduced (Murray *et al.*, 2002). This possibly decreased the NGF producing cells which also caused decrease in the number of responding cells. The involvement of the p^{75} NGF receptors in cellular apoptosis was also reported (Casaccia-Bonnefil *et al.*, 1998). The re-expression of p^{75} NGFR was reported in the Ods in the anterior region of the rat incisors, whereas its expression was limited to the SOd during primary dentinogenesis (Mitsiadis *et al.*, 1993). This could keep the density of the Ods constant in continuous growing teeth by apoptosis control of the NGFR expressed Ods (Mitsiadis *et al.*, 2008). This pattern of NGFR expression was also evident in this study, where the labelling of these receptors was only limited to SOd before tooth eruption. After tooth eruption, these receptors became apparent both within Ods and SOds (Figure 5.32). Furthermore, cellular ageing signs were also recorded within the pulp reaction to the second trauma site which appear different than its reaction to the first trauma. However, there were no older age groups included within the present study which could show what may happen further. Therefore, further ages can be suggested for future studies. Finally, we can conclude that the presence of NGF and

NGFR signalling system during different stages of the tooth life could suggest its multiple functions, which could be altered depending on age required circumstances.

5.4.5 Sensory nerve markers

Although occlusal attrition is a well known phenomenon within the rat molar, none of the previous studies used this physiological trauma to analyse its effect on sensory nerve fibre distribution and sprouting (Kimberly and Byers, 1988; Taylor *et al.*, 1988; Taylor and Byers, 1990). This study observed the immunoreactivities of two nerve markers (CGRP and Nf). In addition, quantitative analysis and comparison between densities of the CGRP nerve fibres within Od layer on the two sides of the mesial cusps within different age groups were performed. This was because the CGRP fibres were the common detected axons within Od and PD and the most observed reaction with trauma insult. Additionally, CGRP fibres are important considering their relation to inflammation and tissue response to trauma, by releasing neuropeptides, which have important effects on circulatory regulation, inflammation, and wound healing (Taylor *et al.*, 1988; Taylor and Byers, 1990). This study also linked pulp innervation data with other information obtained from previous sections to provide new insights about tooth developmental stages, pulp inflammation and repair.

It was obvious in this study model that tooth sensory innervation was delayed in its development until tooth crown formation was completed. The innervation was limited to few fibres running in association with pulp core blood vessels during developmental stages and primary dentinogenesis. Nerves then showed oriented development toward the cusp Od and dentine which became apparent after tooth eruption. This is in line with previous studies (Corpron and Avery, 1973; Byers *et al.*, 1990; Fristad *et al.*, 1994). The presence of NGF-IR within secretory Od and OPs, in addition to NGFR within SOds and CPC, may suggest the role of NGF as a nerve guiding development factor (Davies, 2000). The action of NGF may control the sensory nerve growth from CPC through SOd, Ods and into inner region of the dentine. NGF working on both p75 and trkA neurotrophic receptors together, can effectively regulate neuron survival and control growth of axons and neurites (Davies, 2000). Lacking one of these receptors effectively limited nerve growth within oral and dental tissue (Matsuo *et al.*, 2001).

It is unclear from the results obtained in the current study whether the CGRP or Nf fibres within Od and SOd were myelinated or not. However, and depending on the

calculated diameters, the CGRP were smaller than Nf fibres and contained varicosities. Mainly unmyelinated nerve fibres which contained microvesicles, were reported within Ods and inner dentine, while both myelinated and unmyelinated nerves were observed within SOds (Corpron and Avery, 1973). Myelinated and unmyelinated axons were reported to pass through the apical tooth foramen with an average diameter between 2-4µm (Byers, 1984). Although sympathetic nerves (unmyelinated) were also seen within pulp tissue, they were very few and found along large blood vessels within pulp core (Fristad *et al.*, 1994). The rest of the pulp axons were mainly sensory axons whose cell bodies were located in the trigeminal ganglia (Byers, 1984). These sensory axons are either fast fibres (A delta) or slow-conducting fibres (C). The latter nerves have been distinguished to be responsive to CGRP depending on their secretory microvesicles (Taylor *et al.*, 1988; Taylor and Byers, 1990). The other type (Nf axons), which were recorded in the current study, were mainly located within SOd, partially in Od (smaller diameter), and rarely in PD. The neurofilament is part of the structural skeleton of the nerve axons (Tsuzuki and Kitamura, 1991), and considered as a marker for the myelinated sensory fibres (Luthman *et al.*, 1992).

As mentioned previously, the tree-like OPs disappeared form the crown Ods after accomplishment of primary dentinogenesis. This was also associated with increase axonal development within Ods layer. Additionally, these processes persisted within root Ods until 12w old rats, with very rare intercellular nerves being evident. This could support the hypothesis of the relationship between these actin tree-like OPs and the sensing mechanism of the Ods during this period of tooth development. However, these OPs disappeared even from root Ods in 24w rats with no change within intercellular root innervation. This could reflect the effect of tooth ageing, with thicker secondary dentine deposited on root surfaces, which may decrease the activity of the root Ods and their required external sensation.

The effect of wear trauma was apparent on CGRP afferent axons both morphologically and quantitatively. Localised depletion of CGRP fibres within traumatised Od regions was observed, which appeared similar to previous studies observations (Taylor *et al.*, 1988; Taylor and Byers, 1990). The exact mechanism controlling this transient retraction of the nerve fibres from traumatised Ods regions is unknown, but it could be part of inflammatory changes resulting from tissue insult.

Additionally, the changing in the expression of the NGF from traumatised Ods to the underlying SOd could be the mediator for this retraction (see D in Figure 5.32).

This was followed by a significant increase in the number of CGRP fibres in the trauma side of the cusp in 6w rats (Figure 5.29). This could be mediated by NGF which is produced by both Od and SOds in this age. As a result, the increased production of NGF within trauma region may promote more nerve growth, which promoted nerve proliferation and sprouting (Chao, 2003). The CGRP nerves are primarily sensory as is assumed from the physiology of C fibres (Abd-Elmeguid and Yu, 2009), and their trigeminal ganglia origin (Pan *et al.*, 2003). This observed CGRP nerve proliferation possibly increases the pain sensitivity of the inflamed pulp. Alternatively, it could increase the release of CGRP and substance P as neuromodulators, and have an effect on the inflammatory process. This effect could include; pulp blood flow (Brain *et al.*, 1985), histamine release (Ottosson and Edvinsson, 1997), modulation of immune cells function and mitosis (Hahn and Liewehr, 2007). Therefore, increasing nerve densities within the trauma region could enhance the delivered amount of CGRP and other vasoactive neuropeptides which promote neurogenic inflammation and tissue healing process (Taylor and Byers, 1990). Additionally, the structural re-establishment of the Ods, with reappearance of OPs, could be in part mediated by this neurogenic inflammation.

The distal nerve density continued to increase in 9w samples, although the mesial nerve density looked similar. The cause for this profound nerve proliferation within this time is unknown. However, it could be in part due to the neurogenic inflammatory process, which may result in hyper innervation and hypersensitivity of the tooth cusp. After re-establishment of the Ods layer, new tubular dentine was also secreted. Therefore, the persistence of the neurogenic inflammatory period could promote tissue healing and enhancing tubular reactionary dentine deposition. Additionally, the continuous expression of NGF by both Ods and SOds even after this period from the onset time of trauma (image E Figure 5.32) may promote CGRP nerve sprouting and proliferation.

At 12w both mesial and distal nerve densities reached their maximum levels (Figure 5.32). As mentioned previously, 12w is the age of the complete mesial root formation and closure of the apical foramen. This is the tooth maturation age. It has been reported that, the number of axons increased during the maturation period and

reached its maximum number after complete root formation (Byers, 1984). Therefore, the increasing number of nerves entering the tooth, could be the cause for increasing axons arborisation within both sides of the mesial cusp. Additionally, the subodontoblast nerve plexus became more developed within this age (Figure 5.27). However, the distal nerve density was still higher than the mesial. This could reflect the effect of neurogenic inflammation which could be extended until this age.

In 24w samples, both mesial and distal nerve densities were reduced in comparison to the 12w values. This was probably part of the ageing process and may have contributed to age related reduction in the number of nerve fibres (Swift and Byers, 1992). Additionally, this could also reflect the age reduction of the NGF and NGFR cells recorded within the current study. Moreover, the distal nerve density showed more significant changes than the mesial one. This could be due to the appearance of new trauma region on the distal side of the cusp which showed disappearance of CGRP axons from traumatised Ods. According to the obtained data, the consequences for this new trauma site on the CGRP nerve sprouting is unknown. However, previous research reported higher CGRP nerve sprouting after cavity preparation in older compared to younger rat ages (Swift and Byers, 1992).

5.4.6 Ion transporter markers (NaK-ATPase and NHE-1)

Primary dentinogenesis

NaK-ATPase or sodium pump is the cell membrane enzyme maintaining the Na^+ and K^+ gradient across the plasma membrane of animal cells. It is responsible for a relatively high concentration of intracellular K^+ and extracellular Na^+. It actively exchanges 3 Na^+ out of the cell for every $2K^+$ into the cell. This keeps the membrane resting potential with one positive charge gradient (Kaplan, 2002). This gradient is important in regulating cell volume, cytoplasmic pH and Ca ions (Ca^{2+}) levels through Na^+/H^+ (NHE) and Na^+/Ca^{2+} exchangers respectively, and in driving a variety of secondary transport processes such as Na^+-dependant glucose and amino acid transport (Therien and Blostein, 2000). Because the pulp is a form of tissue with high transport function, it possibly possesses high NaK-ATPase activity (Mornstad, 1978). This can be manifested in the results of this study, which showed activity for this enzyme within Ods and with more IR in SOd during primary dentiogenesis. Alternatively, there is no evidence of expression during the cell division and differentiation period of these cells (Figure 5.34). The exact role of the NaK-ATPase during this stage of primary dentine formation is not known, however it could play a

role in Ca^{2+} transportation required for dentine mineralisation. Although, there were several studies on the role of NaK-ATPase and NHE in maturation and mineralisation of enamel (Josephsen *et al.*, 2010; Wen *et al.*, 2014), their action within dental pulp and dentine mineralisation is so far not known (Duan, 2014). Therefore, this study proposed a model to explain the possible function of these transporters. They could be involved with other ion transporters (which are possibly present) in the process of Ca^{2+} translocation during dentine formation (Figure 5.35). The selection of the other ion transporters in this model is dependent on data available in the published studies on pulp cells or other cells of the body dealing with Ca^{2+} transportation such as salivary gland (Onishi *et al.*, 1999), bone (Boonrungsiman *et al.*, 2012), and enamel organ (Josephsen *et al.*, 2010).

During dentinogenesis, Ca^{2+} transport to the sites of mineralization is reported to be under cellular control, in that the ions are primarily transported intracellularly through the odontoblasts (Lundgren and Linde, 1992; Linde and Lundgren, 1995). Studying the Ca^{2+} transporting system within Ods should basically deal with mechanisms to maintain a low steady state Ca^{2+} concentration within cytosol (Linde and Lundgren, 1995). The major reported influx route for the Ca^{2+} ions is through the L-type Ca^{2+} channels (group I, image A, Figure 5.35), as their blocking *in vivo* caused severe impairment of radioactive Ca^{2+} uptake within dentine minerals (Lundgren and Linde, 1997). After influx of Ca^{2+} intracellularly, these ions are immediately buffered by calcium binding proteins such as calbindin (Berdal *et al.*, 1993). The latter is a high affinity, intracellular soluble protein, present in various Ca^{2+} transporting tissue such as salivary gland (Onishi *et al.*, 1999), enamel organ, and bone (Berdal *et al.*, 1996). Cellular organelles could also play a pivotal role in controlling the concentration of intracellular Ca^{2+} such as endoplasmic reticulum by active Ca pumping (SERCA) mechanism (Granström *et al.*, 1979) and mitochondria via Na/Ca exchanger (Linde and Lundgren, 1995). The plasma membrane also exhibits a transport mechanism to extrude the excess Ca^{2+}, to control their concentration within cytosol by plasma membrane active pump (PMCA) (Granström and Linde, 1976) or by secondary active Na/Ca exchanger (NCX), depending on decreasing intracellular Na^{+} ions concentration caused by function of NaK-ATPase (Tsumura *et al.*, 2010). Furthermore, inorganic phosphate (P_i) translocation through Ods was also reported to be Na^{+} concentration dependant via the Na/P_i cotransporter (Lundquist *et al.*, 2002). This could reflect the high expression of the NaK-ATPase within Ods in the

present study during primary dentinogenesis. This could play a crucial role in regulation of calcifying ions (Ca^{2+}, P_i) transportation and concentration within Od cells by maintenance Na^+ gradient crossing plasma membrane (Therien and Blostein, 2000).

In addition to formation of organic matrix protein, the primary aim for cells forming mineralised tissue such as Ods, is to transport ions to their mineralisation front to perform tissue calcification (Tjäderhane *et al.*, 2012). This requires a unidirectional bulk flow of intracellularly ions (Ca^{2+} and P_i) from the cellular basal part toward efflux sites, near mineralisation zone, where hydroxyapatite crystal nucleation occurs (Lundgren and Linde, 1992). Very little is however known about this intracellular ion translocation within Ods (Linde and Lundgren, 1995). Studies reported that the Ca^{2+} activity in predentine was three times higher its concentration than in pulp extracellular fluid. This reflects their concentration across Od layer within mineralisation front (Lundgren *et al.*, 1992). The extrusion of Ca^{2+} and P_i ions and formation of calcified nodules was also reported to be dependent on Na^+ ions concentration through Na/Ca exchanger and Na/P_i cotransporter respectively (Lundquist *et al.*, 2002). Additionally, the expression of presence of NCX1 and NCX3 were reported to play an active role in the extrusion system and unidirectional transport pathway of Ca^{2+} within Ods (Tsumura *et al.*, 2010). This supports the detected high expression of the NaK-ATPase within OPs during primary dentinogenesis in the current study, which suggest the role of Na^+ pumping enzyme in mineralising ion translocation. Other possible ions extrusion pathway which could be suggested is through membrane vesicles by the activity of Ca^+-ATPase which reported to concentrate Ca^+ within these vesicles at the apical region of the Ods to be exported near the mineralisation front (Granström, 1984; Lundgren and Linde, 1987).

On the other hand, the presence of NaK-ATPase as an active Na pumping enzyme is also required to maintain other cellular requirements such as, intracellular pH (Therien and Blostein, 2000) (see group II, image A, Figure 5.35). This can be achieved through its correlation with the pH regulating ion transporters including NHE-1. The latter has been recorded in the current study within Od cell bodies and initial region of the OPs during primary dentinogenesis (see B Figure 5.34). There is another pH regulating Na dependent ion transporter which can be suggested such as Na/HCO_3 cotransporter (NBCe1) which plays a pivotal role in enamel and bone

development (Riihonen *et al.*, 2010; Jalali *et al.*, 2014). The coordination between NaK-ATPase and this group of transporter is possibly instrumental to keep Od cellular vitality during primary dentinogensis. Additionally, they could also be the main transporter which regulates the pH within predentine region. This pH was measured to be around 7 (Lundgren *et al.*, 1992), which is possibly essential to allow crystal nucleation and development at the mineralisation front. Furthermore, the presence of different K^+ channels was also reported to be present within Od (Allard *et al.*, 2000; Magloire *et al.*, 2003). The K-channels could be the way to efflux excess of intracellular K^+ that could be accumulated during NaK-ATPase action.

The other region within dental pulp which expresses high NaK-ATPase activity during primary dentinogenesis, even higher than Ods, is the SOd cells (image B Figure 5.34). The physiology that could be probed by the NaK-ATPase within Ods is by the possible role of Na^+ in mineral translocation and hydroxyapatite crystal formation at the dentine mineralisation front. But this is not the case for the SOd region. These cells have the highest NaK-ATPase, and they are the closest to the feeding capillaries during this stage of dentine formation (Ohshima and Yoshida, 1992). The Ods are connected to each other by junctional complexes which keep other cells of the pulp separated from dentine and limited minerals translocation just intracellularly within Ods (Linde and Lundgren, 1995). However, studies showed that the functional barrier between developing rat Ods appeared between 15-28 days, which means that these junctions were permeable prior to this time (Turner *et al.*, 1989). Therefore, the SOd cells could play a role during this stage of dentine formation, yet this is still unclear. But, an indicator of what SOd cells might be doing, is possibly gleaned from its cellular changes during trauma time which will be raised later.

Secondary dentinogenesis

As noted previously, after tooth eruption the activity of dentine formation by the Ods is dramatically reduced. These cells change to be dentine maintaining and sensing cells, rather than their previous function before tooth eruption (Magloire *et al.*, 2009; Femiano *et al.*, 2014). This is also manifested in the structural changes that occur within Ods and OPs (Figure 5.31) (for more details see section ‘Non-trauma regions:‘). The differences in the expression of NaK-ATPase appeared minimum in comparison to the changes occurred for NHE-1 within Ods and OPs after tooth eruption (Figure 5.34). The coordination between these ion transporters during this stage could be by their homeostatic function in maintaining cellular vitality, in addition

to their suggested role in Ca^{2+} translocation during secondary dentinogenesis. However, the reason behind chronological increasing activity for these two homeostatic markers especially NHE-1 is not yet clarified. The processes of dentine formation require specific pH value (7), to allow nucleation and development of hydroxyapatite crystals (Lundgren *et al.*, 1992). The reduction in pH possibly reduces this process and enhances dentine demineralisation (Marshall *et al.*, 1997). Changes in pH were also detected during enamel formation, which was associated with the process of cyclical changes of the ameloblasts from ruffle to smooth border cells at maturation stage (Josephsen *et al.*, 2010). During the ruffled border phase, the pH drops to be about 6 in front of these cells within enamel mineralisation region. This could allow dissolving of the enamel organic matrix and reduction of the crystal growth, which could facilitate removal of the dissolved matrix during smooth border ameloblasts when the pH returns to 7 at that stage (Sasaki *et al.*, 1991; Josephsen *et al.*, 2010). Alteration in pH also occurs in association with the bone remodelling process, by the function of osteoclast cells. These cells release more H^+ to reduce the pH value at the interface between the cell and the bone. This possibly facilitates dissolving organic matrix, and aids bone demineralisation (Rousselle and Heymann, 2002). Therefore, the increase in NHE-1 expression within Od in this stage possibly caused an increase in the concentration of H^+ within predentine region. The H^+ within Ods could be obtained from the decomposition of the carbonic or phosphoric acids intracellularly according to the following equations (Silverthorn *et al.*, 2007):

$$H_2CO_3 \leftrightarrow H^+ + HCO_3^-$$

$$H_2PO^-_4 \leftrightarrow H^+ + HPO_4^{2-}$$

This released H^+ is possibly to control pH value (Josephsen *et al.*, 2010), which in turn controls the rate of dentine mineralisation. Decreasing pH to a certain limit possibly causes delay in the time of mineral growth and development (Linde and Goldberg, 1993). This could be associated with reduction in the Ods synthesis ability for the organic matrix of the dentine and changing from secretory to mature cells (Couve, 1986). As a result, the rate of dentine formation is dramatically reduced during secondary dentinogenesis (Tjäderhane *et al.*, 2012).

Similarly, the detected expression of the NHE-1 in the OPs especially the outer region could also be for pH control within intratubular fluid (image B Figure 5.35). It was reported that the dentinal fluid is quite similar in its ion concentrations to the

plasma and interstitial fluid (Haldi *et al.*, 1961; Coffey *et al.*, 1970). This means that it contains high Ca^{2+} and P_i ion concentrations, which could enhance crystal formation and cause obliteration of the dentinal tubules. However, the dentinal tubules remain open, except for some regions where sclerosis of dentinal tubules occurs. This is possibly associated with dentine hypersensitivity (Stanley *et al.*, 1983; Yoshiyama *et al.*, 1989; Mjör and Nordahl, 1996). The possible controlling feature for the continuous crystal formation within this region to prevent tubule obliteration could be by controlling pH. This possibly occurs by the release of H^+ to the intratubular fluid by the function of NHE associated with NaK-ATPase in the OPs. Additionally, this suggests continuous remodelling of the dentinal tubules, which could also reflect the source for high concentration of Ca^{2+} and P_i within the intradentinal fluid according to the following equation:

$$10Ca(OH)_2 + 6H_3PO4 \leftrightarrow Ca_{10}(PO4)_6(OH)_2 + 18H_2O$$

Unfortunately, there is no record in previous studies of the pH within the intratubular fluid. This could be suggested as a further study to support our hypothesis. Therefore, the presence of both NaK-ATPase and NHE after tooth eruption, could suggest the dynamic cellular controlling role of dentine remodelling performed by the Ods and OPs.

Trauma region

The major tissue alteration which happened during the period of occlusal attrition was the loss of the junctional contacts between Od cells (image C, Figure 5.35). Studies reported the presence of a macromolecular tracer between traumatised Ods and within predentine and reparative dentine beyond the trauma site (Turner *et al.*, 1989). This means that due to the trauma effect, the Od layer became more permeable extracellularly to the passage of reparative macromolecules and ions to perform tissue repair (Turner, 1992). This also could be the case for the extracellular transportation of the mineralisation ions during this stage of trauma response of the pulp which provides rapid diffusion of these ions. This probably aid in fast mineralisation of the atubular dentine matrix plug. Although traumatised Ods still expressed NaK-ATPase during this time, the SOds beyond them were the highest labelled cells within the trauma region. The rich vasculature and massive abundance of NaK-ATPase within SOd cells suggest that their active Na^+ ions pumping possibly play a pivotal role in reparative dentine plug formation during this stage. This was

associated with the increase in packing of SOd cells between each other, and their actin been highly expressed during this period. This probably aided in the unidirectional guiding of the ions, to be directed towards the repair zone. Following this lead, during trauma time the role of SOds can be hypothesised to maintain a negative cell potential and electrochemical Na^+ gradient which is possibly required for the extracellular translocation of the mineralisation ions. This coupling between cytosol can be mediated by the presence of massive CGRP innervation which connected cells and dilated capillaries within SOd region. Unfortunately, the inadequate data about the ion transportation mechanism during trauma time from previous studies, impaired further speculation within the model suggested by the current study.

Another important parameter that should be considered within this model is the pH value. The extracellular space between pulp cells within trauma time became connected to the predentine zone above the Ods. In addition, high Ca^{2+} and P_i ion transportation is expected to be present between the cells. The possibility of crystal nucleation behind the Ods became valid if the pH within this region remained neutral. Therefore, in a homeostasis model of this study (image C Figure 5.35), we suggested that to prevent this abnormal crystal formation, the pH of the extracellular fluid between the pulp cells should be controlled to be more acidic, to prevent mineral nucleation within this region. This was built on the SOds expression of NHE within this stage (image D Figure 5.34). This could cause a release of H^+ ions within extracellular fluid to decrease pH, to limit abnormal or pathological crystallisation. Additionally, the fact that pulp could deposit calcified tissue behind the Ods cells is also recorded, by formation of pulp stones, which is still a physiologically little-understood mechanism (Goga *et al.*, 2008). The organic matrix of these stones were shown to be consisted mainly of collagen type I and osteopontin (Ninomiya *et al.*, 2001), and the latter has been commonly found within pathological calcifications induced by pulp fibroblasts in case of reparative dentine (Cajazeira Aguiar and Arana-Chavez, 2007), also in other organ pathological conditions such as urinary stones (Kohri *et al.*, 1993). Therefore, in order to control ion passage and normal crystallisation growth within the predentine region, the present model suggested that the pH control could be the main key that should be considered.

According to this hypothesis, the role of high pH, pulp treatment cements and their mechanism of action in enhancing the calcified dentine formation can be understood.

All the pulp medication applied during direct and indirect pulp capping such as calcium hydroxide, MTA, biodentine and hydraulic calcium silicate cement are alkaline material with pH value more than 9 (Darvell and Wu, 2011; Grech *et al.*, 2013; Rajasekharan *et al.*, 2014). Effect of alkaline pulp treatment during direct and indirect pulp capping is not totally understood and always linked to antimicrobial nature of high pH material (Sipert *et al.*, 2005). None of the previous research employed this high pH in the direct physiological stimulation of the pulp to produce the mineralised matrix. This alkaline treatment could act as a promotor by providing the alkaline environment for the mineralised tissue to be deposited at the pulp border. In the same way, they could act as a director for the pulp cells to deposit their mineralised product toward the high alkaline side of the restoration.

After the effect of trauma subsided, the reestablishment of the apical junction of the Ods and appearance of secondary OPs (image E Figure 5.34) were definitely associated with reorganisation of the mineralisation front and reformation of new dentinal tubules. This suggests returning of the normal ion transportation and dentine calcification which was suggested within this hypothesis (images A and B Figure 5.35).

5.5 Conclusions

As a summary, this model of the rat molar offered important advantages to study different stages of normal tooth development and the pathological and repair processes associated with wear trauma (Figure 5.36). Linking data and results obtained from different structural, cell division, growth factor, nerve and ion transporter markers, helped to provide better understanding about cellular processes within intact and injured dental tissue. It also helped to link this information with that already present in the field, to hypothesise a homeostatic model which could improve the knowledge regarding some well-known dental mysteries.

Several detectable cellular changes have been identified during normal tooth growth. These include the period of cytodifferentiation in the early developmental stages, followed by tooth eruption time, maturation period and ageing process. The first change was associated with structural reorganisation of the cellular cytoskeleton, which could be mediated by the presence of an autocrine or paracrine induction mechanism. This probably caused withdrawal of the Ods from cell division cycle, into specialised secretory cells. Following this was the primary dentinogenesis period,

including hard tissue deposition, development of the OPs and formation of the dentinal tubules. This was associated with activation of the ion transporting mechanism to deliver mineral ions at the cellular mineralisation front. This process could also be self-mediated, by the secretory and other pulp cells, with the absence of neuronal intervention. This was followed by tooth eruption after complete crown formation and commencement of root development. The crown Ods showed major morphological and cytoskeletal alteration as they changed from secretory into maintaining cells. This change was associated with sensory nerve invasion, probably by a continuous cellular mediating process. Additionally, another ion transporter (NHE) became apparent within Od and OPs possibly to control dentine formation by managing extracellular pH. This was followed by complete nerve growth which was associated with the completion of root formation and the tooth maturation period. Changes in pulp space and varied cellular responses to the markers used, were obviously detected in tooth ageing samples.

The trauma model represented by the tooth wear process also showed different cellular changes starting with early protection alterations and ending with tissue repair and regeneration. In the initial trauma responses, both cellular and neuronal changes were obtained and mediated other cellular modifications, to decrease trauma invasion and localise the effect of the trauma insult. This was associated with the appearance of the role of the SOd cells which showed various structural and functional alterations. These aimed to decrease damage and facilitate passages of the repairing material to the injured Ods and region above. This caused formation of an atubular plug for the exposed dentinal tubules, to provide a protected environment for the established repair mechanism. These features possibly aided in damaged tissue repair and reestablishment of the new tubular dentine.

Therefore, the advantages obtained from this model are expected to give new and valuable insights to improve dental knowledge about normal tooth development in addition to pathological responses associated with the trauma of tooth wear.

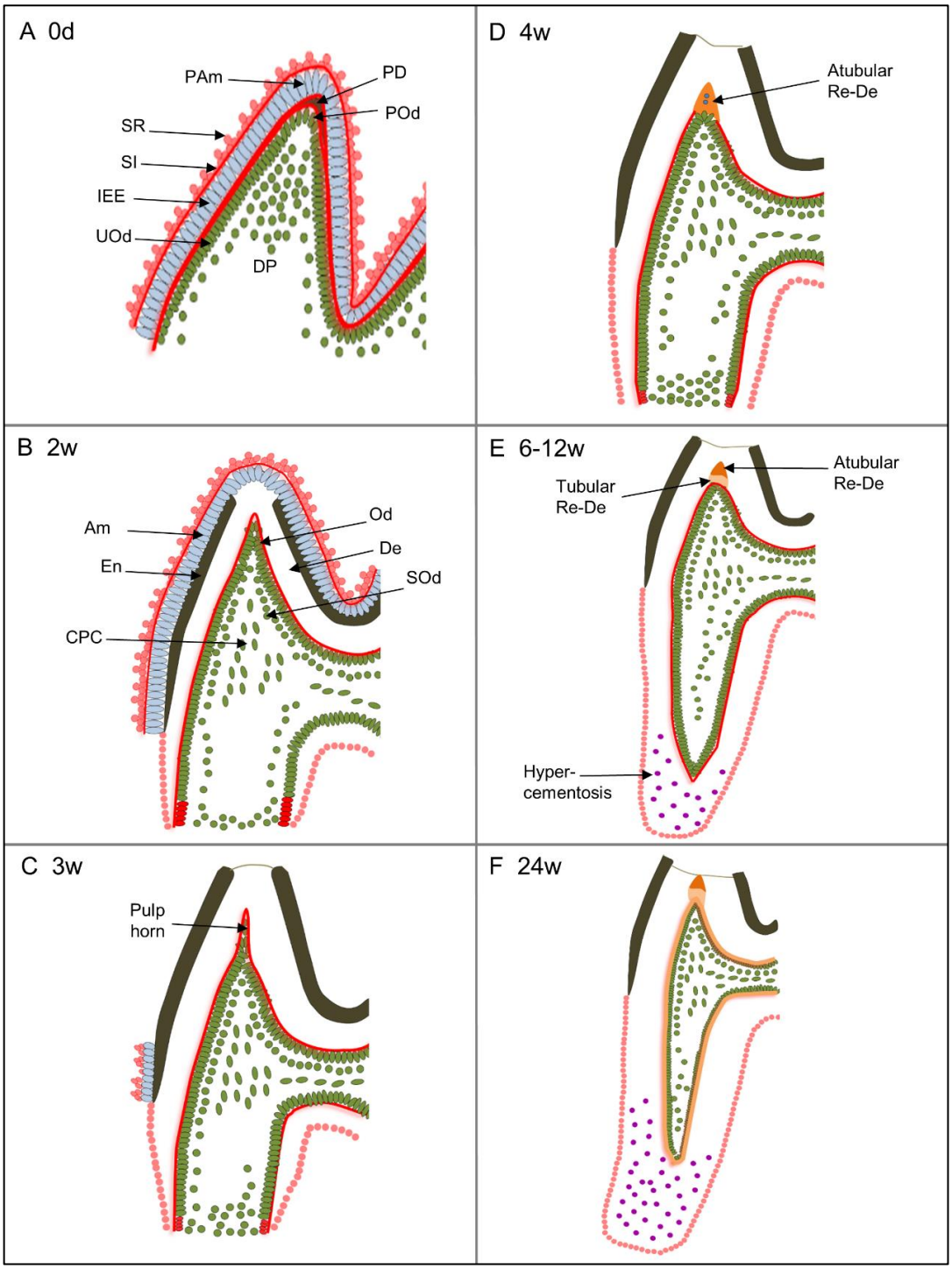

Figure 5.30: Illustration of the saggital section for the mesial side of the rat mandibular 1st molar for the different age groups within current study.
Following structures have been identified: pre-ameloblast (Pam), predentine (PD), pre-odontoblast (POd), stratum intermedium (SI), stellate reticulum (SR), inner enamel epithelium (IEE), undifferntiated odontoblast (UOd), dental papilla (DP), odontoblast (Od), subodontoblast (SOd), central pulp cells (CPC), enamel (En),and dentine (De). Two images A and B represented the crown developmental stages, C is the tooth eruption age (3w), D is the wear start age (4w), E shows the ages of tooth repair process (6-12w) and F is the older age group (24w).

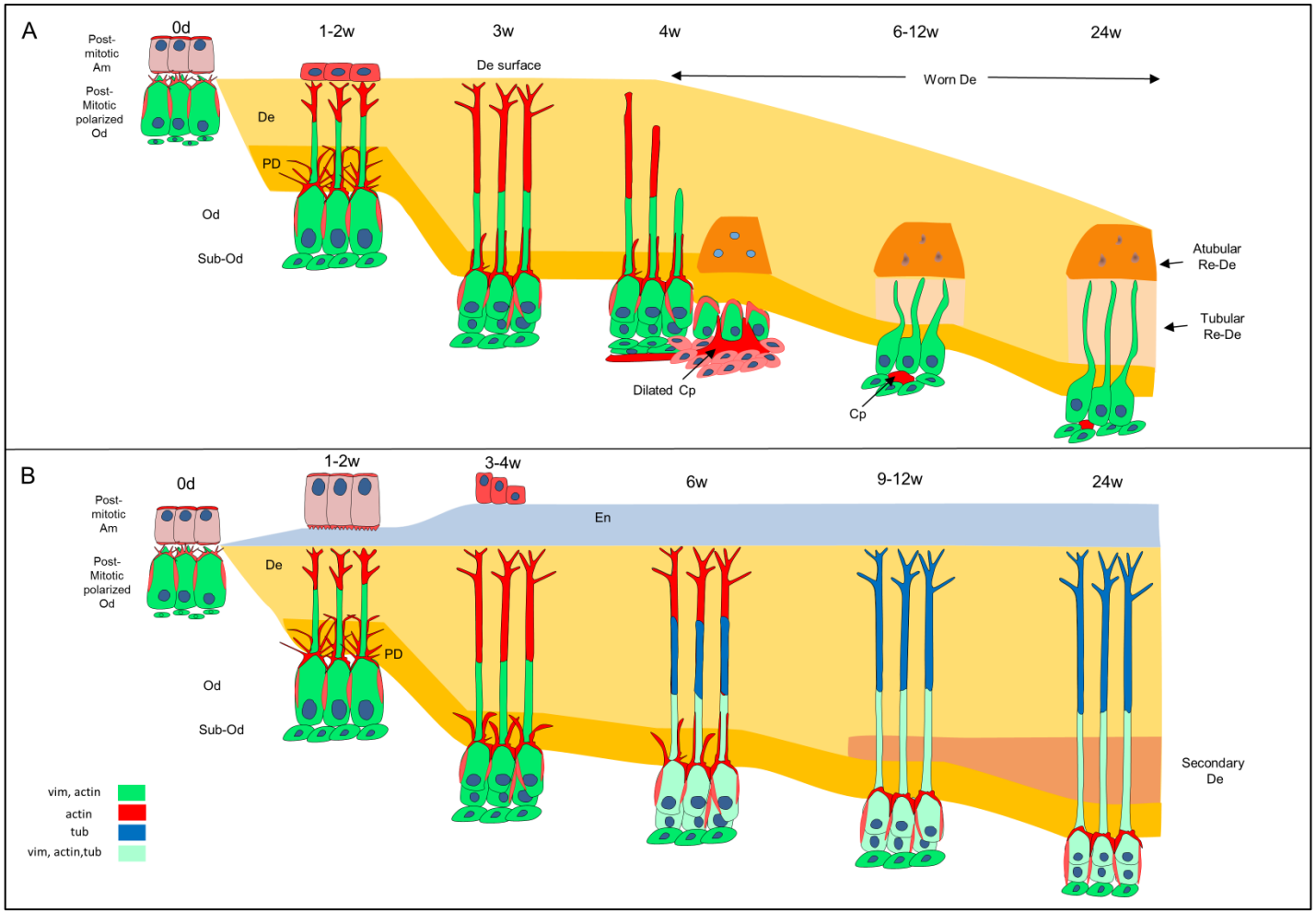

Figure 5.31: Schematic illustration of the Od, OPs and SOd cellular structural changes within different age groups of the current study. A represents the worn cusp surface, and B illustrates the other unworn dentine surfaces within tooth crown. Time line started from 0d to 24w to show the structural changes occurred within pulp celles morphology and responses to different structural marker including vimentin, actin, and tubuluin.

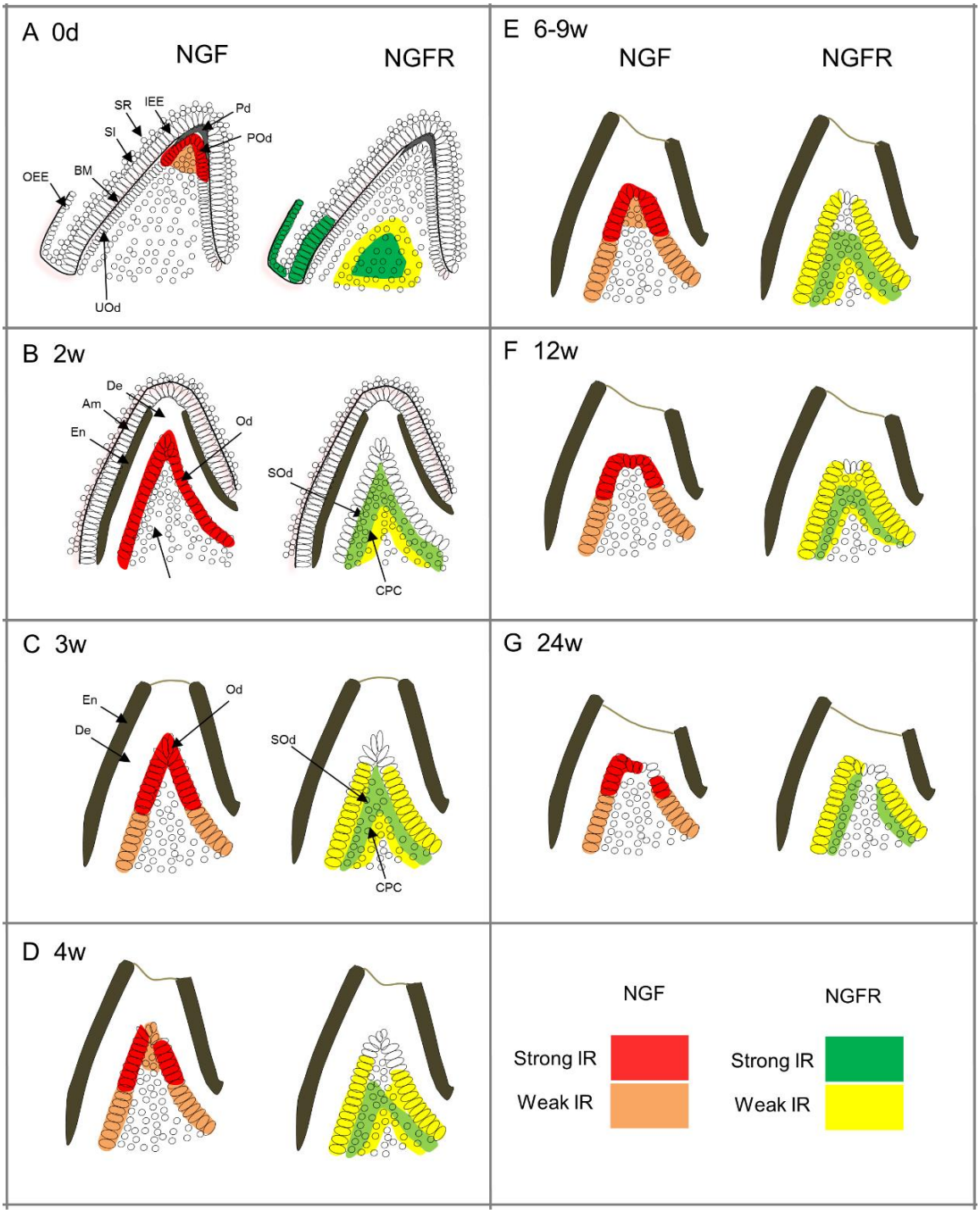

Figure 5.32: Schematic representation of NGF and NGFR immunoreactivities within all study groups.
Following structures have been identified: predentine (PD), pre-odontoblast (POd), stratum intermedium (SI), stellate reticulum (SR), inner enamel epithelium (IEE), undifferentiated odontoblast (UOd), outer enamel epithelium (OEE), odontoblast (Od), subodontoblast (SOd), central pulp cells (CPC), enamel (En), and dentine (De). Each image shows two drawings to identify the NGF and NGFR immunoreactivities respectively, which could be either strong or weak IR. Different panels represent different ages.

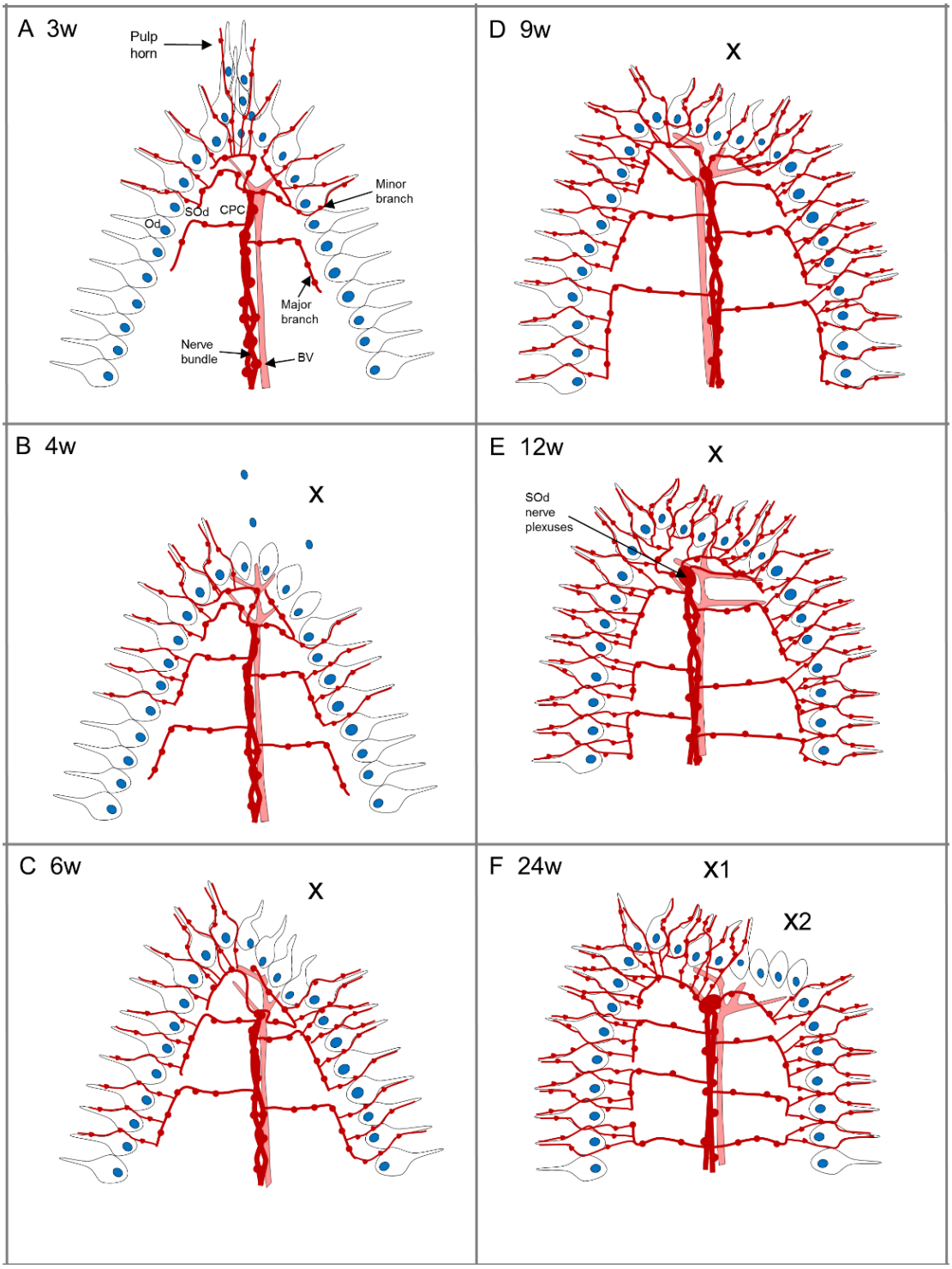

Figure 5.33: Schematic representation for the CGRP-IR nerve disribution within different groups of the current study.
The following structures have been identified: odontoblasts (Od), sub-odontoblast (SOd), central pulp cells (CPC), blood vessels (BV), and the region of wear trauma (×). CGRP nerves are represented by dotted red lines with different thickness depending on their position within the pulp. Additionally, the associated blood vessels are also represented within each figure. Different panels represent different ages.

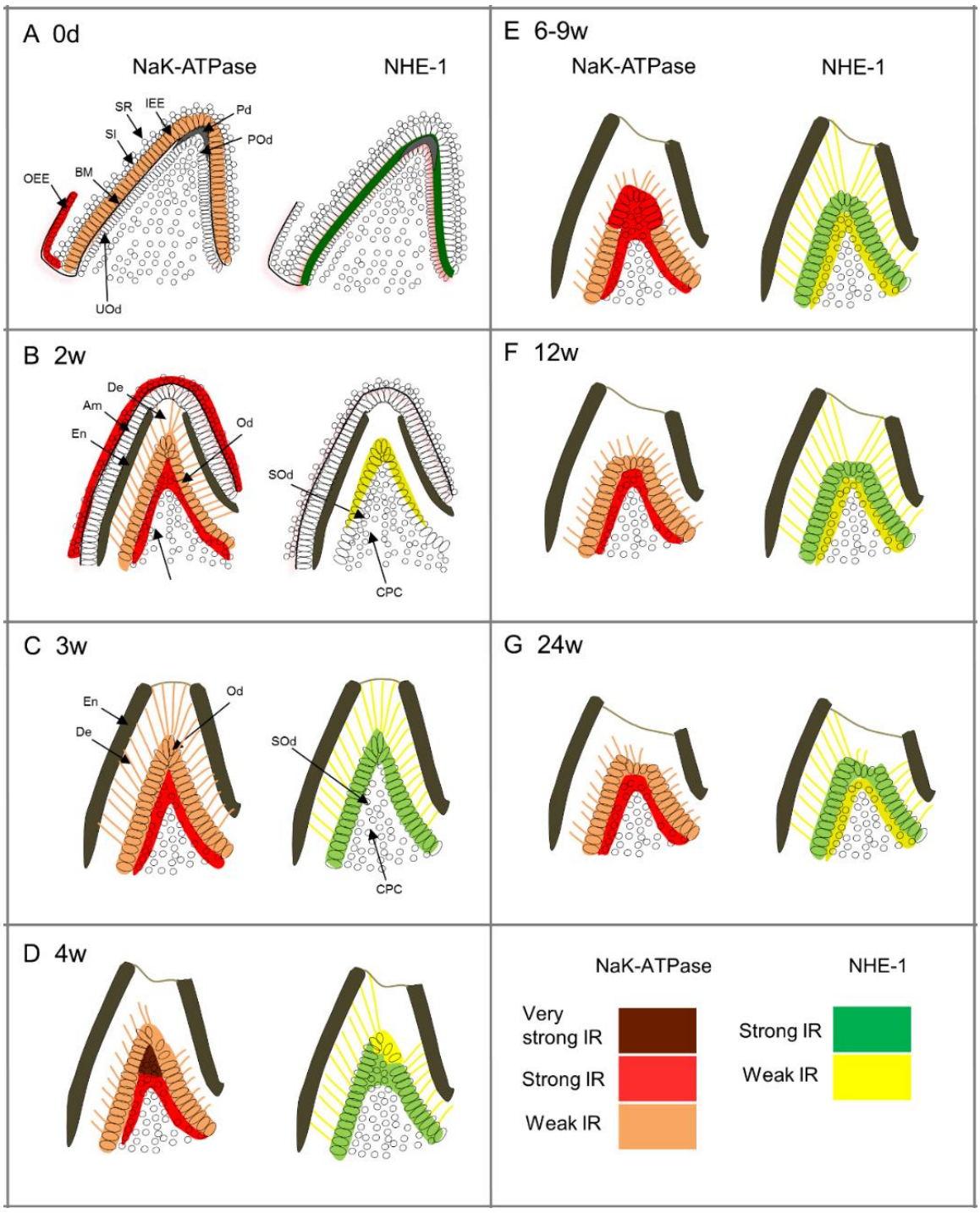

Figure 5.34: Schematic representation of NaK-ATPase and NHE-1 immunoreactivities within all study groups.
Following structures have been identified: predentine (PD), pre-odontoblast (POd), stratum intermedium (SI), stellate reticulum (SR), inner enamel epithelium (IEE), un-differntiated odontoblast (UOd), outer enamel epithelium (OEE), odontoblast (Od), subodontoblast (SOd), central pulp cells (CPC), enamel (En), and dentine (De). Each image shows two drawings to identify the NaK-ATPase and NHE immunoreactivities respectively, which could be either very strong, strong or weak IR. Different ages are shown in different panels.

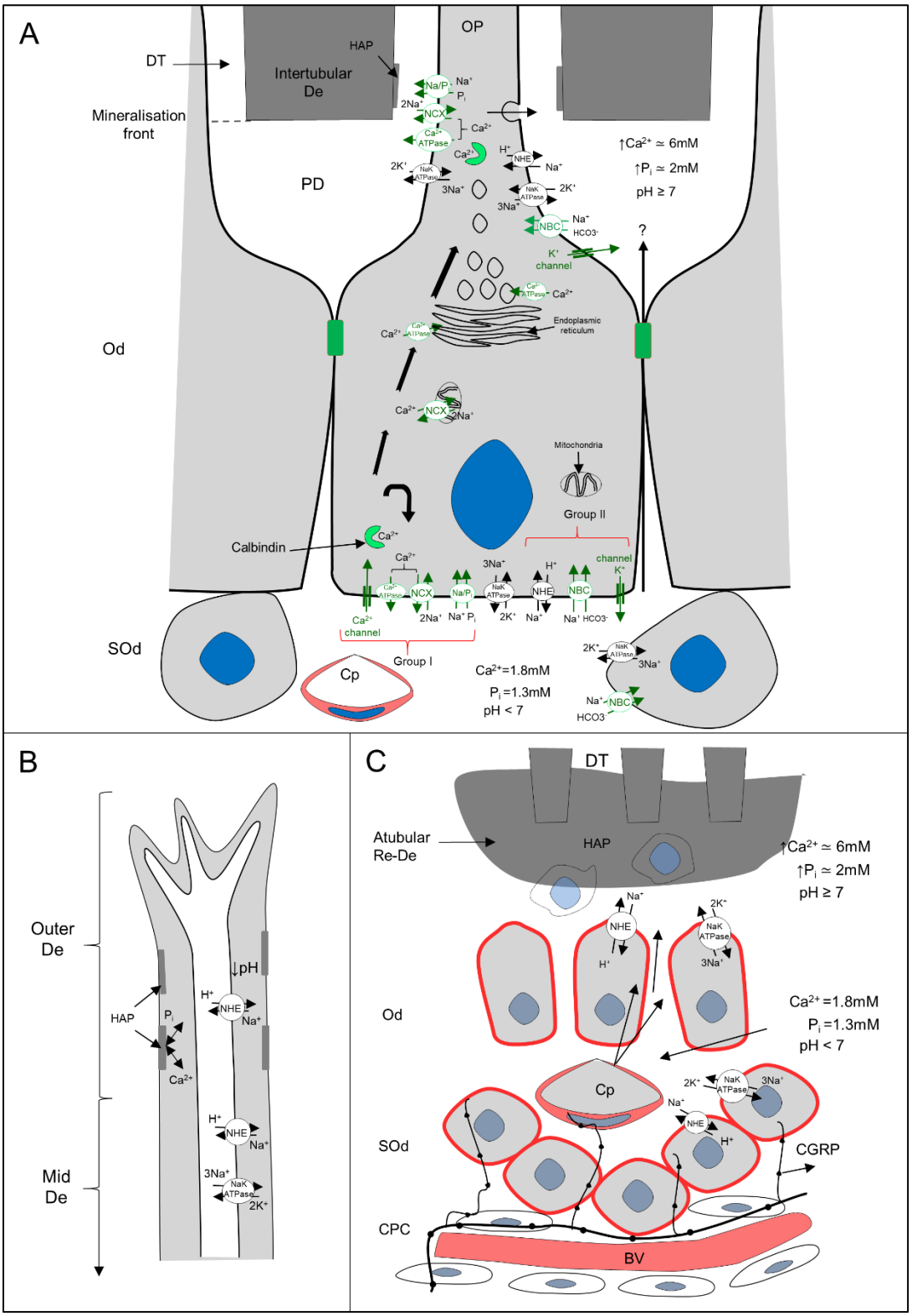
A
DT
HAP
Intertubular De
OP
Mineralisation front
PD
Od
SOd
Calbindin
Mitochondria
Group II
Group I
Cp
Endoplasmic reticulum
K+ channel
Ca2+ channel
↑Ca2+ ≃ 6mM
↑Pi ≃ 2mM
pH ≥ 7
?
Ca2+=1.8mM
Pi=1.3mM
pH < 7
B
Outer De
Mid De
HAP
↓pH
C
DT
Atubular Re-De
HAP
Od
SOd
Cp
CPC
BV
CGRP
↑Ca2+ ≃ 6mM
↑Pi ≃ 2mM
pH ≥ 7
Ca2+=1.8mM
Pi=1.3mM
pH < 7

Figure 5.35: Homeostatic and ion transporter illustration representing the hypothesis of this study according to different stages of dentine formation.
A primary dentinogenesis, B odontoblast process in secondary dentiongenesis, and C is ion transportation during early trauma period. The following structures have been identified: (OP) odontoblast process, (DT) dentinal tubule, (PD) predentine, (JC) junction complex, (Od) odontoblast, (SOd) subodontoblast, (Cp) capillary, (De) dentine, (CPC) central pulp cells and (HAP) hydroxyapatite. The black ion transporters represent those observed within this study while the green identify those cited from published papers. A) shows transcellular translocation of Ca^{2+} ions via Od cell layer from pulp capillaries to the mineralisation front, however the intercellular route can also be suggested (long arrow with question mark). Two groups of ion transporter have been shown: group I including mineral ions related transporter and group II contains other homeostatic ion transporter mainly dealing with controlling pH. Group I shows Ca^{2+}influx through Ca channel. To maintain cytosolic Ca^{2+} concentration, Ca^{2+} either bind to transferring protein such as calbindin or possibly using membrane ATP-dependant (Ca-ATPase) and Na/Ca exchanger used for extruding the excess of Ca^{2+}. Na/P_i cotransporter use for transcellular transportation for P_i. Cellular transferring for both Ca^{2+} and P_i cause increase intracellular Na^+ which activate NaK-ATPase to remove excess Na^+. Cellular organelles take part in buffering the activity of cytosolic Ca^{2+}. Mitochondria use Na/Ca exchanger, while endoplasmic reticulum using Ca^{2+}-ATPase. Intravesicular Ca-ATPase is also used to accumulate Ca^{2+} within intracellular vesicles to obtain controlled transportation toward mineralisation front. The efflux of Ca^{2+} is suggested by Ca-ATPase and NCX which also requires membrane Na^+ gradient to extrude Ca^{2+}. Another Ca^{2+} extrusion route could be via membrane vesicle exocytosis. The Na/P_i cotransporter is also proposed near mineralisation front to extrude Pi. Group II shows possible role of Na/H exchanger (NHE) and Na/HCO_3 cotransporter in controlling intracellular and extracellular pH. This process also required NaK-ATPase to regenerate membrane Na^+ ion gradient and K-channels required to balance the concentration of intracellular K^+. The pH suggested within this hypothesis should be less than 7 within the extracellular fluid between the Ods and SOds to prevent crystal development behind the Ods. Whilst the pH at the mineralisation front should be equal or may be more that 7 to enhance crystal formation and growth. Panel B shows the possible function of the detected ion transporter (NaK-ATPase and NHE) in decreasing the pH of intratubular fluid to control the apposition of hydroxyapatite during secondary dentinogenesis. Panel C illustrates the proposed early trauma extracellular ion transportation mechanism due to loss of cellular junctional contacts between Ods. The role of detected NaK-ATPase and NHE ion transporters was shown to be the key factor in controlling extracellular pH in front and behind the traumatised Ods.

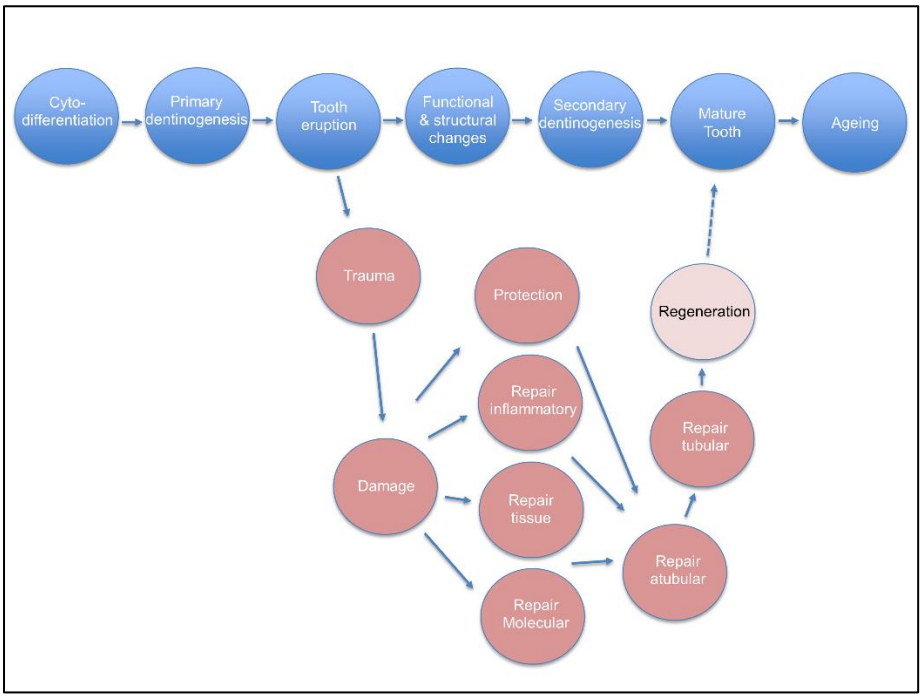

Figure 5.36: Flow diagram to summarise normal and pathological processes within the study model (rat molar).
The blue circles represent the normal tooth flow process, while the red circles illustrate the cellular processes occurring within trauma and tooth repair.

Chapter 6 **Exploration of early gene activation or inactivation in the re-modelling of the pulp after trauma**

6.1 Introduction

The dentine-pulp complex shows a great similarity to other connective tissues within the body. However, it has considerable complexity and several unparalleled features, due to its enclosure within the hard and non-compliant shell of the tooth in all directions except the small apical foramen (Tjäderhane *et al.*, 2012). This encirclement may limit the pulps' inflammatory and reparative ability to neutralise and recover from different injuries. This represents the most obvious challenge facing the dental pulp, as it faces the onslaught of injuries including acute trauma, tooth wear, dental caries, and operative dental surgery.

The tooth crown within the oral cavity environment, is covered by symbiotic harmless microbial communities which are mainly composed of Gram-positive bacteria. These communities normally adhere to the highly mineralised enamel surface in a form of biofilm. A high sugar environment within this biofilm enhances bacterial acid production, which leads to tooth surface demineralisation and the formation of dental caries (Farges *et al.*, 2015). After disruption of the tooth enamel barrier, lesions progress into dentine, with tissue degradation. During this phase, Gram-positive bacteria compose about 70% of the recoverable microflora (Bjørndal and Larsen, 2000). This percentage changes as the lesion advances and becomes deeper, providing a perfect habitat for the survival and proliferation of Gram-negative bacteria (Love and Jenkinson, 2002). The major pathogenic component for these bacteria is endotoxin, or lipopolysaccharide (LPS), which is reported to be involved in pulpitis (Martin *et al.*, 2002) following direct invasion of the dental pulp through patent dentinal tubules (Love and Jenkinson, 2002; Chung *et al.*, 2011). In a previous study of Alhelal (2016), it was determined that a short incubation (3h) of rat incisor pulp tissue in LPS-treated media significantly activated specific pro-inflammatory and anti-inflammatory genes. LPS was also reported to promote differentiation of cultured dental pulp stem cells and to enhance formation of calcified nodules after 2w incubation (He *et al.*, 2015). Other studies have shown that LPS suppressed the transformation of cultured pulp stem cells into Od-like cells by inhibiting alkaline phosphatase, dentine sialophosphoprotein, and restricting mineralised nodule

formation (Nomiyama *et al.*, 2007). LPS-specific binding receptors (TLR-4) have been reported to be present within the odontoblast cell membrane (Botero *et al.*, 2006). It is logical to think that treatment of pulp tissue with LPS can be recognised by host defence systems through interaction with its specific receptors, which could indirectly stimulate structural and homeostatic genes within stimulated pulp tissue.

Cellular degradation is a possible effect of pulp injury caused by different harmful stimuli including caries and trauma (Mitsiadis *et al.*, 2008). This causes release of cytosolic ATP to the extracellular fluids (Liu *et al.*, 2012). Extracellular ATP is reported to serve as a vital signalling molecule, especially in injured tissue through its function on ATP receptors (purinoceptors) (Alavi *et al.*, 2001). These receptors were found to be expressed by the odontoblast cell membrane and nociceptive pulp nerves, which suggests the role of ATP in the mechanism of dental pain (Alavi *et al.*, 2001; Cook and McCleskey, 2002). Additionally, ATP causes changes to cyclooxygenase level within injured tissue, which suggests its indirect effect on tissue inflammatory responses (Alhelal, 2016). However, none of the previous studies identify its possible effect on housekeeping genes including cytoskeletal and ion transporters.

In Ch 5, we used IHC to study different housekeeping markers within rat dental pulp, which included structural markers (α-actin and α-tub), and ion transporter markers (NaK-ATPase and NHE-1). During IHC work, the sample preparation, demineralisation, and staining procedures were very time consuming. This limited the use of other markers because of specimen depletion and time required for preparing new samples. Also, the high cost for each antibody marker had to be considered. It now becomes necessary to develop a simpler technique which requires less time and allows us to scan for different homeostatic genes within the same sample. The molecular techniques including end-point polymerase chain reaction (PCR) and quantitative reverse transcription polymerase chain reaction (qRT-PCR) were chosen as complementary techniques in this work. Therefore, the aims for this work were as follows:

- To employ molecular techniques to identify the expression of key cellular and signalling elements that have been identified using IHC techniques in pulp tissue, in addition to other related elements.
- To explore the idea that damage could cause an active change of gene expression immediately after pulp removal from the tooth and during incubation in media for up to three hours.
- To explore the possibility that LPS and ATP could alter the expression of targeted genes after short incubation periods.

6.2 Material and methods

Methods and materials were described in detail in section (2.6.). The work was divided into three experiments as follows:

6.2.1 Effect of incubation time on gene expression (Table 2.7)

Fifteen male Wistar rats (age= 9 weeks, weight 260-400 G) were killed in a CO_2 chamber before surgically extracting only right mandibular incisor teeth. The teeth were divided into 3 groups (n=5) as follows:

Group A (control): fresh pulps were carefully extracted as previously described in Ch 2 section 2.1.2. The dissected pulp (average weight = 14.5 mg) was immediately stored in 500 µL RNA stabilization agent (RNAlater, Cat. No. 76106, Qiagen, Germany) at 4ºC.

Group B: the extracted pulp was incubated for one hour in in 500µl DMEM solution supplied with foetal calf serum (1% Sigma) and penicillin-streptomycin (50 IU/ml-µg/ml Sigma) before transfer to 500 µL RNA stabilization agent.

Group C: same as B but with 3h incubation time.

6.2.2 Effect of LPS treatment

Seven male, Wistar rat (age= 9 weeks, weight 260-400 G) were killed as above. For each rat, the left mandibular incisor was assigned for the control and the right for the test group for direct comparison. Fresh pulps were carefully dissected as described previously and divided into control and test groups (n=5). The pulps were incubated in a 12 well plate (one pulp per well contained 500µl of incubation solution mentioned above). For the test group, *Escherichia Coli* serotype 026:B6 LPS (10 µg/ml) (Sigma Aldrich, UK) was added. After three hours of incubation, each pulp tissue was stored in 500µl of RNAlater solution at 4º C.

6.2.3 Effect of ATP treatment

This study was conducted in the same manner as for LPS (above) with ATP analogue 2'(3')-O-(4-benzoylbenzoyl) adenosine-5-triphosphate triethylammonium salt (100 µM) (Sigma Aldrich, UK) added to the incubation media of test samples instead of LPS. Media were renewed every hour, since ATP is known to dissociate over time.

At the end of each experiment, the samples underwent RNA extraction, reverse transcription to cDNA and PCR procedures were accomplished (for more details see 2.6.2 to 2.6.9).

Quality control

Two reference genes were used within this study GAPDH and B-actin. The results obtained from GAPDH were consistent and showed unchanged Ct value in qRT-PCR within all conditions and treatment used. Alternatively, the Ct value for the B-actin was affected similarly to the target genes during different incubation experiments. Therefore, only the GAPDH was considered to be the reference gene during these experiments.

The accuracy of PCR quantification depends on two important parameters: linearity and efficiency (see Appendix B image III). These parameters were measured using double standard curve samples generated by progressive dilution of cDNA samples. For quality control within each run, all samples were tested in duplicate, with the inclusion of internal negatives and positive controls (for more details see 2.6.9). Additionally, the duplicates must be within no more than a half cycle in between, or the whole reading was repeated. The Ct for each gene were normalised with the reference gene Ct to obtain a ΔCt value to be used for the statistical analysis.

The numerical data of the qRT-PCR were analysed by using ANOVA and *post hoc* analysis (Bonferroni test) to compare between groups within different incubation experiments. The unpaired T-test was also used to compare between treated and untreated samples within LPS and ATP treatment experiments. Additionally, fold change views were also prepared for all experiments. This was accomplished depending on the ΔCt values for the target gene in the test group to be normalised with the ΔCt of the same gene within the control group of the same experiment.

Therefore, ΔΔCt = ΔCt (test) – ΔCt (control). The fold change was equivalent to the value obtained from ($2^{-\Delta\Delta Ct}$).

6.3 Results

To determine whether or not the target genes were expressed in normal animals, conventional PCR technique and gel electrophoresis were used. This revealed that all target genes were present in single bands within correct base pair length (Figure 6.1), while all negatives were blank.

Serial dilution for the reference gene (GAPDH) showed proportional relationship between the intensity of the band and the cDNA template concentration used (Figure 6.2). The negative control showed no band.

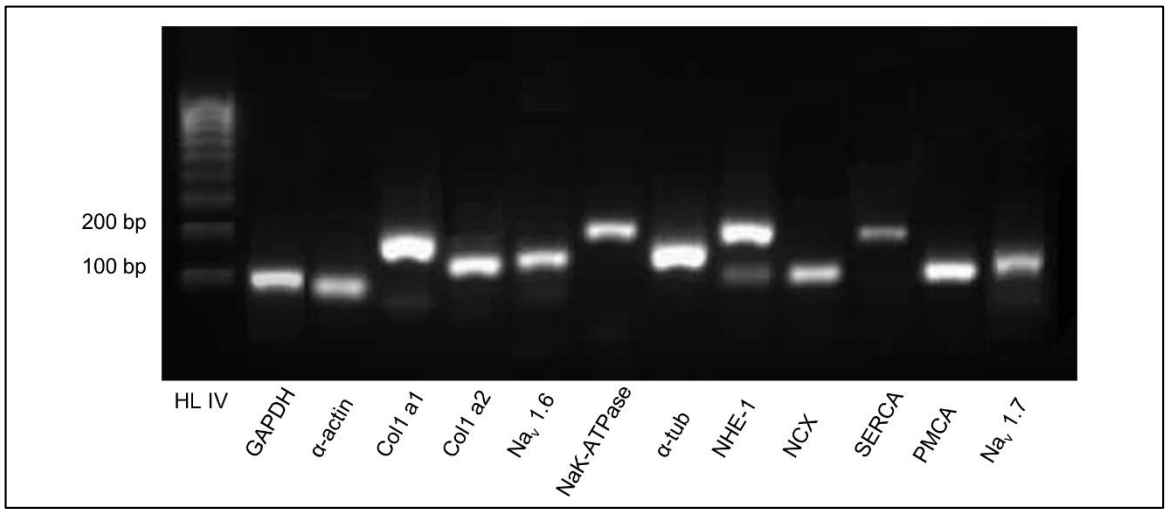

Figure 6.1: Conventional PCR (end point) gel electrophoresis for the genes within this study represented in rat mandibular incisor pulp.
Bands of appropriate base pair (bp) values are shown (as correlated to the hyper ladder IV to the left side) for all target genes. GAPDH was used as a positive internal control. The concentration of the cDNA template was 10ng.

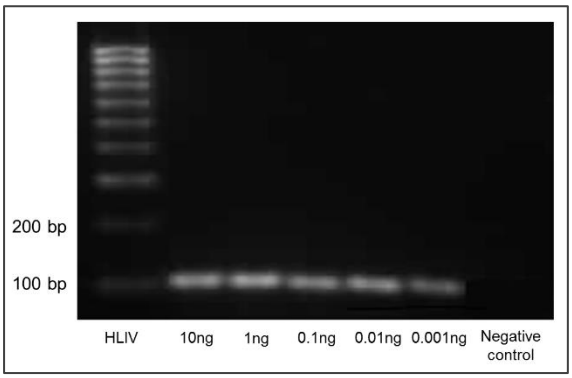

Figure 6.2: Conventional PCR (end point) gel electrophoresis for different concentrations of GAPDH gene.
The intensity of the band decreased when the concentration of the cDNA template decreased, and no band represents the negative control.

6.3.1 Different incubation times

The effects of short incubation time periods on the target genes are shown (Figure 6.3). It shows that the ΔCt values for all targeted genes increase with increasing time of incubation. These changes appear with high statistical significant differences in the following genes: Col1 a1, a2, NaK-ATPase, NHE-1, PMCA and SERCA (Table 6.1). Less significant differences were found in other genes (Na_v 1.7 and 1.6). Additionally, no statistical significant differences were seen in the other genes in comparison to their control groups including: α-actin, α-tub, and NCX-1. The increase in ΔCt value means that these genes were down-regulated with time and this is apparent after normalising their ΔCt values against the control group for each gene (Figure 6.4).

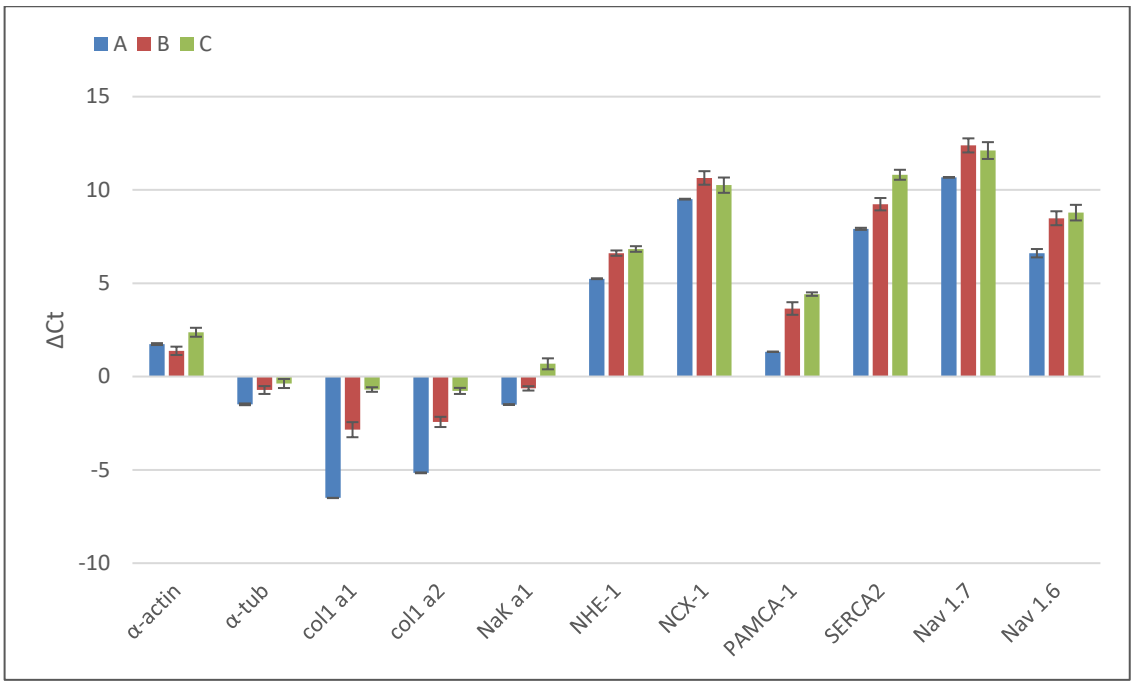

Figure 6.3: qRT-PCR quantification for target genes after different incubation periods. The levels of gene expression were calculated after normalising with the Ct value of the positive control (GAPDH) and presented in relative ΔCt for mRNA expression units of each gene. ΔCt are inversely proportional to the actual mRNA expression. Values are means of ΔCt ± standard error (SE) (n=5). The values of ΔCt for α-tub, col1 a1,a2, and NaK-ATPase are shown in the negative side of the x-axis because their actual mRNA concentrations were higher than the reference gene (GAPDH) within the pulp. This means that their Ct values are less than those of the reference gene.

Groups		α-actin	α-tub	Col1a1	Col1a2	NaK-ATPase	NHE-1	NCX-1	PMCA	SERCA	Na_v 1.7	Na_v 1.6
A	**B**	NS	NS	***	***	*	***	NS	***	**	*	*
	C	NS	**	***	***	***	***	NS	***	***	NS	**
B	**C**	*	NS	***	***	***	NS	NS	NS	**	NS	NS

Table 6.1: ANOVA and Bonferroni post hoc analysis to compare between groups for each gene and their response to trauma and incubation period.
*(A) without incubation, (B) 1h incubation, and (C) 3h incubation. NS is $p>0.05$, * is $p< 0.05$, ** is $p< 0.01$, *** is $p< 0.001$.*

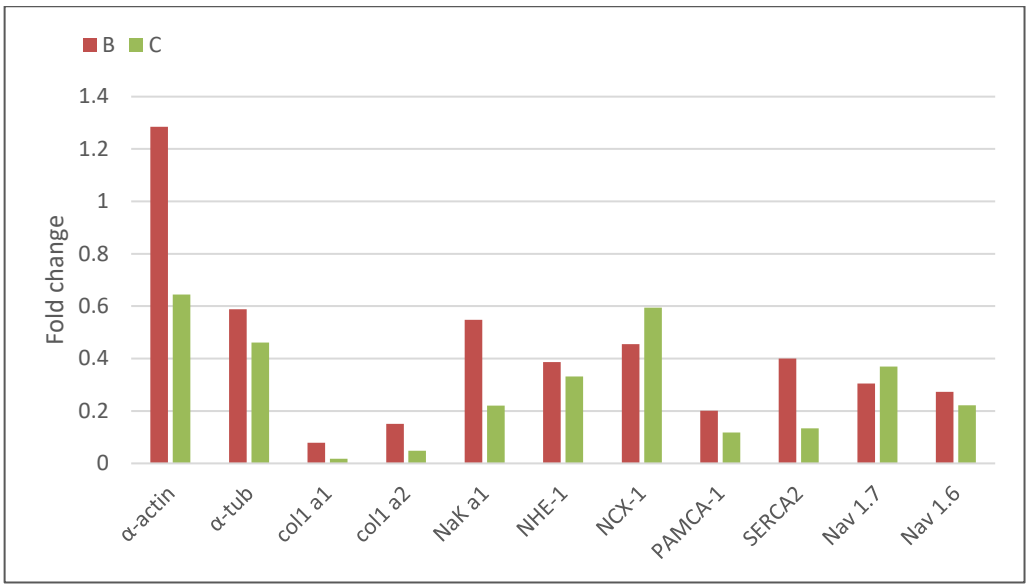

Figure 6.4: Fold change representative values after normalising ΔCt for each gene in groups with incubation periods against ΔCt of group A (without incubation group) for the same gene. The fold change can be calculated according to the formula = $2^{-\Delta\Delta Ct}$.

6.3.2 Treatment with LPS and ATP

Neither LPS nor ATP treatment showed remarkable effects on the target genes within this study (Figure 6.5 and Figure 6.7). No statistical significant difference was obtained between the treated and untreated groups for both treatments except NaK-ATPase which showed a statistically significant difference at $p<0.05$ after treatment with ATP (Figure 6.7).

Additionally, minor fold change values were obtained after normalising the treated ΔCt against untreated values for all genes in both treatments. The highest upregulated gene after LPS treatment was Na_v 1.6 which showed more than 2 fold-change. The greatest down-regulation was for Na_v 1.7 gene. After in ATP treatment, the highest upregulated gene was the NaK-ATPase.

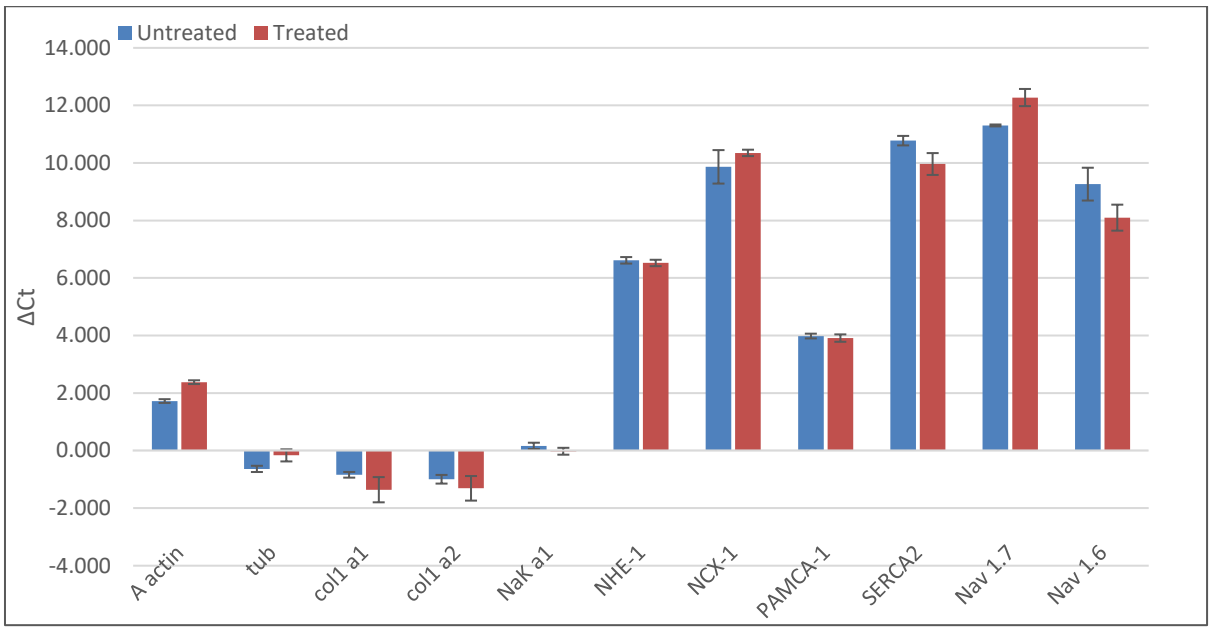

Figure 6.5: qRT-PCR quantitation for the target genes within treated group with LPS and their corresponding non-treated group.
Samples were operated in the presence of GAPDH as a reference gene. The level of gene expression was calculated after normalising against GAPDH in each sample and presented as ΔCt values. Values are mean ΔCt ± SE (n=5). The values of ΔCt for α-tub, col1 a1,a2, and NaK-ATPase are shown in the negative side of the x-axis because their actual mRNA concentrations are higher than the reference gene (GAPDH) within the pulp. Note: the Ct values are inversely proportional to the actual mRNA expression. No statistical significant difference was obtained in Unpaired T-test (p>0.05) between test and control samples.

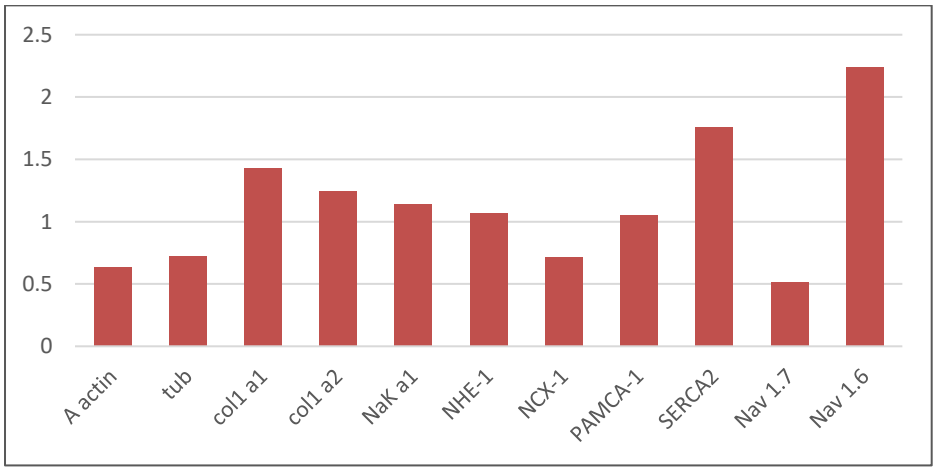

Figure 6.6: Interpretation of the modulating effect of LPS incubation on the expression of target genes in terms of fold change.
Fold-change was determined after normalising the ΔCt value after treatment of each gene with ΔCt of the incubated, untreated group. The fold value= $2^{-\Delta\Delta Ct}$.

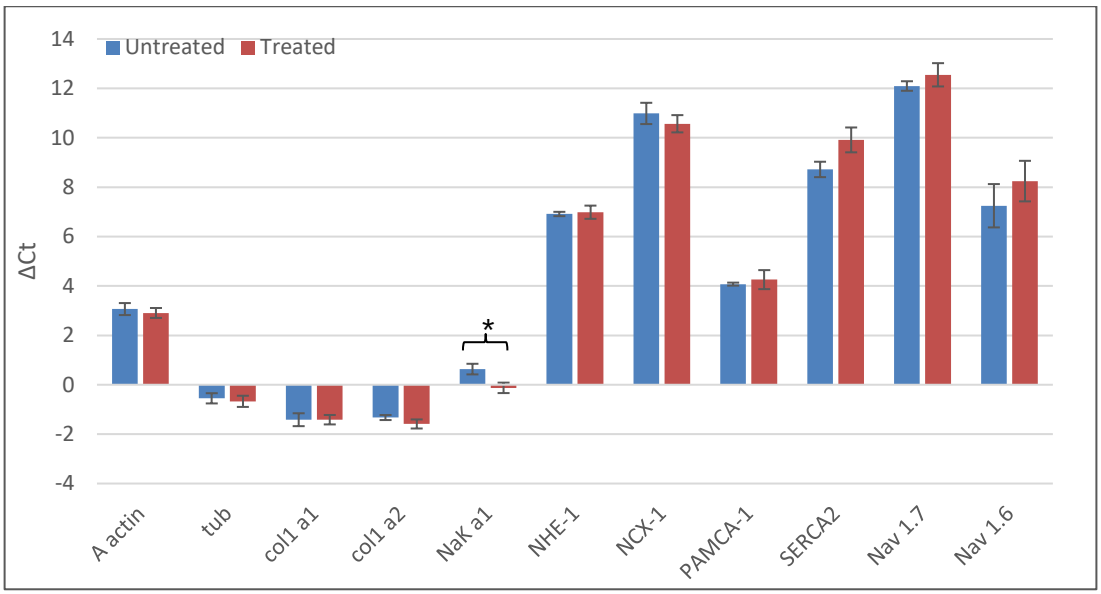

Figure 6.7: qRT-PCR quantitation for the target genes within treated group with ATP and their corresponding non-treated group.
Samples operated in the presence of GAPDH as a reference gene. The level of gene expression was calculated after normalising against GAPDH in each sample and is presented as ΔCt values. Values are mean ΔCt ± SE (n=5). The values of ΔCt for α-tub, col1 a1,a2, and NaK-ATPase are shown in the negative side of the x-axis because their actual mRNA concentrations are higher than the reference gene (GAPDH) within the pulp. Note: the Ct values are inversely proportion to the actual mRNA expression. Unpaired T-test only shows statistical significant difference (*) between control and test groups for the NaK-ATPase at ($p < 0.05$).

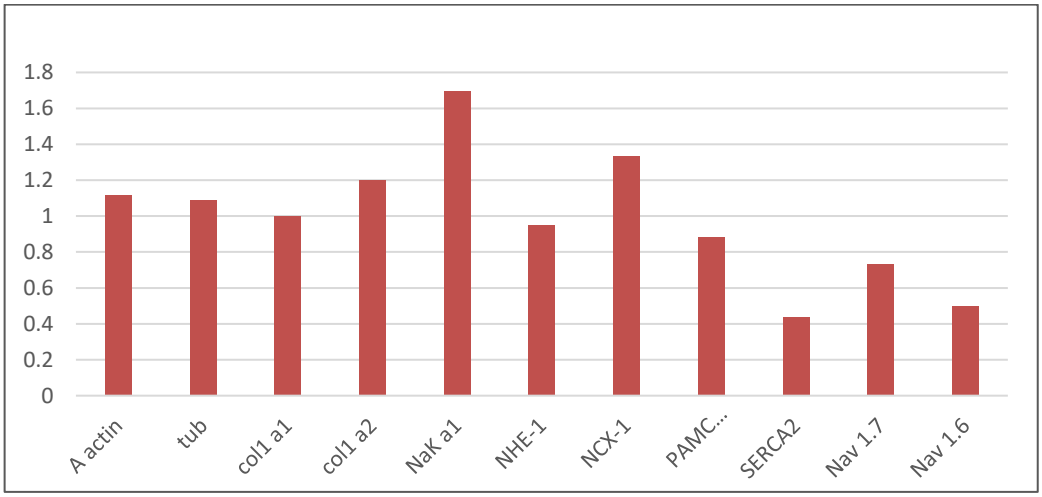

Figure 6.8: Illustration of the change in expression of target genes in response to ATP incubation in terms of fold-change.
Fold-change was obtained after normalising the ΔCt value after treatment of each gene with ΔCt of the incubated, untreated group. The fold value= $2^{-\Delta\Delta Ct}$.

6.4 Discussion

These investigations demonstrated that all target genes were expressed in the rat dental pulp. The presence of this mRNA provides molecular confirmation for the previous chapters which used the same protein markers in IHC including α-actin, α-tubulin, NaK-ATPase, and sodium hydrogen antiporter (NHE-1). Additionally, other structural and ion transporter genes were identified to help broaden our understanding about possible pulp responses to short incubation periods with and without treatment. The latter genes included structural genes: collagen (Col1 a1 and a2) (McLachlan *et al.*, 2003), and ion transporter genes: sodium calcium exchanger (NCX-1) (Lundquist *et al.*, 2000), plasma membrane calcium ATPase (PMCA) (Lundgren and Linde, 1997), sarcoplasmic reticulum calcium ATPase (SERCA) (Granström *et al.*, 1979), and voltage gated sodium channels (Na_v 1.6 and 1.7) (Byers and Westenbroek, 2011). The use of extracted pulp as a model in this work may not reflect the exact *in vivo* environment of tooth trauma and inflammation. However, it could provide a valuable model for studying pulp responses to these insults within a tissue in a lab-based environment.

Studies reported that most of the Ods (87.5%) remain attached to the pulp tissue of the rat incisor teeth after extirpation of this tissue from the tooth at room temperature and only few remain attached to dentine wall (McLachlan *et al.*, 2003). This suggests that the pulp used within this study still maintains a pulp-odontoblast cellular complex, though this was not specifically examined in the current work. Within this complex the main affected cells would be the Ods. It would be valuable to examine an odontoblast cell population only, isolated from dental pulp because they are the cells which are likely to be first to confront external stimuli. However, a large number of teeth were reported in order to obtain a detectable amount of RNA for such analysis (Palosaari *et al.*, 2000). In our own preliminary data, small teeth such as rat molars were also insufficient to provide a detectable amount of RNA, even after using tissues from three molars of the same segment.

The dental pulp is a complex system, which is subjected to different harmful stimuli from its surroundings including mechanical, thermal stimulation and bacterial infection. In all events, the pulp may be damaged, either reversibly or irreversibly depending on the insult (Smith *et al.*, 2008). Reversible damage usually includes the injury or death of the damaged cells followed by healing induction, often including the

secretion of reactionary and reparative dentine matrix. Irreversible damage usually includes a series of pathological events which may end with partial or complete pulp necrosis (Farges *et al.*, 2015).

The purpose of short time incubation period experiments was to identify how fast the targeted genes could respond to the trauma caused by extraction of the pulp tissue from the hard shell of the tooth. Most of the target genes showed statistically significant differences after 1h incubation (group B) when compared to control group without incubation (group A). This change, including down regulation, is compared to group A. This could be due to deterioration of the tissue and RNA destruction during the incubation period. This has no biological explanation. However, not all the genes behaved similarly. α-actin, α-tub and NCX-1 showed no significant differences after one hour of incubation. Moreover, other genes such as Na_v 1.7 changed from significant after one hour to non-significant after 3 hours incubation. This specific gene change could reflect a specific tissue response against trauma which causes different transcriptional changes within a short period after tissue injury. The possible explanation for such gene expression differences is unknown at this level. However, development of this technique could allow us to see in the future the possibilities for such change.

None of the targeted genes exhibited a biologically significant change during short periods of incubation after treatment with LPS and ATP. This could mean that none of these genes were quickly activated at a transcriptional level to give significant up or down regulation values by the effect of the applied treatment. This work complements a previous project of Alhelal (2016) who found that there was rapid pulpal activation of pro-inflammatory and anti-inflammatory genes in response to short incubation periods with LPS. The most upregulated genes were for cyclooxygenase 1 and 2. The latter gives upregulation up to 20-fold within a 3h incubation period. Other genes such as prostaglandin receptors (EP1, EP2), interleukin 1 (IL1), IL1 receptors, interleukin 6 (IL6), IL6 receptors and nitric oxide synthase (NOS1) showed upregulation values ranged between 3-6.5. This may suggest that the tissue inflammation represented by these inflammatory genes were the first line of tissue defence mechanism to be activated. This may supposedly be followed by a series of molecular and cellular events in the course of the inflammatory process. This leads to activation of the structural and homeostatic genes which aims to enhance defence mechanisms ending with tissue repair and

regeneration (Cooper *et al.*, 2014). Additionally, results in Ch 5 revealed that all examined structural and ion transporter markers showed a remarkable increase in expression within the traumatised pulp region after the commencement of tooth wear. Higher expressions of α-actin, NaK-ATPase and NHE were detected within the traumatised Od and associated SOd cells in 4w rat samples (Figures 5-31 and 5-34). The incubation time was only limited to a short period (3h) within the current study to maintain tissue vitality. The targeted genes possibly required more time to be stimulated and to process their function. This function would probably control cellular events that may enhance tissue defence mechanisms and lead to repair and regeneration. However, the exact time required for this process is still not known. Therefore, further research with a longer incubation period can be suggested to identify exactly the time required for such genes to be activated.

In conclusion, early remodelling has been identified within rat pulp samples within specific genes, while others remained unchanged. LPS and ATP treatment did not cause detectable transcriptional changes in the target genes. This possibly required longer incubation times (more than 3h) to allow tissue inflammation, proceeding to generate the stimulatory mechanisms for these molecular changes.

Chapter 7 **Discussion, reflections and opportunities for future work**

This work was initiated by reviewing literature relating to pulp biology and general cellular physiology. The assumption at the outset was that the physiology of the dentine-pulp complex was well understood. Much of the widely held knowledge contained in standard textbooks is based on studies performed many decades ago, and many of the hypotheses explaining tissue behaviour are based on these. This may partly explain the relative lack of focus on basic pulp biology research until recent times, when growing interest in pulp regeneration/revascularisation has reignited interest. It is essential to build therapies on the basis of deep understanding of normal tissue structure and function, and to continue to challenge assumptions on tissue reaction patterns in the face of injury. Without this foundation, opportunities may be missed to discover new and more effective ways of controlling symptoms, managing disease and promoting helpful tissue responses. The relatively low level of knowledge and exploration in fundamental pulp biology could also account for the lack of coherent explanation for several well-known dental mysteries such as pulp stone development, dentine sclerosis and the mode of action of high pH materials (calcium hydroxide, and hydraulic calcium silicate cements).

From many aspects, the dental pulp is regarded as a unique tissue. Much of this relates to its structural and functional intermingling with hard tissues, making its study and its behaviour complicated. New aspects of this complexity have been revealed within the current work. Three broad statements can be made. First, dental pulp is composed of several cellular elements, many of which are heterogeneous in nature, with all cellular elements performing distinctive roles in tissue formation, maintenance and response patterns. Second, changes in cellular structure and morphology always reflect changes in physiology and function. Third, all fine details should be taken into consideration when building hypotheses on tissue behaviour, even if the historic literature neglect this, or consider these details as not useful. Using these concepts helped to direct the present work to elaborate traditional hypotheses or develop new ones that could provide new insights.

Figure 7.1 provides a diagrammatic summary of the new observations, challenges to established knowledge, opportunities for human translational research and possible therapeutic interventions that have emerged from the current work.

This work was focussed on the well-established rat model, which has many similarities with human tissue, but also with important differences. The rat molar is the closest model for human teeth because its growth is not continuous. The continuously growing rat incisor is a particularly good model for the study of different stages of tooth development (Ohshima and Yoshida, 1992). Its size also provides the opportunity for adequate volumes of RNA extraction, compared with the much smaller rat molar (McLachlan *et al.*, 2003; Alhelal, 2016).

Through sections of this thesis, attempts were made to address a number of targeted issues in the following way. In Ch 3, the structural complexity of the Od and its cellular process were explored. The reaction of OPs to cavity preparation into dentine was also investigated. The already published Ch 4 used the physiological occlusal wear of the rat molar to compare cellular responses within areas of the tooth exposed to the oral environment and those that remained intact. Structural and homeostatic cellular elements were the main focus of exploration. The same model was studied in a broader way in Ch 5, including animals of different age and tooth wear experience, and exploring different markers including structural, cell division, growth factors, neurons, and ion transporters. Finally, Ch 6 focused on possible homeostatic gene transcription in early stages after pulp trauma with and without exposure to pro-inflammatory treatments.

There were important new observations in each section (see Figure 7.1 for summary):

Ch 3, the most striking finding was the detection of actin-IR tree-like OPs within the PD region, which were separate from the primary cellular processes. The structural complexity of these tree-like OPs and their spatial relationship to the apical region of the Ods suggested different possibilities for their intervention. These could include possible roles in preserving cellular stability, dentine deposition and/or sensing mechanisms of Od cells following fluid movement or tooth flexion. Moreover, great complexity and regional heterogeneity of primary OPs in terms of different IR to different antibodies within different dentine thickness was also identified. Previously, OPs may have been considered relatively homogenous. Furthermore, the cavity model provided possible new insights on the structural response of OPs to dentine exposure, with evidence of a programmed retraction of OPs toward the Od cell body.

Based on the observed complexity within pulp cells, IR to structural and ion transporter markers, the interactions of these two elements and their corresponding components were chosen to be the focus of this thesis. Nevertheless, other structural elements including tooth innervation and blood supply were also explored for their fundamental structural relationship with Od, and SOd cellular populations.

In Ch 4, the new observations included confirmation of architectural cellular heterogeneity within the Od population. In addition, the regional heterogeneity of the OPs in response to different antibody markers was confirmed in the rat molar. Focusing on the region of the tooth affected by cusp wear, meandering OPs and dentinal tubules were discovered. This observation led to a re-direction of the project, by expanding the investigation of tooth wear and reaction patterns (Ch 5).

A key new finding from studies in Ch 5 was the presence in younger samples (before tooth eruption) of obvious actin tree-like OPs in the coronal pulp; as primary dentinogenesis continued. Once primary dentine formation was complete, these processes disappeared. This observation supports the assertion that these processes have a function in dentine deposition. However, their persistence within root samples even after tooth maturation may indicate other possible functions. Another important observation was the regional heterogeneity of OPs which was found to be age-dependant, and further suggests age-dependant functional changes within the OPs. An additional important finding was the two-staged pulp repair mechanism in areas of the tooth affected by wear. This included the formation of an atubular dentine plug as an early pulp response, followed by a second tubular form within the reactionary dentine region. This was associated with an apparent supportive role from the SOd cells during the period of trauma and defensive reaction. The obvious activation of these cells as evidenced by IR to a range of markers including actin, growth factors, and ion transporters (NaK-ATPase and NHE-1) during early stages of trauma, supports the proposal that these cells provide support to the traumatised Ods. This role helps to support a new homeostatic hypothesis. This hypothesis provides a hitherto undescribed way of mineral ion translocation during normal and pathological conditions depending on the pH controlling ability of the pulp cells (due to active NaK-ATPase and NHE-1 expression).

The results of Ch 6 showed specific transcriptional gene changes within homeostatic genes following a short period of trauma to pulp tissue explants. However, no biologically significant changes occurred after short-term exposure of pulp tissue to LPS and ATP. The lack of response may be time-dependant, with longer exposures needed for tissue inflammatory process to react (Alhelal, 2016) and indirectly activate these genes.

Several existing dental hypotheses and ideas have been challenged through sections of this thesis (challenges in Figure 7.1) as follows:

- One of these ideas was the normal physiological events during cellular developmental period and the associated signalling mechanisms. The identification of the actin tree-like processes and the presence of NaK-ATPase within Ods, OPs, and SOd raise new questions about the role of these new observations during tooth developmental period. Increasing the knowledge about cellular structural changes and possible signalling mechanisms between different cellular populations during the developmental stages probably improve understanding about the possible cellular interactions during trauma and repair.
- Challenging the hydrodynamic theory during normal physiological condition of the tooth by identifying the structural complexity of the OPs and dentinal tubules and how these structures are correlated spatially and functionally. It is suggested that the hydrodynamic fluid movement is more applicable during pathological conditions when more spaces would be available within dentinal tubules after retraction of the OPs. Therefore, this suggests two different modes of tooth sensing mechanism during normal and pathological conditions.
- Challenging the previous ideas about tertiary dentine and the reactionary mechanism of the traumatised pulp tissue, by identifying two-stage reactionary dentine responses to the wear trauma. This new observation revealed that the pulp cells respond to trauma in a controlled mechanism which aims to plug the exposed dentinal tubules as a first response. This allows the pulp cells to overcome the immediate inflammatory period and initiate a second stage of repair and regeneration, with the deposition of more tubular tissue.
- Challenging the previous hypothesis about Ca^{2+} ion transportation and deposition during dentinogenesis. This hypothesis neglected the role of pH as a pivotal parameter during Ca^{2+} deposition and hydroxy apatite crystal

formation and growth (Linde and Lundgren, 1995). Our new hypothesis focused on homeostatic ion transporters which are complementary to Ca^{2+} transportation mechanisms and important in regulating cellular pH and linking that with changes in cellular morphology during normal and pathological conditions. All these helped in developing this hypothesis which theoretically provides a scientific explanation for several unknown pathological phenomena such as the formation of pulp stones. Additionally, this hypothesis can be used to explain the possible physiological mode of action for some existing pulp therapies. This could include the role of high pH cements such as calcium hydroxide, and hydraulic calcium silicates in promoting mineralised tissue formation by traumatised pulp regions (Grech *et al.*, 2013; Sangwan *et al.*, 2013).

- Although there is a huge interest in the field of regenerative endodontics, this work challenges the hypothesis of the present of adult stem cells within differentiated pulp cell populations. The absence of the cell division marker within traumatised pulp tissue raised a question about the reliability of this hypothesis. Instead, this work supports the ability of other pulp cells to de-differentiate and change into other cell types to replace the degenerated Ods.
- The inactivation of homeostatic genes within the short period of time examined in this work identifies the presence of two sets of genes: fast activated inflammatory genes and slow activated repair genes. This supports our concepts about the presence of complex inflammatory and reparative interactions that require to be understood further in the process of developing new therapies.

Although there are many advantages of performing laboratory research on animal samples, this work should be translated in future work to human samples. This may include human teeth maintained within a tissue culture environment, or undertaking clinical experiments on teeth needing extraction for orthodontic purposes. Either option would be technically challenging, costly and time consuming.

Building on the observations and hypotheses emerging from this work, there may be helpful therapeutic implications (see benefits and therapies in Figure 7.1). This may open the possibility for introducing new pharmacological interventions stemming from more detailed understanding of complex cell to cell signalling mechanisms. The use of growth factors could be one of these interventions. In addition to the cellular

released NGF and its NGFR receptors, there are other growth factors including the TGFβ family released during tissue differentiation, preserved within dentine matrix and released during dentine trauma (Goldberg and Smith, 2004). Better understanding of these growth factors and their receptors during normal and pathological conditions could provide new insights in pulp therapies. Furthermore, understanding tissue repair mechanisms and the process of cellular replacement may identify the key cell types within the pulp which can be employed therapeutically in tooth revascularisation process.

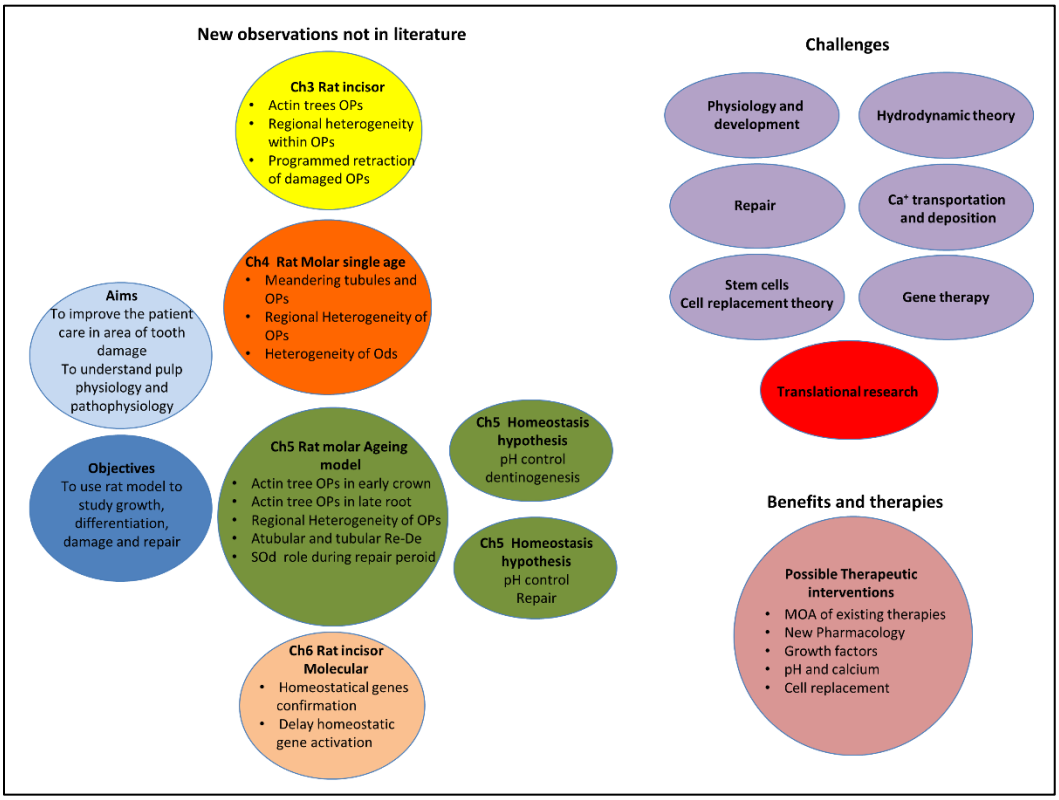

Figure 7.1: Diagram summarising the new observations, challenges to existing knowledge, opportunities for human translation research and possible therapeutic interventions emerging from current studies.

Appendix A

Experiment to determine optimal EDTA concentration for specimen demineralisation

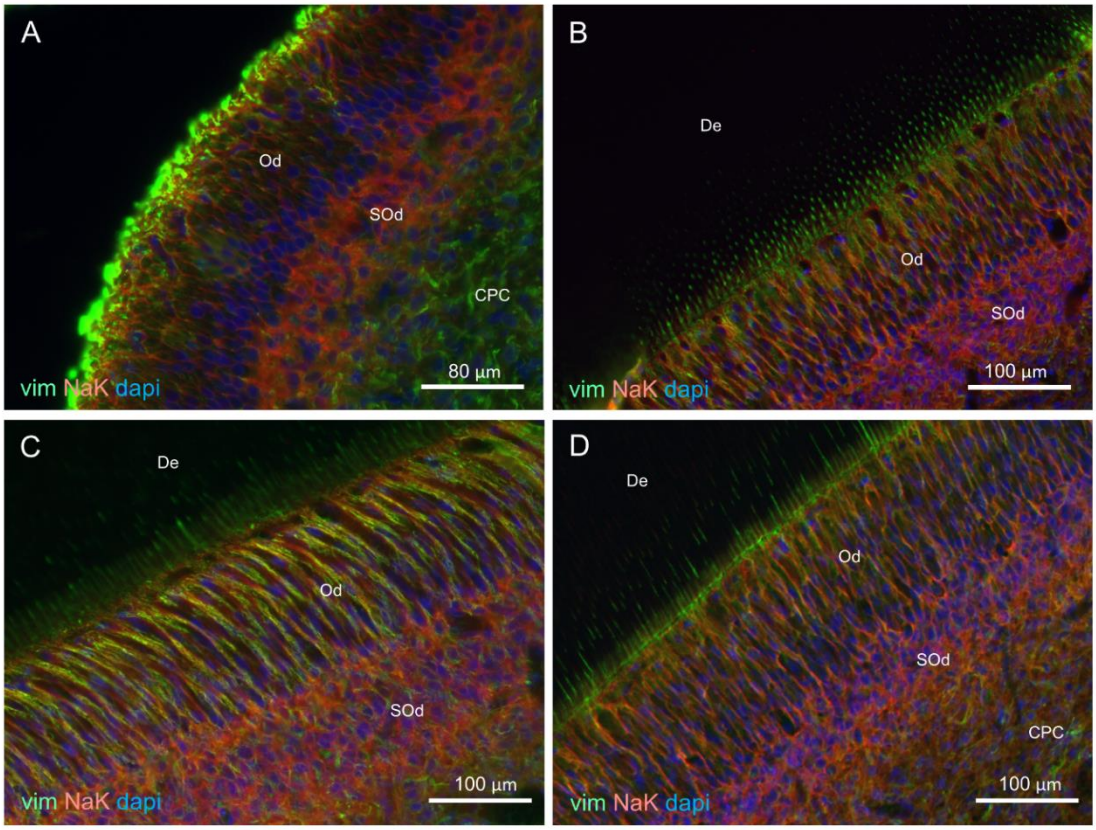

An example of IHC staining in rat mandibular incisor extracted pulp (A) and decalcified sections treated with different EDTA concentrations (4.3% in B,12% in C and 17% in D). All images stained for NaK-ATPase (red), vim (green), and dapi (blue). The following structures have been identified: odontoblast layer (Od), subodontoblast cells (SOd), dentine (De), and central pulp cells (CPC). All images show similar IR to both vim and NaK-ATPase staining.

Appendix B

qRT-PCR quality control

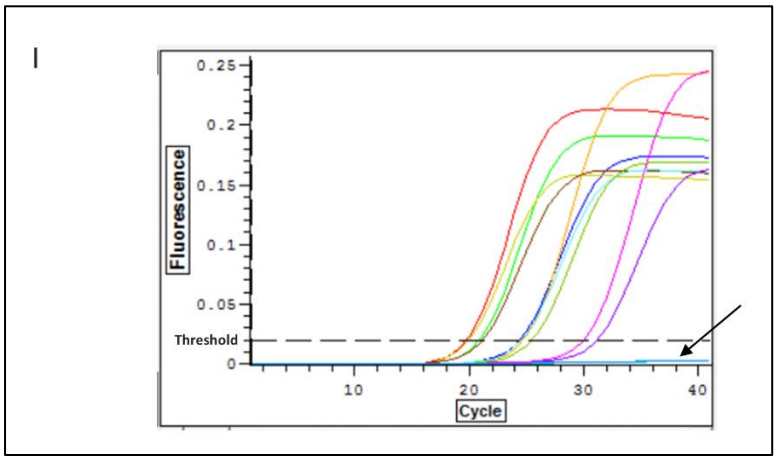

I. Fluorescence amplification versus cycle number for GAPDH (control gene) with serial dilutions of templet cDNA (0.001- 10ng). The curves represent the highest to lowest input mRNA from left to right. Duplicates were used for each input amount and are reflected by overlapping curves on the graph. The relative quantity of GAPDH transcript from each concentration is reflected at the exponential phase of the amplification curve and determined by the Ct value. The threshold bar is the point at which the mRNA levels were estimated. The arrow points to the amplification of RT-ve mRNA, with no amplification or fluorescence was observed. This indicates the complete absence of any genomic DNA contamination.

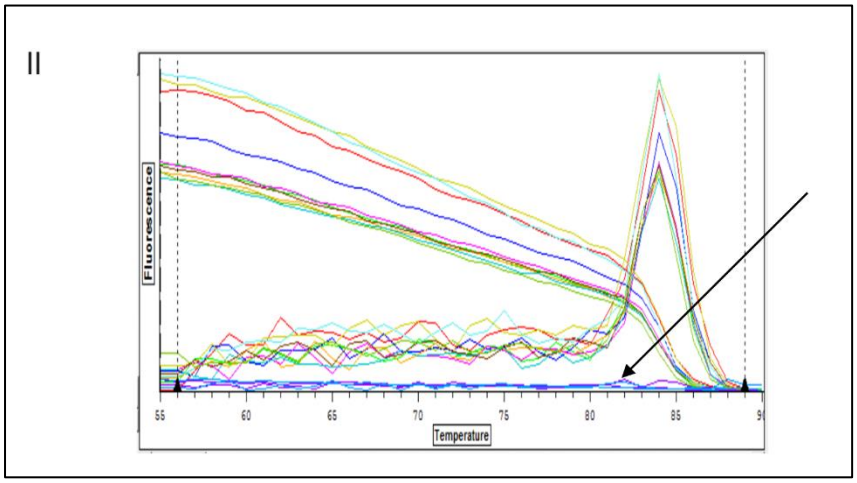

II. Fluorescence versus temperature (melting curve) for GAPDH (control gene) with serial dilutions of templet cDNA (0.001- 10ng). After amplification, the samples were slowly heated in order to detect the loss of fluorescence that occurs at the melting temperature which is recognised by a specific melting peak for each PCR product. All the peaks are located at the same temperature point. This pattern refers to the specificity of the product, as any product has one melting temperature and confirms the specificity of the primers. Note that the peaks are not at the same height because each peak represents a different concentration. The arrow refers to the NTC and RT^{-ve} reaction.

III

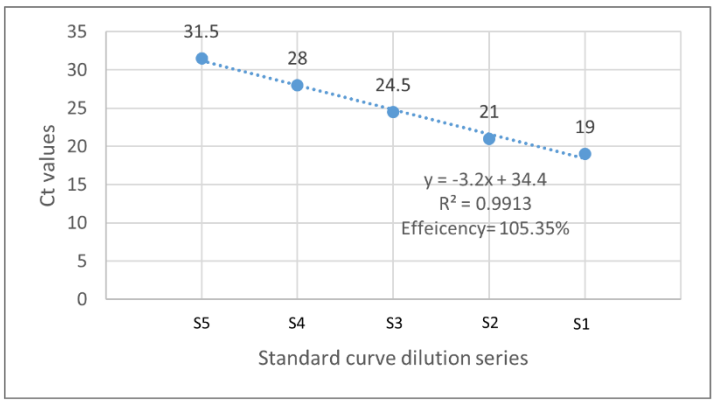

III. A representative of plot of standard curve threshold values (Ct) versus the log of the amount of total cDNA (0.001- 10ng) added to the reaction for GAPDH, showing the R^2 and efficiency values. The correlation coefficient (R^2) for the standard curves ranged from 0.97-1.00 and the efficiency ranged from 90-110 %. X axis represent the serial dilution of target cDNA where S1 represent the neat cDNA, S2 represent S1 diluted ten times and so on.

Appendix C

List of publications and conference presentations Publications:

Mahdee, A., Alhelal, A., Eastham, J., Whitworth, J. and Gillespie, J. (2016). Complex cellular responses to tooth wear in rodent molar. *Arch Oral Biol*, 61, pp. 106-114.

Alhelal, A., Mahdee, A., Eastham, J., Whitworth, J. and Gillespie, J. (2016). Complexity of Odontoblast and Subodontoblast Cell Layers in Rat Incisor. *J Dent Sci*, 4(2), pp. 68-74.

Conference presentations:

Mar. 2017: Spring Scientific Meeting of the British Endodontic Society, London, UK (poster presentation).

Pulp responses to tooth wear in the rodent molar.

June 2016: 10th World Endodontic Congress of the International Federation of Endodontic Association, Cape Town, South Africa (poster presentation).

Presence and putative role of actin-containing odontoblast processes in the rodent molar.

Sep. 2015: European Society of Endodontology Biennial Congress, Barcelona, Spain (oral presentation).

Complexity and extension of odontoblast processes in intact and damaged rodent dentine.

Mar. 2015 General Session & Exhibition of the International Association for Dental Research (IADR), Boston, USA (poster presentation).

Complexity and extension of the odontoblast processes.

References

Abd-Elmeguid, A. and Yu, D. (2009) 'Dental pulp neurophysiology: part 1. Clinical and diagnostic implications', *J Can Dent Assoc*, 75(1), pp. 55-9.

About, I., Bottero, M.-J., de Denato, P., Camps, J., Franquin, J.-C. and Mitsiadis, T.A. (2000) 'Human dentin production in vitro', *Exp Cell Res*, 258(1), pp. 33-41.

About, I., Murray, P., Franquin, J.-C., Remusat, M. and Smith, A. (2001) 'The effect of cavity restoration variables on odontoblast cell numbers and dental repair', *J Dent*, 29(2), pp. 109-117.

Addy, M. (2002) 'Dentine hypersensitivity: new perspectives on an old problem', *Int Dent J*, 52(S5P2), pp. 367-375.

Alavi, A., Dubyak, G. and Burnstock, G. (2001) 'Immunohistochemical evidence for ATP receptors in human dental pulp', *J Dent Res*, 80(2), pp. 476-483.

Alhelal, A. (2016) *Physiological and molecular responses in the pulp associated with early inflammatory process*. PhD thesis submitted to Newcastle University.

Alhelal, A., Mahdee, A., Eastham, J., Whitworth, J. and Gillespie, J. (2016) 'Complexity of Odontoblast and Subodontoblast Cell Layers in Rat Incisor', *J Dent Sci*, 4(2), pp. 68-74.

Allard, B., Couble, M., Magloire, H. and Bleicher, F. (2000) 'Characterization and gene expression of high conductance calcium-activated potassium channels displaying mechanosensitivity in human odontoblasts', *J Biol Chem*, 275(33), pp. 25556-25561.

Allard, B., Magloire, H., Couble, M.L., Maurin, J.C. and Bleicher, F. (2006) 'Voltage-gated sodium channels confer excitability to human odontoblasts: possible role in tooth pain transmission', *J Biol Chem*, 281(39), pp. 29002-10.

Arana-Chavez, V.E. and Massa, L.F. (2004) 'Odontoblasts: the cells forming and maintaining dentine', *The international journal of biochemistry & cell biology*, 36(8), pp. 1367-73.

Aranda, R., Dineen, S.M., Craig, R.L., Guerrieri, R.A. and Robertson, J.M. (2009) 'Comparison and evaluation of RNA quantification methods using viral, prokaryotic, and eukaryotic RNA over a 10 4 concentration range', *Anal Biochem*, 387(1), pp. 122-127.

Assas, B.M., Pennock, J.I. and Miyan, J.A. (2014) 'Calcitonin gene-related peptide is a key neurotransmitter in the neuro-immune axis', *Front Neurosci Doi*, 8, p. Art 23.

Beertsen, W. and Niehof, A. (1986) 'Root-analogue versus crown-analogue dentin: A radioautographic and ultrastructural investigation of the mouse incisor', *Anat Rec*, 215(2), pp. 106-118.

Bègue-Kirn, C., Ruch, J., Ridall, A. and Butler, W. (1998) 'Comparative analysis of mouse DSP and DPP expression in odontoblasts, preameloblasts, and experimentally induced odontoblast-like cells', *Eur J Oral Sci*, 106(S1), pp. 254-259.

Beniash, E., Traub, W., Veis, A. and Weiner, S. (2000) 'A transmission electron microscope study using vitrified ice sections of predentin: structural changes in the dentin collagenous matrix prior to mineralization', *J Struct Biol*, 132(3), pp. 212-225.

Berdal, A., Hotton, D., Pike, J.W., Mathieu, H. and Dupret, J.-M. (1993) 'Cell-and stage-specific expression of vitamin D receptor and calbindin genes in rat incisor: regulation by 1, 25-dihydroxyvitamin D3', *Dev Biol*, 155(1), pp. 172-179.

Berdal, A., Hotton, D., Saffar, J., Thomasset, M. and Nanci, A. (1996) 'Calbindin-D9k and calbindin-D28k expression in rat mineralized tissues in vivo', *J Bone Miner Res*, 11(6), pp. 768-779.

Berod, A., Hartman, B. and Pujol, J. (1981) 'Importance of fixation in immunohistochemistry: use of formaldehyde solutions at variable pH for the localization of tyrosine hydroxylase', *J Histochem Cytochem*, 29(7), pp. 844-850.

Bertassoni, L., Stankoska, K. and Swain, M. (2012) 'Insights into the structure and composition of the peritubular dentin organic matrix and the lamina limitans', *Micron*, 43(2), pp. 229-236.

Bjørndal, L. and Larsen, T. (2000) 'Changes in the cultivable flora in deep carious lesions following a stepwise excavation procedure', *Caries Res*, 34(6), pp. 502-508.

Bleicher, F. (2014) 'Odontoblast physiology', *Exp Cell Res*, 325(2), pp. 65-71.

Boonrungsiman, S., Gentleman, E., Carzaniga, R., Evans, N., McComb, D., Porter, A. and Stevens, M. (2012) 'The role of intracellular calcium phosphate in osteoblast-mediated bone apatite formation', *Proceedings of the National Academy of Sciences*, 109(35), pp. 14170-14175.

Boskey, A. (2003) 'Biomineralization: an overview', *Connect Tissue Res*, 44(1), pp. 5-9.

Botero, T.M., Shelburne, C.E., Holland, G.R., Hanks, C.T. and Nör, J.E. (2006) 'TLR4 mediates LPS-induced VEGF expression in odontoblasts', *J Endod*, 32(10), pp. 951-955.

Boyde, A. and Reith, E. (1977) 'Qualitative electron probe analysis of secretory ameloblasts and odontoblasts in the rat incisor', *Histochemistry*, 50(4), pp. 347-354.

Brain, S., Williams, T., Tippins, J., Morris, H. and MacIntyre, I. (1985) 'Calcitonin gene-related peptide is a potent vasodilator', *Nature*, 313(5997), pp. 54-56.

Brown, M., Reed, R.B. and Henry, R.W. (2002) 'Effects of dehydration mediums and temperature on total dehydration time and tissue shrinkage', *J Int Soc Plastination*, 17, pp. 28-33.

Burke, F. and Samarawickrama, D. (1995) 'Progressive changes in the pulpo-dentinal complex and their clinical consequences', *Gerodontology*, 12(2), pp. 57-66.

Byers, M. (1984) 'Dental sensory receptors', *Int Rev Neurobiol*, 25, pp. 39-94.

Byers, M. and Lin, K.Y. (2003) 'Patterns of fluoro-gold entry into rat molar enamel, dentin, and pulp', *J Dent Res*, 82(4), pp. 312-317.

Byers, M. and Matthews, B. (1981) 'Autoradiographic demonstration of ipsilateral and contralateral sensory nerve endings in cat dentin, pulp, and periodontium', *Anat Rec*, 201(2), pp. 249-260.

Byers, M. and Narhi, M. (1999) 'Dental injury models: experimental tools for understanding neuroinflammatory interactions and polymodal nociceptor functions', *Crit Rev Oral Biol Medicine*, 10(1), pp. 4-39.

Byers, M.R. (1985) 'Terminal arborization of individual sensory axons in dentin and pulp of rat molars', *Brain Res*, 345(1), pp. 181-185.

Byers, M.R., Schatteman, G. and Bothwell, M. (1990) 'Multiple functions for NGF receptor in developing, aging and injured rat teeth are suggested by epithelial, mesenchymal and neural immunoreactivity', *Development*, 109(2), pp. 461-471.

Byers, M.R. and Sugaya, A. (1995) 'Odontoblast processes in dentin revealed by fluorescent Di-I', *J Histochem Cytochem*, 43(2), pp. 159-168.

Byers, M.R. and Westenbroek, R.E. (2011) 'Odontoblasts in developing, mature and ageing rat teeth have multiple phenotypes that variably express all nine voltage-gated sodium channels', *Arch Oral Biol*, 56(11), pp. 1199-1220.

Byers, M.R., Wheeler, F. and Bothwell, M. (1992) 'Altered expression of NGF and P75 NGF-receptor by fibroblasts of injured teeth precedes sensory nerve sprouting', *Growth Factors*, 6(1), pp. 41-52.

Cajazeira Aguiar, M. and Arana-Chavez, V.E. (2007) 'Ultrastructural and immunocytochemical analyses of osteopontin in reactionary and reparative dentine formed after extrusion of upper rat incisors', *J Anat*, 210(4), pp. 418-427.

Carafoli, E. (1987) 'Intracellular calcium homeostasis', *Annu Rev Biochem*, 56(1), pp. 395-433.

Carda, C. and Peydro, A. (2006) 'Ultrastructural patterns of human dentinal tubules, odontoblasts processes and nerve fibres', *Tissue Cell*, 38(2), pp. 141-150.

Casaccia-Bonnefil, P., Kong, H. and Chao, M.V. (1998) 'Neurotrophins: the biological paradox of survival factors eliciting apoptosis', *Cell Death Differ*, 5(5), pp. 357-364.

Celio, M., Norman, A. and Heizmann, C. (1984) 'Vitamin-D-dependent calcium-binding-protein and parvalbumin occur in bones and teeth', *Calcif Tissue Int*, 36(1), pp. 129-130.

Chao, M.V. (2003) 'Neurotrophins and their receptors: a convergence point for many signalling pathways', *Nat Rev Neurosci*, 4(4), pp. 299-309.

Chiego Jr, D. (1992) 'An ultrastructural and autoradiographic analysis of primary and replacement odontoblasts following cavity preparation and wound healing in the rat molar', *Proceedings of the Finnish Dental Society Suomen Hammaslaakariseuran toimituksia*, 88, pp. 243-256.

Cho, A., Suzuki, S., Hatakeyama, J., Haruyama, N. and Kulkarni, A.B. (2010) 'A method for rapid demineralization of teeth and bones', *Open Dent J*, 4, p. 223.

Chung, M.-K., Lee, J., Duraes, G. and Ro, J. (2011) 'Lipopolysaccharide-induced pulpitis up-regulates TRPV1 in trigeminal ganglia', *J Dent Res*, 90(9), pp. 1103-1107.

Ciucchi, B., Bouillaguet, S., Holz, J. and Pashley, D. (1995) 'Dentinal fluid dynamics in human teeth, in vivo', *J Endodont*, 21(4), pp. 191-194.

Coffey, C., Ingram, M. and Bjorndal, A. (1970) 'Analysis of human dentinal fluid', *Oral Surg Oral Med Oral Pathol*, 30(6), pp. 835-837.

Consolidated version of ASPA 1986 (6 May 2014). Available at: https://www.gov.uk/government/publications/consolidated-version-of-aspa-1986.

Cook, S. and McCleskey, E. (2002) 'Cell damage excites nociceptors through release of cytosolic ATP', *Pain*, 95(1), pp. 41-47.

Cooper, P.R., Holder, M.J. and Smith, A.J. (2014) 'Inflammation and regeneration in the dentin-pulp complex: a double-edged sword', *J Endod*, 40(4), pp. S46-S51.

Corpron, R. and Avery, J. (1973) 'The ultrastructure of intradental nerves in developing mouse molars', *Anat Rec*, 175(3), pp. 585-605.

Couve, E. (1986) 'Ultrastructural changes during the life cycle of human odontoblasts', *Arch Oral Biol*, 31(10), pp. 643-651.

Daculsi, G., LeGeros, R., Jean, A. and Kerebel, B. (1987) 'Possible physico-chemical processes in human dentin caries', *J Dent Res*, 66(8), pp. 1356-1359.

Dahl, E. and Mjör, I.A. (1973) 'The structure and distribution of nerves in the pulp-dentin organ', *Acta Odontologica*, 31(6), pp. 349-356.

Darvell, B. and Wu, R. (2011) '"MTA"—an hydraulic silicate cement: review update and setting reaction', *Dent Mater*, 27(5), pp. 407-422.

Davies, A.M. (2000) 'Neurotrophins: neurotrophic modulation of neurite growth', *Curr Biol*, 10(5), pp. R198-R200.

De Azambuja, E., Cardoso, F., de Castro, G., Colozza, M., Mano, M., Durbecq, V., Sotiriou, C., Larsimont, D., Piccart-Gebhart, M. and Paesmans, M. (2007) 'Ki-67 as prognostic marker in early breast cancer: a meta-analysis of published studies involving 12 155 patients', *Brit J cancer*, 96(10), pp. 1504-1513.

Dobie, K., Smith, G., Sloan, A. and Smith, A. (2002) 'Effects of alginate hydrogels and TGF-β1 on human dental pulp repair in vitro', *Connect Tissue Res*, 43(2-3), pp. 387-390.

Duan, X. (2014) 'Ion channels, channelopathies, and tooth formation', *J Dent Res*, 93(2), pp. 117-125.

El Karim, I., Linden, G., Curtis, T., About, I., McGahon, M., Irwin, C. and Lundy, F. (2011) 'Human odontoblasts express functional thermo-sensitive TRP channels: implications for dentin sensitivity', *Pain*, 152(10), pp. 2211-2223.

Farges, J., Alliot-Licht, B., Renard, E., Ducret, M., Gaudin, A., Smith, A. and Cooper, P. (2015) 'Dental pulp defence and repair mechanisms in dental caries', *Mediators Inflamm*, 2015.

Farris, E.J. and Griffith, J.Q. (1949) 'The Teeth', in Schour, I. and Massler, M. (eds.) *The rat in laboratory investigation*

New York: Hafner Press, A Division of Macmillan Publishing Co, Inc., pp. 102-161.

Femiano, F., Femiano, L., Festa, V.M., Rullo, R. and Perillo, L. (2014) 'Reactionary and reparative dentinogenesis a review', *Int J Dent Clin*, 6(4).

Fitzgerald, M., Chiego, D. and Heys, D. (1990) 'Autoradiographic analysis of odontoblast replacement following pulp exposure in primate teeth', *Arch oral biol*, 35(9), pp. 707-715.

Fox, C.H., Johnson, F.B., Whiting, J. and Roller, P.P. (1985) 'Formaldehyde fixation', *J Histochem Cytochem*, 33(8), pp. 845-853.

Frank, R. (1990) 'Structural events in the caries process in enamel, cementum, and dentin', *J Dent Res*, 69(2 suppl), pp. 559-566.

Frank, R. and Steuer, P. (1988) 'Transmission electron microscopy of the human odontoblast process in peripheral root dentine', *Arch Oral Biol*, 33(2), pp. 91-98.

Fristad, I., Heyeraas, K. and Kvinnsland, I. (1994) 'Nerve fibres and cells immunoreactive to neurochemical markers in developing rat molars and supporting tissues', *Arch oral biol*, 39(8), pp. 633-646.

Gage, G.J., Kipke, D.R. and Shain, W. (2012) 'Whole animal perfusion fixation for rodents', *J Vis Exp*, 65, p. 3564.

Gajjeraman, S., Narayanan, K., Hao, J., Qin, C. and George, A. (2007) 'Matrix macromolecules in hard tissues control the nucleation and hierarchical assembly of hydroxyapatite', *J Biol Chem*, 282(2), pp. 1193-1204.

Garant, P. (1972) 'The organization of microtubules within rat odontoblast processes revealed by perfusion fixation with glutaraldehyde', *Arch Oral Biol*, 17(7), pp. 1047-I059.

Gerdes, J., Lemke, H., Baisch, H., Wacker, H., Schwab, U. and Stein, H. (1984) 'Cell cycle analysis of a cell proliferation-associated human nuclear antigen defined by the monoclonal antibody Ki-67', *J Immunol*, 133(4), pp. 1710-1715.

Gillespie, J.I., Markerink-van Ittersum, M. and De Vente, J. (2006) 'Interstitial cells and cholinergic signalling in the outer muscle layers of the guinea-pig bladder', *BJU Int*, 97(2), pp. 379-85.

Goga, R., Chandler, N. and Oginni, A. (2008) 'Pulp stones: a review', *Int Endod J*, 41(6), pp. 457-468.

Goldberg, M. (2014) 'Pulp anatomy and characterization of the pulp cells', in Goldberg, M. (ed.) *The Dental Pulp Biology Pathology and Regenerative Therapies*. Springer, pp. 13-34.

Goldberg, M., Escaig, F., Feinberg, J. and Weinman, S. (1987) 'Ultrastructural localization of calmodulin in rat incisor ameloblasts and odontoblasts during the early stages of development', *Adv Dent Res*, 1(2), pp. 227-235.

Goldberg, M. and Lasfargues, J.-J. (1995) 'Pulpo-dentinal complex revisited', *J Dent*, 23(1), pp. 15-20.

Goldberg, M. and Septier, D. (1996) 'A comparative study of the transition between predentin and dentin, using various preparative procedures in the rat', *Eur J Oral Sci*, 104(3), pp. 269-277.

Goldberg, M. and Smith, A.J. (2004) 'Cells and Extracellular Matrices of Dentin and Pulp: A Biological Basis for Repair and Tissue Engineering', *Crit Rev Oral Biol M*, 15(1), pp. 13-27.

Goldberg, M. and Takagi, M. (1993) 'Dentine proteoglycans: composition, ultrastructure and functions', *Histochem J*, 25(11), pp. 781-806.

Golub, E. (2009) 'Role of matrix vesicles in biomineralization', *Biochimica et Biophysica Acta (BBA)-General Subjects*, 1790(12), pp. 1592-1598.

Gomes, R., Omar, F., Neves, J., Narvaes, O. and Novaes, D. (2010) 'Increase of MT1-MMP, TIMP-2 and Ki-67 proteins in the odontogenic region of the rat incisor post-shortening procedure', *J Mol Hist*, 41(6), pp. 333-341.

Goracci, G., Mori, G. and Baldi, M. (1999) 'Terminal end of the human odontoblast process: a study using SEM and confocal microscopy', *Clin Oral Investig*, 3, pp. 126-132.

Gotliv, B. and Veis, A. (2007) 'Peritubular dentin, a vertebrate apatitic mineralized tissue without collagen: role of a phospholipid-proteolipid complex', *Calcif Tissue Int*, 81(3), pp. 191-205.

Gotliv, B.A. and Veis, A. (2008) 'The composition of bovine peritubular dentin: matching TOF-SIMS, scanning electron microscopy and biochemical component distributions', *Cells Tissues Organs*, 189(1-4), pp. 12-19.

Granström, G. (1984) 'Further evidence of an intravesicular Ca2+-pump in odontoblasts from rat incisors', *Arch Oral Biol*, 29(8), pp. 599-606.

Granström, G., Jontell, M. and Linde, A. (1979) 'Separation of odontoblast Ca 2+-ATPase and alkaline phosphatase', *Calcif Tissue Int*, 27(1), pp. 211-217.

Granström, G. and Linde, A. (1976) 'A comparison of ATP-degrading enzyme activities in rat incisor odontoblasts', *J Histochem Cytochem*, 24(9), pp. 1026-1032.

Granström, G., Linde, A. and Nygren, H. (1978) 'Ultrastructural localization of alkaline phosphatases in rat incisor odontoblasts', *J Histochem Cytochem*, 26(5), pp. 359-368.

Grech, L., Mallia, B. and Camilleri, J. (2013) 'Characterization of set intermediate restorative material, Biodentine, Bioaggregate and a prototype calcium silicate cement for use as root-end filling materials', *Int Endod J*, 46(7), pp. 632-641.

Grötz, A., Duschner, H., Reichert, E., De Aguiar, G., Götz, H. and Wagner, W. (1998) 'Histotomography of the odontoblast processes at the dentine–enamel junction of permanent healthy human teeth in the confocal laser scanning microscope', *Clin Oral Invest*, 2(1), pp. 21-25.

Guerini, D. (1998) 'The Ca2+ pumps and the Na+/Ca2+ exchangers', *Biometals*, 11, pp. 319-330.

Gunji, T. and Kobayashi, S. (1983) 'Distribution and Organization of Odontoblast in Human Dentin', *Arch Histo Jap*, 46(2), pp. 213-219.

Gunning, P.W., Ghoshdastider, U., Whitaker, S., Popp, D. and Robinson, R.C. (2015) 'The evolution of compositionally and functionally distinct actin filaments', *J Cell Sci*, p. jcs. 165563.

Hahn, C.-L. and Liewehr, F.R. (2007) 'Innate immune responses of the dental pulp to caries', *J Endod*, 33(6), pp. 643-651.

Haldi, J., Wynn, W. and Culpepper, W. (1961) 'Dental pulp fluid—I: Relationship between dental pulp fluid and blood plasma in protein, glucose and inorganic element content', *Arch Oral Biol*, 3(3), pp. 201IN11-206.

Harada, H., Kettunen, P., Jung, H.-S., Mustonen, T., Wang, Y.A. and Thesleffl. (1999) 'Localization of Putative Stem Cells in Dental Epithelium and Their Association with Notch and Fgf Signaling', *The Journal of Cell Biology*, 147(1), pp. 105-120.

Harada, H., Mitsuyasu, T., Toyono, T. and Toyoshima, K. (2002) 'Epithelial stem cells in teeth', *Odontology*, 90, pp. 1-6.

Harada, H. and Ohshima, H. (2004) 'New perspectives on tooth development and the dental stem cell niche', *ArchHisolCytol*, 67(1), pp. 1-11.

He, W., Wang, Z., Luo, Z., Yu, Q., Jiang, Y., Zhang, Y., Zhou, Z., Smith, A.J. and Cooper, P.R. (2015) 'LPS promote the odontoblastic differentiation of human dental pulp stem cells via MAPK signaling pathway', *J Cell Physiol*, 230(3), pp. 554-561.

Holland, G.R. (1985) 'The odontoblast process: form and function', *J Dent res*, 64, pp. 499-514.

Holland, G.R. and Botero, T.M. (2014) 'Pulp biology: 30 years of progress', *Endod Top*, 31(1), pp. 19-35.

Homann, V., Kinne-Saffran, E., Arnold, W., Gaengler, P. and Kinne, R. (2006) 'Calcium transport in human salivary glands: a proposed model of calcium secretion into saliva', *Histochem Cell Biol*, 125(5), pp. 583-591.

Ibuki, T., Kido, M., Kiyoshima, T., Terada, Y. and Tanaka, T. (1996) 'An ultrastructural study of the relationship between sensory trigeminal nerves and odontoblasts in rat dentin/pulp as demonstrated by the anterograde transport of wheat germ agglutinin-horseradish peroxidase (WGA-HRP)', *J Dent Res*, 75(12), pp. 1963-1970.

Ikawa, M., Komatsu, H., Ikawa, K., Mayanagi, H. and Shimauchi, H. (2003) 'Age-related changes in the human pulpal blood flow measured by laser Doppler flowmetry', *Dent Traumatol*, 19(1), pp. 36-40.

Ikeda, H. and Suda, H. (2013) 'Odontoblastic syncytium through electrical coupling in the human dental pulp', *J Dent Res*, 92(4), pp. 371-375.

Inoue, H., Kurosaka, Y. and Abe, K. (1992) 'Autonomic nerve endings in the odontoblast/predentin border and predentin of the canine teeth of dogs', *J Endod*, 18(4), pp. 149-151.

Jalali, R., Guo, J., Zandieh-Doulabi, B., Bervoets, T., Paine, M., Boron, W., Parker, M., Bijvelds, M., Medina, J.F. and DenBesten, P. (2014) 'NBCe1 (SLC4A4) a potential pH regulator in enamel organ cells during enamel development in the mouse', *Cell Tissue Res*, 358(2), pp. 433-442.

Jernvall, J. and Fortelius, M. (2002) 'Common mammals drive the evolutionary increase of hypsodonty in the Neogene', *Nature*, 417(6888), pp. 538-540.

Johnsen, D. (1985) 'Session III: Innervation of the Dentin, Predentin, and Pulp—HO Trowbridge, Chairman: Innervation of Teeth: Qualitative, Quantitative, and Developmental Assessment', *J Dent Res*, 64(4), pp. 555-563.

Johnson, R. (2004) 'Effects of multiple dentinal lesions on the rat pulp', *J endodont*, 30(12), pp. 868-871.

Josephsen, K., Takano, Y., Frische, S., Praetorius, J., Nielsen, S., Aoba, T. and Fejerskov, O. (2010) 'Ion transporters in secretory and cyclically modulating ameloblasts: a new hypothesis for cellular control of preeruptive enamel maturation', *Am J Physiol Cell Ph*, 299(6), pp. C1299-C1307.

Kagayama, M., Sasano, Y., Sato, H., Kamakura, S., Motegi, K. and Mizoguchi, I. (1999) 'Confocal microscopy of dentinal tubules in human tooth stained with alizarin red', *Anat Embryol*, 199(3), pp. 233-238.

Kaplan, J.H. (2002) 'Biochemistry of Na,K-ATPase', *Annu Rev Biochem*, 71, pp. 511-35.

Kawagishi, E., Nakakura-Ohshima, K., Nomura, S. and Ohshima, H. (2006) 'Pulpal responses to cavity preparation in aged rat molars', *Cell Tissue Res*, 326(1), pp. 111-122.

Kawasaki, K., Tanaka, S. and Ishikawa, T. (1979) 'On the daily incremental lines in human dentine', *Arch Oral Biol*, 24(12), pp. 939-943.

Kawashima, N., Wongyaofa, I., Suzuki, N., Kawanishi, H.N. and Suda, H. (2006) 'NK and NKT cells in the rat dental pulp tissues', *Oral Surg Oral Med O*, 102(4), pp. 558-63.

Kelley, K.W., Bergenholtz, G. and Cox, C.F. (1981) 'The extent of odontoblast process in Rhesus monkeys (Macaca Mulatta) as observed by scanning electron microscopy.', *Arch oral Biol*, 26, pp. 893-897.

Kido, J., Kasahara, C., Ohishi, K., Nishikawa, S., Ishida, H., Yamashita, K., Kitamura, S., Kohri, K. and Nagata, T. (1995) 'Identification of osteopontin in human dental calculus matrix', *Arch Oral Biol*, 40(10), pp. 967-972.

Kimberly, C. and Byers, M. (1988) 'Inflammation of rat molar pulp and periodontium causes increased calcitonin gene-related peptide and axonal sprouting', *Anat Rec*, 222(3), pp. 289-300.

Kitamura, C., Kimura, K., Nakayama, T., Toyoshima, K. and Terashita, M. (2001) 'Primary and secondary induction of apoptosis in odontoblasts after cavity preparation of rat molars', *J Dent Res*, 80(6), pp. 1530-1534.

Kohri, K., Nomura, S., Kitamura, Y., Nagata, T., Yoshioka, K., Iguchi, M., Yamate, T., Umekawa, T., Suzuki, Y. and Sinohara, H. (1993) 'Structure and expression of the mRNA encoding urinary stone protein (osteopontin)', *J Biol Chem*, 268(20), pp. 15180-15184.

Kuboki, Y. and Mechanic, G. (1982) 'Comparative molecular distribution of cross-links in bone and dentin collagen. Structure-function relationships', *Calcif Tissue Int*, 34(1), pp. 306-308.

Kuratate, M., Yoshiba, K., Shigetani, Y., Yoshiba, N., Ohshima, H. and Okiji, T. (2008) 'Immunohistochemical analysis of nestin, osteopontin, and proliferating cells in the reparative process of exposed dental pulp capped with mineral trioxide aggregate', *J Endod*, 34(8), pp. 970-4.

Landis, W. (1996) 'Mineral characterization in calcifying tissues: atomic, molecular and macromolecular perspectives', *Connect Tissue Res*, 34(4), pp. 239-246.

Lesot, H., Begue-Kirn, C., Kubler, M., Meyer, J., Smith, A., Cassidy, N. and Ruch, J. (1993) 'Experimental Induction of Odontoblast Differentiation and Stimulation During Preparative Processes', *Cells and Materials*, 3(2), pp. 201-217.

Lesot, H., Lisi, S., Peterkova, R., Peterka, M., Mitolo, V. and Ruch, J. (2001) 'Epigenetic signals during odontoblast differentiation', *Adv Dent Res*, 15(1), pp. 8-13.

Lesot, H., Meyer, J., Ruch, J., Weber, K. and Osborn, M. (1982) 'Immunofluorescent localization of vimentin, prekeratin and actin during odontoblast and ameloblast differentiation', *Differentiation*, 21(1-3), pp. 133-137.

Linde, A. and Goldberg, M. (1993) 'Dentinogenesis', *Crit Rev Oral Biol M*, 4(5), pp. 679-728.

Linde, A. and Lundgren, T. (1995) 'From serum to the mineral phase. The role of the odontoblast in calcium transport and mineral formation', *Int J Dev Biol*, 39, pp. 213-222.

Liu, X., Yu, L., Wang, Q., Pelletier, J., Fausther, M., Sévigny, J., Malmström, H., Dirksen, R. and Ren, Y.-F. (2012) 'Expression of ecto-ATPase NTPDase2 in human dental pulp', *J Dent Res*, 91(3), pp. 261-267.

Love, R. and Jenkinson, H. (2002) 'Invasion of dentinal tubules by oral bacteria', *Crit Rev Oral Biol Medicine*, 13(2), pp. 171-183.

Lovschall, H., Fejerskov, O. and Josephsen, K. (2002) 'Age-related and site-specific changes in the pulpodentinal morphology of rat molars', *Arch Oral Biol*, 47(5), pp. 361-367.

Lucchini, M., Couble, M.-L., Romeas, A., Staquet, M.-J., Bleicher, F., Magloire, H. and Farges, J.-C. (2004) 'αvβ3 integrin expression in human odontoblasts and co-localization with osteoadherin', *J dent res*, 83(7), pp. 552-556.

Lundgren, T. and Linde, A. (1987) 'Regulation of free Ca2+ by subcellular fractions of rat incisor odontoblasts', *Arch Oral Biol*, 32(7), pp. 463-468.

Lundgren, T. and Linde, A. (1988) 'Na+/Ca2+ antiports in membranes of rat incisor odontoblasts', *J Oral Pathol Med*, 17(9-10), pp. 560-563.

Lundgren, T. and Linde, A. (1992) 'Calcium ion transport kinetics during dentinogenesis: effects of disrupting odontoblast cellular transport systems', *Bone Miner*, 19(1), pp. 31-44.

Lundgren, T. and Linde, A. (1997) 'Voltage-Gated Calcium Channels and Nonvoltage-Gated Calcium Uptake Pathways in the Rat Incisor Odontoblast Plasma Membrane', *Calcif Tissue Int*, 60, pp. 79-85.

Lundgren, T., Nannmark, U. and Linde, A. (1992) 'Calcium ion activity and pH in the odontoblast-predentin region: ion-selective microelectrode measurements', *Calcif Tissue Int*, 50(2), pp. 134-136.

Lundquist, P., Lundgren, T., Gritli-Linde, A. and Linde, A. (2000) 'Na+/Ca 2+ exchanger isoforms of rat odontoblasts and osteoblasts', *Calcif Tissue Int*, 67(1), pp. 60-67.

Lundquist, P., Ritchie, H., Moore, K., Lundgren, T. and Linde, A. (2002) 'Phosphate and Calcium Uptake by Rat Odontoblast-Like MRPC-1 Cells Concomitant With Mineralization', *J Bone Miner Res*, 17(10), pp. 1801-1813.

Luthman, J., Luthman, D. and Hökfelt, T. (1992) 'Occurrence and distribution of different neurochemical markers in the human dental pulp', *Arch Oral Biol*, 37(3), pp. 193-208.

Luukko, K., Kettunen, P., Fristad, I. and Berggreen, E. (2011) 'Structure and functions of the dentin-pulp complex.', in Hargreaves, K. and Cohen, S. (eds.) *Cohen's pathways ofthe pulp* Mosby Elsevier.

Luukko, K., Moshnyakov, M., Sainio, K., Saarma, M., Sariola, H. and Thesleff, I. (1996) 'Expression of neurotrophin receptors during rat tooth development is developmentally regulated, independent of innervation, and suggests functions in the regulation of morphogenesis and innervation', *Dev Dyn*, 206(1), pp. 87-99.

Magloire, H., Couble, M.L., Thivichon-Prince, B., Maurin, J.C. and Bleicher, F. (2009) 'Odontoblast: a mechano-sensory cell', *J Exp Zool B Mol Dev Evol*, 312B(5), pp. 416-24.

Magloire, H., Joffre, A. and Bleicher, F. (1996) 'An in vitro model of human dental pulp repair', *J Dent Res*, 75(12), pp. 1971-1978.

Magloire, H., Lesage, F., Couble, M.L., Lazdunski, M. and Bleicher, F. (2003) 'Expression and localization of TREK-1 K+ channels in human odontoblasts', *J dent res*, 82(7), pp. 542-545.

Magloire, H., Romeas, A., Melin, M., Couble, M.-L., Bleicher, F. and Farges, J.-C. (2001) 'Molecular regulation of odontoblast activity under dentin injury', *Adv Dent Res*, 15(1), pp. 46-50.

Mahdee, A., Alhelal, A., Eastham, J., Whitworth, J. and Gillespie, J. (2016) 'Complex cellular responses to tooth wear in rodent molar', *Arch oral biol*, 61, pp. 106-114.

Marshall, G., Inai, N., Magidi, I.-C., Balooch, M., Kinney, J., Tagami, J. and Marshall, S. (1997) 'Dentin demineralization: effects of dentin depth, pH and different acids', *Dent Mater*, 13(5-6), pp. 338-343.

Martin, F.E., Nadkarni, M.A., Jacques, N.A. and Hunter, N. (2002) 'Quantitative microbiological study of human carious dentine by culture and real-time PCR: association of anaerobes with histopathological changes in chronic pulpitis', *J Clin Microbiol*, 40(5), pp. 1698-1704.

Matsuo, S., Ichikawa, H., Henderson, T., Silos-Santiago, I., Barbacid, M., Arends, J. and Jacquin, M. (2001) 'trkA modulation of developing somatosensory neurons in oro-facial tissues: tooth pulp fibers are absent in trkA knockout mice', *Neuroscience*, 105(3), pp. 747-760.

Maurin, J.-C., Couble, M.-L., Didier-Bazes, M., Brisson, C., Magloire, H. and Bleicher, F. (2004) 'Expression and localization of reelin in human odontoblasts', *Matrix Biol*, 23(5), pp. 277-285.

McLachlan, J., Smith, A., Sloan, A. and Cooper, P. (2003) 'Gene expression analysis in cells of the dentine–pulp complex in healthy and carious teeth', *Arch oral biol*, 48(4), pp. 273-283.

Mendis, B. and Darling, A. (1979a) 'Distribution with age and attrition of peritubular dentine in the crowns of human teeth', *Arch Oral Biol*, 24(2), pp. 131-139.

Mendis, B. and Darling, A. (1979b) 'A scanning electron microscope and microradiographic study of closure of human coronal dentinal tubules related to occlusal attrition and caries', *Arch Oral Biol*, 24(10), pp. 725-733.

Mitsiadis, A., De Bari, C. and About, I. (2008) 'Apoptosis in developmental and repair-related human tooth remodeling: a view from the inside', *Exp cell res*, 314(4), pp. 869-877.

Mitsiadis, T.A., Couble, P., Dicou, E., Rudkin, B.B. and Magloire, H. (1993) 'Patterns of nerve growth factor (NGF), proNGF, and p75 NGF receptor expression in the rat incisor: comparison with expression in the molar', *Differentiation*, 54(3), pp. 161-175.

Mitsiadis, T.A., Dicou, E., Joffre, A. and Magloire, H. (1992) 'Immunohistochemical localization of nerve growth factor (NGF) and NGF receptor (NGF-R) in the developing first molar tooth of the rat', *Differentiation*, 49(1), pp. 47-61.

Mjör, I. and Nordahl, I. (1996) 'The density and branching of dentinal tubules in human teeth', *Arch Oral Biol*, 41(5), pp. 401-412.

Mori, H., Ishida-Yamamoto, A., Senba, E., Ueda, Y. and Tohyama, M. (1989) 'Calcitonin gene-related peptide containing sensory neurons innervating tooth pulp and buccal mucosa of the rat: an immunohistochemical analysis', *J Chem Neuroanat*, 3(3), pp. 155-163.

Mori, S., Sawai, T., Teshima, T. and Kyogoku, M. (1988) 'A new decalcifying technique for immunohistochemical studies of calcified tissue, especially applicable to cell surface marker demonstration', *J Histochem Cytochem*, 36(1), pp. 111-114.

Mornstad, H. (1978) 'Demonstration of a K+-stimulated and ouabain-sensitive p-nitrophenyl phosphatase activity in enamel-and dentin-forming tissues in the rat', *Eur J Oral Sci*, 86(1), pp. 12-20.

Morse, D.R. (1991) 'Age-related changes of the dental pulp complex and their relationship to systemic aging', *Oral Surg Oral Med O*, 72(6), pp. 721-745.

Moses, K.D., Butler, W.T. and Qin, C. (2006) 'Immunohistochemical study of small integrin-binding ligand, N-linked glycoproteins in reactionary dentin of rat molars at different ages', *Eur J Oral Sci*, 114(3), pp. 216-222.

Moxham, B.J., Webb, P.P., Benjamin, M. and Ralphs, J.R. (1998) 'Changes in the cytoskeleton of cells within the periodontal ligament and dental pulp of the rat first molar tooth during ageing', *Eur j oral sci*, 106(S1), pp. 376-383.

Murray, P., About, I., Lumley, P., Franquin, J.-C., Remusat, M. and Smith, A. (2000) 'Human odontoblast cell numbers after dental injury', *J Dent*, 28(4), pp. 277-285.

Murray, P., Stanley, H., Matthews, J., Sloan, A. and Smith, A. (2002) 'Age-related odontometric changes of human teeth', *Oral Surg Oral Med O*, 93(4), pp. 474-482.

Murray, P.E., Smith, A.J., Garcia-Godoy, F. and Lumley, P.J. (2008) 'Comparison of operative procedure variables on pulpal viability in an ex vivo model', *Int Endod J*, 41(5), pp. 389-400.

Nanci, A. (2012) 'Dentin-pulp complex', in Nanci, A. (ed.) *Ten Cate's Oral Histology*. 8th edn. Mosby Elsevier, pp. 165-204.

Ninomiya, M., Ohishi, M., Kido, J., Ohsaki, Y. and Nagata, T. (2001) 'Immunohistochemical localization of osteopontin in human pulp stones', *J Endod*, 27(4), pp. 269-272.

Nishikawa, S. (2007) 'Developmental changes in pulpal sensory innervation of rat incisors and molars shown on a single injection of the fluorescent dye AM1-43', *Anat sci inter*, 82(4), pp. 227-232.

Nishikawa, S. and Kitamura, H. (1986) 'Localization of actin during differentiation of the ameloblast, its related epithelial cells and odontoblasts in the rat incisor using NBD-phallacidin', *Differentiation*, 30(3), pp. 237-243.

Nishikawa, S. and Kitamura, H. (1987) 'Microtubules, intermediate filaments, and actin filaments in the odontoblast of rat incisor', *Anat Rec*, 219(2), pp. 144-151.

Nishikawa, S. and Sasa, S. (1989) 'Immunofluorescent Localization of Myosin, Alpha-actinin and Tropomyosin in odontoblast microfilament bundles of rat incisor ', *Cell Struct Funct* 14, pp. 407-414.

Nomiyama, K., Kitamura, C., Tsujisawa, T., Nagayoshi, M., Morotomi, T., Terashita, M. and Nishihara, T. (2007) 'Effects of Lipopolysaccharide on Newly Established Rat Dental Pulp–derived Cell Line with Odontoblastic Properties', *J Endod*, 33(10), pp. 1187-1191.

Obrien, W.J., Lingrel, J.B. and Wallick, E.T. (1994) 'Ouabain Binding Kinetics of the Rat Alpha Two and Alpha Three Isoforms of the Sodium-Potassium Adenosine Triphosphate', *Arch Biochem Biophys*, 310(1), pp. 32-39.

Ohshima, H. (1990) 'Ultrastructural changes in odontoblasts and pulp capillaries following cavity preparation in rat molars', *Arch Histo Cytol*, 53(4), pp. 423-438.

Ohshima, H., Sato, O., Kawahara, I., Maeda, T. and Takano, Y. (1995) 'Responses of immunocompetent cells to cavity preparation in rat molars: an immunohistochemical study using OX6-monoclonal antibody', *Connect Tissue Res*, 32(1-4), pp. 303-311.

Ohshima, H. and Yoshida, S. (1992) 'The relationship between odontoblasts and pulp capillaries in the process of enamel- and cementum-related dentin formation in rat incisors', *Cell Tissue Res*, 268, pp. 51-63.

Ohshima, K.N., Watanabe, J., Kenmotsu, S. and Ohshima, H. (2003) 'Possible role of immunocompetent cells and the expression of heat shock protein-25 in the process of pulpal regeneration after tooth injury in rat molars', *J Electron Microsc* 52(6), pp. 581-591.

Oka, S., Oka, K., Xu, X., Sasaki, T., Bringas, P. and Chai, Y. (2007) 'Cell autonomous requirement for TGF-β signaling during odontoblast differentiation and dentin matrix formation', *Mech Dev*, 124(6), pp. 409-415.

Okiji, T., Kosaka, T., Kamal, A., Kawashima, N. and Suda, H. (1996) 'Age-related changes in the immunoreactivity of the monocyte/macrophage system in rat molar pulp', *Arch oral biol*, 41(5), pp. 453-460.

Okumura, R., Shima, K., Muramatsu, T., Nakagawa, K., Shimono, M., Suzuki, T., Magloire, H. and Shibukawa, Y. (2005) 'The odontoblast as a sensory receptor cells? The expression ot TRPV1 (VP1) channels', *Arch Histol Cytol* 68(4), pp. 251-257.

Onishi, T., Ooshima, T., Sobue, S., Tabata, M., Maeda, T., Kurisu, K. and Wakisaka, S. (1999) 'Immunohistochemical localization of calbindin D28k during root formation of rat molar teeth', *Cell Tissue Res*, 297(3), pp. 503-512.

Ottosson, A. and Edvinsson, L. (1997) 'Release of histamine from dural mast cells by substance P and calcitonin gene-related peptide', *Cephalalgia*, 17(3), pp. 166-174.

Palosaari, H., Wahlgren, J., Larmas, M., Rönkä, H., Sorsa, T., Salo, T. and Tjäderhane, L. (2000) 'The expression of MMP-8 in human odontoblasts and dental pulp cells is down-regulated by TGF-β1', *J Dent Res*, 79(1), pp. 77-84.

Pan, Y., Wheeler, E., Bernanke, J., Yang, H. and Naftel, J. (2003) 'A model experimental system for monitoring changes in sensory neuron phenotype evoked by tooth injury', *J Neurosci Methods*, 126(1), pp. 99-109.

Pang, Y.W., Feng, J., Daltoe, F., Fatscher, R., Gentleman, E., Gentleman, M.M. and Sharpe, P.T. (2016) 'Perivascular stem cells at the tip of mouse incisors regulate tissue regeneration', *J Bone Miner Res*, 31(3), pp. 514-523.

Parekh, S., Kyriazidou, A., Bloch-Zupan, A. and Roberts, G. (2006) 'Multiple pulp stones and shortened roots of unknown etiology', *Oral Sur Oral Med O*, 101(6), pp. e139-e142.

Pashley, D.H. (1985) 'Dentin-Predentin Complex and Its Permeability: Physiologic Overviwe', *J Dent Res*, 64(4), pp. 613-620.

Pashley, D.H. (1996) 'Dynamics of the Pulpo-Dentin Complex', *Crit rev oral biol m*, 7(2), pp. 104-133.

Patel, A. and Honoré, E. (2001) 'Properties and modulation of mammalian 2P domain K+ channels', *Trends Neurosci*, 24(6), pp. 339-346.

Peters, S.R. (2010) *A practical guide to frozen section technique*. Springer.

Pollard, D. and Cooper, A. (2009) 'Actin, a central player in cell shape and movement', *Science*, 326(5957), pp. 1208-1212.

Pugach, M., Strother, J., Darling, C., Fried, D., Gansky, S., Marshall, S. and Marshall, G. (2009) 'Dentin caries zones: mineral, structure, and properties', *J Dent Res*, 88(1), pp. 71-76.

Raia, P., Carotenuto, F., Eronen, J. and Fortelius, M. (2011) *Proc R Soc B*. The Royal Society.

Rajasekharan, S., Martens, L., Cauwels, R. and Verbeeck, R. (2014) 'Biodentine™ material characteristics and clinical applications: a review of the literature', *Eur Arch Paediatr Dent*, 15(3), pp. 147-158.

Ricucci, D., Loghin, S., Lin, L.M., Spångberg, L.S. and Tay, F.R. (2014) 'Is hard tissue formation in the dental pulp after the death of the primary odontoblasts a regenerative or a reparative process?', *J Dent*, 42(9), pp. 1156-1170.

Riihonen, R., Nielsen, S., Väänänen, H.K., Laitala-Leinonen, T. and Kwon, T.-H. (2010) 'Degradation of hydroxyapatite in vivo and in vitro requires osteoclastic sodium-bicarbonate co-transporter NBCn1', *Matrix Biol*, 29(4), pp. 287-294.

Rohrer, H., Heumann, R. and Thoenen, H. (1988) 'The synthesis of nerve growth factor (NGF) in developing skin is independent of innervation', *Dev Biol*, 128(1), pp. 240-244.

Rousselle, A.-V. and Heymann, D. (2002) 'Osteoclastic acidification pathways during bone resorption', *Bone*, 30(4), pp. 533-540.

Rozen, S. and Skaletsky, H. (1999) 'Primer3 on the WWW for general users and for biologist programmers', *Bioinformatics methods and protocols*, pp. 365-386.

Ruch, J.V., Lesot, H. and Begue-Kirn, C. (1995) 'Odontoblast differentiation', *Int J Dev Biol*, 39, pp. 51-68.

Rungvechvuttivittaya, S., Okiji, T. and Suda, H. (1998) 'Responses of macrophage-associated antigen-expressing cells in the dental pulp of rat molars to experimental tooth replantation', *Arch Oral Biol*, 43(9), pp. 701-710.

Saghiri, M.A., Oranji, J., Asatourian, A. and Sheibani, N. (2015) 'Validity and Variability of Animal Models Used in Dentistry', *Adv Hum Biol*, 5(2), pp. 1-16.

Sangwan, P., Sangwan, A., Duhan, J. and Rohilla, A. (2013) 'Tertiary dentinogenesis with calcium hydroxide: a review of proposed mechanisms', *Int Endod J*, 46(1), pp. 3-19.

Sasaki, S., Takagi, T. and Suzuki, M. (1991) 'Cyclical changes in pH in bovine developing enamel as sequential bands', *Arch Oral Biol*, 36(3), pp. 227-231.

Sasaki, T. and Garant, P.R. (1996) 'Structure and organization of odontoblasts', *Anat Rec*, 245(2), pp. 235-249.

Schilke, R., Lisson, J.A., Bauß, O. and Geurtsen, W. (2000) 'Comparison of the number and diameter of dentinal tubules in human and bovine dentine by scanning electron microscopic investigation', *Arch Oral Biol*, 45(5), pp. 355-361.

Scholzen, T. and Gerdes, J. (2000) 'The Ki-67 protein: from the known and the unknown', *J cell physiol*, 182(3), pp. 311-322.

Serper, A. and Çalt, S. (2002) 'The demineralizing effects of EDTA at different concentrations and pH', *J Endod*, 28(7), pp. 501-502.

Shi, S. and Gronthos, S. (2003) 'Perivascular Niche of Postnatal Mesenchymal Stem Cells in Human Bone Marrow and Dental Pulp', *J bone miner res*, 18(4), pp. 696-704.

Shibukawa, Y. and Suzuki, T. (2003) 'Ca2+ Signaling Mediated by IP3-Dependent Ca2+ Releasing and Store-Operated Ca2+ Channels in Rat Odontoblasts', *J Bone Miner Res*, 18(1), pp. 30-38.

Sigal, M., Aubin, J. and Ten Cate, A. (1985) 'An immunocytochemical study of the human odontoblast process using antibodies against tubulin, actin, and vimentin', *J Dent Res*, 64(12), pp. 1348-1355.

Sigal, M., Aubin, J., Ten Cate, A. and Pitaru, S. (1984a) 'The odontoblast process extends to the dentinoenamel junction: an immunocytochemical study of rat dentine', *J Histochem Cytochem*, 32(8), pp. 872-877.

Sigal, M., Pitaru, S., Aubin, J. and Ten Cate, A. (1984b) 'A combined scanning electron microscopy and immunofluorescence study demonstrating that the odontoblast process extends to the dentinoenamel junction in human teeth', *Anat Rec*, 210(3), pp. 453-462.

Silverthorn, D.U., Ober, W.C., Garrison, C.W., Silverthorn, A.C. and Johnson, B.R. (2007) *Human physiology: an integrated approach*. 4th edn. Pearson/Benjamin Cummings.

Simon, S. and Goldberg, M. (2014) 'Regenerative endodontics: regeneration or repair?', in *The Dental Pulp*. Springer, pp. 267-276.

Simon, S., Smith, A.J., Lumley, P.J., Cooper, P.R. and Berdal, A. (2012) 'The pulp healing process: from generation to regeneration', *Endod Top*, 26(1), pp. 41-56.

Sipert, C., Hussne, R., Nishiyama, C. and Torres, S. (2005) 'In vitro antimicrobial activity of fill canal, sealapex, mineral trioxide aggregate, Portland cement and endorez', *Int Endod J*, 38(8), pp. 539-543.

Six, N., Decup, F., Lasfargues, J.-J., Salih, E. and Goldberg, M. (2002) 'Osteogenic proteins (bone sialoprotein and bone morphogenetic protein-7) and dental pulp mineralization', *J Mater Sci Mater Med*, 13(2), pp. 225-232.

Sloan, A.J., Shelton, R.M., Hannc, A.C., Moxhamc, B.G. and Smith, J.A. (1998) 'An in vitro approach for the study of dentinogenesis by organ culture of the dentine-pulp complex from rat incisor teeth', *Arch Oral Biol*, 43, pp. 421-430.

Sloan, A.J. and Smith, A.J. (1999) 'Stimulation of dentine-pulp complex of rat incisor teeth by transforming growth factor-B isoforms 1-3 in vitro ', *Arch Oral Biol*, 44, pp. 149-156.

Smith, A. and Lesot, H. (2001) 'Induction and regulation of crown dentinogenesis: embryonic events as a template for dental tissue repair?', *Crit Rev Oral Biol Medicine*, 12(5), pp. 425-437.

Smith, A., Scheven, B., Takahashi, Y., Ferracane, J., Shelton, R. and Cooper, P. (2012) 'Dentine as a bioactive extracellular matrix', *Arch Oral Biol*, 57(2), pp. 109-121.

Smith, A.J. (2003) 'Vitality of the Dentin-Pulp Complex in Health and Disease: Growth Factors as Key Mediators', *J Dent Educ*, 67(6), pp. 678-689.

Smith, A.J., Cassidy, N., Perry, H., Begue-Kirn, C., Ruch, J.V. and Lesot, H. (1995) 'Reactionary dentinogenesis', *Int J Dev Biol*, 39, pp. 273-280.

Smith, A.J., Lumley, P.J., Tomson, P.L. and Cooper, P.R. (2008) 'Dental regeneration and materials: a partnership', *Clin Oral Investig*, 12(2), pp. 103-108.

Smith, C.E. and Warshawsky, H. (1975) 'Histological and three dimensional organization of the odontogenic organ in the lower incisor of 100 gm rats', *THE AMERICAN JOURNAL OF ANATOMY*

142(4), pp. 403-430.

Solé-Magdalena, A., Revuelta, E., Menénez-D., Calavia, M., Cobo, T., García-Suárez, O., Pérez-Piñera, P., De Carlos, F., Cobo, J. and Vega, J. (2011) 'Human odontoblasts express transient receptor protein and acid-sensing ion channel mechanosensor proteins', *Microsc Res Tech*, 74(5), pp. 457-463.

Son, A.R., Yang, Y.M., Hong, J.H., Lee, S.I., Shibukawa, Y. and Shin, D.M. (2009) 'Odontoblast TRP channels and thermo/mechanical transmission', *J Dent Res*, 88(11), pp. 1014-9.

Stains, J. and Gay, C. (1998) 'Asymmetric Distribution of Functional Sodium-Calcium Exchanger in Primary Osteoblasts', *J Bone Miner Res*, 13(12), pp. 1862-1869.

Stanley, H., Pereira, J., Spiegel, E., Broom, C. and Schultz, M. (1983) 'The detection and prevalence of reactive and physiologic sclerotic dentin, reparative dentin and dead tracts beneath various types of dental lesions according to tooth surface and age', *J oral pathol med*, 12(4), pp. 257-289.

Staquet, M.-J., Couble, M.-L., Romeas, A., Connolly, M., Magloire, H., Hynes, R., Clezardin, P., Bleicher, F. and Farges, J.-C. (2006) 'Expression and localisation of αv integrins in human odontoblasts', *Cell Tissue Res*, 323(3), pp. 457-463.

Swift, M. and Byers, M. (1992) 'Effect of ageing on responses of nerve fibres to pulpal inflammation in rat molars analysed by quantitative immunocytochemistry', *Arch Oral Biol*, 37(11), pp. 901-912.

Takano, Y., Sakai, H., Baba, O. and Terashima, T. (2000) 'Differential involvement of matrix vesicles during the initial and appositional mineralization processes in bone, dentin, and cementum', *Bone*, 26(4), pp. 333-339.

Taylor, P. and Byers, M. (1990) 'An immunocytochemical study of the morphological reaction of nerves containing calcitonin gene-related peptide to microabscess formation and healing in rat molars', *Arch oral biol*, 35(8), pp. 629-638.

Taylor, P., Byers, M. and Redd, P. (1988) 'Sprouting of CGRP nerve fibers in response to dentin injury in rat molars', *Brain Res*, 461(2), pp. 371-376.

Téclès, O., Laurent, P., Zygouritsas, S., Burger, A.S., Camps, J., Dejou, J. and About, I. (2005) 'Activation of human dental pulp progenitor/stem cells in response to odontoblast injury', *Arch oral biol*, 50(2), pp. 103-108.

Therien, A.G. and Blostein, R. (2000) 'Mechanisms of sodium pump regulation', *Am J Physiol Cell Physiol*, 279, pp. c541-c566.

Thesleff, I. (2003) 'Epithelial-mesenchymal signalling regulating tooth morphogenesis', *J Cell Sci*, 116(9), pp. 1647-1648.

Thesleff, I., Keranen, S. and Jernvall, J. (2001) 'Enamel knots as signaling centers linking tooth morphogenesis and odontoblast differentiation', *Adv dent res*, 15(1), pp. 14-18.

Thivichon-Prince, B., Couble, M., Giamarchi, A., Delmas, P., Franco, B., Romio, L., Struys, T., Lambrichts, I., Ressnikoff, D. and Magloire, H. (2009) 'Primary cilia of odontoblasts: possible role in molar morphogenesis', *J Dent Res*, 88(10), pp. 910-915.

Thomas, H. (1979) 'The extent of the odontoblast process in human dentin', *J Dent Res*, 58(4 suppl), pp. 2207-2218.

Thomas, H. (1983) 'The effect of various fixatives on the extent of the odontoblast process in human dentine', *Arch Oral Biol*, 28(5), pp. 465-469.

Thomas, H. (1984) 'The lamina limitans of human dentinal tubules', *J Dent Res*, 63(8), pp. 1064-1066.

Thomas, H. and Carella, P. (1983) 'A scanning electron microscope study of dentinal tubules from un-erupted human teeth', *Arch Oral Biol*, 28(12), pp. 1125-1130.

Thomas, H. and Payne, R. (1983) 'The ultrastructure of dentinal tubules from erupted human premolar teeth', *J Dent Res*, 62(5), pp. 532-536.

Tjäderhane, L., Carrilho, M.R., Breschi, L., Tay, F. and Pashley, D. (2012) 'Dentin basic structure and composition—an overview', *Endod Top*, 20(1), pp. 3-29.

Tjäderhane, L. and Haapasalo, M. (2012) 'The dentin–pulp border: a dynamic interface between hard and soft tissues', *Endod Top*, 2012(1), pp. 52-84.

Tsuchlya, M., Sasano, Y., Kagayama, M. and Watanabe, M. (2002) 'The extent of odontoblast processes in the dentin is distinct between cusp and cervical regions during development and aging', *Arch Histo Cytol*, 65(2), pp. 179-188.

Tsumura, M., Okumura, R., Tatsuyama, S., Ichikawa, H., Muramatsu, T., Matsuda, T., Baba, A., Suzuki, K., Kajiya, H. and Sahara, Y. (2010) 'Ca 2+ extrusion via Na+-Ca 2+ exchangers in rat odontoblasts', *J Endod*, 36(4), pp. 668-674.

Tsuruga, E., Sakakura, Y., Yajima, T. and Shide, N. (1999) 'Appearance and distribution of dendritic cells and macrophages in dental pulp during early postnatal morphogenesis of mouse mandibular first molars', *Histochem Cell Biol* 112, pp. 193-204.

Tsuzuki, H. and Kitamura, H. (1991) 'Immunohistochemical analysis of pulpal innervation in developing rat molars', *Arch Oral Biol*, 36(2), pp. 139-146.

Turner, D. (1992) 'Immediate physiological response of odontoblasts', *Proceedings of the Finnish Dental Society Suomen Hammaslaakariseuran toimituksia*, 88, pp. 55-63.

Turner, D., Marfurt, C.F. and Sattelberg, C. (1989) 'Demonstration of physiological barrier between pulpal odontoblasts and its perturbation following routine restorative procedures: a horseradish peroxidase tracing study in the rat', *J dent res*, 68(8), pp. 1262-1268.

Turner, N., Else, P. and Hulbert, A. (2005) 'An allometric comparison of microsomal membrane lipid composition and sodium pump molecular activity in the brain of mammals and birds', *J Exp Biol*, 208(2), pp. 371-381.

Tziafas, D. (1995) 'Basic mechanisms of cytodifferentiation and dentinogenesis during dental pulp repair', *Int J Dev Biol*, 39, pp. 181-290.

Tziafas, D. (2010) 'Dentinogenic potential of the dental pulp: facts and hypotheses', *Endod Top*, 17(1), pp. 42-64.

Veerayutthwilai, O., Byers, M., Pham, T.T., Darveau, R. and Dale, B. (2007) 'Differential regulation of immune responses by odontoblasts', *Oral Microbiol Immunol*, 22(1), pp. 5-13.

Vongsavan, N., Matthews, R. and Matthews, B. (2000) 'The permeability of human dentine in vitro and in vivo', *Arch Oral Biol*, 45(11), pp. 931-935.

Warshawsky, H., Josephsen, K., Thylstrup, A. and Fejerskov, O. (1981) 'The development of enamel structure in rat incisors as compared to the teeth of monkey and man', *The Anatomical Record*, 200(4), pp. 371-399.

Weiner, S., Veis, A., Beniash, E., Arad, T., Dillon, J., Sabsay, B. and Siddiqui, F. (1999) 'Peritubular dentin formation: crystal organization and the macromolecular constituents in human teeth', *J Struct Biol*, 126(1), pp. 27-41.

Wen, X., Lacruz, R.S., Smith, C.E. and Paine, M.L. (2014) 'Gene-expression profile and localization of Na+/K(+)-ATPase in rat enamel organ cells', *Eur J Oral Sci*, 122(1), pp. 21-6.

Wiesmann, H., Höhling, H., Zierold, K. and Barckhaus, R. (1995) 'Elemental distributions in predentine associated with dentine mineralization in rat incisor', *Connect Tissue Res*, 33(1-3), pp. 179-184.

Woodnutt, D., Wager-Miller, J., O'Neill, P., Bothwell, M. and Byers, M. (2000) 'Neurotrophin receptors and nerve growth factor are differentially expressed in adjacent nonneuronal cells of normal and injured tooth pulp', *Cell Tissue Res*, 299(2), pp. 225-236.

Yamada, T., Nakamura, K., Iwaku, M. and Fusayama, T. (1983) 'The extent of the odontoblast process in normal and carious human dentin', *J dent res*, 62(7), pp. 798-802.

Yoshiba, K., Yoshiba, N., Ejiri, S., Iwaku, M. and Ozawa, H. (2002) 'Odontoblast processes in human dentin revealed by fluorescence labeling and transmission electron microscopy', *Histochem Cell Biol*, 118(3), pp. 205-212.

Yoshida, S. and Ohshima, H. (1996) 'Distribution and organization of peripheral capillaries in dental pulp and their relationship to odontoblasts', *Anat Rec*, 245, pp. 313-326.

Yoshiyama, M., Masada, J., Uchida, A. and Ishida, H. (1989) 'Scanning electron microscopic characterization of sensitive vs. insensitive human radicular dentin', *J Dent Res*, 68(11), pp. 1498-1502.

Yoshiyama, M., Noiri, Y., Ozaki, K., Uchida, A., Ishikawa, Y. and Ishida, H. (1990) 'Transmission electron microscopic characterization of hypersensitive human radicular dentin', *J Dent Res*, 69(6), pp. 1293-1297.

Yu, C. and Abbott, P.V. (2007) 'An overview of the dental pulp, its functions and responses to injury', *Aust Dent J*, 52(1 suppl), pp. S4-S16.

Zaslansky, P., Zabler, S. and Fratzl, P. (2010) '3D variations in human crown dentin tubule orientation: A phase-contrast microtomography study', *Dent Mater*, 26(1), pp. e1-e10.

Zhang, M. and Fukuyama, H. (1999) 'CGRP immunohistochemistry in wound healing and dentin bridge formation following rat molar pulpotomy', *Histochem Cell Biol*, 112(5), pp. 325-333.